Synthetic routes towards triazole cannabidiol analogues and substituted cycloparaphenylenes

by
Mari Janse van Rensburg

Thesis presented in partial fulfilment of the requirements for the degree of Master of Science in the Faculty of Science at Stellenbosch University

Supervisor: Prof. Willem A. L. van Otterlo
Co-supervisor: Prof. Gareth E. Arnott
Department of Chemistry and Polymer Science

December 2019

DECLARATION

By submitting this thesis electronically, I declare that the entirety of the work contained therein is my own, original work, that I am the sole author thereof (save to the extent explicitly otherwise stated), that reproduction and publication thereof by Stellenbosch University will not infringe any third party rights and that I have not previously in its entirety or in part submitted it for obtaining any qualification.

Date: December 2019

ABSTRACT

SYNTHESIS OF TRIAZOLE CANNABIDIOL (CBD) ANALOGUES

Cancer is the leading cause of death worldwide and current treatment options often lead to painful and unpleasant side-effects. The active constituents isolated from medicinal plants have been successfully developed into various chemotherapeutic agents. The medicinal plant of interest in this research project, the cannabis plant, along with the constituents isolated, known as cannabinoids, have shown promising proapoptotic, anti-proliferative and anti-angiogenic effects. Interest in non-psychoactive cannabinoids, in particular cannabidiol (CBD), has significantly increased in recent years. CBD offers the hope of improved anticancer therapies that selectively target cancer cells without affecting normal cells, thereby eliminating the unwanted side-effects associated with conventional therapies.

This project involved the design and synthesis of CBD analogues by mimicking the main pharmacophoric groups found on the structure of CBD. The main difference between the natural occurring cannabinoid and the analogues in this study, was the replacement of the benzene ring at the core of the structure with a 1,2,3-triazole ring using click chemistry. A triazole moiety can provide improved solubility and bioavailability, while helping to exploit the chemical space around the compound. Three different systems (Scaffold A, B and C) were explored throughout this project. The transitions between these systems involved systematic alterations of functional groups on the general structure of each system, as well as the introduction of stereochemistry in the synthesis of Scaffold C. Important reactions used during the synthesis of these scaffolds included an epoxide ring opening via nucleophilic substitution, a Michael reaction, an Appel reaction, a nucleophilic substitution reaction resulting in an inversion of stereochemistry, as well as copper- and ruthenium-catalyzed azide alkyne cycloaddition reactions. These reactions provided the 1,4- and 1,5-, as well as 1,4,5-polysubstituted 1,2,3-triazole CBD analogues.

The anticancer activity of these compounds was subsequently evaluated against the MCF-7 cell line, as well as the HeLa cell line. None of the CBD triazole analogues of this study showed particularly appealing activity against these cancer cell lines. One analogue did however show potentially interesting activity against the MCF-7 cell line, and two analogues had an IC_{50} value below 100 µM against the HeLa cell line, with the most promising analogue providing an IC_{50} value of 74.3 µM. In addition, all compounds tested were completely devoid of toxicity below concentrations of 100 µM. The results obtained provide valuable insight into the future design of triazole CBD analogues.

SYNTHESIS OF SUBSTITUTED CYCLOPARAPHENYLENES (CPPS)

The synthesis of complex macrocycles and the study of the structural characteristics and properties displayed by these compounds is a fascinating research field. Cycloparaphenylenes (CPPs) are macrocycles which consist of benzene rings connected through *para*-linkages. This project focused on the synthesis of functionalized CPPs as these macrocycles could provide new host−guest

possibilities, possible use in chemosensors and nanoporous materials and the option of connecting these CPP macrocycles to various surfaces.

A method was developed for the synthesis of substituted [8]CPPs containing a thioether functionality, which provides the option of effortlessly transforming the substituents throughout the synthesis to give access to the previously synthesized ether-containing [8]CPP macrocycle. The series of reactions used during the synthesis of this CPP linker system included a Sonogashira coupling reaction, a dibromination reaction and a macrocyclization reaction, among others.

A linear test system was developed with a similar backbone structure to the substituted CPPs. The synthesis of the linear test system allowed investigation of the optimum route for the formation of the thioether functionality, which was then directly applied to the CPP linker system to gain access to the sulfur-containing CPP macrocycle.

UITTREKSEL

SINTESE VAN TRIASOOL KANNABIDIOL (CBD) ANALOË

Kanker is tans wêreldwyd die hoofoorsaak van sterftes. Die verskeie vorme van behandeling wat beskikbaar is lei dikwels tot pynlike en onaangename newe-effekte. Die aktiewe komponente, wat van medisinale plante verkry is, is reeds suksesvol tot verskeie chemoterapeutiese middels ontwikkel. Die medisinale plant in hierdie navorsingsprojek ter sprake, is die cannabis plant, asook die komponente, kannabinoïede, wat uit hierdie plant geïsoleer is. Dit toon belowende proapoptotiese, anti-proliferatiewe en anti-angiogeniese effekte. Belangstelling in nie-psigoaktiewe kannabinoïede, in besonder kannabidiol (CBD), het aansienlik verhoog in die afgelope paar jaar. CBD bied hoop op verbeterde anti-kankerterapieë, wat kankerselle selektief teiken, sonder om normale selle te beïnvloed. Dit skakel dus die ongewenste newe-effekte, geassosieer met konvensionele terapie, uit.

Hierdie projek behels die ontwerp en sintese van CBD analoë deur die farmakoforiese groepe, wat in die struktuur van CBD gevind word, na te boots. Die hoof verskil tussen die kannabinoïd wat natuurlik voorkom, en die analoë in hierdie studie, is die vervanging van die benseenring, in die kern van die struktuur, met ’n 1,2,3-triasool ring, deur middel van kliek chemie. ‘n Triasool komponent kan verbeterde oplosbaarheid en biobeskikbaarheid bied, terwyl dit terselfdertyd help om die chemiese spasie rondom die verbinding te benut. Drie verskillende sisteme (Steier A, B en C) is tydens hierdie projek ondersoek. Die oorgang tussen sisteme behels die sistematiese wysiging van funksionele groepe op die algemene struktuur van elke sisteem, sowel as die invoer van stereochemie in die sintese van Steier C. Belangrike reaksies wat tydens die sintese van die steiers gebruik is sluit in ’n epoksied ring-opening, deur middel van nukleofiele vervanging, ’n Michael-reaksie, ’n Appel-reaksie, ’n nukleofiele vervangingsreaksie wat lei tot ‘n inversie van stereochemie, asook koper- en rutenium-gemedïeerde azied alkyn sikloaddisie reaksies. Hierdie reaksies het die 1,4- en 1,5-, sowel as 1,4,5-gesubstitueerde 1,2,3-triasool CBD analoë verskaf.

Die anti-kanker aktiwiteit van hierdie verbindings is vervolgens teen die MCF-7 sellyn, asook die HeLa sellyn, geëvauleer. Geen van die CBD triasool analoë in hierdie studie het besondere belowende aktiwiteit teen die twee sellyne getoon nie. Een verbinding het egter potensieël interessante aktiwiteit teen die MCF-7 sellyn getoon en twee analoë het ’n IC_{50} waarde minder as 100 µM, teen die HeLa sellyn gehad. Die mees belowende analoog het ‘n IC_{50} waarde van 74.3 µM verskaf teen die HeLa sellyn. Daarbenewens is alle verbindings wat getoets is, heeltemal vry van toksisiteit onder konsentrasies van 100 µM. Die resultate verskaf waardevolle insig in toekomstige ontwikkeling van triasool CBD-analoë.

SINTESE VAN GESUBSTITUEERDE SIKLOPARAFENILENE (CPPS)

Die sintese van kompleks makroringe, asook die studie van die strukturele kenmerke en eienskappe wat hierdie verbindings toon, is ’n baie interessante navorsingsveld. Sikloparafenilene (CPPs) is

makroringe wat bestaan uit benseenringe wat deur *para*-skakeling verbind word. Hierdie projek fokus op die sintese van gefunksioneerde CPPs omdat hierdie makroringe nuwe gasheer-gas moontikhede, moontlike gebruik in chemosensors en nano-poreuse materiale, asook die opsie om hierdie CPP makroringe met verskeie ander oppervlaktes te verbind, kan bied.

'n Metode is ontwikkel vir die sintese van gesubstitueerde [8]CPPs wat n tioeter funksionaliteit bevat, wat die opsie bied om die substituente deur die loop van die sintese te transformeer om toegang tot die vorige gesintetiseerde eter-bevattende [8]CPPs te verskaf. Die reeks reaksies wat tydens die sintese van hierdie CPP skakelsisteem gebruik is, sluit 'n Sonogashira-koppelingsreaksie, 'n dibrominasie-reaksie en 'n makrosikloserings-reaksie, onder andere, in.

'n Lineêre toetssisteem is ontwikkel met 'n soortgelyke ruggraatstruktuur as die gesubstitueerde CPPs. Die sintese van die lineêre toetssisteem het die geleentheid gebied om die optimale roete vir die formasie van die tioeter funksionaliteit te ondersoek, wat toe direk op die CPP skakelsisteem toegepas is om toegang tot die swael-bevattende CPP makroring te verkry.

ACKNOWLEDGEMENTS

“Research is formalized curiosity. It is poking and prying with a purpose. It is a seeking that he [/she] who wishes may know the cosmic secrets of the world and they that dwell therein.” Zora Neale Hurston, American writer and anthropologist. Dust tracks on a road (1942) an autobiography.

PROFESSIONAL ACKNOWLEDGEMENTS

I am very fortunate to have worked with several talented scientists during my MSc, each of whom had taught me valuable lessons along the way. First of all, I would like to extend my gratitude to my supervisor, Prof. Willem A. L. van Otterlo. The amazing opportunities you have given me has helped me to grow on a personal and professional level. Thank you for all your support, patience and guidance during my MSc and honours degree. It has truly been an honour to work with you. To my co-supervisor, Prof. Gareth E. Arnott, thank you for your advice and guidance during my undergraduate and postgraduate studies at Stellenbosch University. Your passion and enthusiasm for Organic Chemistry inspires us all and is certainly one of the reasons I chose to further my studies in Organic Chemistry. I will always be grateful for having the opportunity to have started my research career under these two inspirational supervisors! You have taught me where to poke and pry and how to formalise my curiosity.

Next, I would like to acknowledge Prof. Dr Hermann A. Wegner from the Justus-Liebig University in Giessen, Germany. Thank you for inviting me into your research group for four months and giving me the opportunity to work on a second project which is also discussed in this dissertation. Your guidance and advise related to this project is highly appreciated.

To Prof. Ivan R. Green, you are truly a pillar in the Organic Chemistry department at Stellenbosch University. I am honoured to have had the opportunity to work with you on two additional projects during my MSc under the supervision of Prof. Willem A. L. van Otterlo. Thank you for all the stimulating conversations and for sharing your knowledge about organic chemistry and natural products. For one of the additional projects conducted during my MSc, I would like to thank Prof. Antonio Evidente and Dr Marco Masi from the University of Naples Federico II, Naples, Italy. Thank you for allowing me to work in your research group for a period of one month and giving me the opportunity to explore an interesting branch of organic chemistry that I have not previously been involved in.

For the research conducted at Stellenbosch University, I would like to thank Ms Elsa Malherbe and Dr Jaco Brand for the NMR analysis and Dr Maritjie Stander for the MS analysis. I would also like to thank all the members of the group of medicinal and organic chemistry (GOMOC), thank you for being supportive colleagues that turned into treasured friends. In particular, I would like to acknowledge Dr Tanya Mabank and Leandi van der Westhuizen. Thank you for teaching me the finer art of purification and inert reaction conditions and for always providing advice in and out of the laboratory. Finally, for the biological tests conducted on the compounds produced from my main MSc

project, I would like to thank two our collaborators for their contribution towards this section. The first is Dr Kabamba B. (Alex) Alexandre and Dr Asongwe Lionel Tantoh from the Council for Scientific and Industrial Research in Pretoria, South Africa. The second is Dr Snezna Rogelj from the New Mexico Institute of Mining and Technology in Socorro, the United States of America, and the students involved in these evaluations, namely Maximo Santarosa, Danielle Turner and Shishir Acharya.

PERSONAL ACKNOWLEDGEMENTS

To all my friends, thank you for rejoicing in my triumphs and lifting me up during difficult times. Ilze Barnard, my NMR expert, thank you for all your help during the past few months, even though you are working on your own thesis, you were always willing to help me when needed. Stephanie M.R. Dassonville, my friend, there is no words to describe how grateful I am for your never-ending support. Thank you for all your help with this dissertation, for editing, proof reading, and so much more (at least now you know a thing or two about Organic Chemistry). Friends like you are precious and few! To my two families - Thank you for providing me with two loving homes where I can always relax and recharge, even during the quick weekend visits. Thank you for giving me the opportunity to study at Stellenbosch University and for all the sacrifices you have made so that I could get the best opportunities life has to offer, I will be eternally grateful. To my 'baby' sister, thank you for taking on the role of the big sister in times when I need encouragement and for always seeing the best in me. To my amazing mother, thank you for always standing by me in whatever decision I make, and for all the invaluable lessons you have taught me throughout my life. Not only are you one of my best friends but you are also the best role model a girl can ask for. To my two grandmothers, thank you for your unwavering support and guidance, especially during the course of my postgraduate studies. Always ready to jump on a bus and come for a Stellenbosch visit when you could hear I was in need of some love. I will always treasure the memories we made on these Stellenbosch streets!

FUNDING ACKNOWLEDGEMENTS

Firstly, and most importantly, I would like to extend my gratitude to The Harry Crossley Foundation for supporting this research in the form of a bursary. Secondly, I would like to thank the National research foundation (NRF) for their contribution in the form of a Grant holder's bursary during the first year of my MSc, as well as Stellenbosch University for giving me a merit award in the form of a Murray Bursary. Additionally, I would like to thank the Justus Liebig University for funding my four-month research stay in Germany, in the form of a Liebig-College Scholarship. This scholarship allowed me to conduct the research of the second project discussed in this dissertation. I would also like to thank the Italian Ministry, as part of the Italian Science Ministry-RSA National Research Foundation's bilateral exchange program, for funding my one-month research stay at the University of Naples Federico II, in Italy. Finally, I would like to thank the IUPAC Postgraduate Summer School on Green Chemistry for awarding me with a scholarship which allowed me to attend the 2018 Summer School in Venice, Italy.

TABLE OF CONTENT

LIST OF ABBREVIATIONS

AcOH – Acetic acid

$CB_{'x'}$ – Cannabinoid-binding receptor type 'x'

CBD – Cannabidiol

CNTs – Carbon nanotubes

COD – Cyclooctadiene

CP* – Pentamethylcyclopentadiene

CPPs – Cycloparaphenylenes

CSIR – Counsel for Scientific and Industrial Research

CuAAC – Copper-catalyzed azide alkyne cycloaddition

DEAD – Diethyl azodicarboxylate

DCM – Dichloromethane

DIPEA – *N*,*N*-Diisopropylethylamine (Hünig's base)

DMF – *N,N*-Dimethylformamide

DMSO – Dimethyl sulfoxide

ECS – Endocannabinoid system

EtOAc – Ethyl acetate

MeCN – Acetonitrile

MOMCl – Chloromethyl methyl ether

MP – Melting point

MS – Mass spectrometry

MsCl – Methanesulfonyl chloride

MTT – (3-(4,5-Dimethylthiazol-2-yl)-2,5-diphenyltetrazolium bromide)

NBD – Norbornadiene

***n*BuLi** – *n*-Butyllithium

NMR – Nuclear magnetic resonance

NMT – The New Mexico Institute of Mining and Technology

R_f – Retention factor

RT – Room temperature

RuAAC – Ruthenium-catalyzed azide alkyne cycloaddition

SWNTs – Single-walled carbon nanotubes

TBAB – Tetrabutylammonium bromide

THC – Tetrahydrocannabinol

THF – Tetrahydrofuran

TLC – Thin layer chromatography

PREFACE
A NOTE TO THE READER

My MSc degree has truly been a unique journey. I had the opportunity to work on four different projects, of which some were in slightly different fields of specialization. Two of these projects also gave me the opportunity to work in two European countries for extended periods.

Of the four projects I worked on during my MSc, two are discussed in this document, as can be seen in the joined title of this dissertation.

THESIS LAYOUT

The first project, which is also the main project of my MSc, is titled “Synthesis of triazole cannabidiol (CBD) analogues”. This is an organic chemistry project which focused on the synthesis of small molecules as potential anti-cancer agents. Pages 1 to 123 contains all the information of this project, including the introduction (Chapter 1 and 2), results and discussion (Chapter 3), biological evaluation (Chapter 4), conclusion and future work (Chapter 5), experimental (Chapter 6), as well as the appendix pertaining to the work of this project (labelled as Appendix 1). All the experimental work for this project was conducted at Stellenbosch University, under the supervision of Prof. Willem A. L. van Otterlo and Prof. Gareth Arnott, except for the biological tests. The bioactivity of these compounds was independently determined by our collaborators at the CSIR in Pretoria and at NMT in the United States of America.

The second project discussed in this document, is titled “Synthesis of substituted cycloparaphenylenes (CPPs)”. This project focused on designing novel synthetic routes for the synthesis of these unique macrocycles. The reactions involved in this project, as well as the possible applications of these macrocycles are completely different when compared to the main project discussed in this dissertation. Pages 124 to 164 contains all the information of this project, including the introduction (Chapter 7), results and discussion (Chapter 8), conclusion and future work (Chapter 9), experimental (Chapter 10), as well as the appendix for this project (labelled as Appendix 2). For this project I spent approximately 4 months in Giessen, Germany, at the Justus Liebig University as part of the Liebig-College Scholarship in the research group of Prof. Dr Hermann A. Wegner.

Please note – In order to show the complete division between these two projects, the compound numbering and NMR spectra numbering for the second project was restarted at 1.

Finally, a combined reference list can be found in pages 165 to 174 containing all the references used for both of these projects.

ADDITIONAL PROJECTS AND PUBLICATIONS

Apart from the two projects discussed in this document, I was involved in another two research endeavors. During my MSc degree at Stellenbosch University, I had the opportunity to work with Dr Tanya Mabank, Prof. Ivan R. Green and Prof. Willem A. L. van Otterlo on finalizing some important

aspects of a ring closing metathesis project. This research, titled "Observations concerning the synthesis of heteroatom-containing 9-membered benzo-fused rings by ring-closing metathesis", was published in Tetrahedron in 2017.[1]

The final project which I was involved in focused on the isolation and characterization of alkaloids from an indigenous unexplored South African plant. The initial experimental work for this project was conducted at Stellenbosch University with Prof. Ivan R. Green and Prof. Willem A. L. van Otterlo, after which I got the opportunity to continue with this project in the research group of Prof. Antonio Evidente at the University of Naples Federico II, Naples, Italy. The manuscript for this research, titled “Alkaloids isolated from Haemanthus humilis Jacq., an indigenous South African Amaryllidaceae: Anticancer activity of coccinine and montanine” was accepted on 28 January 2019 by the South African Journal of Botany and has been send to production.[2]

During my MSc I attended two conferences, one local (Frank warren, 2016 in Grahamstown, South Africa) and one international (IUPAC Postgraduate Summer School on Green Chemistry 2018 in Venice, Italy), where I presented my main MSc project (Synthesis of triazole cannabidiol (CBD) analogues) by means of poster presentations. At the IUPAC Summer school on Green Chemistry 2018 in Venice, Italy, I received a certificate of recognition from Eni (main sponsor of the summer school) for the research presented in the poster presentation.

INTERPRETATION OF NMR SPECTRA

Please note that the atom numbering of the compounds in this dissertation is different compared to the numbering used when naming these compounds. This was done in an attempt to simplify the NMR spectra analysis, allowing the comparison of the same atom on different compounds in a more convenient way.

[1] B. A. Aderibigbe, I. R. Green, T. Mabank, M. Janse van Rensburg, G. L. Morgans, M. A. Fernandes, J. P. Michael and W. A. L. van Otterlo, *Tetrahedron*, 2017, **73**, 4671–4683.
[2] M. Masi, S. Van slambrouck, M. Janse van Rensburg, P. C. James, J. G. Mochel, P. S. Heliso, A. S. Albalawi, A. Cimmino, W. A. L. van Otterlo, A. Kornienko, I. R. Green and A. Evidente, in press, on invitation to *S. Afr. J. Bot.*, January 2019.

SYNTHESIS OF TRIAZOLE CANNABIDIOL (CBD) ANALOGUES

CHAPTER 1
INTRODUCTION TO CANCER AND CANNABIS

1.1. CANCER

1.1.1. DEFINITION OF CANCER

The American Cancer Society's formal definition describes cancer as 'a group of diseases characterized by uncontrolled growth and spread of abnormal cells'.[1] Cancer is one of the leading causes of mortality worldwide, causing more deaths than AIDS, tuberculosis and malaria combined. Although considerable progress has been made in cancer treatment, a universal cure is still out of reach.[2,3]

Cancer can affect people across the globe, of any race or age; and the severity of the global cancer epidemic is demonstrated in recent cancer statistics.[1]

1.1.2. CANCER STATISTICS

In 2008, the International Agency for Research on Cancer, estimated that 12.7 million new cancer cases and 7.6 million cancer deaths occurred, of which 63% of cancer deaths occurred in less developed countries.[4,5] This might be due to late diagnoses in less developed countries along with limited access to the necessary treatment centers, as shown in Figure 1:1.

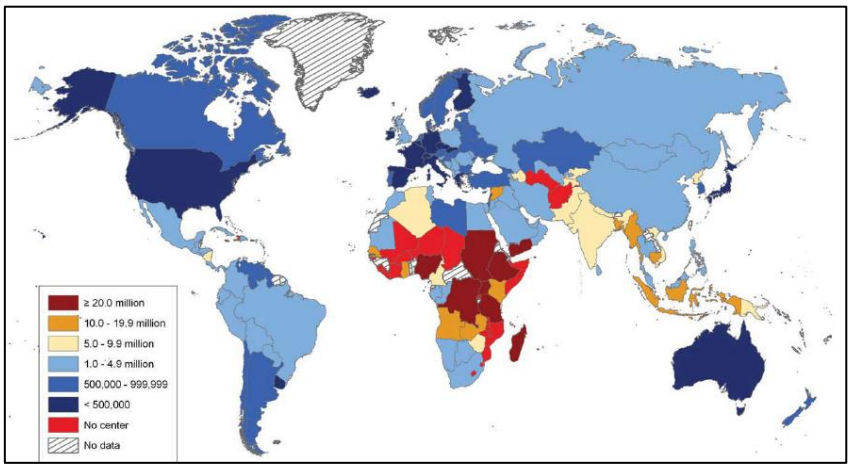

Figure 1:1 Number of patients at treatment centers in 2008.[5]

The 2012 statistics, estimated that 14.1 million new cases and 8.2 million deaths occurred; of which more than half of the morbidity and mortality rates were once again assigned to less developed countries, as illustrated in Figure 1:2.[3]

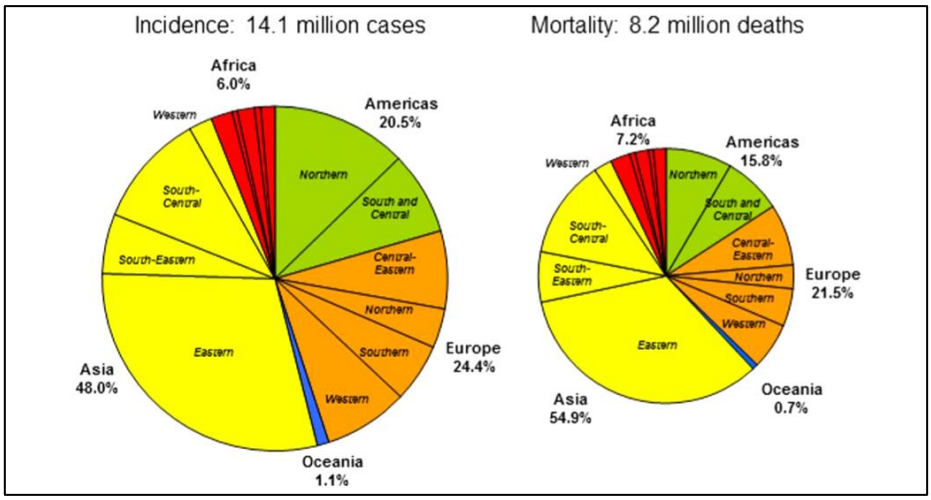

Figure 1:2 Estimated global morbidity and mortality rates in 2012.[3]

To visualize the impact cancer has on the South African population, cancer statistics for African countries were also consulted. An estimated 715 000 new cases and 542 000 deaths occurred in 2008; with the highest overall death rates being assigned to Southern Africa (Table 1:1).[6]

Table 1:1 Cancer Death rates in Africa, 2008.[6]

	All Africa	Sub-Saharan Africa	Southern Africa	Eastern Africa	Middle Africa	Northern Africa	Western Africa
	[a]Rate	[a]Rate	[a]Rate	[a]Rate	[a]Rate	[a]Rate	[a]Rate
Males All sites [b]	95.7	98.1	172.1	105.4	78.5	89.5	80.1
Females All sites [b]	86.5	92.8	108.1	95.9	75.6	68.2	91.2

[a] Rates are per 100 000 and age-standardized to the world population.
[b] Excluding nonmelanoma skin cancer.

Through extrapolation of these recent increasing trends, the global cancer statistics are estimated to increase to 20.3 million new cases and 13.2 million deaths in 2030.[7]

These cancer-related mortalities also have a significant influence on the economy of developing countries, due to a loss in productivity. In a recent study, five economically developing countries were evaluated; and South Africa exhibited the highest economic impact per cancer death.[8]

These statistics clearly illustrates the need for affordable new cancer treatments, especially in less developed countries like South Africa. When researching new cancer treatments, a thorough understanding of the biology involved in cancer formation and progression is required.

1.1.3. BRIEF CANCER BIOLOGY

This group of diseases, consisting of more than 100 different types, are all characterized by changes, or mutations, to the processes involved in normal cell division; resulting in clusters of abnormal cells, known as tumours.[9] Tumours that remain in their position of origin, are called benign tumours; but invasive tumours that can spread, or metastasize, to other regions in the body, are known as malignant tumours (Figure 1:3).[10,11]

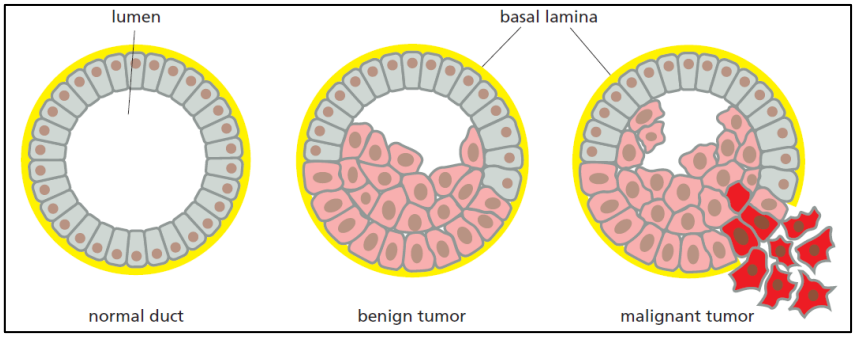

Figure 1:3 Benign tumours compared to malignant tumours.[10]

Lifestyle and environmental factors (radiation, tobacco, infectious organisms and viruses among others), as well as genetic factors (gene mutations or hormones) can lead to these unwanted mutations, thus resulting in cancer.[12]

To appreciate current insights into the biology and treatments of cancer, the history of cancer research must be considered.

1.1.4. HISTORY OF CANCER

Paleopathologists have suggested the presence of animal 'tumours' in prehistoric times, and some believe that cancer can be traced back to the beginning of mankind; however, there are no accurate scientific records to confirm these beliefs.[13] The first written description of 'cancer' dates back to approximately 3000 BC; located in an ancient Egyptian surgery manuscript, called the Edwin Smith Papyrus (Figure 1:4).[13]

Figure 1:4 The Edwin Smith Papyrus.[13]

The Edwin Smith Papyrus manuscript, described 'cancer' as an untreatable disease. Nevertheless, the ancient Egyptians did attempt treating this disease by means of cauterization, or through the use of salts and an arsenic paste, known as ''Egyptian ointment''. Their medical beliefs were guided by their trust in religion and magic, which is why ancient Egyptians believed that the "will of the Gods" was responsible for several diseases, including cancer.[13,14]

One of the first relevant milestones in cancer history, is when Hippocrates of Cos (460-375 BC), a Greek physician known as the "Father of Medicine", formulated the humoral theory of cancer.

1.1.4.1. HUMORAL THEORY

This theory stated that an imbalance of internal humours (believed to be blood, phlegm, yellow bile and black bile) was the cause of most diseases. Hippocrates believed that an excess of black bile was responsible for the formation of cancer. His approach towards cancer treatment was to surgically remove superficial tumours, but to avoid any interference with internal tumours as he believed these surgeries were perilous endeavours. The Hippocratic Corpus (the collected writings of Hippocrates, Figure 1:5) introduced the terms, *karkinos* and *karkinoma*, referring to malignant tumours and ulcer forming malignant tumours. These Greek terms refer to a crab, as Hippocrates thought tumours resemble the shape of this decapod species; and a subsequent translation to Latin led to the term - cancer.[13,14]

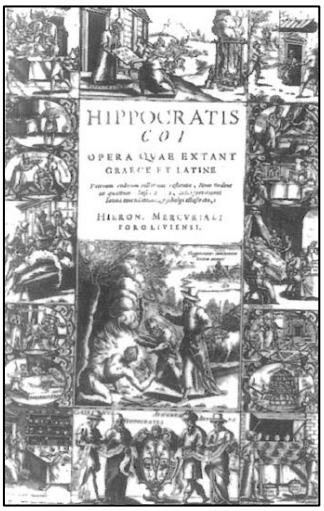

Figure 1:5 The collected writings of Hippocrates.[13]

The humoral theory remained unchallenged for over 1000 years, until René Descartes (1596-1650), a French philosopher and physician, proposed the lymph theory of cancer.[14]

1.1.4.2. LYMPH THEORY

The lymph theory stated that tumours originate in a localized area, after which lymph nodes are responsible for the development of secondary malignant tumours. A French Surgeon, Henry François le Dran (1685-1770) also supported the lymph theory and his treatment involved a complete

removal of the tumour, as well as the surrounding lymph nodes. During the lymph theory era, various scientists were interested in cancer epidemiology, and this led to some interesting discoveries linking cancer to specific lifestyle and occupational choices. For example, in 1713, Bernardino Ramazzini (1633-1714) revealed the link between the celibate lifestyle of nuns to the low number of cervical cancer cases among them.[15] Subsequently, the first reported example of occupational cancer was described by Percival Pott (1714-1788) in 1775, when he exposed the link between chimney sweeping and scrotal cancer.[14,16] These discoveries provided essential information for the control and possible prevention of cancer; and has a major influence on modern occupational safety regulations.

The next significant milestone in cancer history took place in 1838, when a German physiologist, Johannes Müller (1801-1858), gave rise to the cellular theory of cancer.[16]

1.1.4.3. CELLULAR THEORY OF CANCER

Müller initiated this theory by proving that cancerous tissue consists of cells, rather than black bile or lymph, by examining tumours under a light microscope. One of Müller's students, Rudolf Virchow (1821-1902), took this theory a step further by stating that cancer cells are either generated by chronic cellular irritation or an inherited predisposition. The cellular theory soon gained the support of several other scientists, including Karl Thiersch (1822-1925). Thiersch reinforced this theory in 1865, by proving that cancer spreads through malignant cells, and not through an unknown liquid substance. Karl von Rokitansky (1804-1878) also made a significant contribution to this theory by proving that tumours consist of two main components, namely, the framework and the cancer mass.[14,16]

Modern understanding of the biology behind cancer is a combination of the revolutionary discoveries made by Müller, Virchow and Rokitansky. The insights obtained from these discoveries led to major advances in effective cancer treatments.

1.1.5. CANCER TREATMENTS

When considering current treatment options, there are three main modes of treatments at our disposal, namely surgery, radiation therapy and chemotherapy. A number of additional treatment options have become available in recent years, including hormonal-, immune- and antiangiogenesis therapy.[17,18] For the purpose of this research, only the three main treatment options will be discussed in greater detail.

Surgery was the first, and for many years, the only treatment option available in the fight against cancer.

1.1.5.1. SURGERY

One of the first breakthroughs in the history of cancer surgery was reached in 1809, by an American surgeon, Ephraim McDowell. McDowell disproved the belief established by Hippocrates concerning the treatment of internal cancer masses, by successfully removing an ovarian tumour; leading to numerous advances in cancer surgery. In the last two centuries, with the discovery of anaesthetics in 1846 and the introduction of antiseptics in 1867, cancer surgery has evolved into a successful treatment for localized tumours.[19] The surgery related mortality rates have also significantly decreased with the continuous improvements made in this field. Despite these great strides, cancer surgery is still inadequate when attempting to treat progressive tumours and this led to the hunt for a new tool to use in the fight against cancer.

1.1.5.2. RADIATION THERAPY

Radiation therapy was set in motion by Wilhelm C. Röntgen (1845-1923) in 1895 with the discovery of X-rays, and the subsequent realization that X-rays are capable of reducing tumour growth. The discovery of radium shortly after, in 1898 by Antoine H. Becquerel (1852-1908), Pierre Curie (1859-1906) and Marie S. Curie (1867-1934), combined with Röntgen's breakthrough, accelerated research in this field. Each of these remarkable discoveries received Nobel Prizes for their contribution to physics.[20] Radiation therapy proved successful in the treatment of breast-, skin- and cervical cancer; and with the introduction of fractionated radiation, the treatment of head and neck cancers were also accomplished in 1928. In 1950, the discovery of cobalt therapy revolutionized this treatment option; and as a result, cobalt is still used in modern radiation therapy.[19]

In recent years, there has been major advancements in cancer surgery as well as radiation therapy; and although these can be used in combination, several cancers are still incurable when only relying on these two treatment options.[21] The next option that came to light, involved the incorporation of chemicals into the treatment of cancer.

1.1.5.3. CHEMOTHERAPY

Chemotherapy was initially defined as "the science dealing with the treatment of internal parasitic diseases by means of preparations synthesized with the object of combining the maximum power of efficiency in the destruction of the greatest variety of protozoa with the minimum poisonous action upon the patient's tissues".[22] A few years later, a modified definition was provided, describing chemotherapy as "the specific treatment of infections by artificial remedies".[23] The term 'chemotherapy', originated with Paul Ehrlich (1854-1915) in 1897, when he started the search for suitable chemicals with potential activity against cancer cells.[24] The majority of research done in the decades to follow was aimed at model development. Finally, in 1943, an alkylating agent with the ability to alter the DNA of abnormal cells, was discovered. This compound, called nitrogen mustard, showed promise in the treatment of non-Hodgkin's lymphoma and was the first chemical used as an

anti-cancer agent. This initiated the search for more selective and reliable chemical drugs; slowly leading to the development of modern combination chemotherapy.[24,25] Chemotherapy has developed into a very effective cancer treatment, which can either be used independently or in combination with the aforementioned options. It is known to increase the lifespan of patients; and in combination with radiation therapy, several cancers have been cured.[24] Nevertheless, the effectiveness of these chemicals is often limited to a specific type of cancer; and the price associated with this treatment limits this option to a certain group of patients. Chemotherapy is also associated with several unpleasant side-effects, which can significantly reduce the patient's quality of life.[26]

In the search for cheaper, less toxic chemotherapeutic drugs with reduced side-effects; natural products, specifically medicinal plants, have become a promising source of inspiration.

1.2. MEDICINAL PLANTS

A medicinal plant can be defined as "any plant used in order to relieve, prevent or cure a disease or to alter a physiological and pathological process"; or alternatively as "any plant employed as a source of drugs or their precursors".[27] Natural products, including various plant species with interesting biological properties, have been used in traditional medicine for thousands of years. Several developing countries, including the majority of the African population, still rely on plant-based traditional medicine (phytomedicines) to treat various diseases.[28,29] Although the focus of modern drug discovery has partially shifted towards synthetic organic techniques and molecular modelling, medicinal plants remain an important component due to their incomparable chemical diversity and bioactivity.[30] It is now known that each medicinal plant contains a set of unique pharmacologically active compounds which give rise to the observed bioactivity of that specific plant. The isolation of these compounds has become a vital aspect in modern drug discovery.

1.2.1. ISOLATION OF PHARMACOLOGICALLY ACTIVE COMPOUNDS FROM PLANT SPECIES

The isolation of these active compounds started in the nineteenth century; when morphine became the first pure pharmacologically active compound to be isolated from a plant. Friedrich Sertürner isolated morphine from opium poppy (*Papaver somniferum* L., Figure 1:6 A) in 1805, but the elucidation of its chemical structure (Figure 1:6 B) was only achieved in 1923.[28–30]

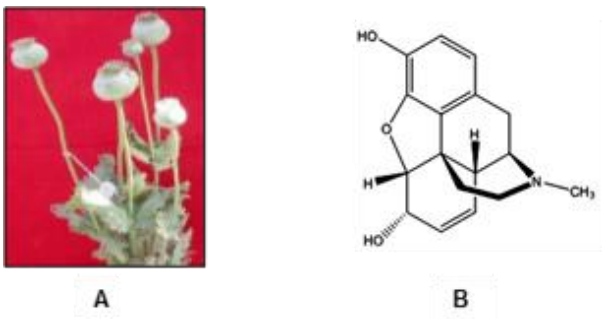

Figure 1:6 A: Opium poppy (*Papaver somniferum L.*);[31] B: Structure of morphine.[32]

After the successful isolation of morphine, numerous plant active compounds have been isolated and successfully developed into a variety of therapeutic materials, including chemotherapeutic agents.[33] The earliest pharmaceutical drugs from this category include cocaine (isolated from Erythroxylum coca), codeine (from *Papaver somniferum* L.), digitoxin (from Digitalis purpurea) and quinine (from Cinchona calisaya Wedd.).[26] This approach, in which the active compounds are used directly in their natural form, does however come with certain drawbacks. The isolation process is highly time consuming, structure elucidation requires expertise, and only limited amounts of pure compound is obtained from each plant. In addition, the cultivation of medicinal plants in less developed countries are not well regulated, leading to a decline in biodiversity.[34] These factors subsequently affect the sustainability of the plant population as well as the resulting pharmaceutical drugs. In order to overcome these restrictions, an alternative option came to light where the isolated active compounds can also be used as drug templates or precursors.[27,29]

Thus far, great success has been achieved in this field and various plant derived drugs are currently being used for a number of different diseases.

1.2.2. PLANT-DERIVED DRUGS

Some well-known plant derived active compounds currently on the market are summarized in Table 1:2. This table also provides the specific plant from which these compounds were isolated (or alternatively, the name of the isolated compound which acted as a template), as well as the disease for which each drug is used.

Table 1:2 Examples of plant derived drugs.

Name of active compound	Source of inspiration/ Plant	Medicinal use
Arteether[35]	Derivative of artemisinin, isolated from *Artemisia annua*	Malaria
Galantamine[36]	Isolated from *Galanthus nivalis* and Galanthus woronowii	Alzheimer's disease
Apomorphine hydrochloride[37]	Derivative of morphine, isolated from *Papaver somniferum* L.	Parkinson's disease
Tiotropium bromide[38]	Derivative of atropine, isolated from *Atropa belladonna*	COPD (chronic obstructive pulmonary disease)
Nitisinone[39]	Derivative of leptospermone isolated from *Callistemon citrinus*	Tyrosinemia

Apart from the above-mentioned bioactive compounds, several plant-derived active compounds have shown promising anti-cancer activity and has been developed into successful cancer treatments.

1.2.3. PLANT-DERIVED CHEMOTHERAPEUTIC DRUGS

This trend was initiated with the isolation of two vinca alkaloids from *Catharanthus roseus* G. Don., namely vincristine and vinblastine (Figure 1:7).[12,40] These alkaloids showed promising anti-cancer activity and were subsequently developed into novel anticancer drugs. Vincristine is used in the treatment of leukaemia, while vinblastine is used for breast-, lung- and testicular cancer.[12] The efficiency shown by these alkaloids prompted a wider investigation, and this led to the development of novel analogues, namely vindesine and vinorelbine, which is used in combination with other chemotherapeutic agents.[40]

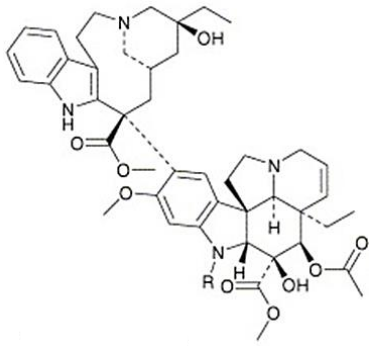

Figure 1:7 Structure of the vinca alkaloids; Vincristine (R = CHO) and Vinblastine (R = CH_3).[40]

The success achieved with the vinca alkaloids, instigated the search for more efficient plant derived chemotherapeutic agents. Relevant compounds already developed into successful anti-cancer treatments, include teniposide and etoposide (derivatives of podophyllotoxin, isolated from *P. peltatum Linnaeus*, and *P. emodii Wallich*), as well as Topotecan (derivative of camptothecin, isolated from *Camptotheca acuminata Decne*). The structures of the above-mentioned compounds are illustrated in Figure 1:8.[40,41]

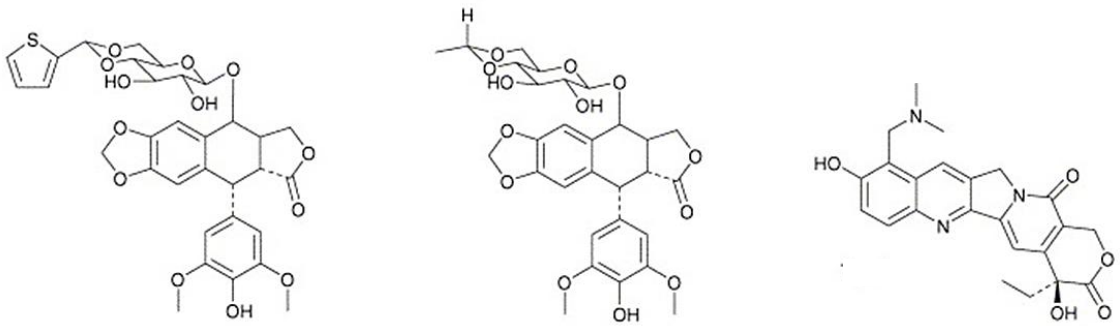

A **B** **C**

Figure 1:8 Structure of A: Teniopside; B: Etoposide; C: Topotecan.[40]

The medicinal potential concealed in Mother Nature can clearly be seen when considering the chemotherapeutic drugs approved in the last 70 years as more than half were derived from natural products.[26,28] One of the most renowned plant derived compounds approved as an anticancer drug, is known as paclitaxel (Taxol®,

Figure 1:9 A). This taxane diterpene was initially isolated by Wani and co-workers from *Taxus brevifolia Nutt*. (Figure 1:9 B) in 1967 (published in 1971)[42] and was subsequently approved as an ovarian cancer treatment in 1992.[43] Despite the drug resistance associated with this compound, paclitaxel is now obtained through a semi-synthetic procedure and is currently used in the treatment of various cancers (including ovarian-, breast- and non-small-cell lung cancer).[12,26,28] A potent semi-synthetic analogue of paclitaxel, namely docetaxel (Figure 1:9 C), has also been developed and is primarily used in the treatment of breast cancer.[12]

A **B** **C**

Figure 1:9 A: Structure of paclitaxel (Taxol®);[43] B: Bark of *Taxus brevifolia Nutt;* C: Structure of docetaxel.[44]

The success achieved thus far, clearly illustrates the potential of medicinal plants in the development of novel chemotherapeutic agents.

The medicinal plant of interest in this research project is one of the most controversial bioactive plants yet to be discovered, namely *Cannabis* (*C. sativa*).

1.3. THE CANNABIS PLANT

"It is a plant - this thing that we are about to discuss: a green plant, a very abundant and ubiquitous plant, an unusually valuable economic plant, possibly a dangerous plant, certainly in many ways a mysterious plant."[45]

1.3.1. TAXONOMY AND BOTANY OF CANNABIS

The *Cannabis* genus (a member of the *Cannabaceae* family[46] was originally divided into three distinct species, namely *Cannabis sativa* L., *Cannabis indica* Lam. and *Cannabis ruderalis* Janisch.[47] Nowadays, *Cannabis* is often treated as a monotypic species, namely *Cannabis sativa (C. sativa)* with various subspecies and varieties, for example, *C. sativa subsp. sativa* or *C. sativa subsp. indica* var. *kafiristanica.*[46,48,49] Even with the publication of several articles on the classification of *Cannabis*, including a recent comprehensive review,[50] more research needs to be conducted to determine the

exact taxonomy of the *Cannabis* plant.[51] For the purpose of this research, the latter taxonomy will be used, in which the term "*C. sativa*" refers to the monotypic species with various subspecies and varieties. In addition, the less scientific term, "marijuana", refers to the plant when used as a recreational drug.

C. sativa is predominantly classified as a dioecious plant, meaning an individual plant is either classified as male (staminate) or female (pistillate); however, monoecious plants are occasionally encountered where an individual plant bears both male and female flowers.[45,46] Although the entire plant (excluding the seeds) contains pharmacologically active compounds, the dried resin extracted from the glands of the female flowers contains the highest concentration of these compounds (Figure 1:10).[46]

Figure 1:10 Example of a female plant of *C. sativa* with visible clusters of individual flowers.[46]

1.3.2. HISTORY OF CANNABIS

This is but a brief summary of the history of *C. sativa*, for a more in-depth account, please consult the review article published by Russo in 2007.[52]

Through archaeological findings and scientific writings, it has been determined that *C. sativa* found its origin in Central Asia, more particularly in China. For more than 10 millennia, the Chinese population have realized the tremendous potential of this triple-purpose economic plant.[53] Initially, only the *C. sativa* stem was used to produce strong fibers (for ropes, cloths and paper); but shortly after, the value of the *C. sativa* seeds as edible oils was also recognized. Later on, it was discovered that the resin from its flowers (as well as other parts of the plant) could be used for medicinal purposes.[45] As a result, the cultivation of this useful plant started in China more than 6000 years ago; and some of the earliest medicinal texts mentioning *C. sativa*, were found in approximately 2000-year-old Chinese literature.[53,54]

The medicinal use of *C. sativa* started circulating through Asia, and finally in the 19th century, an Irish physician, William B. O'Shaughnessy, observed the therapeutic properties of *C. sativa* while working in India. O'Shaughnessy then conducted animal and human trials with *C. sativa* extracts and found that these extracts contains a wide variety of medicinal properties. After the publication of these results in Europe in 1842, the medicinal use of *C. sativa* experienced a dramatic increase.[55] The United States of America (USA) officially authorized the medicinal use of *C. sativa* in 1851, and by mid-20th century, more than twenty-five *C. sativa*-based medications could be easily obtained for a number of different maladies.[55,56] This new trend led to the search for more reliable and consistent *C. sativa*-based drugs which resulted in a number of patented preparations, indicated either as a sedative, an antispasmodic or an analgesic drug (some of which are illustrated in Figure 1:11).[57]

Figure 1:11 Labels of two patented *C. sativa*-based drugs.[57]

Several obstacles were however encountered with these drugs; and as a result, *C. sativa* research started to decline. One of these stumbling blocks was the method of administration as these *C. sativa* extracts proved to be non-water-soluble. These drugs were also often prescribed without standardized quality and dosage control, resulting in various unwanted side-effects. Above all these, the most significant obstacle was the social and political bias surrounding the use of *C. sativa* due to the psychotropic effects displayed by this plant.[46]

1.3.3. LEGAL ASPECTS SURROUNDING CANNABIS

In 1914, the first relative political intervention with the use of *C. sativa* took place in the USA, with the approval of the Harrison Narcotics Tax Act. Due to the fact that this act stipulated specific regulations for the distribution and production of narcotic drugs; society started viewing *C. sativa* as a dangerous drug, and the medicinal use systematically decreased.[58]

By 1937, the medicinal use of *C. sativa* was outlawed in the USA, under the Marijuana Tax Act; and similar legislations were approved throughout the Occident.[55,59] After numerous invalidation attempts, the Marijuana Tax Act was ultimately overturned in 1969, more than 3 decades after its approval, due to a violation of the Fifth Amendment. However, the following year, the USA Controlled Substance Act was passed as part of the Comprehensive Drug Abuse Prevention and Control Act of 1970, labelling *C. sativa* (marijuana) as a "Schedule I" drug with no medicinal use (Table 1:3).[58]

Table 1:3 USA Controlled Substance act criteria: "marijuana" classified as Schedule I.

Classification	Schedule I	Schedule II	Schedule III	Schedule IV	Schedule V
Uses	No Medical Use	Medical Use			
Abuse Potential	Very High	Gradual → Decrease			Very Low
Psychological or Physiological Dependence	Severe Psychological or Physiological	Gradual → Decrease			Low Psychological or Physiological

1.3.3.1. THE SOUTH AFRICAN PERSPECTIVE

When briefly considering the political history of *C. sativa*, out of a South African perspective, it is interesting to note that the use of *C. sativa* was prohibited 9 years before the approval of the Marijuana Tax Act in the USA. In South Africa, the use of *C. sativa* was outlawed in 1928, with the approval of the Medical, Dental and Pharmacy Act; which was subsequently modified in 1954, with increased consequences for transgression. In the decades to follow, two additional acts were approved, firstly the Abuse of Dependence-producing Substances and Rehabilitation Centres Act (in 1971), followed by the Drugs and Drug Trafficking Act (in 1992). Both of these provided hefty prison sentences for possession and dealing of *C. sativa* preparations.[60,61]

1.3.3.2. DECRIMINALIZATION OF CANNABIS

Despite these political restrictions, research on the plant and its constituents have continued across the globe, providing ample evidence for the undisputed medicinal value of *C. sativa*. These new scientific insights are slowly shifting the social and legal perspectives, leading to a movement known as the "decriminalization of Cannabis", in an effort to change the legal status of *C. sativa*. The medicinal use of *C. sativa,* under medical prescription, has already been legalized in several

countries (including Switzerland, India, Uruguay, Spain, Canada, Australia, and over 20 states in the USA).[62,63]

South Africa joined this movement in February 2014, with the introduction of the Medical Innovation Bill.[64] In March 2017, inconsistencies were found between the Drugs and Drug Trafficking Act and the Medicine and Related Substances Act, declaring certain sections invalid, thus ruling in favour of the private use of *C. sativa* by adults.[65] Even though these political restrictions have long delayed the study of *C. sativa* in South Africa; this research will certainly start gaining more support, following this landmark judgement. With well-constructed scientific research, it is certainly possible to distinguish between the medicinal and narcotic use, as shown with the opiates isolated from *Papaver somniferum* L., as mentioned earlier.

Although many aspects of the chemistry of *C. sativa* is already known, novel research is essential for the development of successful *C. sativa*-based or *C. sativa*-derived medical treatments. The wide variety of medicinal properties hidden within this plant, the exact mechanism of action, as well as the constituents responsible for these properties is still under investigation.

1.4. Chemistry of Cannabis

1.4.1. Cannabis constituents

The dried resin from the female flower, the most abundant source of pharmacologically active compounds found within the cannabis plant, contains a variety of constituents including flavonoids, terpenes, and cannabinoids.[66] The bio-activity of *C. sativa* has thus far mainly been assigned to the cannabinoid constituents; and therefore, for the purpose of this research, only the cannabinoids will be discussed in more detail.

C. sativa was the first plant from which cannabinoids were successfully isolated. Assuming other members of the *Cannabaceae* family could also contain cannabinoids would be a reasonable deduction; however, this is not the case. The *Humulus* genus, a member of the *Cannabaceae* family, acts as a good example. Despite various similarities between these two genera, no cannabinoids have thus far been found within the *Humulus* plant.[67,68] It is therefore commonly thought that cannabinoids are exclusively found within the *C. sativa* plant; but some exceptions have been reported. The presence of a few cannabinoid constituents has not only been confirmed in other plant species (including *Helichrysum umbraculigerum* Less.), but also in a few fungal and liverwort species.[69,70] Nevertheless, the *C. sativa* plant produces the greatest quantity and diversity of cannabinoids compared to any other source found in nature. The *C. sativa* plant is therefore a vital tool when investigating this diverse group of chemical compounds.

1.4.2. DEFINING THE TERM "CANNABINOID"

"Cannabinoid" does not only refer to the naturally occurring constituents (phytocannabinoids) isolated from the plant, but also to manufactured analogues (synthetic cannabinoids), as well as endogenous analogues produced within the animal and human body (endocannabinoids).[71] The majority of these chemical compounds are either part of, or are able to interact with a unique pleiotropic signaling system, known as the endocannabinoid system.

1.4.3. THE ENDOCANNABINOID SYSTEM

The endocannabinoid system (ECS) is a neuromodulatory system found within most mammalian species, known to be involved in several aspects of basic physiology and pathology. The ECS comprises of endocannabinoid ligands (along with the enzymes responsible for its biosynthesis, transport and degradation), as well as their specific binding sites known as the cannabinoid receptors.[72]

1.4.3.1. THE CANNABINOID RECEPTORS

The discovery of the ECS was initiated in 1988 with the identification of the first cannabinoid receptor, 'cannabinoid-binding receptor type 1' (CB_1), by Howlett and co-workers.[73] This breakthrough expedited research in this field; and only a few years later, Munro and co-workers discovered a second cannabinoid receptor, 'cannabinoid-binding receptor type 2' (CB_2).[74]

The cannabinoid receptors, CB_1 and CB_2, are both members of the G-protein-coupled receptor family.[75] The CB_1 receptor is predominantly located in the central nervous system, with the highest concentrations found in the hippocampus and cerebellum. As a result, the CB_1 receptor plays a role in regulating pain and the release of various neurotransmitters, among other important functions.[76] On the other hand, the CB_2 receptor is mainly found in the immune system; especially in the tonsils and spleen, with a variety of functions including inflammation regulation.[59]

After the discovery of CB_1 and CB_2, scientists started searching for endogenous ligands responsible for the activation of these receptors; thereby producing specific biological responses.

1.4.3.2. ENDOCANNABINOIDS

In contrast to other neurotransmitters which are produced in advance, and stored until needed; endocannabinoids are produced on demand, causing immediate changes in intercellular signaling upon receptor binding.[72]

The first endogenous ligand successfully isolated, is known as N-arachidonoyl-ethanolamine (AEA, Figure 1:12 A), and shows high affinity for the CB_1 receptor.[77] Another important endocannabinoid, with a high affinity for both the CB_1 and CB_2 receptors, was subsequently isolated and identified as 2-arachidonoyl-glycerol (2-AG, Figure 1:12 B).[78,79] When considering the structural similarities

between AEA and 2-AG, it is interesting to note that these bioactive lipids have distinctly different enzymatic routes.[72]

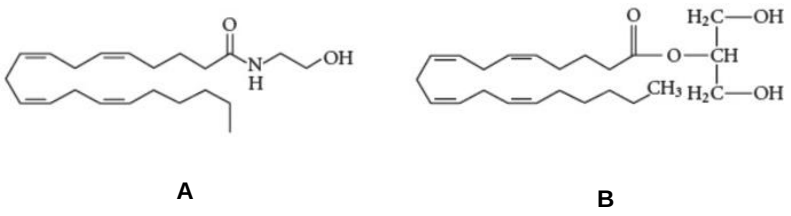

A **B**

Figure 1:12 A: Structure of AEA; B: Structure of 2-AG.[79]

A number of additional endocannabinoids, including O-arachidonoylethanolamine and N-arachidonoyldopamine has been identified, but AEA and 2-AG are regarded as the 'major endocannabinoids'.[80] It is now known that endocannabinoids are non-psychoactive compounds involved in a number of important functions within the human body. These ligands, along with the cannabinoid receptors, could therefore be a potentially interesting therapeutic target; however, their short half-life and lipophilic nature is problematic for the development of endocannabinoid-based therapies.[81]

When considering the presence of these cannabinoid-like structures within the human body, their affinity towards the cannabinoid receptors, and their role in the regulation of several bodily functions, the bioactivity of phytocannabinoids and their possible interaction with the endocannaboinoid system also comes to mind. The focus of the current research project is specifically directed towards the medicinal potential, particularly the anti-cancer activity of phytocannabinoids, in order to use the chosen phytocannabinoid as a template in the design of synthetic cannabinoids with potential anti-cancer activity. This focus will be discussed in more detail in the following section.

1.4.4. PHYTOCANNABINOIDS

A wide variety of these naturally occurring cannabinoids have been found within the *C. sativa* plant. When considering the isolated cannabinoids in their original form, as well as the additional cannabinoids formed under degradation, more than 90 phytocannabinoids have been identified.[66]

Each compound in this diverse group has a different chemical structure, which determines the specific mechanism of action and pharmacological profile of said cannabinoid.[80]

The first report on the anticancer-activity of phytocannabinoids surfaced in 1975, when Muton et al. discovered that phytocannabinoid administration inhibited the growth of Lewis lung adenocarcinomas in animal models.[82] In the last few decades, it has been shown that certain phytocannabinoids, as well as a number of synthetic cannabinoids possess proapoptotic, anti-proliferative and anti-angiogenic effects.[83]

One of the cannabis constituents that showed promising antineoplastic activity is the notorious phytocannabinoid, known as (−)-trans-Δ^9-tetrahydrocannabinol (THC, Figure 1:13), which is also the main psychoactive constituent found in the cannabis plant. Raphael Mechoulam, known as the 'father of cannabis research' was the first to successfully isolate,[84] determine the structure,[84] and successfully complete the total synthesis of THC.[85] THC has shown high affinity for both the CB_1 and CB_2 receptor, and the observed psycho-active effects is believed to be caused through the activation of the CB_1 receptor.[46]

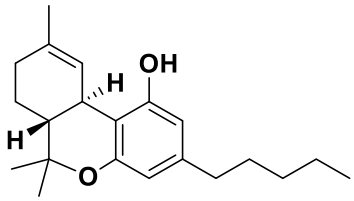

Figure 1:13 Structure of THC.[84]

These unwanted psycho-active side-effects limits the clinical use of THC-based treatments. For this reason, interest in non-psychoactive phytocannabinoids such as cannabidiol (CBD) has significantly increased in recent years. This interest will be further explored in the section to follow.

1.5. CANNABIDIOL

Although CBD was already isolated from the cannabis plant in 1940 by Adams *et al.*,[86] the intensive study of this phytocannabinoid staggered for many years. This can clearly be seen by the fact that the structure of CBD (Figure 1:14) was only elucidated 23 years after its initial isolation.[87] The cannabis pioneer, R. Mechoulam, was once again at the forefront of this structure elucidation.

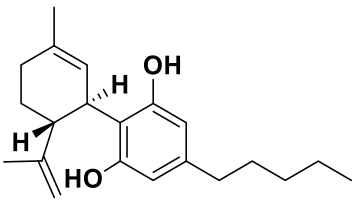

Figure 1:14 Structure of CBD.[87]

CBD and THC have similar structural characteristics and share several therapeutic properties. Nevertheless, one major difference between these two phytocannabinoids, is the minimal energy conformation adopted by these compounds. CBD adopts a conformation in which the two rings are perpendicular to each other (Figure 1:15 A), while THC adopts a rigid planar conformation (Figure 1:15 B).[88,89] It is believed that these conformational differences prohibit CBD from binding to, or activating the CB_1 receptor, thereby accounting for the lack of psychotropic activity of this phytocannabinoid.[89]

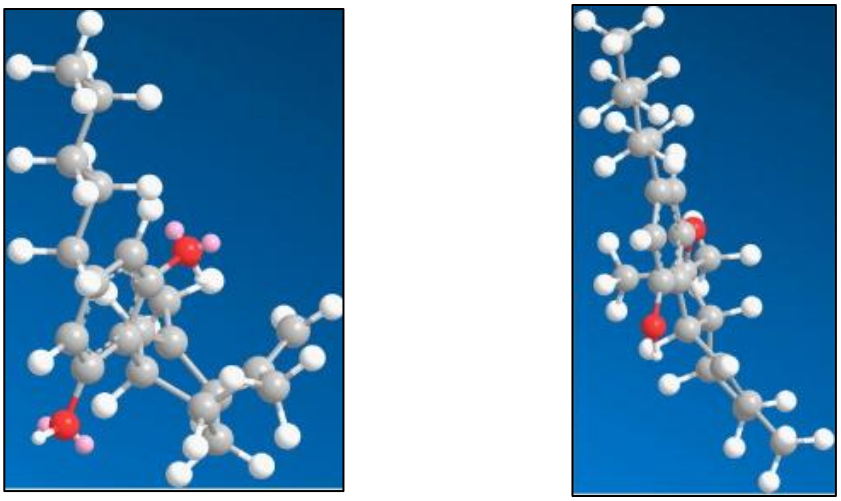

Figure 1:15 Minimal energy conformation of A: CBD; and B: THC.[88]

The *in vitro* and *in vivo* anticancer activity of CBD has recently been demonstrated by showing that CBD is capable of selectively inhibiting the growth and migration of human gliomas and breast carcinomas, while having no effect on normal cell lines.[90,91]

When considering these exciting reports on the anticancer activity of CBD, it is interesting to note that this phytocannabinoid has little to no direct affinity for either one of the cannabinoid receptors.[92] It has however been speculated that the anticancer effects of CBD could be due to indirect activation of the CB_2 receptor, as well as the possible activation of the transient receptor potential vanilloid type-1 and type-2 (TRPV1 and TRPV2) channels.[93,94] It is however important to note that the exact mechanism of action of phytocannabinoids, including CBD, is still under investigation. For a detailed review on the reported anticancer activity of CBD in several types of cancers and their possible mode of action in each of these cases, please refer to the review by Massi *et al.*[95]

The promising activity displayed by CBD, encourages the development of CBD-based anticancer treatments as CBD provides access to new treatment options without the unpleasant side effects affiliated with conventional therapies. As already mentioned, a number of major disadvantages are associated with natural product-based treatments including the time-consuming and expensive isolation process and the unsustainability of this route.[34] Taking this into consideration, we placed our interest in the design of synthetic CBD analogues in the hope that these synthetic cannabinoids show similar or even improved anticancer activity compared to CBD, while retaining the non-psychotropic property of this phytocannabinoid.

Often the design of synthetic drugs is based on the interaction of a ligand with a receptor known to control a specific function and the affinity of a ligand to the specific receptor is often calculated in advance through molecular modeling. However, with the uncertainty surrounding the mechanism of

action of phytocannabinoids, current designs of synthetic cannabinoids are based on the structure, and pharmacophoric groups on the structure of the phytocannabinoid exhibiting promising activity.

This research project is specifically directed towards the design and synthesis of CBD analogues, modified with a triazole moiety, as potential anticancer agents. The next section (Chapter 2) will therefore provide a brief introduction to click chemistry and discuss the rationale behind the design of the triazole CBD analogues of the study, followed by the aim and objectives set out for this project.

CHAPTER 2
CLICK CHEMISTRY AND PROJECT AIM

2.1. A BRIEF INTRODUCTION TO "CLICK CHEMISTRY"

The term "click chemistry", was defined by Sharpless and co-workers in 2001.[96] According to this definition, "click chemistry" is a collection of selective and highly reliable reactions capable of rapidly combining small separate units to produce larger molecules through irreversible carbon-heteroatom bond formations. These researchers also provided a list of stringent criteria that must be adhered to in order for a reaction to be subsumed under the umbrella of "click chemistry".[96] These criteria specify that a "click chemistry" reaction must use readily available substrates and benign solvents to provide the desired product stereospecifically and in a high yield. In addition, the product purification must be effortless and these reactions must only produce harmless by-products.[96]

A variety of well-known chemical transformations which adhere to these criteria have been identified. These include a number of oxidative addition reactions to carbon-carbon multiple bonds (for instance dihydroxylations, sulfenyl halide additions, aziridinations and epoxidations), as well as a number of nucleophilic ring-opening reactions of strained heterocycles (including aziridines and epoxides). Another important group of chemical transformations that meet these criteria are cycloaddition reactions of unsaturated species, including hetero-Diels-Alder reactions, as well as Huisgen dipolar cycloadditions.[96,97]

Among the products obtained from these chemical transformations, the 1,2,3-triazole moiety is of most interest in this project. The Huisgen [3+2] 1,3-dipolar cycloaddition reaction is one method that can be used for the 1,2,3-triazole synthesis. This involves the concerted addition of organic azides with terminal alkynes at elevated temperatures. Although this was a remarkable transformation at the time of its discovery in 1893,[98] this is a slow reaction and usually provides a mixture of the 1,4- and 1,5 regioisomers as depicted in Scheme 2:1.[99]

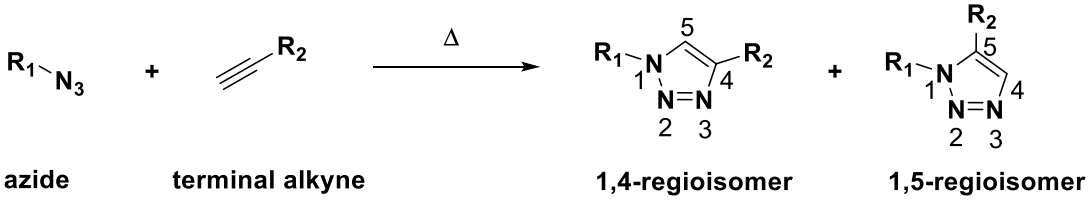

Scheme 2:1 Schematic representation of the general Huisgen azide-alkyne cycloaddition at elevated temperatures.[99]

This lack of regioselectivity was subsequently addressed by two separate research groups, namely Sharpless and co-workers, as well as Meldal and co-workers, who simultaneously published in 2002.[100,101] These researchers reported a copper(I)-mediated azide-alkyne cycloaddition reaction to obtain the 1,4-isomer regioselectively and in high yields.

2.1.1. COPPER-CATALYZED AZIDE ALKYNE CYCLOADDITION (CUAAC)

The CuAAC reaction is regarded as a prime example of "click chemistry" and is therefore frequently called the "click" reaction. This cycloaddition reaction has a broad scope and a remarkable tolerance for a variety of different solvents.[100] Various copper catalysts can be used for the CuAAC reaction on the condition that a copper(I) [Cu(I)] species is formed before the addition of the two substrates. One option is using a Cu(I) catalyst directly, for example, copper(I) halides; however, these copper sources require the addition of a stabilizing ligand (often a basic compound) and the reaction is frequently conducted in the absence of light to counteract the instability of the Cu(I) species.[102] The use of a Cu(II) pre-catalyst, for example, copper(II) sulphate pentahydrate, has also been reported.[100] The *in situ* generation of the Cu(I) species through the use of a pre-catalyst normally requires the addition of a mild reducing agent, but eliminates the need for a stabilizing ligand.[77] In addition, the use of certain Cu(II) pre-catalysts, in particular, copper(II) acetate, in alcohol solvents, without the deliberate addition of a reducing agent, has also been reported.[104,105] Brotherton *et al.* initially speculated that a catalytic amount of the Cu(I) species was generated via the reduction of the Cu(II) species through the oxidation of the alcohol solvent used (Scheme 2:2 A).[104] However, after successful triazole formation was observed in an alcohol solvent not prone to oxidation, these researchers presented a second hypothesis for the formation of the Cu(I) species. This hypothesis stated that catalytic amounts of the Cu(I) species was generated through a Glaser coupling reaction, or more accurately in this case an Eglinton reaction, between the Cu(II) pre-catalyst and the terminal alkyne (Scheme 2:2 B).[104]

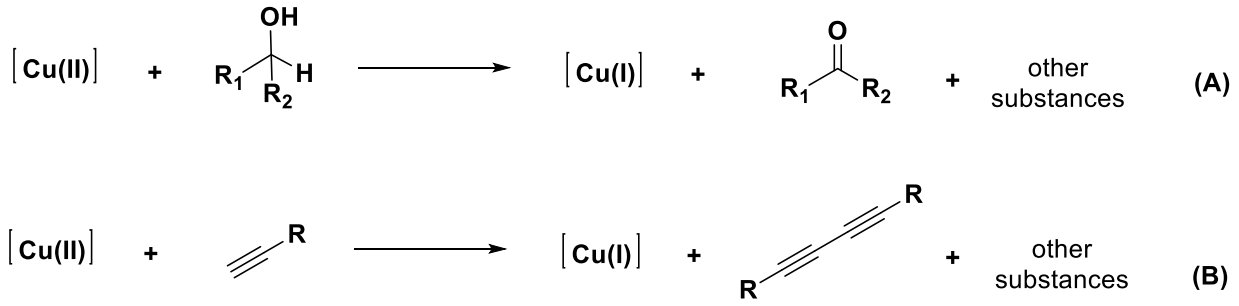

Scheme 2:2 Reduction of the Cu(II) pre-catalyst ($Cu(II)(OAc)_2$) to the Cu(I) species in alcohol solvents.[104]

A possible mechanism for the CuAAC reaction was first reported by Sharpless and co-workers in the same paper in which they introduced the copper-mediated cycloaddition reaction.[100] This was followed by a modified mechanism by Fokin and co-workers in 2005.[106] This modified mechanism was widely accepted, until Fokin and co-workers reported a new mechanism in 2013, which included a dinuclear copper intermediate, not seen in the previous versions.[107] This latest proposed mechanism for the CuAAC reaction is depicted in Scheme 2:3. This sequence begins with the coordination of the terminal alkyne to the Cu(I) species to form a π-complex. The active complex (a σ-bound dinuclear copper acetylide) is subsequently formed upon entry of a second Cu(I) species.

This is followed by the reversible coordination of the organic azide to the dinuclear copper acetylide. These researchers have proven that the direct cycloaddition does not take place, but that a step-wise annulation event rather occurs during which the β-carbon of the acetylene takes part in a nucleophilic attack at the nitrogen distal to the azide substituent. This leads to the formation of the first carbon-nitrogen bond. A second carbon-nitrogen bond is subsequently formed between the α-carbon of the acetylene and the nitrogen proximal to the azide substituent, resulting in a copper triazolide intermediate. Subsequent protonation provides the 1,4-disubstituted 1,2,3-triazole compound and regenerates the Cu(I) species.[107]

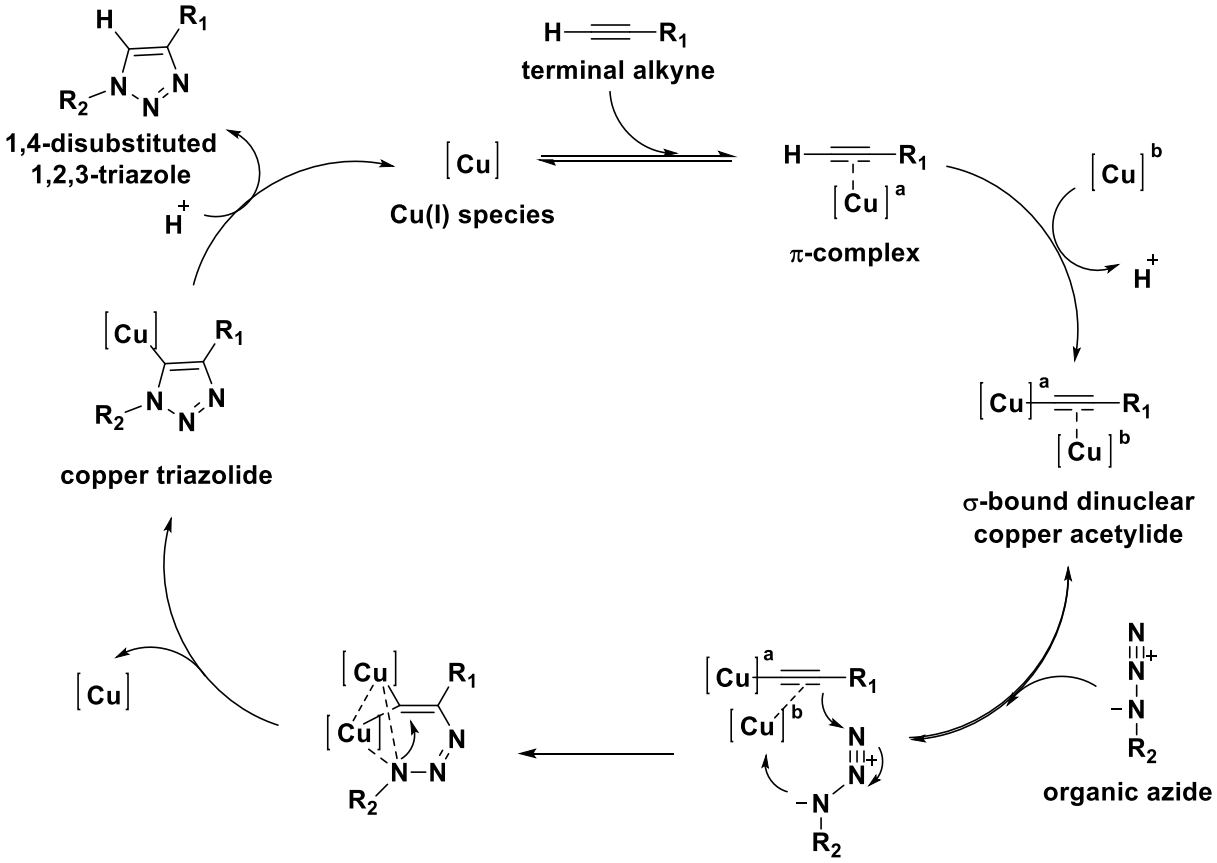

Scheme 2:3 Most recent proposed mechanism reported for the CuAAC reaction.[107]

After the successful implementation of the CuAAC reaction and the successes seen with this reaction in chemistry, biology and material science applications, selective access to the complementary isomer, the 1,5-disubstituted triazole, was investigated. Although a few procedures for the regioselective synthesis of the 1,5-isomer have previously been reported, including the reaction of bromomagnesium acetylides and organic azides,[108] these methods lack the scope and convenience of the CuAAC process. Jia and co-workers subsequently started searching for a catalytic procedure for this conversion and were the first to report a ruthenium-mediated azide-alkyne cycloaddition (RuAAC) reaction, which provides the 1,5-isomer regioselectively.[109]

2.1.2. RUTHENIUM-CATALYZED AZIDE ALKYNE CYCLOADDITION (RUAAC)

Jia, Fokin, Sharpless and co-workers investigated a variety of ruthenium catalysts for the selective synthesis of 1,5-disubstituted 1,2,3-triazoles from organic azides and terminal alkynes. Initially these researches discovered a cyclopentadienyl ruthenium complex, $CpRuCl(PPh_3)_2$, that could be used as a catalyst to provide the desired product. Even though this catalyst provided mainly the 1,5-isomer, the formation of the complimentary 1,4-isomer was also observed as minor product. In the search for a more selective catalyst, this complex was subsequently modified by exchanging the cyclopentadiene (Cp) group with the pentamethylcyclopentadiene derivative (Cp*). By using this modified catalyst, $Cp^*RuCl(PPh_3)_2$, a higher conversion of the starting materials was observed and the desired 1,5-regioisomer was obtained exclusively.[109]

It has been speculated that the electronic and steric properties of the Cp* group contributes to the stabilization of the higher formal oxidation states of the ruthenium atom, causing the bystander ligands to be more labile, thereby facilitating the formation of the active azide-[Cp*RuCl]-alkyne complex (see mechanism in Scheme 2:4 below).[110] A further investigation on different pentamethylcyclopentadienyl ruthenium chloride [Cp*RuCl] complexes revealed that $(Cp^*RuCl_2)_2$, Cp*RuCl(NBD), $Cp^*RuCl(PPh_3)_2$ and Cp*RuCl(COD) are the most efficient catalysts for the selective formation of 1,5-disubstituted 1,2,3-triazoles from primary azides and terminal alkynes. Two of these [Cp*RuCl]-based catalysts, namely $Cp^*RuCl(PPh_3)_2$ and Cp*RuCl(COD), proved to be superior as these also showed successful coupling with secondary azides. Unfortunately, the reaction rates and the product yields were much lower when compared to primary azides. This cycloaddition was also attempted with tertiary azides, but these proved to be much less reactive and most of the attempted tertiary azides did not participate in the coupling reaction.[110]

These researchers (Jia, Fokin, Sharpless and co-workers) also studied the solvent effect and found toluene, THF, benzene, 1,2-dichloroethane and dioxane to be compatible, but discovered that protic solvents negatively affect the yield and selectivity of this reaction.[109] From these results it is clear that the RuAAc reaction is more sensitive to solvents and the steric effects of the participating azide substituents when compared to the CuAAC reaction. After successfully establishing the suitable catalysts and solvents for this conversion, Jia, Fokin, Sharpless and co-workers explored the use of internal alkynes in this cycloaddition reaction. Due to the presence of copper(I) acetylide intermediate in the CuAAC reaction (Scheme 2:3), this transformation is limited to the use of terminal alkynes as already mentioned. The [Cp*RuCl] catalysts, or the two superior catalysts in particular, ($Cp^*RuCl(PPh_3)_2$ and Cp*RuCl(COD)) have the remarkable ability of engaging internal alkynes in catalysis, thereby providing access to 1,4,5-trisubstituted 1,2,3-triazoles.[109–111]

A possible mechanism for the RuAAC reaction was proposed in 2008 by Fokin and co-workers (Scheme 2:4, illustrated with a terminal alkyne for simplicity).[110] The ability to use internal alkynes ruled out the involvement of a ruthenium acetylide intermediate as seen in the CuAAC reaction.[109]

These researchers proposed that the two bystander ligands of the ruthenium catalyst are displaced upon addition of the alkyne and azide reagents, resulting in the activated azide-[Cp*RuCl]-alkyne complex. Azides prone to decomposition can react with the ruthenium catalyst to form a [Cp*RuCl]-tetrazenide complex which has no catalytic activity. To prevent the formation of this complex, the alkyne must be introduced before the azide. The azide and alkyne in this complex subsequently undergo oxidative coupling forming the metallacycle, or in this case a ruthenacycle intermediate. The new carbon-nitrogen bond is formed between the nitrogen distal to the azide substituent and the less sterically hindered carbon of the alkyne. When working with internal alkynes, the electronegativity of the substituents also plays a role in this bond-forming step. In addition, it has been speculated that internal alkynes containing a hydrogen bond donor group forms additional hydrogen bonds with the chloride atom on the ruthenium centre.[111] All these factors can influence the outcome of the cycloaddition reaction which is why the oxidative coupling step is thought to govern the regioselectivity of this cycloaddition reaction. The regioselectivity of internal alkynes will be discussed in more detail in Section 3.1.6. The resulting metallacycle intermediate then undergoes reductive elimination to provide the 1,5-disubstituted 1,2,3-triazole compound (in the case of terminal alkynes) and regenerates the ruthenium catalyst.[110]

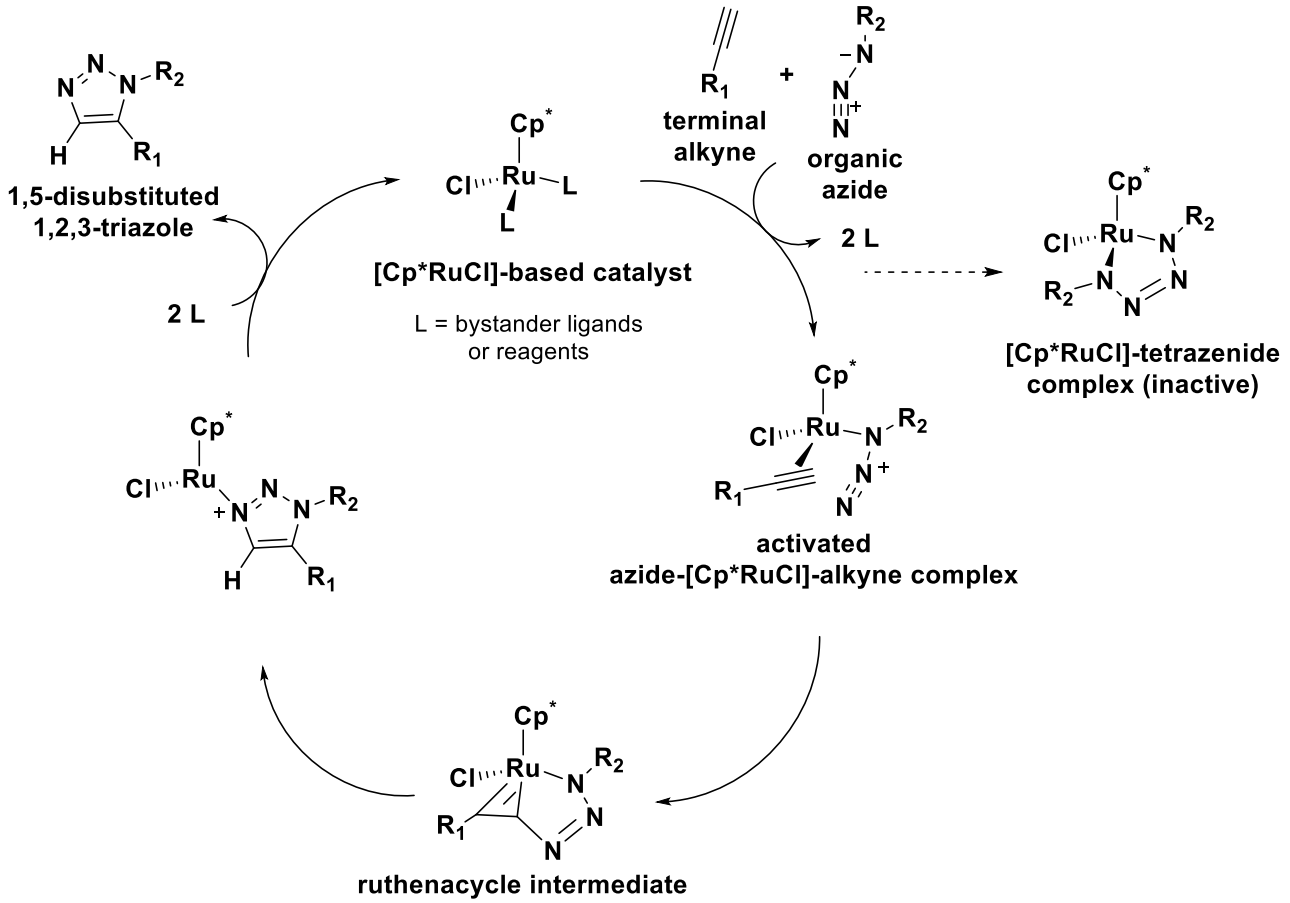

Scheme 2:4 Possible mechanism for the RuAAc reaction.[110]

Note that this mechanism is valid for all the ruthenium catalysts mentioned above (which are all 18-electon ruthenium complexes). Nolen and co-workers reported a set of coordinatively unsaturated 16-electron ruthenium complexes, which could also be used for the RuAAC reaction and proposed a slightly different mechanism for these complexes.[112] However, only the 18-electon ruthenium complexes and the mechanism shown in Scheme 2:4 is of importance in this project.

These two regioselective “click” reactions have recently been shown to be valuable tools in various different disciplines, as they have found applications in dendrimer synthesis,[113] activity-based protein profiling,[114] and cell surface engineering.[115] The triazole functional group generated through these “click” reactions have also demonstrated diverse biological functions, and is an increasingly common structural unit in various bioactive molecules, including anticancer agents.[116,117]

Our interest in cannabinoids (as discussed in Chapter 1), combined with our interest in the triazole moiety, led us to investigate previously designed triazole cannabinoid analogues and the applications for which they were designed.

2.2. PROPOSED TRIAZOLE CANNABINOID ANALOGUES

To our knowledge, the first report discussing the synthesis of potential triazole cannabinoid analogues, was published in 2007 by Di Marzo and co-workers.[118] Examples of the analogues designed in this study can be seen in Figure 2:1.

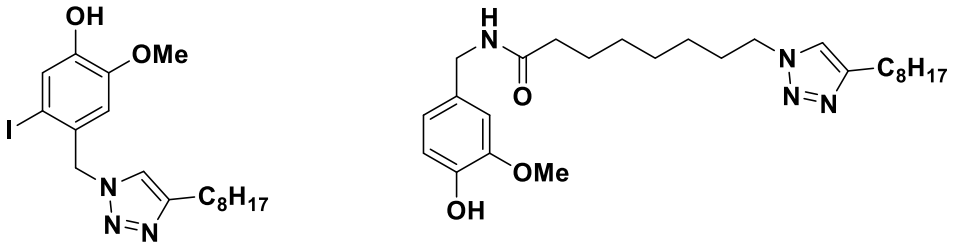

Figure 2:1 First reported of potential triazole cannabinoid analogues.[118]

Two years later, Hung and co-workers presented a fully substituted symmetrical triazole cannabinoid analogue (Figure 2:2) which showed high levels of *in vitro* activity for the CB_1 receptor. This compound was designed as a novel anti-obesity drug.[119]

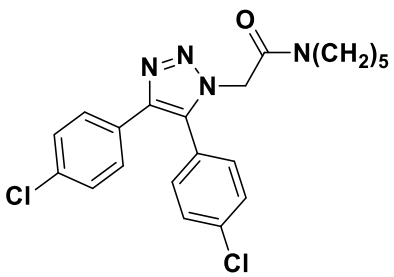

Figure 2:2 Potential triazole cannabinoid analogue designed as an anti-obesity drug.[119]

Around the same time, Trudell and co-workers reported the synthesis of a possibly triazole cannabinoid analogue containing an ester functionality, as can be seen in Figure 2:3.[120] This analogue was designed as a potential treatment against drug abuse.

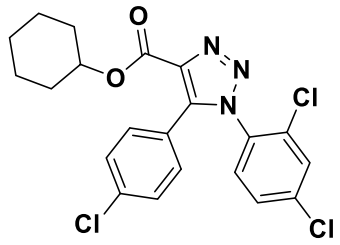

Figure 2:3 Potential triazole cannabinoid analogue targeting drug-abuse.[120]

None of the abovementioned proposed cannabinoid analogues were specifically designed as an anti-cancer treatment, and the structure of these compounds have more aromatic character than that of the traditional phytocannabinoids (THC and CBD) known to have anti-proliferative and pro-apoptotic effects. By combing the literature for previously synthesized cannabinoid analogues with potential anti-cancer activity, we came across a paper published in 2013, in which Szafrański *et al.* synthesized a set of novel 1,4-disubstituted triazole cannabinoid ligands with varying lengths of lipophilic side chains (Figure 2:4).[121] The strategy involved a CuAAC reaction between a previously synthesized 1,2-azido alcohol and different terminal aliphatic alkynes to obtain the hexyl, heptyl, octyl, decyl and dodecyl side chain triazole cannabinoid analogues.

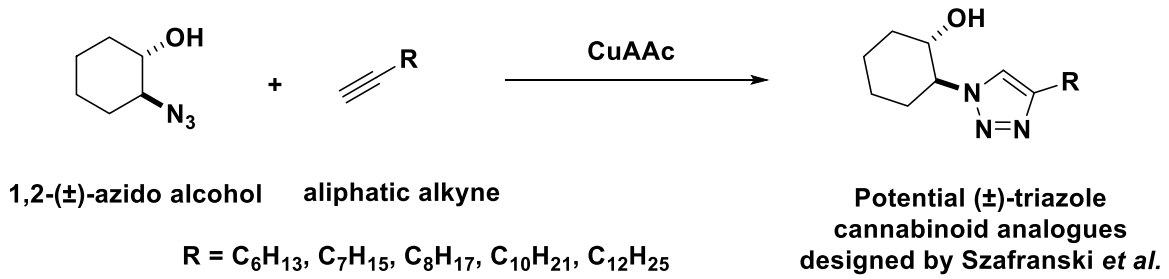

Figure 2:4 Approach used by Szafrański et al.[121]

In this paper, the cannabinoid on which they based their scaffold, was a synthetic cannabinoid (known as CP55940) with similar pharmacophoric groups as that of the cannabinoid of interest in this project, CBD. One of the main differences between these structures, is the length of the lipophilic side chain, as the synthetic cannabinoid has a longer side chain compared to CBD. The main change the researchers made to the structure was to replace the benzene ring present at the centre of most cannabinoids, including CP55940, THC and CBD, with a triazole ring.[121]

Unfortunately, relatively low affinities towards the CB_1 and CB_2 receptor was reported for these analogues synthesized by Szafrański *et al.* This might be a result of the longer side chain than that found in the phytocannabinoids like CBD, as well as the lack of other important pharmacophoric groups found in the structure of CBD.

2.3. AIM AND OBJECTIVES

In this research project, the issue of low potency shown by Szafrański *et al.*'s compounds will be addressed by considering all functional groups on the structure of CBD and designing novel triazole CBD analogues with the same side chain length as found on the structure of CBD. Although we initially considered molecular modelling in our quest to design new CBD analogues, only the crystal structure of CB_1 (PDB: 5TGZ) was solved at the time of this research.[122] However, as already mentioned, activation of the CB_1 receptor causes the unwanted psycho-active effects.[46] As luck would have it, the crystal structure of CB_2 (PDB: 5TGZ) only became available in 2019,[123] just before submission of this dissertation. Future work might therefore include molecular modelling to design novel CBD analogues selective for the CB_2 receptor.

When we considered pharmacophoric groups of interest on the structure of CBD, six main groups could be identified; the lipophilic tail (pentyl side chain), a benzene ring, the phenolic hydroxyl group, the cyclohexyl ring, the methyl group attached at the top of the cyclohexyl ring and the isopropenyl group attached to the bottom of the cyclohexyl ring (Figure 2:5).

When designing the CBD analogues for this study, two significant changes to these main pharmacophoric groups will be considered. The first and most important change will be to incorporate a triazole ring at the core, instead of the benzene ring. This change is possible as a similar spatial distribution can be achieved when incorporating a triazole ring.[121] Several natural products and pharmaceutical drugs have been modified with a triazole moiety to diversify the drug structure and exploit the chemical space around the compound.[124] This modification has also shown to provide improved solubility and bioavailability, and offer the additional option of attaching a biotin label or a fluorophore to the structure at a later stage in the synthesis.[124] The second modification will be to investigate the presence of an additional hydroxyl group at the top of the cyclohexyl ring, instead of the methyl group found in CBD. It has been shown that this alteration resulted in increased activity and selectivity of certain phytocannabinoids including THC and CBD.[46] The general structure of the triazole CBD analogues that will be investigated is depicted in Figure 2:5 B. This figure also shows a comparison between the analogues designed in this study and the structure of CBD (Figure 2:5 A), while emphasizing the two main changes that will be considered.

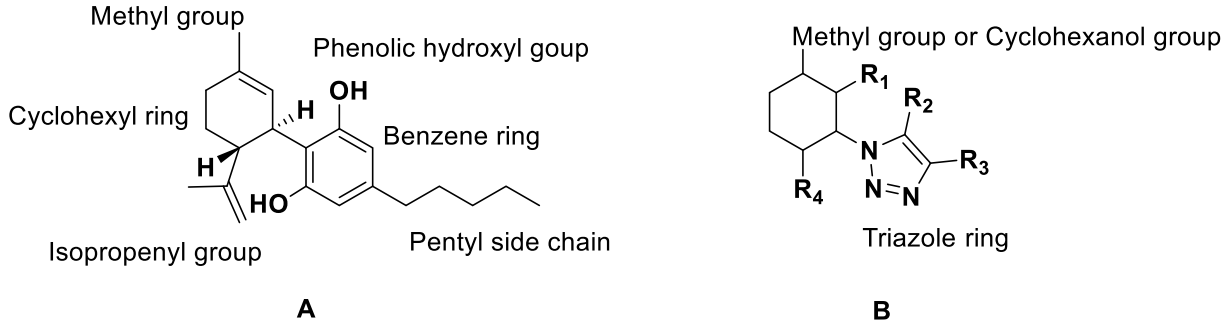

Figure 2:5 A: CBD with relative functional groups; B: General structure of triazole CBD analogues in this study.

To this end, three different systems (Scaffold A, B and C) will be investigated during this project, each with a unique structure and purpose. The design of each of these systems will be discussed below in sections 2.4.1, 2.4.2 and 2.4.3, and the syntheses of these three systems will be discussed in sections 3.1, 3.2 and 3.3.

2.4. RATIONALE BEHIND DESIGN OF TRIAZOLE CBD ANALOGUES

In this project, we will initially investigate a model system (Scaffold A) containing a set of triazole CBD analogues based on the scaffold designed by Szafrański *et al.*[121]

2.4.1. SCAFFOLD A

The lipophilic tail and the cyclohexyl ring are considered the two most important groups for the synthesis of Scaffold A. The pentyl side chain, which Szafrański *et al.* did not investigate, will be used as the standard length throughout this project, because this is the same side chain length found in the structure of CBD. An additional aspect that will be considered in the synthesis of Scaffold A, is to include the cyclohexanol group, similar to the scaffold reported by Szafrański *et al.*[121]

The 1,4- and 1,5-, as well as the 1,4,5-polysubstituted 1,2,3-triazoles, will be investigated by making use of both CuAAC and RuAAC methods. In the 1,5-disubstituted triazole, the pentyl side chain will adopt a different orientation to where we would normally expect it to be. The primary reason for investigating the 1,5-disubstituted triazole is to test the RuAAC reaction and find the optimum reaction conditions for the RuAAC reaction for this system. With optimized RuAAC conditions in hand, we hope to synthesize the 1,4,5-trisubstituted triazole analogue which will introduce an additional hydroxyl group at the center of the structure to mimic the phenol hydroxyl group found in the CBD structure. The general approach that will be followed to synthesize Scaffold A is illustrated in Scheme 2:5.

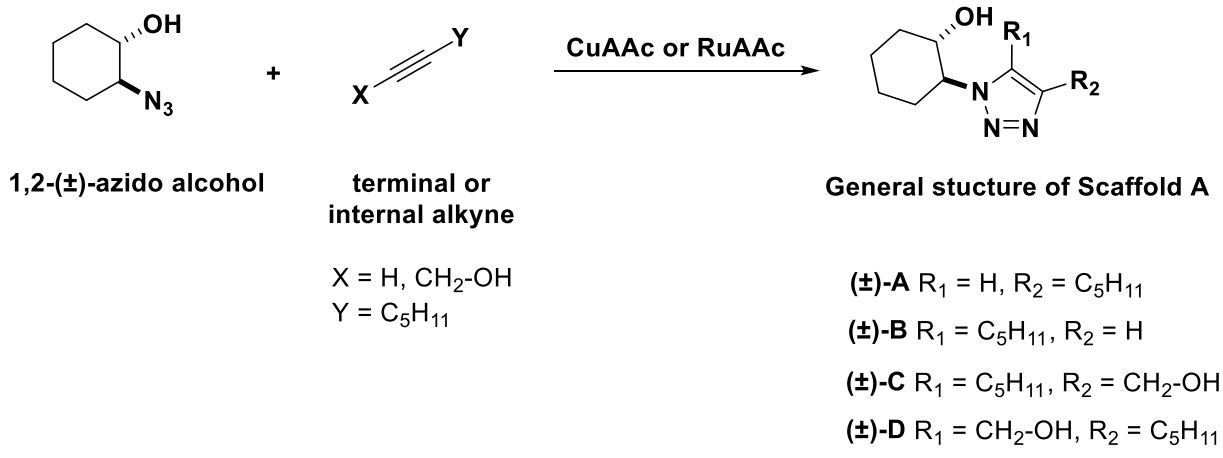

Scheme 2:5 General approach for the synthesis of Scaffold A.

2.4.2. SCAFFOLD B

In the next section, we will explore novel CBD triazole analogues, while still focussing on the three main functionalities as in Scaffold A (the lipophilic tail, the cyclohexyl ring as well as the cyclohexanol group). The main difference between the analogues of Scaffold A and Scaffold B, will be the position of the cyclohexanol group. In Scaffold B, the cyclohexanol group will be one carbon atom further away from the triazole functionality than in Scaffold A (where the cyclohexanol group is attached to the carbon adjacent to the triazole ring). This was done in order to have the hydroxyl group in the same position as the methyl group on the cyclohexane ring in the structure of CBD. For this scaffold, only the 1,4- and 1,5-disubstituted triazoles will be explored, as the main aim of this section is to compare the difference in activity with this hydroxyl shift. Once activity results of Scaffold A can be obtained, we can determine whether the 1,4,5-trisubstituted 1,2,3-triazole analogues (with the additional hydroxyl group at the center of the structure) would be a viable option to explore in Scaffold B. The general approach for the synthesis of Scaffold B is shown in Scheme 2:6.

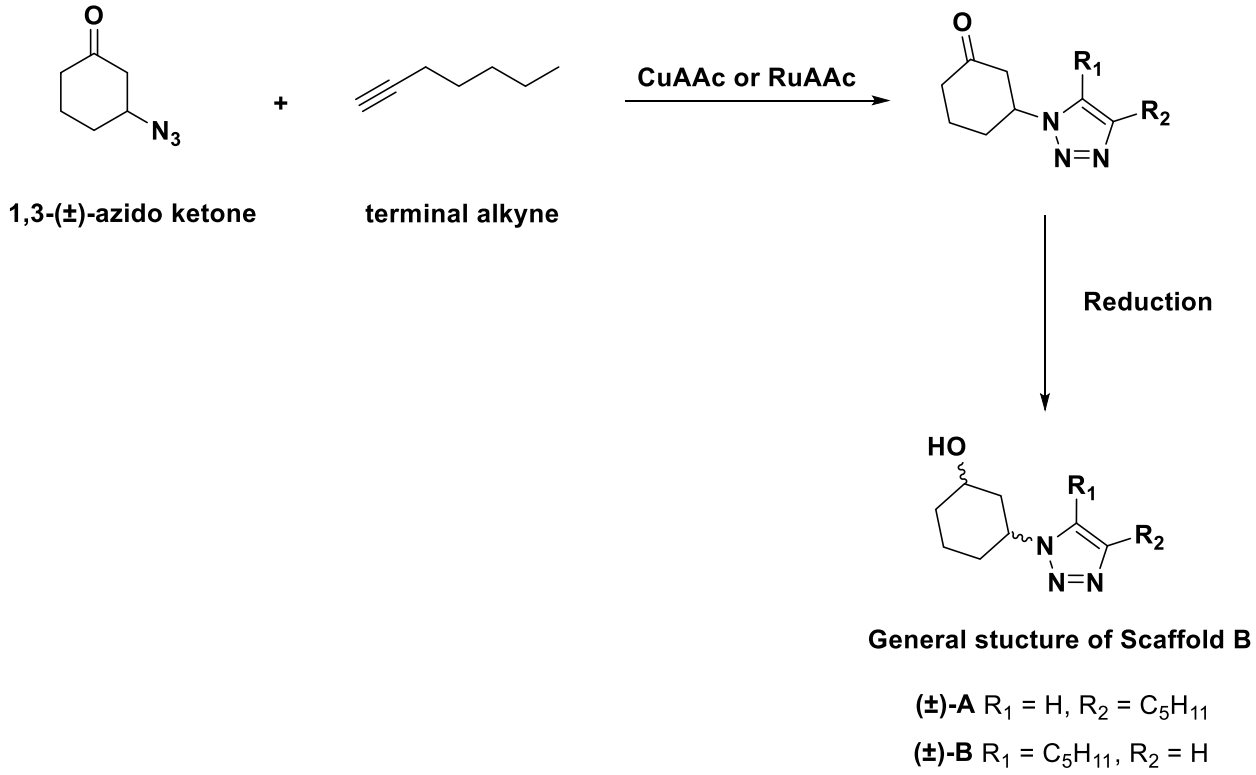

Scheme 2:6 The general approach for the synthesis of Scaffold B.

2.4.3. SCAFFOLD C

In the last section, the three main functionalities focused upon in Scaffold A and B (the lipophilic tail, the cyclohexyl ring as well as the cyclohexanol group) will still be taken into consideration, along with an additional group found on the structure of CBD. There are three main differences between the general structure of Scaffold C and the general structures of the previous two scaffolds. The first is the methyl group present at the top of the cyclohexane ring instead of the cyclohexanol group, and

the second is the introduction of an isopropyl group at the bottom of the cyclohexyl ring. The isopropyl group will be introduced to mimic the isopropenyl group at the same position on the structure of CBD. Since many groups in the general structure of these analogues have been altered during the design of Scaffold C, compared to the structure of CBD, it was decided to rather incorporate the methyl group at the top section of the cyclohexyl ring, as this is the exact group found in the structure of CBD. In doing so, the Scaffold C analogues can be directly compared to CBD. This will enable us to determine the influence of the changes we set out to make (the triazole ring and the isopropyl group) on the activity of these compounds. The third difference between the general structure of Scaffold C compared to the previous two systems, is the introduction of stereochemistry on substituents found on the cyclohexyl ring, similar to that of CBD. For this scaffold, only the 1,4-disubstituted triazoles will be explored, as the main aim of the synthesis of this scaffold is to compare the activity difference between these chiral triazole compounds and the previous two scaffolds (A and B). This will provide information on whether the isopropyl group at the bottom of the cyclohexyl ring is an important functional group to consider when designing CBD analogues in the future. The general approach for the synthesis of Scaffold C is illustrated in Scheme 2:7.

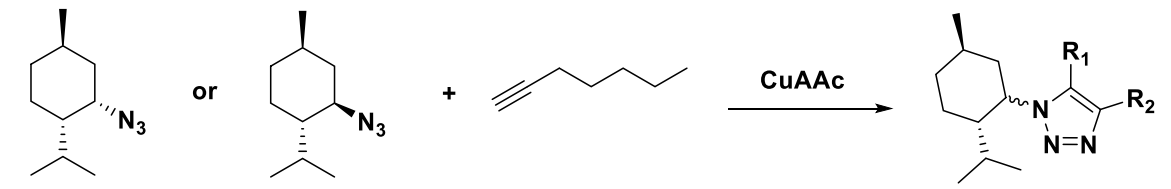

(1*S*,2*S*,4*R*)-azide **(1*S*,2*R*,4*R*)-azide** **terminal alkyne** **General stucture of Scaffold C**

(1*S*,2*S*,4*R*)-A R_1 = H, R_2 = C_5H_{11}

(1*S*,2*R*,4*R*)-B R_1 = H, R_2 = C_5H_{11}

Scheme 2:7 The general approach for the synthesis of Scaffold C.

Upon successful synthesis of the proposed analogues, biological tests will be conducted by our collaborators to determine the activity of these compounds on cancer cell lines. These results should potentially give a good indication on which functional groups play the most important role and will provide valuable insight into future design of CBD analogues by this click approach.

CHAPTER 3
RESULTS AND DISCUSSION

3.1. SYNTHESIS OF SCAFFOLD A

3.1.1. SYNTHESIS OF (±)-*TRANS*-2-AZIDOCYCLOHEXAN-1-OL 1

The synthesis of Scaffold A started with the transformation of cyclohexene oxide into the *trans* 1,2-azido alcohol **(±)-1** (Scheme 3:1) based on the procedure published by Krasnova and Yudin.[125,126] An epoxide functionality is more electrophilic than linear ethers due to the added ring strain. The nucleophilic attack causes the carbon-oxygen bond to break, resulting in a ring opening and thereby relieving the ring strain. Since the azide anion is a strong nucleophile, no acid catalyst was needed to activate the epoxide as would be required when working with weaker nucleophiles. After work-up and purification by column chromatography, the pure 1,2-azido alcohol **(±)-1** was obtained in a high yield of 95%.

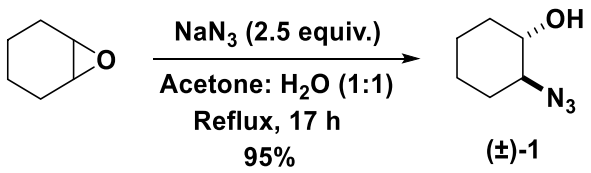

Scheme 3:1 Synthesis of 1,2-azido alcohol (±)-1 for Scaffold A.

NMR spectra 1 and 2, located in Appendix 1, were used to characterize product **(±)-1**. In the ^{1}H spectrum, a multiplet was observed at 3.36 – 3.30 ppm which represented the proton of the carbon attached to the hydroxyl group. The multiplet seen at 3.15 – 3.09 ppm corresponded to the proton of the carbon atom next to the nitrogen atom (of the azide functionality) and the broad singlet at 2.48 ppm could be assigned to the proton of the hydroxyl group. These two peaks appeared at a slightly higher chemical shift value due to the electronegativity of the oxygen and nitrogen atoms to which they were connected.[127] The ^{13}C spectrum also contained two deshielded peaks at 73.46 ppm and 66.98 ppm which represented the carbon attached to the hydroxyl group and the carbon attached to the nitrogen atom (of the azide moiety), respectively.[127] If this conversion was unsuccessful, these two carbon atoms would have been in the same chemical environment and only one peak would have been observed. All other proton and carbon atoms were accounted for, and were in accordance with previously reported spectral data.[125]

The 1,2-azido alcohol **(±)-1** was subsequently subjected to an initial CuAAC reaction to test the triazole formation. The general structure aimed for throughout this project contained an aliphatic pentyl side chain as previously mentioned; however, all of these desired structures were not UV active, making the tracking of reactions by TLC very difficult. For this reason, an alkyne derivative containing a UV active group (phenylacetylene) was specifically chosen for this test reaction.

3.1.2. SYNTHESIS OF (±)-*TRANS*-2-(4-PHENYL-1*H*-1,2,3-TRIAZOL-1-YL)CYCLOHEXAN-1-OL 2

The pure 1,2-azido alcohol **(±)-1** was subsequently subjected to a standard CuAAC reaction with phenylacetylene as the chosen UV active alkyne (Scheme 3:2). Copper(II) sulphate pentahydrate was used as a copper source along with sodium ascorbate as a reducing agent (see Chapter 2 – Click Chemistry Introduction). This specific copper source was chosen for this test reaction because it was the same copper source used by Szafrański *et al.* with this specific azide.[121] In literature, a solvent mixture of dimethyl sulfoxide and water was used for this reaction; however, it was decided to alter the solvent system to a mixture of methanol and water. This copper source has been shown to be compatible with a mixture of water and other polar solvents (including methanol or butanol), which indicated this to be an appropriate alteration.[97] By using methanol instead of dimethyl sulfoxide, the work-up and purification procedure of this novel triazole compound was made simpler. After work-up and removal of the organic solvent, the residue was purified by recrystallization (in a minimum amount of ethyl acetate), to obtain the pure UV active triazole **(±)-2** in an acceptable yield of 63%.

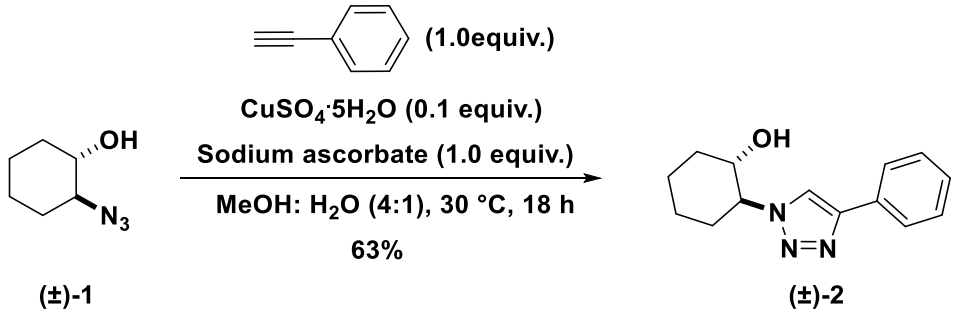

Scheme 3:2 Test reaction for CuAAC reaction with a UV active alkyne.

Product **(±)-2** was characterized by studying NMR spectra 3 and 4 in Appendix 1. The ^{1}H NMR spectrum showed a singlet at 7.76 ppm which represented the proton attached to the unsubstituted carbon of the triazole ring. Additionally, three multiplets were observed in the aromatic region (7.73 – 7.27 ppm) which corresponded to the five protons of the phenyl ring. It was also interesting to note that the proton atoms of the carbons attached to the hydroxyl group and the nitrogen atom (of the newly formed triazole ring) both appeared more downfield compared to the spectrum of compound **(±)-1** (which contained the azide functionality). These high chemical shift values could be a result of the magnetic anisotropy induced by the nearby triazole ring. Compared to the spectrum of **(±)-1**, the ^{13}C NMR spectrum presented six new peaks in the aromatic region, which corresponded to the two carbon atoms of the triazole ring as well as the six carbon atoms of the phenyl ring. As expected, only four peaks appeared for the six phenyl carbons. This was a consequence of the free rotation around the triazole-phenyl bond, causing a plane of symmetry along the center of the phenyl ring. The four carbons on either side of this plane therefore appeared as only two peaks, as the carbons across from each other were seen as chemically equivalent. The substituted carbon atom of the

triazole ring was represented by the largest chemical shift value (147.18 ppm) found in this spectrum. This can be explained by the combined ring current effects of the triazole ring and the attached phenyl ring. We worked on the assumption that the obtained product was indeed the 1,4-disubstituted regioisomer, as a large volume of literature has proven that the CuAAC reaction provides the 1,4-regioisomer selectively.[100–105] However, two-dimensional NMR experiments, in particular the nuclear overhauser effect spectroscopy (NOESY) sequence must be conducted to confirm this assumption. Furthermore, the mass spectroscopic analysis result confirmed successful synthesis of product **(±)-2**, as the result of 244.1452 amu was in agreement with the calculated value of 244.1450 amu. This high resolution mass spectrometry (HRMS) result, labeled as Mass Spectrum 1, can be seen in Appendix 1.

After the successful synthesis of the UV active triazole **(±)-2**, along with confirmation of the triazole formation, the synthesis of the 1,4-disubstituted triazole CBD analogue **(±)-3** was investigated.

3.1.3. Synthesis of (±)-*trans*-2-(4-pentyl-1*H*-1,2,3-triazol-1-yl)cyclohexan-1-ol 3

Optimization of the copper-catalyzed azide alkyne cycloaddition (CuAAC) reaction

As can be expected, a wide collection of literature procedures are available on this cycloaddition reaction. As a result, a variety of copper sources (both Cu(I) and Cu(II) sources) along with different reaction conditions were investigated in this project. This was done to obtain the optimum yield and the most convenient method for the CuAAC reaction between the 1,2-azido alcohol **(±)-1** and the chosen alkyne (1-heptyne) used to synthesize the desired 1,4-disubstituted 1,2,3-triazole **(±)-3** of Scaffold A. Due to the similarities between the three scaffolds of this study, the outcome of this optimization can be directly applied to Scaffold B and C. Each method will be discussed below and characterization of compound **(±)-3** will follow.

3.1.3.1. CuAAC with Copper(I) sulphate pentahydrate

The first CuAAC procedure explored for the synthesis of compound **(±)-3** utilized the same copper source as above, in the synthesis of compound **(±)-2**. As already mentioned, this was also the same copper source used by Szafrański *et al.* in the synthesis of a similar group of compounds.[97,121] The 1,2-azido alcohol **(±)-1** was reacted with the chosen alkyne, 1-heptyne, along with copper(II) sulphate pentahydrate and sodium ascorbate as a reducing agent (Scheme 3:3, see Chapter 2 – Click Chemistry Introduction). Initially, the copper source and reducing agent were dissolved in water and left to stir, allowing time for the reduction to occur. We assumed that the CuAAC reaction provides the 1,4-regioisomer as per above explanation. After standard work-up and purification by column chromatography, the pure 1,4-disubstituted analogue **(±)-3** was obtained in a good yield of 79%.

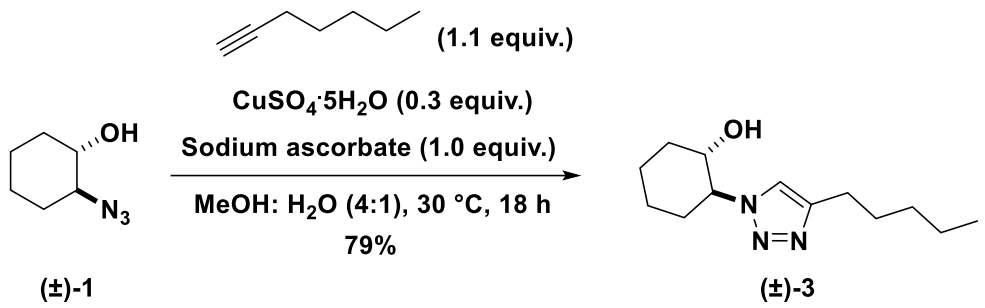

Scheme 3:3 Synthesis of 1,4-disubstituted triazole (±)-3 with $CuSO_4 \cdot H_2O$.

Although this was a pleasing result, the set-up of this reaction was fairly time-consuming and we were curious to see what yield would be obtained with different copper sources.

3.1.3.2. CuAAC with Copper(I) iodide

Various literature procedures using copper(I) iodide in CuAAC reactions have been published.[102,128,129] When using the Cu(I) catalyst, a stabilizing ligand (frequently a basic compound) is required and the reaction must preferably be conducted in the absence of light, (see Chapter 2 – Click Chemistry Introduction). Three different reaction conditions with copper(I) iodide as copper source were investigated and are discussed below. During all three reaction conditions investigated, *N,N*-diisopropylethylamine (DIPEA) was used as base.

3.1.3.2.1. First approach with Copper(I) iodide (DCM at room temperature (RT))

The first set of reaction conditions investigated, was the copper(I) iodide-catalyzed click reaction using dichloromethane as a solvent while running the reaction at room temperature (Scheme 3:4).[128] Under these conditions, a low yield of 39% was obtained after work-up and purification by column chromatography.

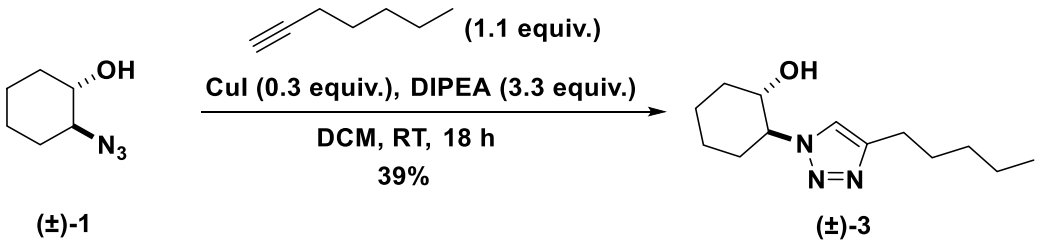

Scheme 3:4 Synthesis of 1,4-disubstituted triazole (±)-3 with CuI (DCM at RT).

Despite this poor yield, the successful recovery of both starting materials during the purification step, acted as a decent consolation prize. The presence of the residual starting materials indicated that the reaction either needed to run for a longer period or needed more heat energy (to increase the reaction rate) so that it would go to completion in the time period utilized. Since the reaction was already permitted to run for 18 hours; increasing the reaction time was deemed not to be a feasible option. However, adding additional heat energy into the system, by means of an increased reaction temperature, was a viable modification.

3.1.3.2.2. Second approach with copper(I) iodide (DCM at 40 °C)

The second set of reaction conditions investigated was the copper(I) iodide-catalyzed click reaction, still using dichloromethane as a solvent, but setting the reaction to a slightly elevated temperature of 40 °C (Scheme 3:5). By just increasing the temperature from room temperature to 40 °C, the reaction yield was significantly increased, as a yield of 83% was obtained under these conditions.

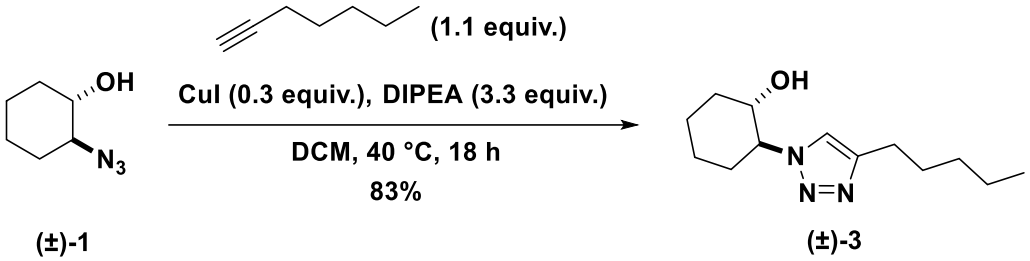

Scheme 3:5 Synthesis of 1,4-disubstituted triazole 3 with CuI (DCM at 40 °C).

Even though an acceptable yield was obtained during this attempt, a higher yield (88%) was obtained by Szafrański et al.,[121] even when working on a much larger scale. In a subsequent attempt at optimizing the CuAAC reaction for this system, a solvent with a higher boiling point (but still compatible with the copper(I) iodide-catalyzed click reaction) was investigated, allowing us to add even more heat energy into the system.

3.1.3.2.3. Third approach with copper(I) iodide (MeCN at 65 °C)

The third set of reaction conditions explored was to use copper(I) iodide with acetonitrile as solvent and setting the reaction to a temperature of 65 °C (Scheme 3:6). This option was considered after finding literature in which acetonitrile was used as a solvent with this copper source.[102,129] For this reaction a slight increase in the yield was observed in comparison to the previous conditions described, as a yield of 86% was obtained for product **(±)-3**.

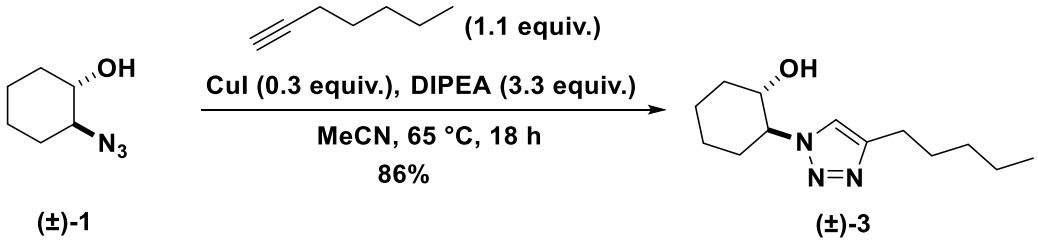

Scheme 3:6 Synthesis of 1,4-disubstituted triazole (±)-3 with CuI (MeCN at 65 °C).

Although good yields were obtained while using the copper(II) sulphate pentahydrate or the optimized copper(I) iodide-catalyzed conditions (described in the three different reactions above), both require the addition of an additive (whether it be a reducing agent or a stabilizing ligand). Furthermore, the copper(I) iodide-catalyzed reaction has the additional requirement in which the

reaction must be conducted in the dark (see Chapter 2 – Click Chemistry Introduction). Due to these drawbacks it was decided to investigate a third copper source.

3.1.3.3. CuAAC WITH COPPER(II) ACETATE

In the final method investigated for the synthesis of compound **(±)-3**, the 1,2-azido alcohol **(±)-1** was reacted with the chosen alkyne, 1-heptyne, along with copper(II) acetate at 30 °C (Scheme 3:7).[104] After standard work-up and purification by flash chromatography, the pure 1,4-disubstituted triazole **(±)-3** was obtained in a good yield of 89%.

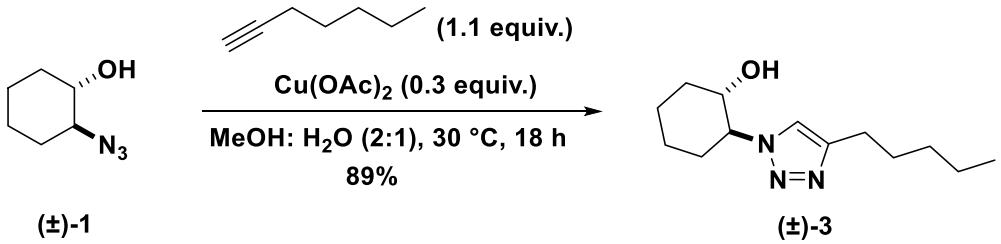

Scheme 3:7 Synthesis of 1,4-disubstituted triazole (±)-3 with $Cu(OAc)_2$.

Although optimum reaction conditions for all three copper sources were determined with acceptable yields (79% and above), the present set of reaction conditions had additional benefits. When using copper(II) acetate, no additional additives (for example reducing agents or basic compounds) were required (see Chapter 2 – Click Chemistry Introduction),[104] which in turn made the set-up and reaction work-up faster and less troublesome. Another benefit of this method, is the fact that a good yield (89%) was obtained even under a reaction temperature of 30 °C. The copper(II) acetate-catalyzed conditions would therefore be used for all the CuAAC reactions throughout this project. The assumption that these conditions will also be compatible with Scaffold B and C is valid as the azide and alkyne structures used in system B and C are relatively similar to that used for optimization in System A.

NMR spectra 5 and 6, found in Appendix 1, were used to characterize the 1,4-disubstituted triazole **(±)-3**. In the ^{1}H NMR spectrum, a signal was observed at 7.28 ppm which represented the proton attached to the unsubstituted carbon in the triazole ring. It was interesting to note that the triazole proton of **(±)-3** (with the pentyl side chain substituent) appeared more upfield in comparison with **(±)-2** (which contained the phenyl ring substituent). This could be due to the lack of the phenyl ring current present in compound **(±)-2**. In addition, a multiplet was observed at 4.09 – 3.95 ppm which represented the two protons of the carbons attached to the hydroxyl group (H_1) and the nitrogen atom (H_2, newly formed triazole ring). In the ^{13}C NMR spectrum of **(±)-3**, the substituted carbon atom of the triazole ring was observed at the highest chemical shift value of 147.48 ppm. Furthermore, the unsubstituted carbon atom of the triazole ring could be seen at 120.55 ppm. The ^{13}C spectrum also contained two deshielded peaks at 72.41 ppm and 66.80 ppm, which corresponded to the carbons

adjacent to the hydroxyl group (C_1) and the nitrogen atom (C_2, newly formed triazole ring), respectively. All other proton and carbon atoms were accounted for, and the NMR spectroscopic data was consistent with values provided in literature.[121] This compound was further characterized with Mass Spectrum 2, located in Appendix 1. The mass spectroscopic analysis confirmed isolation of product **(±)-3,** as the result of 238.1920 amu corresponded favourably with the calculated value of 238.1919 amu.

The optimization attempts for the CuAAC reaction are summarized in Table 3:1 below. During all attempts, the alkyne was initially added to the active copper source and the mixture was left to stir to allow coordination of the alkyne (1.1 equiv., see Chapter 2 – Click Chemistry Introduction). This was followed by the addition of the azide (1.0 equiv.). In addition, the reaction time for all five attempts was held constant at 18 hours.

Table 3:1 Summary of CuAAC reaction conditions attempted with azide (±)-1, 1,2-azido alcohol, and the chosen alkyne, 1-heptyne, for the synthesis of the 1,4-disubsituted triazole (±)-3.

Attempts	Copper source (0.3 equiv.)	Additive	Solvent	Temp. (°C)	Yield (%)
1	$CuSO_4{\cdot}H_2O$	Sodium ascorbate	MeOH: H_2O (4:1)	30	79
2	CuI	DIPEA	DCM	RT	39
3	CuI	DIPEA	DCM	40	83
4	CuI	DIPEA	MeCN	65	86
5	$Cu(OAc)_2$	-	MeOH: H_2O (1:1)	30	89

The next step involved the synthesis of the 1,5-disubstituted triazole **(±)-4**. This compound contained the same pentyl side chain as shown for compound **(±)-3** (and also in the structure of CBD), but in a different position on the triazole ring.

3.1.4. SYNTHESIS OF (±)-*TRANS*-2-(5-PENTYL-1*H*-1,2,3-TRIAZOL-1-YL)CYCLOHEXAN-1-OL 4

Optimization of the ruthenium-catalyzed azide alkyne cycloaddition (RuAAC) reaction

In this reaction, the 1,2-azido alcohol **(±)-1** was reacted with the alkyne, 1-heptyne, along with a ruthenium catalyst to obtain the 1,5-disubstituted triazole **(±)-4**, exclusively (Scheme 3:8). Once again, we worked on the assumption that the 1,4-regioisomer was obtained under the CuAAC reaction and by comparing the NMR spectra it was clear that the product obtained under the RuAAC

reaction conditions was different than the product obtained above. The catalyst chosen for this reaction was chloro(pentamethylcyclopentadienyl)(cyclooctadiene)-ruthenium(II), Cp*RuCl(COD). The cyclooctadiene ligands of this catalyst are easier to displace than ligands of other applicable catalysts (see Chapter 2 - Click Chemistry Introduction for mechanism), which is why this catalyst is considered superior to other ruthenium catalysts.[110] The Cp*RuCl(COD) catalyst has also been shown to achieve successful coupling, with high yields and 100% regioselectivity, under milder reaction conditions compared to other pertinent catalysts.[110]

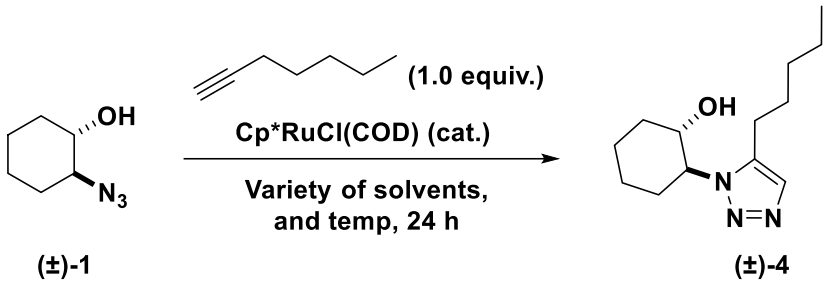

Scheme 3:8 Synthesis of 1,5-disubstituted triazole (±)-4.

Different solvents and temperatures were investigated in order to obtain the best possible yield for this specific system, as illustrated in Table 3:2. All three solvents investigated were shown to be compatible with the chosen catalyst, Cp*RuCl(COD).[110,130] During all of these attempts, the alkyne was added to the ruthenium catalyst solution in a Schlenk tube and the mixture was left to stir, to allow the coordination of the alkyne, 1-heptyne (1.0 equiv., see Chapter 2 - Click Chemistry Introduction). This was followed by the addition of the azide **(±)-1** (1.0 equiv.). In addition, all attempts were carried out with a reaction time of 24 hours. In order to make a viable comparison, all six attempts were also done at the same scale: azide, (±)-*trans*-2-azidocyclohexan-1-ol **(±)-1**: 200mg. Each method will once again be discussed, followed by the characterization of compound **(±)-4**.

Table 3:2 Summary of RuAAC reaction conditions attempted with azide (±)-1, (±)-*trans*-2-azidocyclohexan-1-ol, and the chosen alkyne, 1-heptyne, for the synthesis of the 1,5-disubsituted triazole (±)-4.

Attempt	Solvent	Solvent vol. (mL)	Cat. amount (mol%)	Degas method	Temperature (°C)	Yield (%)
1	THF	8	10	N_2[a]	50	36
2	Toluene	8	10	N_2[a]	80	39
3	Toluene	8	10	FPT[b]	80	51
4	Toluene	8	4	FPT[b]	80	51
5	Dioxane	8	4	FPT[b]	60	63
6	Dioxane	4	4	FPT[b]	60	57

a = Solvent was purged with nitrogen for 45 min as a degassing method.
b = Solvent was subjected to the freeze-pump-thaw technique in combination with nitrogen purging, as a degassing method.

In the first attempt, 8 mL of dry tetrahydrofuran was used along with 10 mol% of the chosen catalyst, Cp*RuCl(COD). The solvent was degassed by passing nitrogen gas through the reaction vessel for 45 minutes to provide an inert atmosphere and the reaction was set to 50 °C. Unfortunately, a low yield (36%) was obtained under these conditions due to the incomplete consumption of both starting materials (as seen on TLC). Despite of the low yield obtained in the first attempt for the desired 1,5-disubstituted triazole **(±)-4**, both unreacted starting materials were successfully recovered and subsequently used in further attempts.

It was then decided to change the reaction solvent to one with a higher boiling point, so that additional energy could be added into the system. This was done in the hopes that the reaction would be driven to completion by faster reaction kinetics. The second attempt therefore involved 8 mL of anhydrous toluene and the reaction was set to 80 °C, while keeping all other variables constant. This did however not make a significant difference to the yield as only 39% was obtained under these conditions, still owing to incomplete consumption of both starting materials. Even after successful recovery of the azide and alkyne fractions, the search for a procedure providing an acceptable conversion continued.

This led us to investigate the degassing method used, as certain common contaminants (for example water or molecular oxygen) present in the reaction vessel, might be deactivating the catalyst leaving behind the residual unreacted starting materials. As a result, the third attempt involved altering the degassing method from solely passing nitrogen through the reaction set-up to a combination of the freeze-pump-thaw (FPT) technique and nitrogen purging. All other variables were kept constant. In this case a more significant yield increase was observed, from 39% to 51%, confirming that nitrogen purging alone was not a sufficient degassing method. All future attempts were therefore conducted with the FPT degassing technique in combination with nitrogen purging.

After finding a set of conditions providing a yield above 50%, it was decided to investigate the amount of catalyst needed in this cycloaddition reaction. In the fourth attempt, the catalyst amount was thus decreased from 10 mol% to 4 mol%, while keeping all other variables constant. In a pleasing result, this had no influence on the yield and therefore all future RuAAC reactions were conducted with 4 mol% of the Cp*RuCl(COD) catalyst.

Once the catalyst amount was optimized to more economical and environmentally friendly proportions, we set out to further improve the yield for this cycloaddition reaction. During the fifth attempt, a third solvent, 1,4-dioxane, was investigated and the reaction temperature was set to 60 °C while keeping all other variables constant. We were pleased to obtain another significant increase in the reaction yield (from 51% to 63%), even when working at a lower reaction temperature than compared to the fourth attempt.

In a final attempt at optimizing the reaction conditions, we investigated the amount of solvent needed for this cycloaddition reaction to proceed at an acceptable yield. We therefore decreased the solvent volume from 8 mL to 4 mL in the sixth attempt to see what affect this would have on the yield. If the yield was not negatively influenced, we would have been able to decrease the amount of solvent used for this coupling reaction. Unfortunately, by implementing this final modification, the yield decreased from 63% to 57%.

As a result, it was decided to use the fifth attempt as our optimized reaction conditions for the RuAAC reaction throughout the rest of this project. The purification procedure involved when using 1,4-dioxane was also faster and easier compared to the other two solvents investigated, as no work-up step was required and the reaction residue could directly be loaded onto the column. This is possible as 1,4-dioxane is a fairly non-polar solvent and can therefore easily be eluted from the column by using a weak mobile phase, which would not affect the retention of the more polar triazole compounds.

NMR spectra 7 and 8, located in Appendix 1, were examined during the characterization of product **(±)-4**. Figure 3:1 contains the numbered structures of **(±)-3** and **(±)-4**. These atom numbers will be referred to during the NMR spectroscopy discussion of compound **(±)-4** below.

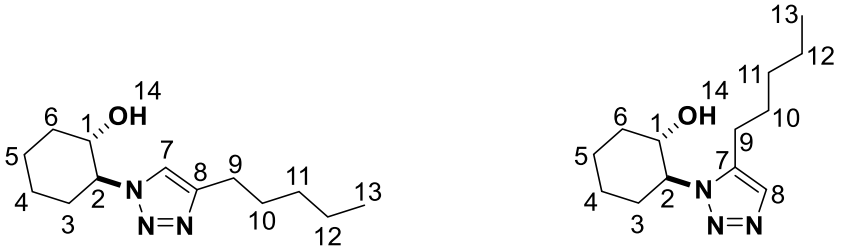

Figure 3:1 Numbered structure of the 1,4- and 1,5-disubstituted triazoles (±)-3 and (±)-4.

In the ^{1}H NMR spectrum of **(±)-4**, a singlet was observed at 7.39 ppm which represented the proton of the unsubstituted carbon atom in the triazole ring. A multiplet was also seen at 3.94 – 3.85 ppm assigned to the proton of the carbon attached to the hydroxyl group (H_1). Another multiplet integrating for three protons appeared at 2.72 – 2.54 ppm. This multiplet was assigned to the proton of the carbon attached to the nitrogen atom (H_2, newly formed triazole ring), as well as the two protons of the aliphatic carbon of the side chain directly attached to the triazole ring (H_9). The presence of these two separate multiplets in the spectrum of the 1,5-disubstituted triazole **(±)-4**, was fascinating, as the H_1 and H_2 protons were seen as an overlapping multiplet at 4.09 – 3.95 ppm in the spectrum for the 1,4-disubstituted triazole **(±)-3**. This separation was observed because of an upfield shift of the H_2 proton of the 1,5-disubstituted triazole **(±)-4**. The precise reason for this upfield shift cannot be provided with certainty, but the new position of the pentyl side chain is definitely the main aspect to consider. In the 1,5-disubstituted triazole **(±)-4**, the side chain was adjacent to the nitrogen atom

attached to the carbon of the proton under discussion (H_2). The conformation adopted by **(±)-4**, due to the new side chain position, might have altered the way in which the nitrogen lone pairs were able to interact, thus affecting the shift on the neighbouring carbon, C_2 (and the corresponding proton, H_2).

In the ^{13}C NMR spectrum of **(±)-4**, a peak was seen at 138.24 ppm which represented the substituted carbon atom of the triazole ring (C_7). The unsubstituted triazole carbon atom was also accounted for at 131.82 ppm (C_8). The carbon peak of C_7 appeared slightly more upfield, and that of C_8 appeared slightly more downfield in comparison to the spectrum of the 1,4-disubstituted triazole **(±)-3**. Note that the unsubstituted triazole carbon of the 1,4-disubstituted triazole analogue **(±)-3** was in close proximity to the cyclohexyl ring, but in the 1,5-disubstituted triazole analogue **(±)-4,** the unsubstituted triazole carbon is further away from the cyclohexyl ring. With this in mind, this observation could once again be attributed to the conformational change between the two triazole analogues (**(±)-3** and **(±)-4**) and the resulting effect on the nitrogen lone pairs. All other proton and carbon atoms were accounted for. Mass spectroscopic analysis further confirmed a successful reaction with the obtained result of 238.1921 amu corresponding well to the calculated value of 238.1919. This HRMS result can be seen in Mass Spectrum 3 in Appendix 1.

Although the synthesis of **(±)-4** was initially seen as a test reaction to determine the optimum reaction conditions for this regioselective cycloaddition reaction, it was considered of interest to compare the 1,4- and 1,5-disubstituted triazole compounds (**(±)-3** and **(±)-4**) to see what effect this side chain shift would entail.

After successful optimisation of the RuAAC reaction conditions, the chosen method could then be directly applied in the synthesis of the 1,4,5-trisubstituted triazole analogue **(±)-7**. The synthesis of the desired 1,4,5-trisubstituted triazole **7** involved the reaction of azide **1** with an internal alkyne, oct-2-yn-1-ol **5**, to provide a triazole analogue with an additional hydroxyl group at the core of the structure to mimic the phenolic hydroxyl group of CBD (Figure 3:2).

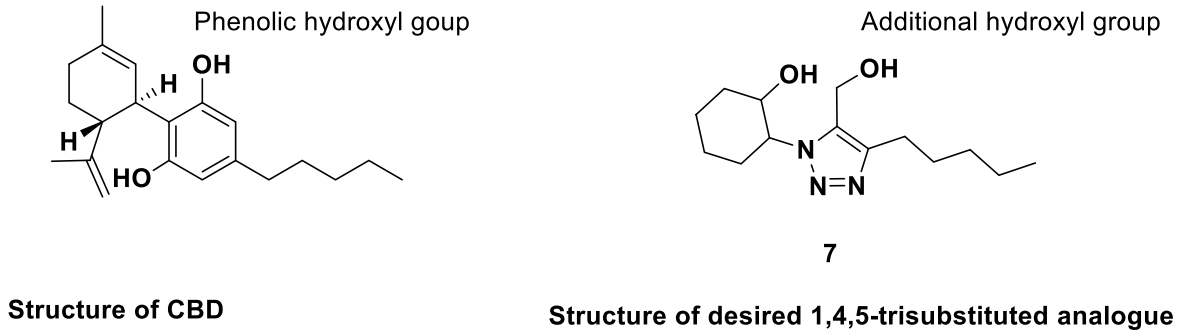

Figure 3:2 Comparison between CBD and 1,4,5-trisubstituted triazole (±)-7.

The next step was therefore to synthesize the desired internal alkyne, oct-2-yn-1-ol **5**, needed for the synthesis of the 1,4,5-trisubstituted triazole **(±)-7**.

3.1.5. SYNTHESIS OF INTERNAL ALKYNE, OCT-2-YN-1-OL 5

The synthesis of the internal alkyne **5** was accomplished by reacting 1-heptyne with *n*-butyllithium in dry tetrahydrofuran to form the corresponding lithium acetylide, which was subsequently reacted with paraformaldehyde (Scheme 3:9).[131,132] After work-up and purification by column chromatography, the desired propargyl alcohol **5** was isolated in a reasonable yield of 67%.

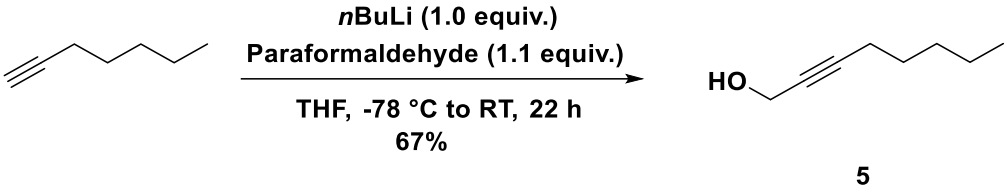

Scheme 3:9 Synthesis of the internal alkyne 5.

NMR spectra 9 and 10 (Appendix 1) were used to characterize this internal alkyne. In the ^{1}H NMR spectrum, a multiplet was observed at 4.24 ppm which represented the two protons in between the hydroxyl group and the triple bond. This multiplicity was unexpected; however, some splitting was also reported in literature which suggested possible long range coupling to the protons on the opposite side of the triple bond.[131] A broad multiplet could also be seen at 1.80 – 1.77 ppm which we assigned to the hydroxyl group. Although one would expect the hydroxyl group to appear at a higher chemical shift value, the shift for this functional group is known to vary; and a discrepancy can be seen between different literature reports on the exact position of the hydroxyl group of this particular compound, oct-2-yn-1-ol **5**.[131,133] In addition, both peaks seen at a higher chemical shift value (compared to the hydroxyl group) integrated for two protons each, and were therefore undoubtedly assigned to the four protons on either side of the triple bond.

In the ^{13}C NMR spectrum of **5**, two peaks could be seen at 86.73 ppm and 78.40 ppm, which represented the two carbon atoms of the triple bond, with the higher chemical shift peak resulting from the triple bond carbon closer to the hydroxyl group. Another significant peak was seen at 51.49 ppm, which corresponded to the carbon atom in between the triple bond and the hydroxyl group. All other relative nuclei were accounted for in the respective spectra. The NMR spectroscopic data corresponded to previously reported results.[131]

With the desired internal alkyne in hand, the synthesis of the 1,4,5-trisubstituted triazole **(±)-7** was attempted by making use of the optimized RuAAC reaction conditions.

3.1.6. SYNTHESIS OF (±)-*TRANS*-2-[4-(HYDROXYMETHYL)-5-PENTYL-1*H*-1,2,3-TRIAZOL-1-YL]CYCLOHEXAN-1-OL 6 AND (±)-*TRANS*-2-[5-(HYDROXYMETHYL)-4-PENTYL-1*H*-1,2,3-TRIAZOL-1-YL]CYCLOHEXAN-1-OL 7

For the synthesis of the desired 1,4,5-trisubstituted triazole **(±)-7,** the 1,2-azido alcohol **(±)-1** was reacted with the synthesized internal alkyne, oct-2-yn-1-ol **5,** under the optimized RuAAc reaction

conditions (8 mL of dioxane, 4 mol% of the Cp*RuCl(COD) catalyst, FPT degassing, 60 °C reaction temperature, Scheme 3:10).

When internal alkynes are used during these cycloaddition reactions, both regioisomers can be obtained. Exclusive regioselectivity is not usually observed with internal alkynes lacking a specific directing group. When some regioselectivity is exhibited by this type of internal alkyne, it could be attributed to either steric or electronic effects. However, when working with internal alkynes containing a hydrogen bond donor group (like a propargylic alcohol as found in the internal alkyne **5**) substantial regioselectivity is usually observed, which can be contributed to a hydrogen bond formation between the propargylic alcohol and the chloride ligand on the ruthenium catalyst (see Chapter 2 – Click Chemistry Introduction).[110]

As per the above explanation, we expected this reaction to yield compound **(±)-7** as the major product along with compound **(±)-6** as the minor product. However, in our hands, this was not the case. Contrary to our expectations, no regioselectivity was observed, as both compounds **(±)-6** and **(±)-7** were isolated at a low yield of 6%.

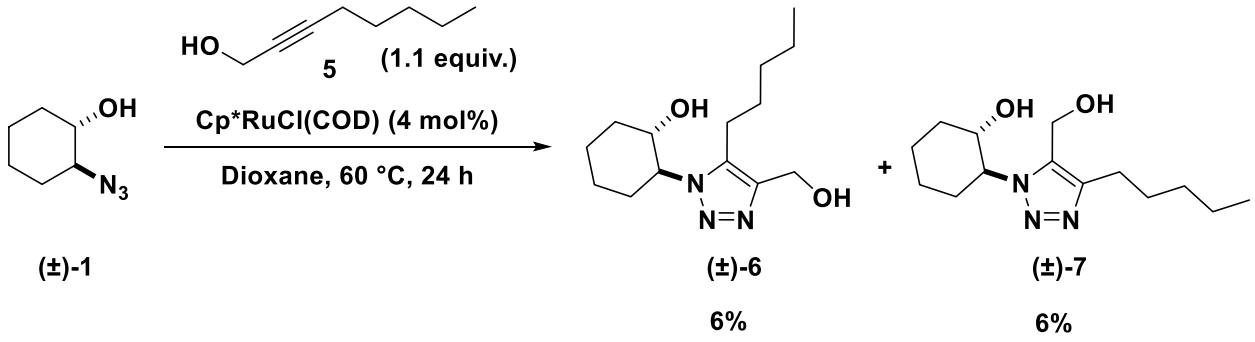

Scheme 3:10 Synthesis of 1,4,5-trisubstituted triazoles (±)-6 and (±)-7.

NMR spectra 11, 12, 13 and 14 (Appendix 1) were subsequently studied during the characterization of compounds **(±)-6** and **(±)-7**.

Note that these two compounds were tentatively assigned with the available ^{1}H and ^{13}C NMR spectra. For a more accurate assignment, or for confirmation of the assignment made in this report, two-dimensional NMR spectra must be obtained. The most important two-dimensional NMR spectroscopy experiments that must be conducted, are the homonuclear correlation spectroscopy (COSY) sequence, as well as the heteronuclear single-quantum correlation spectroscopy (HSQC) sequence. These two experiments will provide information on the proton-proton coupling between adjacent proton nuclei, as well as the proton-carbon coupling between directly attached proton and carbon nuclei, respectively. Additionally, the heteronuclear multiple bond correlation (HMBC) experiment could also be considered, as this would provide long range proton-carbon coupling information. These experiments were not conducted during the scope of this study. Distinct differences were observed between the ^{1}H and ^{13}C NMR spectra of **(±)-6** and **(±)-7,** which allowed

the characterization of these two compounds. These observed differences and the consequential assignments are discussed below.

The numbered structures of **(±)-6** and **(±)-7**, along with the relative pharmacophoric groups, are illustrated in Figure 3:3. These atom numbers and relative pharmacophoric groups will be referred to during the NMR spectroscopy discussion of compound **(±)-6** and **(±)-7** below.

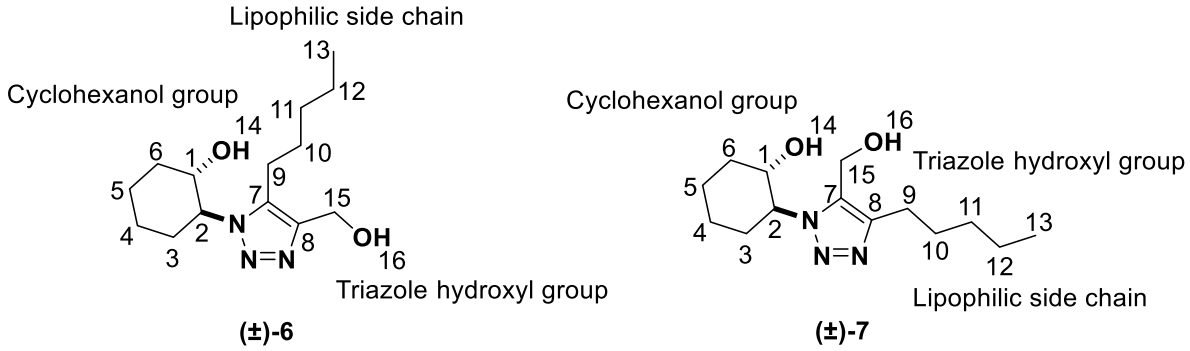

Figure 3:3 Numbered structure of two 1,4,5-trisubstituted triazoles (±)-6 and (±)-7, with the relative pharmacophoric groups.

In the ^{1}H NMR spectra, NMR spectrum 11 for compound **(±)-6** and NMR spectrum 13 for compound **(±)-7**, the cyclohexanol group could be seen as broad singlets at 4.43 and 4.30 ppm, respectively. The cyclohexanol group (H_{14}) of **(±)-7** might have appeared slightly more shielded due to the possibility of additional hydrogen bonding to the nearby triazole hydroxyl group.

The protons of the carbon in between the triazole ring and the triazole hydroxyl group (H_{15}), were observed as a singlet at 4.55 ppm for compound **(±)-6** (NMR Expansion 3:1A), and as an unexpected multiplet (or more accurately, overlapping geminal coupled doublets) at 4.62 – 4.48 ppm for compound **(±)-7** (NMR Expansion 3:1B).

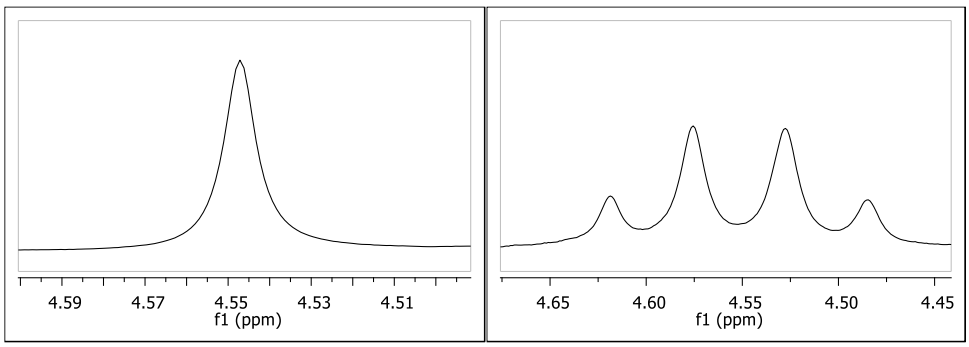

NMR Expansion 3:1 A: Singlet observed for H_{15} in spectra of (±)-6; B: Overlapping germinal doublets observed for H_{15} in spectra of (±)-7.

One would expect to see a singlet for H_{15} for both **(±)-6** and **(±)-7** with no additional coupling due to the absence of neighboring proton nuclei. When first considering the conformation of **(±)-6**, the

carbon atom of the protons under discussion (H_{15}), was positioned away from any other functional groups and could therefore not have any interactions that might have led to additional coupling. These two H_{15} protons of **(±)-6** also appeared chemically equivalent due to free rotation around the bond between C_8 and C_{15}, which appeared as a singlet integrating for two protons as one would expect to see. However, when considering the conformation of **(±)-7**, this same carbon atom attached to H_{15} was positioned more to the center of the structure, in a closer proximity to the cyclohexanol group (H_{14}). Although a definitive explanation for this observation in **(±)-7** could not be provided with the resources at hand, this multiplicity could be a result of an additional hydrogen bonding possibility between the cyclohexanol group (H_{14}) and the triazole hydroxyl group (H_{16}, which is adjacent to the carbon atom of the protons under discussion). It was thought that this possible interaction as well as the specific conformation illustrated for compound **(±)-7**, locks the two protons of H_{15} in chemically non-equivalent positions by restricting the free rotation around the bond between C_8 and C_{15}. This also enhances the diastereotopic effect of these two protons due to the nearby chiral center. Theoretically one would expect to observe geminal doublets; however, we reported this peak as a multiplet as the two doublets appeared overlapped. As already mentioned, two-dimensional NMR spectroscopic results must be obtained to confirm this theory. For both compounds **(±)-6** and **(±)-7**, these protons labeled as H_{15}, appeared at a higher chemical shift value than normally expected for methylene groups, due to the magnetic anisotropy caused by the adjacent triazole ring.

The triazole hydroxyl group was seen as a broad singlet at 5.82 ppm for compound **(±)-6** and as a broad singlet at 3.56 ppm for compound **(±)-7**. The difference observed in the chemical shift values was expected, as the conformation of **(±)-6** caused the triazole hydroxyl group to face away from the crowded core of the structure. This also excluded the possibility of hydrogen bonding between the cyclohexanol group and the triazole hydroxyl group. Both of these conformational traits of **(±)-6** caused the triazole hydroxyl group to appear more deshielded compared to the triazole hydroxyl group of **(±)-7**.

The proton of the carbon attached to the cyclohexanol (H_1) and the proton of the carbon attached to the nitrogen atom (H_2, new formed triazole ring) were seen as a multiplet at 4.10 – 3.95 ppm for compound **(±)-6**. However, for compound **(±)-7**, these two peaks were seen as separate multiplets at 4.23 – 4.15 ppm (H_2) and 3.88 – 3.80 ppm (H_1). H_1 of compound **(±)-7** might have appeared at a slightly lower chemical shift (more shielded) due to possible hydrogen bonding to the nearby triazole hydroxyl group. All other proton atoms were accounted for.

In the ^{13}C NMR spectra, NMR spectrum 12 for compound **(±)-6** and NMR spectrum 14 for compound **(±)-7**, the two carbon atoms that form part of the triazole ring (C_7 and C_8) were observed at 144.93 ppm and 133.37 ppm for compound **(±)-6** and only one aromatic peak was seen at 136.46 ppm for compound **(±)-7**. The absent peak in the spectrum of compound **(±)-7** could be due to an inadequate

acquisition time during the NMR spectroscopy experiment based on the concentration of this specific NMR spectroscopy sample. This is a problem often encountered for quaternary carbons with no protons attached. These carbon atoms (C_7 and C_8) are found at such high chemical shift values due to the deshielding effect caused by the magnetic anisotropy induced by the triazole ring.

The carbon in between the triazole ring and the triazole hydroxyl group (C_{15}) was observed at 51.42 ppm for compound **(±)-6** and 55.56 ppm for compound **(±)-7**. The deshielding effect observed for **(±)-7** may once again be a result of the additional hydrogen bonding possibility between the triazole hydroxyl group and the cyclohexanol group, as already explained. The carbon atom attached to the cyclohexanol group (C_1) and the carbon attached to the nitrogen atom (C_2, newly formed triazole ring) was observed at approximately 73 ppm and 64 ppm for both compound **(±)-6** and **(±)-7**. C_1 was assigned to the higher chemical shift value in both cases as a result of the electronegativity of the oxygen atom of the adjacent hydroxyl group, causing C_1 to be more deshielded. All other carbon atoms were accounted for. In addition, Mass Spectrum 4 (to be seen in Appendix 1), also confirmed the successful formation of the 1,4,5-trisubstituted triazoles as the mass spectroscopic value of 268.2037 amu corresponded well with the calculated value of 268.2025 amu.

The low yields obtained during this reaction were once again due to incomplete consumption of both starting materials, as determined by TLC. The poor yields obtained, even under a relatively long reaction time of 24 hours, indicated that this reaction was a slow process by nature. Although both starting materials were salvaged during the purification process, the yields obtained were not satisfactory, and the lack of regioselectivity meant that the desired compound could not be obtained as the major product under these conditions. Another possible explanation for this low yield might be the presence of two directing groups (the cyclohexanol group and the triazole hydroxyl group) which could have led to coordination to the catalyst thereby shutting down the catalytic cycle. Future attempts at this synthesis might therefore involve protection of the one hydroxyl group, preferably the cyclohexanol group, to prevent this coordination. It would be recommended to repeat this reaction and explore different options which could possibly provide an improved yield and selectivity.

Firstly, one would need to consider the reaction conditions and the changes that can be implemented to provide an improved yield. The solvent used, as well as the ideal solvent volume for this specific scale of 200 mg of the 1,2-azido alcohol **(±)-1**, has already been optimized. For this reason, it would not be advisory to alter these parameters. However, possible options for improving the yield could include increasing the amount of internal alkyne used, and either increasing the reaction time or the reaction temperature in an attempt to drive this reaction to completion. As the reaction was already allowed to run for 24 hours, adjusting the reaction temperature would once again be deemed to be the better option. The additional heat energy could drive this reaction to completion through faster reaction kinetics.

When considering the regioselectivity of this reaction, internal alkynes containing propargyl alcohols normally produce the desired isomer as the major product, with the propargyl alcohol in the 5-position on the 1,2,3-triazole ring, as already explained. However, for this specific system, this was not the case. This could possibly be explained by an additional interaction of the propargyl alcohol with the nearby cyclohexanol group. In order to address this lack of regioselectivity, two other internal alkynes will be discussed which could potentially provide the desired isomer as the major product.

The first option would be to synthesize an internal alkyne with a tertiary amine functionality in the propargylic position instead of the alcohol functionality used in **5**. This group is also known to promote the formation of the desired isomer with the propargyl substituent in the 5-position on the 1,2,3-triazole ring.[111,130] The amine functionality might have a different coordinating interaction with the nearby cyclohexanol group compared to the propargyl hydroxyl group, thereby resulting in a higher selectivity for the desired isomer. Making use of this internal alkyne would however require additional steps after the cycloaddition, in order to transform the amine functionality into the required hydroxyl group. This could be achieved by first converting the tertiary amine into a primary amine,[134] followed by a subsequent conversion into the primary alcohol[135] to obtained the desired triazole CBD analogue **(±)-7**. The general process proposed for the reaction with the propargyl amine alkyne is depicted in Scheme 3:11.

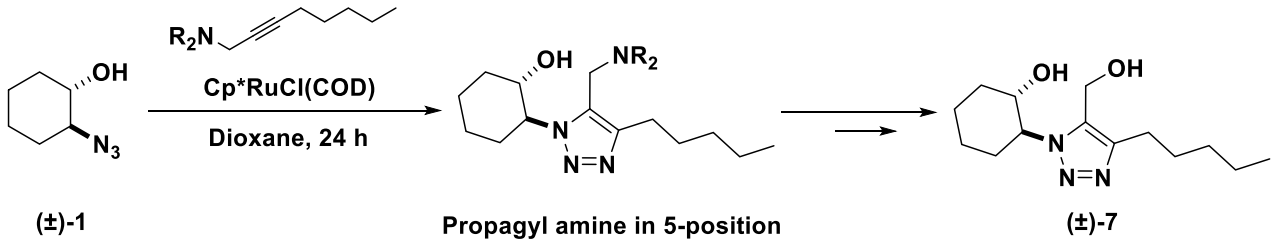

Scheme 3:11 First option to address the lack of regioselectivity (internal alkyne with a propargyl amine).

Another option would be to synthesize an internal alkyne with the required propargyl alcohol on the one side (as in compound **5**), along with an additional electron-withdrawing group on the other side of the triple bond. Internal alkynes with a strong electron-withdrawing group, for instance a carbonyl group, are known to produce the isomer with the electron-withdrawing group on the 4-position on the 1,2,3-triazole ring.[111,130] Keeping in mind that the propargyl alcohol usually favours the 5-position, this internal alkyne would then consist of two directing groups both favouring the formation of the preferred isomer, with the hydroxyl group in the 5-position on the 1,2,3-triazole ring. This option would however also require an additional step in which the carbonyl group must be subjected to a deoxygenation reaction to reduce the ketone functionality to the desired aliphatic side chain. This could be achieved through either a Clemmensen or a Wolff-Kishner reduction.[136]

The general scheme which would be involved when employing the internal alkyne containing an electron-withdrawing group (a ketone), as well as the propargyl alcohol on opposite sides of the triple bond, is illustrated in Scheme 3:12.

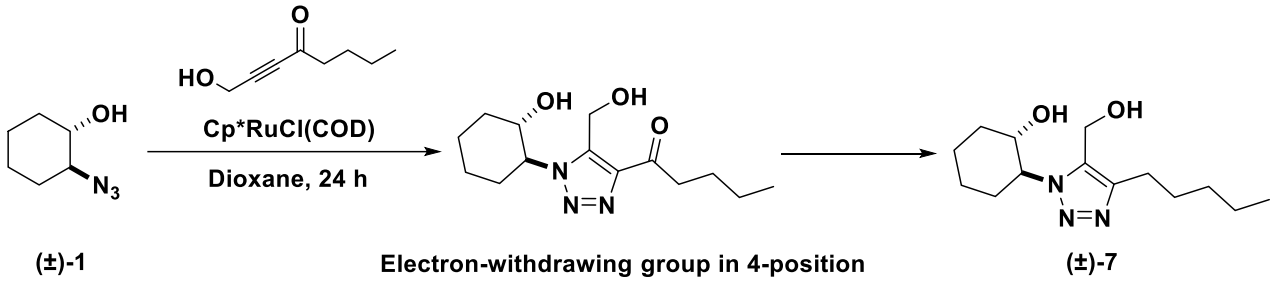

Scheme 3:12 Second option to address the lack of regioselectivity, using an internal alkyne with an electron-withdrawing group and a propargyl alcohol.

The yield and selectivity of this reaction was not further explored during the scope of this research as sufficient amounts of each regioisomer was isolated for biological tests. If larger amounts would be required in the future, this reaction will need to be studied in more detail, and the suggestions provided above could be used as initial attempts at optimization.

After the successful synthesis of the 1,4- ,1,5- and 1,4,5-polysubstituted triazole analogues aimed for in Scaffold A, the synthesis of Scaffold B (in which the cyclohexanol group occupied a new position) was investigated.

3.2. SYNTHESIS OF SCAFFOLD B

As illustrated in the ligand design for Scaffold B, these analogues consisted of the same three pharmacophoric groups as that of Scaffold A, but with the cyclohexanol group in a different position. The azide needed for the synthesis of the triazole analogues of this system, was 3-azidocyclohexan-1-one **11**. Initially, a synthetic route was designed in which this desired β-azido ketone **11** could be obtained in four steps.

3.2.1. ATTEMPTED SYNTHESIS OF AZIDE 11 IN FOUR STEPS

This four-step synthetic route, involved the epoxidation of an α,β-unsaturated ketone, 2-cyclohexen-1-one, to obtain the α,β-epoxyketone **8**, followed by a reductive cleavage to acquire the corresponding β-hydroxy ketone **9**. This β-hydroxy ketone **9** would then be subjected to a mesylation reaction yielding **10**, followed by a nucleophilic substitution reaction to finally access the desired β-azido ketone **11** (Scheme 3:13). Note that during the discussion of this system, the starting material, 2-cyclohexen-1-one, used for the synthesis of the β-azido ketone **11,** will be labeled as $\mathbf{11}_{SM}$.

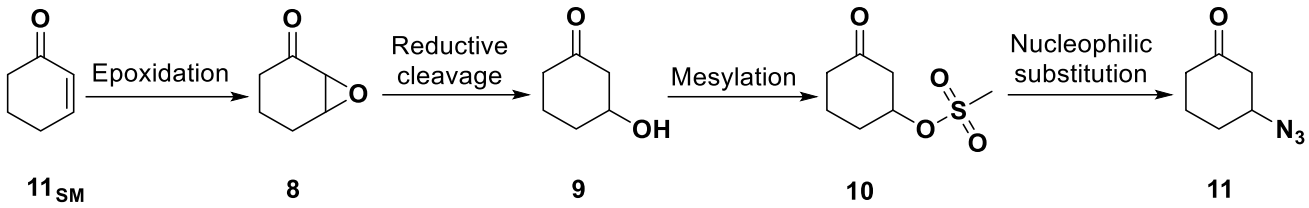

Scheme 3:13 General scheme for the four-step synthesis of azide 11.

Details of the reactions involved, as well as the results obtained for each of these steps are discussed in the sections to follow.

3.2.1.1. SYNTHESIS OF 2,3-EPOXYCYCLOHEXANONE, (7-OXABICYCLO[4.1.0]HEPTAN-2-ONE) 8

The first step involved in the attempted synthesis of the required azide **11**, was the Weitz-Scheffer epoxidation of an electrophilic α,β-unsaturated ketone to obtain the corresponding α,β-epoxyketone **8**. This transformation was achieved by reacting 2-cyclohexen-1-one (**11$_{SM}$**) with a hydrogen peroxide solution, in the presence of a catalytic amount of aqueous sodium hydroxide (Scheme 3:14).[137]

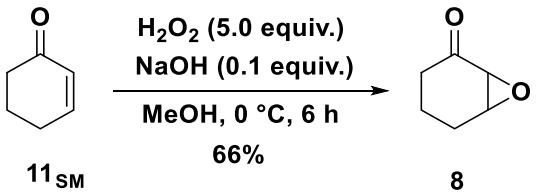

Scheme 3:14 Synthesis of α,β-epoxyketone 8.

The Weitz-Scheffer reaction is considered to be a reliable transformation, since the basic mechanism involved in the epoxidation of electrophilic α,β-unsaturated carbonyls was already published in 1921.[138] This epoxidation proceeded through a two-step addition-elimination mechanism (as determined through kinetic studies)[139] as depicted in Scheme 3:15. This process started with the addition of deprotonated hydrogen peroxide (in the presence of sodium hydroxide) to the β-carbon of the α,β-unsaturated ketone **11$_{SM}$**. This addition led to a β-peroxyenolate intermediate which subsequently underwent an intramolecular ring closure. During the intramolecular ring closure, a new carbon-oxygen bond was formed causing the weak oxygen-oxygen bond to break, during which the hydroxide ion acted as a leaving group.[140] After standard work-up and purification by column chromatography, the pure α,β-epoxyketone **8** was obtained in a yield of 66%.

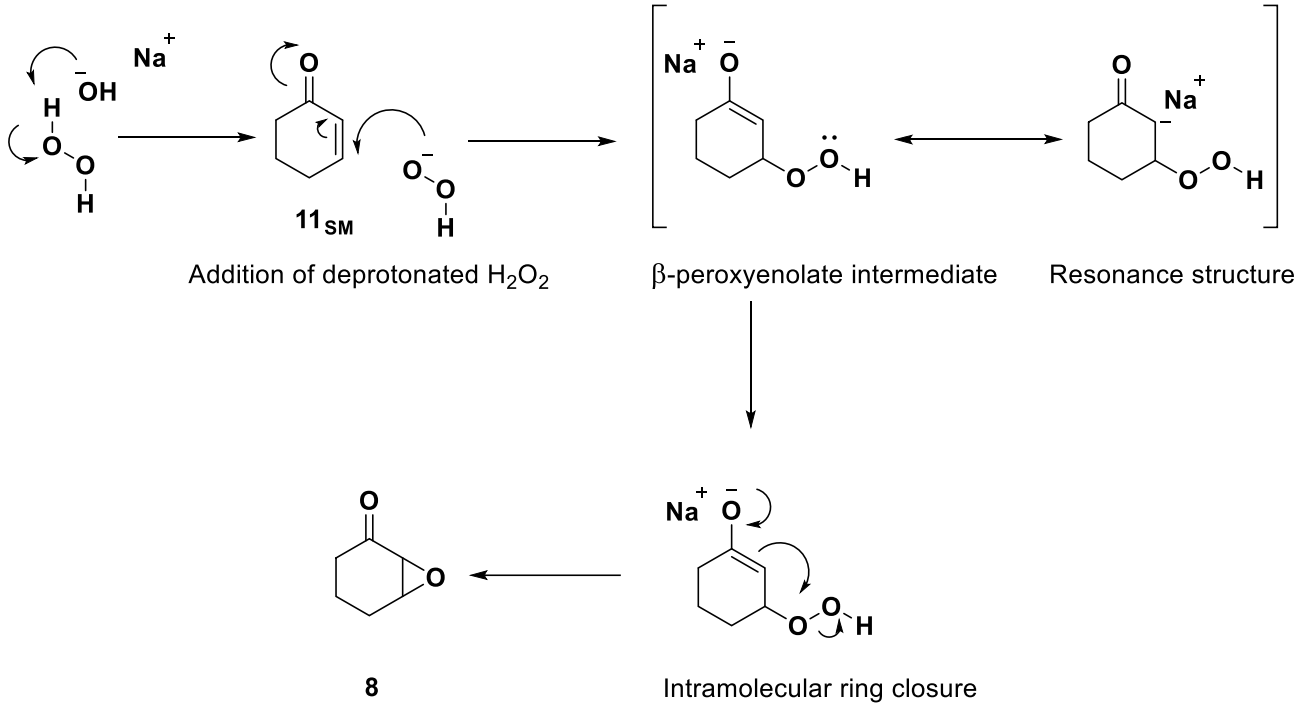

Scheme 3:15 Weitz-Scheffer epoxidation of the α,β-unsaturated ketone 11_{SM} to form the α,β-epoxyketone 8.

Characterization of product **8** was achieved by studying the NMR spectra 15 and 16, located in Appendix 1. In the ^{1}H NMR spectrum, a multiplet was observed at 3.53 – 3.50 ppm which represented the proton of the β-carbon (the epoxide carbon furthest away from the carbonyl functionality). Another noteworthy peak was seen as a doublet at 3.13 ppm which corresponded to the proton attached to the α-carbon (the epoxide carbon adjacent to the carbonyl group). In the ^{13}C NMR spectrum, a peak was observed at 205.85 ppm which indicated the presence of the carbonyl group. In addition, two peaks were seen in the region of 55 ppm which represented the two epoxide carbons. All other proton and carbon atom signals were accounted for and the NMR spectroscopic data was in accordance with literature.[140] The next step involved the conversion of the α,β-epoxyketone **8** into the corresponding β-hydroxy ketone **9**.

3.2.1.2. SYNTHESIS OF 3-HYDROXYCYCLOHEXAN-1-ONE 9

This transformation was achieved by subjecting the α,β-epoxyketone **8** to an organoselenium-mediated reductive cleavage, in which diphenyl diselenide was used along with an appropriate reducing agent (Scheme 3:16).[140]

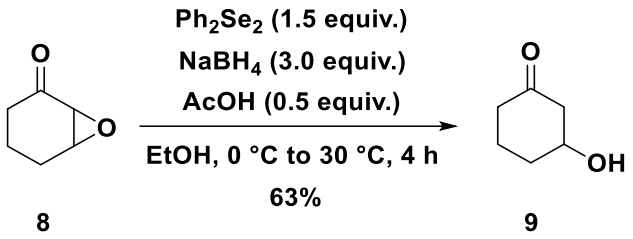

Scheme 3:16 Organoselenium-mediated reductive cleavage for the synthesis of the β-hydroxy ketone 9.

Note that the desired product of this reductive cleavage, the β-hydroxy ketone **9**, consisted of an Aldol structural unit, which means that there was a possibility for the retro-aldol reaction to occur.[141] The general mechanism for the retro-aldol reaction is shown in Scheme 3:17. This unwanted side reaction, would cause a carbon-carbon bond to break (between the α- and β-carbon), normally resulting in two separate molecules, one with an aldehyde functionality (resulting from the hydroxyl fraction) and one with a ketone functionality.

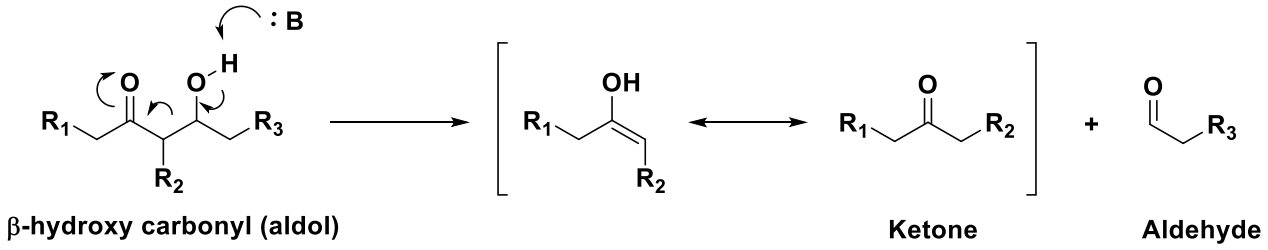

Scheme 3:17 General scheme for the retro-aldol reaction.

However, with the cyclic structure of the β-hydroxy ketone **9**, two separate fractions would not be obtained under the retro-aldol reaction, but rather an open chain structure with a ketone on the one side and an aldehyde on the other, as illustrated in Scheme 3:18.

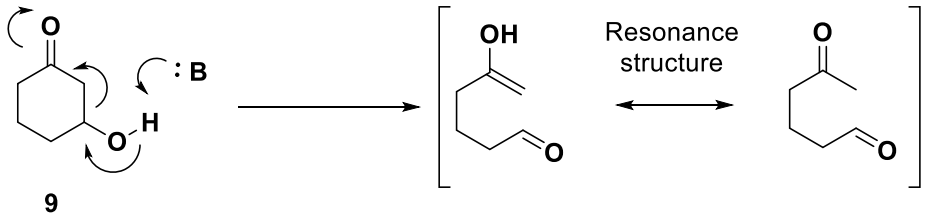

Scheme 3:18 Possible outcome of the unwanted retro-aldol reaction for the β-hydroxy ketone 9.

With this in mind, acetic acid was included with the previously mentioned reagents to suppress this unwanted retro-aldol reaction.[142]

Yoshikoshi and co-workers reported a possible mechanism for this organoselenium-mediated reductive cleavage; however, additional reports were also consulted for the specifics involved.[142–145] Scheme 3:19 depicts this mechanism for the specific system under discussion. The first step involved the *in situ* generation of a phenyl selenium anion, as a phenyl selenyl/borane complex

$Na^+[(PhSe)BH_3]^-$, simplified to $PhSe^-$ in the mechanism shown. The phenyl selenium anion was obtained by reducing diphenyl diselenide (PhSeSePH) with sodium borohydride. The resulting phenyl selenium anion ($PhSe^-$) then participated in a nucleophilic substitution at the α-carbon of the α,β-epoxyketone **8,** to provide the corresponding β-hydroxy selenide. This was followed by a subsequent nucleophilic attack of the second phenyl selenium anion ($PhSe^-$) onto the selenium atom found on this β-hydroxy selenide. This led to the formation of the β-hydroxy enolate which readily converted into the more stable β-hydroxy ketone resonance structure **9**.[142]

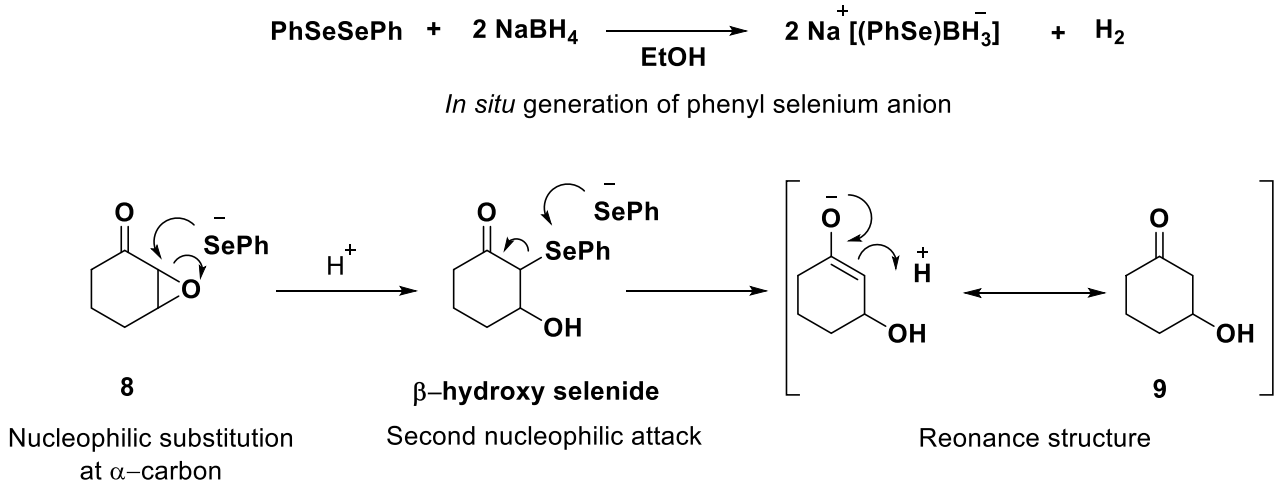

Scheme 3:19 A possible mechanism for the reductive cleavage which yielded the β-hydroxy ketone 9.[142]

After standard work-up and purification by column chromatography, the β-hydroxy ketone **9** was obtained in a yield of 63%, along with the regenerated diphenyl diselenide (PhSeSePH) which was recovered in a yield of 90%. Literature has stated that the recovered diphenyl diselenide (PhSeSePH) could be reused in future reactions;[142] however, this has not been tested during the scope of this project. Under these conditions, only the desired product **9** was obtained, no enones (α,β-unsaturated ketones) or selenenylated ketone derivatives were observed as by-products. In addition, the unwanted retro-aldol product was also not observed.

NMR spectra 17 and 18, located in Appendix 1 were used to characterize product **9**. In the ^1H NMR spectrum, a multiplet was observed at 4.18 – 4.10 ppm which represented the proton on the carbon attached to the hydroxyl group. This deshielding effect was due to the electronegativity of the attached oxygen atom. Compared to the spectrum of the corresponding α,β-epoxideketone **8,** this proton appeared more downfield, as would be expected. The α,β-epoxideketone **8** is a conformationally rigid system, and even though it was also attached to an oxygen atom, the deshielding effect was less due to the added ring strain. In addition, a broad singlet was observed at 3.09 ppm which corresponded to the proton of the hydroxyl group. In the ^{13}C NMR spectrum, the carbonyl peak was observed at 210.75 ppm and the carbon atom attached to the hydroxyl group was observed at 69.68 ppm. The carbon adjacent to the hydroxyl group also appeared more

downfield compared to the spectrum of the corresponding α,β-epoxideketone **8**, which was once again attributed to the ring strain of the epoxide moiety. All other proton and carbon peaks were accounted for, and NMR spectroscopic data was consisted with the values provided in literature.[146]

In the next step we attempted the conversion of the β-hydroxy ketone **9** into the corresponding methanesulfonate derivative **10**.

3.2.1.3. ATTEMPTED SYNTHESIS OF 3-OXOCYCLOHEXYL METHANESULFONATE 10

The β-hydroxy ketone **9** was reacted with methanesulfonyl chloride along with triethylamine in the hopes of obtaining the corresponding electrophilic derivative **10** through a mesylation reaction, as illustrated in Scheme 3:20.[147]

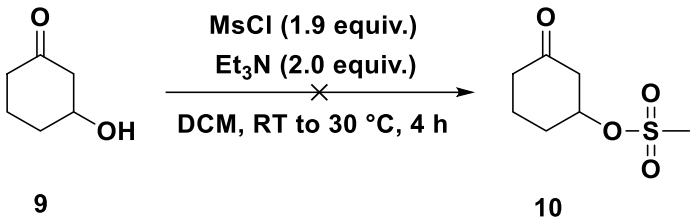

Scheme 3:20 Attempted mesylation reaction to obtain 10.

Before standard work-up procedures were performed, TLC indicated a complete conversion of the β-hydroxy ketone **9** into a less polar compound. This outcome was expected, as the desired methanesulfonate derivative **10** would be less polar than the β-hydroxy ketone **9**. In spite of this observation, neither the β-hydroxy ketone **9** nor the methanesulfonate derivative **10**, or any other side-products were present in the flask after work-up and concentration under high vacuum. Although this baffled us initially, it was believed that the structure of the methanesulfonate derivative **10** caused this compound to be highly volatile. If this was the case, then the formed product, as indicated by TLC could have been vaporized during the use of the rotary evaporator in combination with the high vacuum pump under concentration of the reaction residue. However, another possibility is that the formed product was lost in the aqueous layer during the work-up procedure.

If the methanesulfonate derivative **10** were successfully isolated, the next step would have been a nucleophilic substitution reaction with sodium azide, during which the mesyl group would have acted as a leaving group to obtain the required β-azido ketone **11**. The introduction of a different leaving group instead of the mesyl group was briefly considered and possible alternatives to counteract this volatility problem included either a tosyl or a triflate group. However, after examining the four-step procedure designed for the synthesis of the required azide **11**, relatively low yields were obtained for the first two steps (66% for the epoxidation and 63% for the reductive cleavage). Furthermore, the mesylation attempted in the third step proved to be problematic as explained above. As a result, a literature search was conducted, and an alternative route was revealed in which the desired β-azido ketone **11** could be obtained in only one step.

3.2.2. SYNTHESIS OF AZIDE 11 IN ONE STEP

3.2.2.1. SYNTHESIS OF 3-AZIDOCYCLOHEXAN-1-ONE 11

In this section, the one step transformation of the α,β-unsaturated ketone, 2-cyclohexen-1-one (**11$_{SM}$**) into the β-azido ketone **11**, as illustrated in Scheme 3:21, will be discussed.

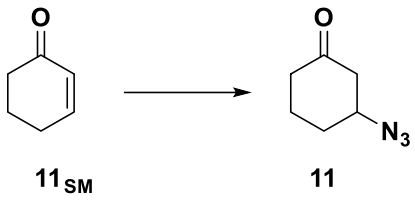

Scheme 3:21 General scheme for the synthesis of the β-azido ketone 11 in one step.

Three different methods were explored for this intermolecular conjugate addition, also known as an example of an aza-Micheal reaction. The reaction conditions and results obtained for these three methods will be discussed below, and the characterization of the β-azido ketone **11** will follow.

3.2.2.1.1. First attempted synthesis of 3-azidocyclohexan-1-one 11 (NaN_3)

The first procedure explored for this conversion, involved the reaction of 2-cyclohexen-1-one (**11$_{SM}$**) with sodium azide and acetic acid, in the presence of a Lewis base catalyst (Scheme 3:22).[148]

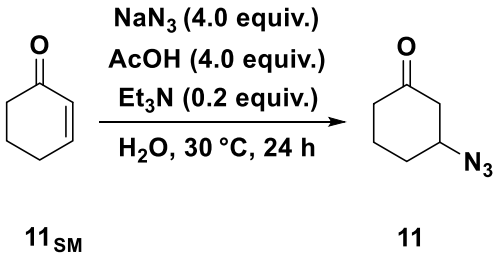

Scheme 3:22 First attempted synthesis of azide 11 with NaN_3.

An azide source frequently used for this transformation is hydrazoic acid (HN_3); however, HN_3 is known to be a highly toxic and explosive compound.[149] The present method therefore involved the *in situ* generation of HN_3 through a disproportionation reaction between glacial acetic acid and sodium azide, as reported by Zhou and co-workers.[148,150] The set-up of this reaction thus required the premixing of these two reagents, which generated the active hydrazoic acid nucleophile, HN_3, along with sodium acetate as by-product. Subsequent addition of the α,β-unsaturated ketone (**11$_{SM}$**), in the presence of a Lewis base catalyst, led to conjugate addition to form the β-azido ketone **11**.

The retention factor (R_f) values of the starting material, cyclohex-2-en-1-one (**11$_{SM}$**) and the desired product, 3-azidocyclohexan-1-one (**11**) were very similar, irrespective of the mobile phase used. This made it very difficult to say for certain whether all the starting material was being consumed during the course of the reaction. To compensate for this, the reaction time was significantly increased

compared to the prescribed literature time, but it could still not be said with certainty whether the reaction was complete. In literature, the pure azido ketone was obtained within 6 hours, without any further purification; but in our hands, some starting material was still present even after running the reaction for 24 hours. After experimenting with different TLC stains, as well as various stain combinations, we found that staining the TLC plate with 10% triphenylphosphine in dichloromethane, followed by immediate staining with ninhidrin, selectively indicated the presence of a compound containing an azide functionality.

After standard work-up and various purification attempts, the pure β-azido ketone **11** could unfortunately not be separated from the unreacted starting material, cyclohex-2-en-1-one (**11_{SM}**). The same reaction was also attempted with pyridine as base instead of triethylamine, as literature reported this to be a compatible catalyst for this reaction.[148] It was thought that the introduction of a bulkier base could help drive the reaction to completion, by positively influencing the activation of the unsaturated ketone. Unfortunately, the same problem was encountered as before.

By combing the literature, we found another procedure for this transformation which required trimethylsilyl azide ($TMSN_3$), along with a polystyrene-supported ammonium fluoride catalyst, namely Amberlite IRA900F.[151]

3.2.2.1.2. Second attempted synthesis of 3-azidocyclohexan-1-one 11 (Amberlite IRA900N_3)

The second attempt for this one step transformation, involved the *in situ* generation of a polymer-supported organocatalyst, Amberlite IRA900N_3, by reacting Amberlite IRA900F with $TMSN_3$ under solvent free conditions (Scheme 3:23).[151]

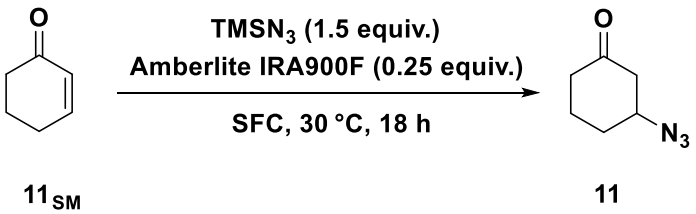

Scheme 3:23 Second attempted synthesis of azide 11 with Amberlite IRA900F and $TMSN_3$.

This procedure was reported by Vaccaro and co-workers in 2006, along with a possible mechanism.[151] This mechanism, as applied to the specific system under discussion, can be seen in Scheme 3:24. This process initially involved an exchange reaction between a polystyrene-supported ammonium fluoride (Amberlite IRA900F) and trimethylsilyl azide ($TMSN_3$) to form the corresponding Amberlite IRA900N_3 organocatalyst. Thereafter, the azido anion which formed part of this newly generated organocatalyst, acted as a Lewis base and coordinated to the silicon atom on a second $TMSN_3$ molecule. This resulted in a pentavalent azido-silicate species with a highly activated silicon-nitrogen bond capable of reacting with the α,β-unsaturated ketone (**11_{SM}**). After the conjugated

addition of the activated azide ion, the corresponding β-azido silyl enol ether derivative was obtained, which was readily converted into the more stable β-azido ketone **11**.

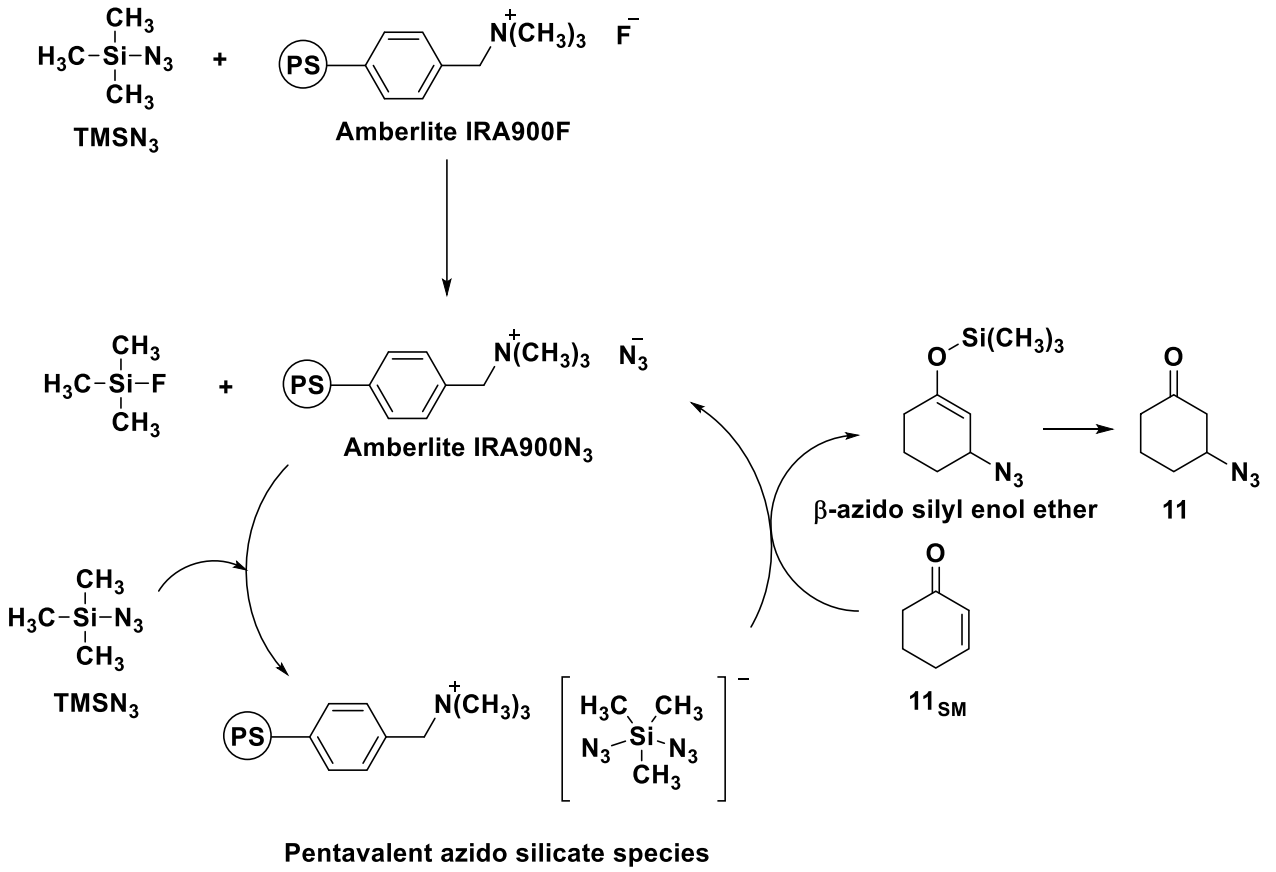

Scheme 3:24 Mechanism reported by Vaccaro and co-workers for the azidation of 11_{SM} with amberlite IRA900F and $TMSN_3$.[151]

The active catalyst in this reaction (Amberlite IRA900N_3), could be recovered and re-used (in up to five consecutive cycles) with no loss of efficiency.[151] However, this was not tested during the scope of this project.

To our dismay, this procedure led to the same problem as explained in the first attempted synthesis of the β-azido ketone **11**, in which residual starting material, the α,β-unsaturated ketone (**11_{SM}**), remained present even after a prolonged reaction time. When taking in to account the conversion and purification problems already explained, as well as the cost associated with the Amberlite IRA900F catalyst, a third procedure for this conversion was explored.

3.2.2.1.3. Third attempted synthesis of 3-azidocyclohexan-1-one 11 ($TMSN_3$)

The third attempt, based on a procedure published by Miller and co-workers, involved the reaction of the α,β-unsaturated ketone (**11_{SM}**) with equimolar amounts of trimethylsilyl azide ($TMSN_3$) and glacial acetic acid, in the presence of a tertiary amine catalyst (Scheme 3:25).[152] $TMSN_3$ is considered to be a safer azide transfer reagent compared to HN_3 and NaN_3.[153]

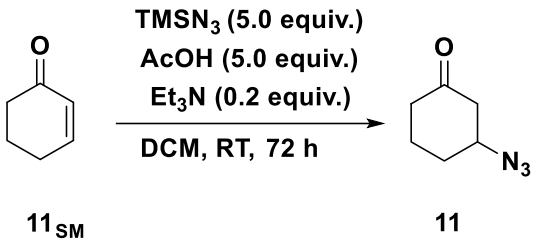

Scheme 3:25 Third attempt for the synthesis of azide 11 in one step with $TMSN_3$.

The reported mechanism[152] of this procedure is similar to that explained in section 3.2.2.1.1 for the first attempt at this transformation. This procedure also involved the *in situ* generation of HN_3 through a disproportionation reaction between glacial acetic acid and an azide source (in this case $TMSN_3$). The set-up of this reaction therefore also required the premixing of these two reagents to yield the active azide nucleophile, HN_3, along with trimethylsilyl acetate (TMSOAc) as byproduct. Subsequent addition of the *α,*β-unsaturated ketone **11_{SM}** in the presence of an amine catalyst, then led to conjugate addition to form the β-azido ketone **11**.

In literature, the crude reaction mixture was directly applied to a silica plug and eluted with a solution of Hexane: EtOAc, 55:45.[152] During various attempts to obtain the pure product, the solvent was removed by evaporation and the crude mixture was dry loaded onto a silica column. Purification was attempted with varying gradients of Hexane: EtOAc, 95:5 – 50:50. Even under these varied purification conditions, the same problem was encountered as in the first two attempts for this transformation. In a subsequent attempt, the reaction time was significantly increased (72 hours), but residual starting material was still detected. The desired product, azidocyclohexan-1-one **11**, could still not be separated from the unreacted starting material, cyclohex-2-en-1-one (**11_{SM}**).

Evaluation by way of NMR spectroscopy showed a 5:1 ratio of the product, 3-azidocyclohexan-1-one **11** to residual starting material, cyclohex-2-en-1-one (**11_{SM}**), under these conditions.

The same reaction was carried out at 30 °C (instead of room temperature) with a slightly higher equivalent of Et_3N (0.35 equiv.) and stirred for 24 hours (instead of 72 hours). We hoped that a slight increase in the temperature and in the amount of Lewis base used, would improve the conversion by driving the reaction to completion. Unfortunately, we obtained an even worse conversion, in which only a 2:1 ratio of product to unreacted starting material was observed (determined from NMR spectra). From these results it is clear that this is a very slow reaction. In our hands the temperature (note that we only attempted a slight increase) or catalyst amount did not significantly influence the conversion, but a long reaction time is a critical factor as the 5:1 ratio was obtained when running the reaction for 72 hours.

NMR spectra 19 and 20, found in Appendix 1, were used to characterize the β-azido ketone **11**. Note that the NMR spectra under discussion concerned the crude spectra of the 5:1 mixture of product **11** to the starting material **11$_{SM}$**.

11$_{SM}$ **11**

The noteworthy peaks which resulted due to the residual starting material (**11$_{SM}$**) will be discussed first for each spectrum, followed by the peaks for the desired product **11**.

In the ^{1}H NMR spectrum, a significant peak indicating the presence of the starting material **11$_{SM}$** was observed as a multiplet at 6.99 – 6.95 ppm. This peak represented the proton of the β-carbon (the alkene carbon furthest away from the carbonyl functionality). A second multiplet was observed at 6.01 – 5.97 ppm due to the proton attached to the α-carbon (the alkene carbon adjacent to the carbonyl group). Both of these protons were present at such high chemical shift values due to the anisotropy of the adjacent double bond. In the same ^{1}H NMR spectrum, a notable peak of the desired product **11** was observed as a multiplet at 3.90 – 3.84 ppm. This peak corresponded to the proton of the β-carbon attached to the nitrogen atom (of the azide moiety).[100] The chemical shift of the proton of the β-carbon moved more upfield compared to the spectrum of **11$_{SM}$**. This proton appeared slightly more shielded due to the absence of the double bond, but still at a relatively high chemical shift value due to the electronegativity of the attached nitrogen atom.

In the ^{13}C NMR spectrum, a peak of the starting material **11$_{SM}$** appeared at 199.78 ppm which represented the carbonyl carbon. In addition, two peaks were observed at 150.74 ppm and 129.97 ppm. These two peaks represented the β-carbon (the alkene carbon furthest away from the carbonyl functionality) and the α-carbon (the alkene carbon adjacent to the carbonyl group), respectively. In the same ^{13}C NMR spectrum, the carbonyl carbon of the desired product **11** was observed at 207.55 ppm. Another noteworthy peak of the desired product **11** was observed at 59.61 ppm. This peak corresponded to the β-carbon attached to the azide functionality.[100] This slight downfield shift observed for the carbonyl carbon peak was expected as the electron density around conjugated carbonyl carbon nuclei (as found in **11$_{SM}$**), are known to be more than the electron density around saturated carbonyl carbon nuclei (as found in **11**). This means that the conjugated carbonyl carbon nucleus (**11$_{SM}$**) would appear more upfield.[154] All other proton and carbon atoms for both **11$_{SM}$** and **11** were accounted for. The NMR spectroscopic data was also in accordance with previously reported spectra.[151,152]

The NMR spectroscopic results confirmed the successful formation of the β-azido ketone **11**; unfortunately, due to the purification problems encountered, the conversion from cyclohex-2-en-1-one (**11$_{SM}$**) into 3-azidocyclohexan-1-one **11** could not be quantified. It was therefore decided that the crude 3-azidocyclohexan-1-one **11** would be used directly in the next step. This was possible because the residual 2-cyclohexen-1-one (**11$_{SM}$**) would not interfere with the following step, as it had no functionalities that could be utilized in the click reaction.

3.2.3. SYNTHESIS OF 3-(4-PENTYL-1*H*-1,2,3-TRIAZOL-1-YL)CYCLOHEXAN-1-ONE 12

As mentioned above, the crude β-azido ketone **11** still containing residual *α,*β-unsaturated ketone **11$_{SM}$** was subsequently subjected to a copper-mediated click reaction to obtain the corresponding 1,4-disubstituted triazole **12**.

In a further attempt to quantify the conversion of the *α,*β-unsaturated ketone **11$_{SM}$** into the β-azido ketone **11**, two of the three azidation methods were subjected to the subsequent copper-mediated click reaction. The yields obtained for triazole **12** was therefore calculated over two steps, based on cyclohex-2-en-1-one **11$_{SM}$**. The two azidation methods chosen, were discussed in section 3.2.2.1.1 and 3.2.2.1.3. The method which involved the use of the organocatalyst (Amberlite IRA900F) was not explored further as this specific catalyst was a more expensive reagent than needed during the other two methods. Another disadvantage of the method utilizing Amberlite IRA900F, was the appearance of an additional spot (as observed by TLC) which indicated the formation of an unwanted side-product. The formation of additional side-products was not observed in the two methods chosen for further investigation.

The CuAAC conditions optimized for Scaffold A, as discussed in section 3.1.1.3, was used to obtain the 1,4-disubstituted triazole **12**. Seeing that the conditions for the CuAAC reaction following these two aza-Micheal reactions were identical, the yields obtained could therefore allow us to compare the two azidation procedures. The reaction conditions and results obtained during the synthesis of **12** with these two procedures will be discussed below, and the characterization of the 1,4-disubstituted 1,2,3-triazole **12** will follow.

3.2.3.1. FIRST SYNTHESIS OF 3-(4-PENTYL-1*H*-1,2,3-TRIAZOL-1-YL)CYCLOHEXAN-1-ONE 12

In the first method investigated for the synthesis of the 1,4-disubstituted triazole **12**, the *α,*β-unsaturated ketone **11$_{SM}$** was converted into the β-azido ketone **11** by using the sodium azide procedure described in section 3.2.2.1.1. The inseparable mixture was then reacted with the chosen alkyne, 1-heptyne, under the optimized copper-mediated click reaction conditions (copper(II) acetate, MeOH: H_2O in a 2:1 ratio, 30 °C, Scheme 3:26Scheme 3:26 First synthesis of the 1,4-disubstituted triazole 12, using sodium azide for the aza-Micheal reaction.). After standard work-up and purification by flash chromatography, the pure 1,4-disubstituted triazole **12** was obtained in a yield of 35%, based on cyclohex-2-en-1-one **11$_{SM}$**.

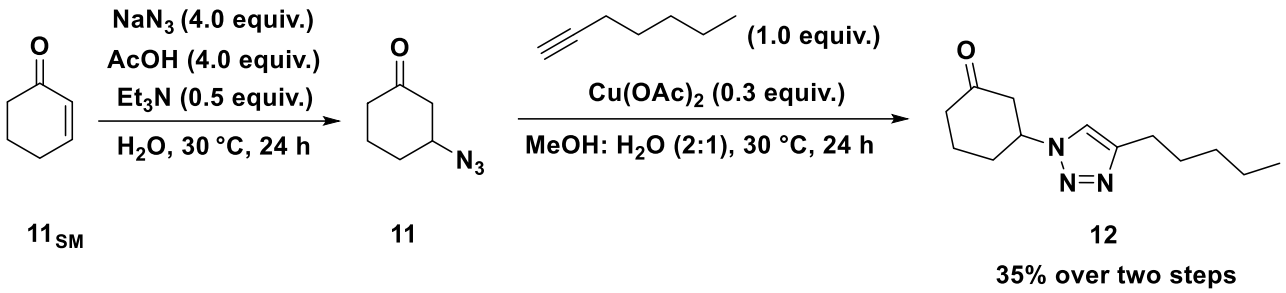

Scheme 3:26 First synthesis of the 1,4-disubstituted triazole 12, using sodium azide for the aza-Micheal reaction.

3.2.3.2. SECOND SYNTHESIS OF 3-(4-PENTYL-1*H*-1,2,3-TRIAZOL-1-YL)CYCLOHEXAN-1-ONE 12

In the second method investigated for the synthesis of the 1,4-disubstituted triazole **12**, the *α,*β-unsaturated ketone $\mathbf{11_{SM}}$ was converted into the β-azido ketone **11** by using the trimethylsilyl azide procedure described in section 3.2.2.1.3. The inseparable mixture was subsequently subjected to a CuAAC reaction with the chosen alkyne, 1-heptyne, under the optimized copper-mediated click reaction conditions (copper(II) acetate, MeOH: H_2O in a 2:1 ratio, 30 °C, Scheme 3:27). After standard work-up and purification by column chromatography, the pure 1,4-disubstituted triazole **12** was obtained in a slightly improved yield of 38%, based on cyclohex-2-en-1-one $\mathbf{11_{SM}}$.

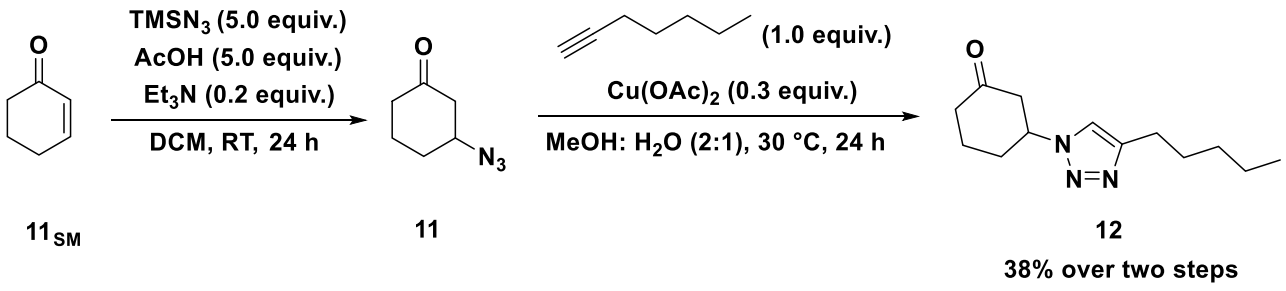

Scheme 3:27 Second synthesis of the 1,4-disubstituted triazole 12, using trimethylsilyl azide for the aza-Micheal reaction.

By comparing these two procedures, a slightly better yield was obtained when using trimethyl azide compared to the sodium azide method. It should be acknowledged that when working on such a small scale (cyclohex-2-en-1-one: 0.3 g), minor changes to the product mass could have a significant influence on the yield obtained. The product mass could have been influenced during various stages in the reaction, including the work-up and purification steps. When considering all of these factors, no definitive conclusion can be drawn regarding which one of these two methods were superior.

The characterization of **12** was achieved by studying the NMR spectra 21 and 22, located in Appendix 1.

In the ^{1}H NMR spectrum, a singlet was observed at 7.27 ppm, which represented the proton of the unsubstituted carbon of the triazole ring. In addition, a multiplet was seen at 4.83 – 4.73 ppm which

corresponded to the proton of the carbon attached to the nitrogen atom (of the newly formed triazole ring). This proton atom appeared more downfield compared to the spectrum of **11** (which contained the azide functionality). The higher chemical shift value observed for **12** could be a result of the magnetic anisotropy induced by the nearby triazole ring causing this proton in **12** to appear more deshielded. All other proton atoms were accounted for.

In the ^{13}C NMR spectrum, a peak was observed at 206.82 ppm which represented the carbonyl carbon. In addition, two peaks were seen at 148.58 ppm and 119.12 ppm, which were assigned to the two triazole carbon atoms, with the higher chemical shift value resulting from the substituted carbon in the triazole ring. Another noteworthy peak was observed at 58.74 ppm which represented the proton of the carbon attached to the nitrogen atom (of the newly formed triazole ring). This carbon appeared slightly downfield compared to the spectrum of **11** (which contained the azide functionality). The higher chemical shift value for **12** could once again be attributed to the magnetic anisotropy induced by the nearby triazole ring causing this carbon in **12** to appear more deshielded. All other carbon atoms were accounted for. Compound **12** was also characterized by examining Mass Spectrum 5 located in Appendix 1. The mass spectroscopic result of 236.1768 amu was in agreement with the calculated value of 236.1763 amu, further confirming the success of this reaction.

As previously explained, we assumed that the CuAAC reaction provided the 1,4-regioisomer due to substantial literature preference for this transformation. However, two-dimensional NMR spectroscopy experiments are recommended for future attempts at this synthesis, to confirm this assumption. With the 1,4-disubstituted triazole **12** in hand, sights were set on the synthesis of the 1,5-disubstituted triazole **13.**

3.2.4. SYNTHESIS OF 3-(5-PENTYL-1*H*-1,2,3-TRIAZOL-1-YL)CYCLOHEXAN-1-ONE 13

During the synthesis of the 1,5-disubstituted triazole **13**, the *α,*β-unsaturated ketone $\mathbf{11_{SM}}$ was converted into the β-azido ketone **11** by using the sodium azide procedure described in section 3.2.2.1.1. The two azidation procedures used during the synthesis of the 1,4-disubstituted triazole **12** provided similar yields, but this specific method was chosen because sodium azide is considered to be a safer and more stable azide source and was readily available.[153]

The inseparable mixture was subsequently reacted with the chosen alkyne, 1-heptyne, along with the Cp*RuCl(COD) catalyst under the optimized RuAAC reaction conditions, as discussed in Section 3.1.4. The route followed during the synthesis of the 1,5-disubstituted triazole **13** can be seen in Scheme 3:28. Working on the assumption that the CuAAC reaction provided the 1,4-regioisomer as mentioned above, the NMR spectra of the product obtained during the aforementioned reaction was compared to the spectra obtained during the RuAAC reaction. This allowed us to determine which of the two regioisomers was the major product in this reaction.

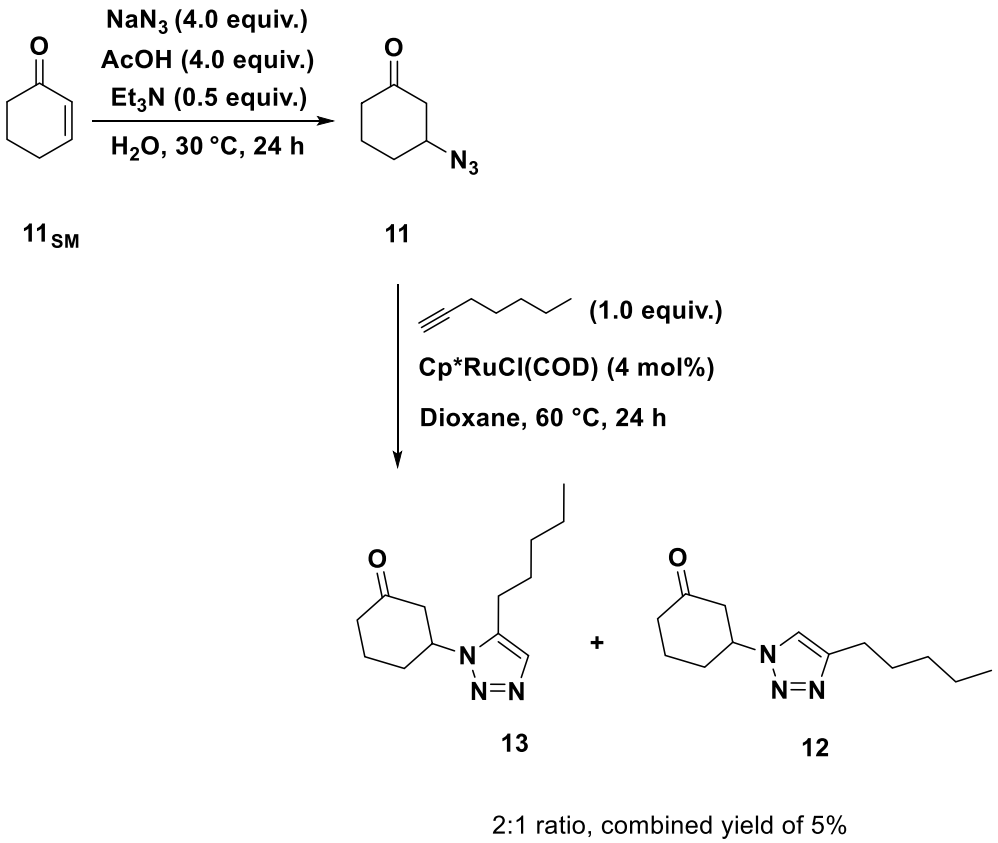

Scheme 3:28 Synthesis of the 1,5-disubstituted triazole 13.

When comparing the results from the CuAAC and RuAAC reactions in Scaffold A, much lower yields were obtained for the RuAAC reaction, as the highest yield obtained for Scaffold A was only 63%. With this in mind, the low yield of 35% obtained over two steps during the synthesis of the 1,4-disubstituted triazole **12** for Scaffold B under the CuAAC conditions, already suggested that the RuAAC reaction conditions would provide a very low yield for this system. When also taking into consideration the problems encountered during the conversion of the *α,*β-unsaturated ketone $\mathbf{11_{SM}}$ into the β-azido ketone **11** as already explained, a high yield was not predicted; however, the exclusive formation of the 1,5-disubstituted triazole **13** was expected.

After standard work-up and attempted purification by column chromatography, the pure 1,5-disubstituted triazole **13** could unfortunately not be successfully isolated. High-resolution mass spectrometry (HRMS) did however indicate the formation of a compound with the mass that was expected for **13**, see Mass Spectrum 6 in Appendix 1. The expected accurate mass calculated for $C_{13}H_{22}N_3O^+$ was 236.1763 amu and the spectroscopic value obtained for the $[M+H]^+$ ion was 236.1770 amu. During purification, 38% of the inseparable azide mixture was recovered which indicated a very low conversion into the desired triazole **13**. Note that this percentage recovered is an approximation as it was based on the theoretical yield for the β-azido ketone **11**. A more polar compound, which was represented by a single spot on the TLC plate, was subsequently isolated in a very low yield of 5%. Evaluation by way of NMR spectroscopy showed that this was a mixture of

the desired 1,5-disubstituted triazole **13** and the regioisomer 1,4-disubstituted triazole **12** in a 2:1 ratio, with compound **13** being the major product. This was definitely unexpected, as the 1,4-regioisomer was not detected in Scaffold A under the RuAAC conditions.

NMR spectra 23 and 24, found in Appendix 1, were used to characterize these two products **12** and **13**. The numbered structures of **12** and **13** are depicted in Figure 3:4. These atom numbers will be referred to during the NMR spectroscopy discussion below.

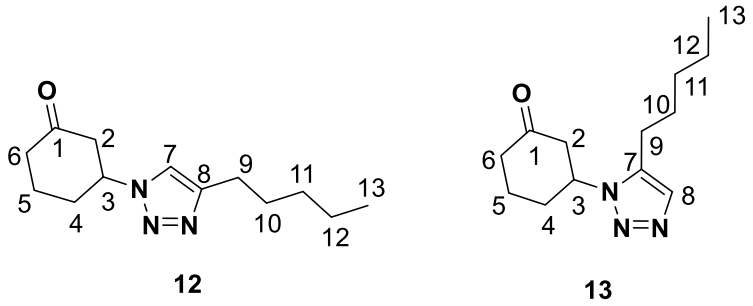

Figure 3:4 Numbered structure of the 1,4- and 1,5-disubstituted triazoles 12 and 13.

In the ^{1}H NMR spectrum, all the peaks that were previously assigned to **12** (as discussed in section 3.2.3.2.) were observed at the expected chemical shift values. All additional peaks corresponded to the 1,5-disubstituted triazole **13**. These peaks included a singlet at 7.45 ppm which represented the proton of the unsubstituted triazole carbon (H_8). This proton appeared slightly downfield compared to the proton of the unsubstituted carbon atom of the 1,4-disubstituted triazole **12**. A similar trend was observed between the 1,4- and 1,5-disubstituted triazoles of Scaffold A. Another noteworthy peak was observed as a multiplet at 4.52 – 4.42 ppm which represented the proton of the carbon attached to the nitrogen atom (of the triazole ring, H_3). This proton appeared more upfield when compared to the 1,4-disubstituted triazole **12**. A similar trend was also observed between the 1,4- and 1,5-disubstituted triazoles of Scaffold A. As previously explained for Scaffold A, the side chain of the 1,5-disubstituted triazole **13**, was adjacent to the nitrogen atom attached to the carbon of the proton under discussion. The conformation adopted by **13**, due to this specific side chain position, might have altered the way in which the nitrogen lone pairs were able to interact, thus affecting the shift on the neighbouring carbon (C_3) and the corresponding proton atom (H_3).

In the ^{13}C NMR spectrum, all 13 peaks assigned to the 1,4-disubstituted triazole **12** (as discussed in section 3.2.3.2.) were observed at the expected chemical shift values. All additional peaks observed corresponded to the structure of the 1,5-disubstituted triazole **13**. An important signal was observed at 207.16 ppm, which represented the carbonyl carbon (C_1) of **13**. Although the carbonyl carbons of **12** and **13** appeared at similar chemical shift values, a clear distinction could be seen between these two peaks. The two triazole carbons (C_7 and C_8) of **13** was observed at 136.46 and 132.12 ppm, with the highest chemical shift once again being assigned to the substituted triazole carbon (C_7). When

comparing the chemical shift of these two carbons to the corresponding carbon positions on **12**, C_7 moved more downfield and C_8 more upfield due to the side chain shift from C_8 to C_7 from **12** to **13**. A similar trend was observed between the 1,4- and 1,5-disubstituted triazole of Scaffold A. In addition, a significant shift was also observed for the carbon atom connected to the nitrogen atom (of the triazole ring, C_3) compared to compound **12**. C_3 was seen at 55.99 ppm for **13** and at 58.74 ppm for **12**. This upfield shift could once again be due to the specific position of the pentyl side chain and the resulting availability of the nitrogen lone pairs. For other minor chemical shift differences observed between these regioisomers, see Section 6.2.4.

As mentioned in Section 2.4.1., the main aim of the synthesis of this scaffold was to assess the effect of the hydroxyl position by comparing the 1,4-disubsituted triazole analogues of Scaffold A with those of Scaffold B. The 1,5-disubsituted triazole **13** was explored as an additional analogue, but the low yield and selectivity observed during this synthesis redirected our focus on completing the synthesis of the 1,4-disubsituted triazole CBD analogue.

The final reaction needed to complete the synthesis of Scaffold B, was a reduction in which the ketone functionality at the top of the cyclohexyl ring would be converted into a hydroxyl group.

3.2.5. SYNTHESIS OF 3-(4-PENTYL-1*H*-1,2,3-TRIAZOL-1-YL)CYCLOHEXAN-1-OL 14

For the synthesis of the desired triazole CBD analogue of Scaffold B, the 1,4-disubstituted triazole **12** was reacted with lithium aluminium hydride in tetrahydrofuran (Scheme 3:29).[155] After standard work-up and purification, the pure compound **14** was obtained in a yield of 88%.

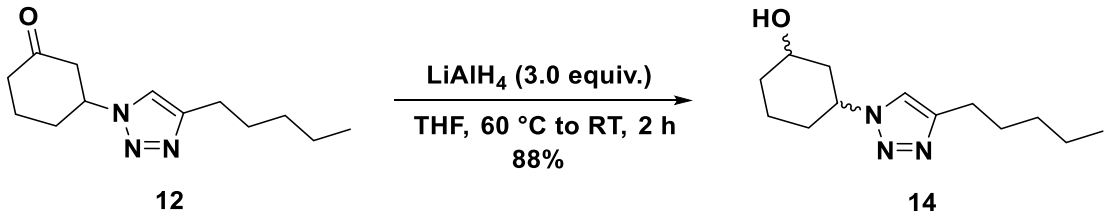

Scheme 3:29 Reduction to obtain the 1,4-disubtituted triazole CBD analogue 14.

NMR spectra 25 and 26, located in Appendix 1, were used to characterize the triazole CBD analogue **14**. In the ^{1}H NMR spectrum, a singlet was observed at 7.27 ppm which corresponded to the proton of the unsubstituted carbon atom of the triazole ring. The chemical shift of the proton is identical to that found in the spectrum of **12**. In addition, a multiplet was seen at 4.52 – 4.40 ppm which represented the proton of the carbon atom attached to the nitrogen atom (of the triazole ring). A second multiplet appeared at 3.86 – 3.73 ppm in the spectrum of **14** which was not present in the spectrum of **12**. This multiplet represented the proton atom of the carbon attached to the oxygen atom (newly formed hydroxyl group). In addition, the proton of the hydroxyl group was observed as part of in overlapping multiplet at 2.75 – 2.41 ppm.

In the ^{13}C NMR spectrum, two peaks were observed at 148.32 ppm and 118.39 ppm, which represented the substituted- and unsubstituted carbon atoms of the triazole ring, respectively. The carbon atom attached to the nitrogen atom (of the triazole ring) was also observed at 58.11 ppm. Compared to the spectrum of **12**, the disappearance of the carbonyl peak was a good indication that **14** was obtained successfully. In addition, a new peak was observed at 68.97 ppm, which represented the carbon attached to the oxygen atom (newly formed hydroxyl group). The ^{13}C NMR spectrum obtained after purification also suggested that the product obtain was not a mixture of diastereomers, but rather one diastereomer with its mirror image. Only slight traces of the other diastereomer was visible in the ^{13}C NMR spectrum. All other proton and carbon atoms were accounted for.

After successfully synthesizing the 1,4-disubstituted triazole **14** aimed for in Scaffold B (with the hydroxyl group in the same position as the methyl group on the structure of CBD), the synthesis of Scaffold C was investigated.

3.3. SYNTHESIS OF SCAFFOLD C

As explained in the ligand design of Scaffold C, three changes were made in this system compared to Scaffold A and B. These differences included the introduction of stereochemistry on the cyclohexyl ring, an additional isopropyl substituent, as well as a methyl group at the top of the cyclohexyl ring instead of the hydroxyl group. After searching for possible starting materials which would inherently consist of these main pharmacophoric groups, we came across (1*R*,2*S*,5*R*)-2-Isopropyl-5-methylcyclohexanol, (–)-menthol. Two different routes were then set out for this system to obtain two enantiomeric azides which could provide two different chiral triazole CBD analogues as depicted in Scheme 3:30. To obtain the one azide, the chosen starting material, (–)-menthol, would be subjected to a mesylation reaction to obtain the methanesulfonate derivative **15**. Compound **15** would then subsequently be transformed into the corresponding azide **16** through a nucleophilic substitution reaction. This nucleophilic substitution reaction would involve an inversion of the stereochemical configuration at the carbon connected to the azide moiety. To obtain the enantiomer of **16**, (–)-menthol would then be subjected to a double inversion strategy. This will involve an Appel reaction to obtain **17**, during which the first inversion would take place. Thereafter, a similar nucleophilic substitution reaction would be explored to convert **17** into the corresponding azide **18**, which would once again involve an inversion of configuration. It should be noted that the axial and equatorial orientations of these compounds were confirmed by Sankararaman and co-workers by means of single crystal XRD data.[156] Subjecting these two azides (**16** and **18**) to a CuAAC reaction with the chosen alkyne, 1-heptyne, would then provide two triazole analogues with opposite stereochemistry at the carbon attached to the triazole ring. Please note that the numbering used in the triazole

analogues of Scaffold C in the scheme below is based on the numbering of the corresponding azides. This was done to illustrate the different *R* and *S* conformations that will be obtained in the final analogues by using these diastereomeric azides.

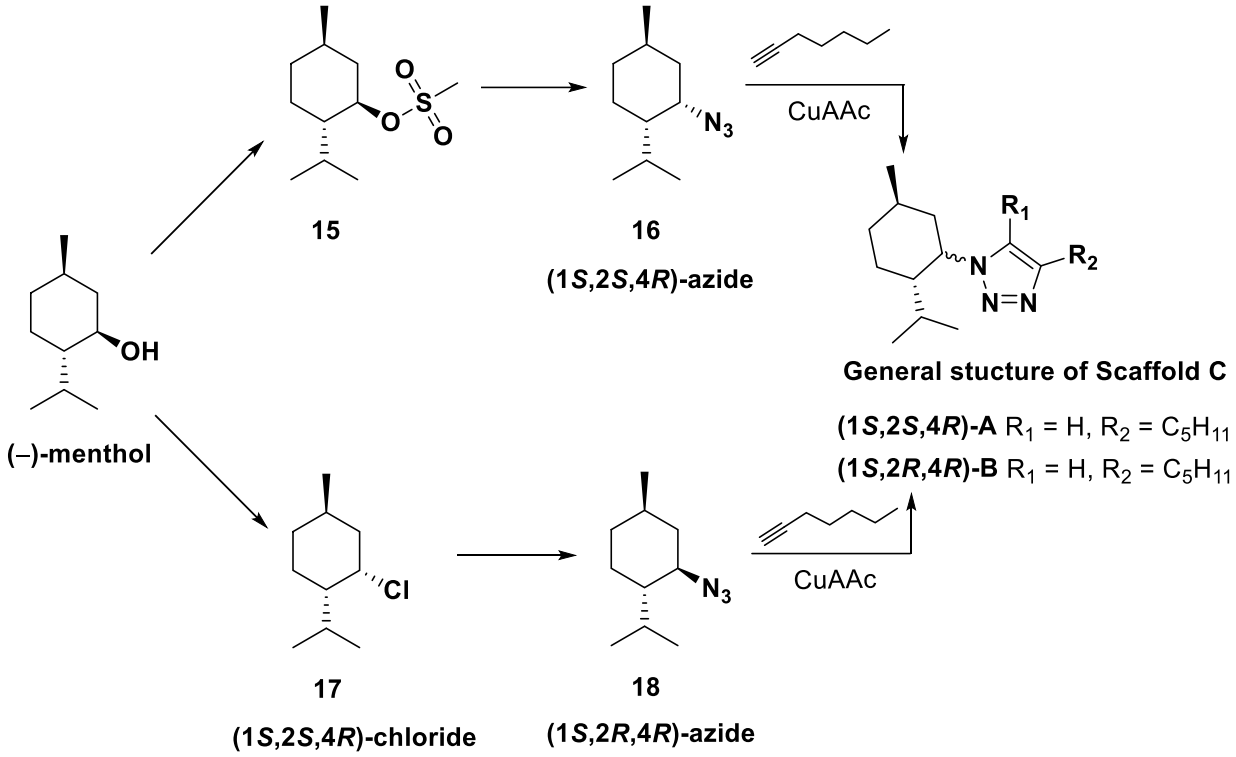

Scheme 3:30 The two routes set out for the synthesis of Scaffolds C.

The synthesis of compounds based on Scaffold C therefore started with the formation of the methanesulfonate derivative **15**.

3.3.1. SYNTHESIS OF (1*R*,2*S*,5*R*)-2-ISOPROPYL-5-METHYLCYCLOHEXYL METHANESULFONATE 15

The convenient starting material, (–)-menthol, was converted into the corresponding methanesulfonate derivative **15**, in the presence of methanesulfonyl chloride and triethylamine as illustrated in Scheme 3:31.[156] After standard work-up and purification by flash chromatography, the pure product **15** was obtained in a good yield of 89%.

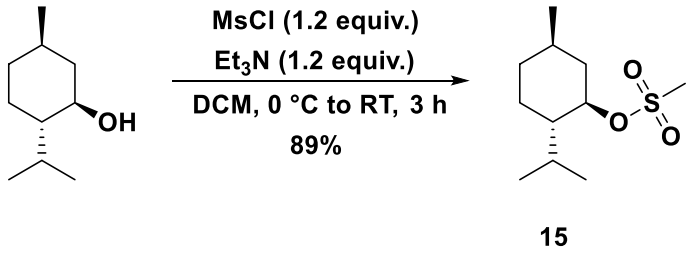

Scheme 3:31 Mesylation reaction to obtain 15.

NMR spectra 27 and 28, located in Appendix 1, were used to characterize this compound. The numbered structures and chair conformation, which will be referred to during the NMR spectroscopy discussion, is depicted in Figure 3:5. Please note that these atom numbers are different to the numbering used when naming this compound.

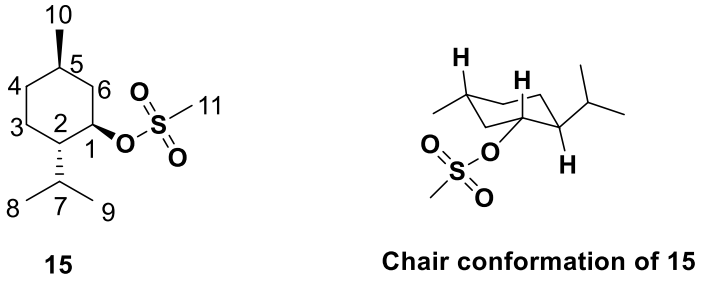

Figure 3:5 Numbered structure and chair conformation of 15.

In the ^{1}H NMR spectrum, a triplet of doublets, with coupling constant values of 10.9 Hz and 4.6 Hz, was observed at 4.55 ppm which represented the proton of the carbon adjacent to the methane sulfonate group (H_1). This splitting pattern was expected. When the chair conformation of this cyclohexyl ring was examined, the isopropyl group was in an equatorial position. It is well known that the most stable chair conformation is one in which the largest group adopts an equatorial position. This therefore also meant that both the methyl group and methanesulfonyl group were in an equatorial position in the chair conformation of **15**. When we considered the coupling to neighbouring proton nuclei, the axial proton under discussion (H_1) coupled to the axial proton of the carbon attached to the isopropyl group (H_2), as well as to the axial and equatorial protons of C_6. The coupling of the two adjacent axial protons resulted in a triplet. This coupling was also responsible for the larger coupling constant of the two values reported above. The adjacent equatorial proton on C_6, would then further split the triplet to form the triplet of doublets observed in this spectrum. This occurred because coupling between two axial protons are bigger than the coupling between an axial proton and an equatorial proton. Another noteworthy peak observed in the ^{1}H NMR spectrum, was a sharp singlet at 3.00 ppm which was due to the three protons of the methyl group introduced by the methane sulfonate functionality (H_{11}). In the ^{13}C NMR spectrum, a deshielded peak was seen at 83.55 ppm, which represented the carbon next to the methane sulfonate group (C_1). In addition, a peak was seen at 42.39 ppm which was assigned to the carbon of the methyl group introduced by the methane sulfonate functionality (C_{11}). Also note the presence of two separate peaks for the two methyl groups (C_8 an C_9) of the isopropyl substituent. Due to free rotation only one peak would be expected for these carbons; however, literature also reported two distinct peaks for this specific compound.[156] All other relevant nuclei were accounted for, and the NMR spectroscopic data was consistent with literature.[156]

The next step was converting this methanesulfonate derivative **15** into the corresponding azide **16**.

3.3.2. SYNTHESIS OF (1*S*,2*S*,4*R*)-2-AZIDO-1-ISOPROPYL-4-METHYLCYCLOHEXANE 16

The methanesulfonate derivative **15** was subsequently subjected to a nucleophilic substitution reaction with sodium azide to obtain the axial azide **16**, as can be seen in Scheme 3:32. During a nucleophilic substitution reaction on a carbon consisting of stereochemistry, the nucleophile will attack from the opposite side than the attached group. During this reaction, with the methane sulfonate group in the front, the azide nucleophile will attack from the back, thereby expelling the methane sulfonate group as the leaving group. As already mentioned, the inversion of stereochemistry observed under these specific conditions was confirmed by Sankararaman and co-workers.[156] Considering that the proton of the carbon adjacent to the methane sulfonate group is a diastereotopic proton, the stereochemistry of this proton will influence the chemical shift and multiplicity of this proton. By comparing the spectroscopic results with that published by Sankararaman and co-workers we confirmed that the inversion of stereochemistry did indeed occur. After standard work-up and purification by column chromatography the pure compound **16** was obtained in a yield of 41%.

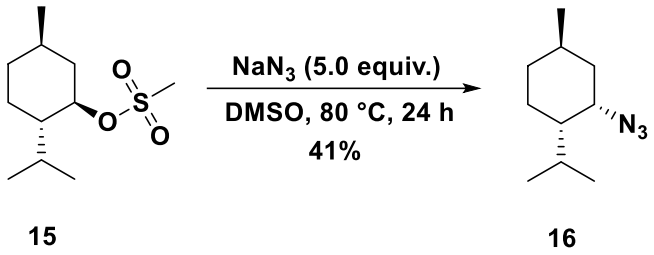

15 **16**

Scheme 3:32 Nucleophilic substitution reaction with sodium azide to obtain the axial azide 16.

Product **16** was characterized by studying the NMR spectra 29 and 30 as seen in Appendix 1. In the ^{1}H NMR spectrum, a multiplet was seen at 3.99 – 3.96 ppm which represented the proton of the carbon adjacent to the nitrogen atom of the azide functionality. Contrary to the ^{1}H spectrum of **15**, this peak appeared less resolved and was therefore assigned as a multiplet. It is interesting to note that this proton moved slightly upfield in comparison to the methanesulfonate derivative **15**. The disappearance of the singlet at 3.00 ppm, which corresponded to the three protons of the methyl of the methane sulfonate group in the spectrum of **15**, was also a good indication that the conversion was successful. In the ^{13}C NMR spectrum, a slightly deshielded peak was present at 60.69 ppm, which represented the carbon next to the nitrogen atom of the azide group. The chemical shift of this carbon shifted upfield by approximately 20 ppm during this azide substitution. Once again, note should be taken of the disappearance of the peak at 42.39 ppm, which corresponded to the carbon of the methyl of the methane sulfonate group in the spectrum of **15**. Based on examination of the ^{13}C NMR spectrum only the one diastereomer was obtained during this reaction. All other proton and carbon peaks were accounted for, and the NMR spectroscopic data was in agreement with previously reported spectra.[156]

With the (1*S*,2*S*,4*R*)-axial azide **16** in hand, the synthesis of the (1*S*,2*R*,4*R*)-equatorial azide **18** was explored. The first step of this endeavour involved an Appel reaction to obtain the axial chloride **17**.

3.3.3. SYNTHESIS OF (1*S*,2*S*,4*R*)-2-CHLORO-1-ISOPROPYL-4-METHYLCYCLOHEXANE 17

Treatment of (–)-menthol with triphenylphosphine and carbon tetrachloride (which also acted as the solvent for this reaction) gave the corresponding axial chloride **17** (Scheme 3:33).

This transformation once again involved an inversion of stereochemistry, as reported by Sankararaman and co-workers.[156] Upon completion of this reaction, the reaction mixture was cooled and the precipitated triphenylphosphine oxide was filtered off. The solvent was then removed under reduced pressure and the residue was purified by flash chromatography to obtain the pure axial chloride **17** in a yield of 45%.

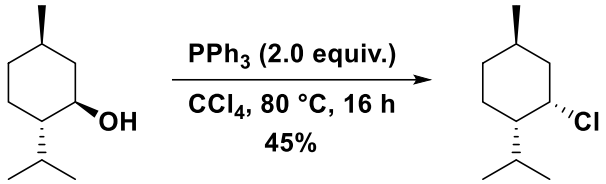

17

Scheme 3:33 Appel reaction to obtain the axial chloride 17.

The mechanism involved in this transformation as applied to this specific system is depicted in Scheme 3:34.[157,158] This mechanism firstly involved the formation of a phosphonium cation by reacting triphenylphosphine with carbon tetrachloride. Subsequent deprotonation of the alcohol functionality of the starting material ((–)-menthol) led to the formation of an alkoxide. The resulting alkoxide then participated in a nucleophilic displacement with the phosphonium cation during which a chloride anion then acted as a leaving group. The resulting oxyphosphonium intermediate then took part in a nucleophilic substitution reaction (S_N2) to produce the desired axial chloride **17**. During this reaction, the previously expelled chloride anion acted as the nucleophile and triphenylphosphine oxide was formed as by-product. Note that an inversion of configuration occurred during the nucleophilic substitution reaction and that the formation of the strong P=O double bond was the driving force behind this reaction.[157,158]

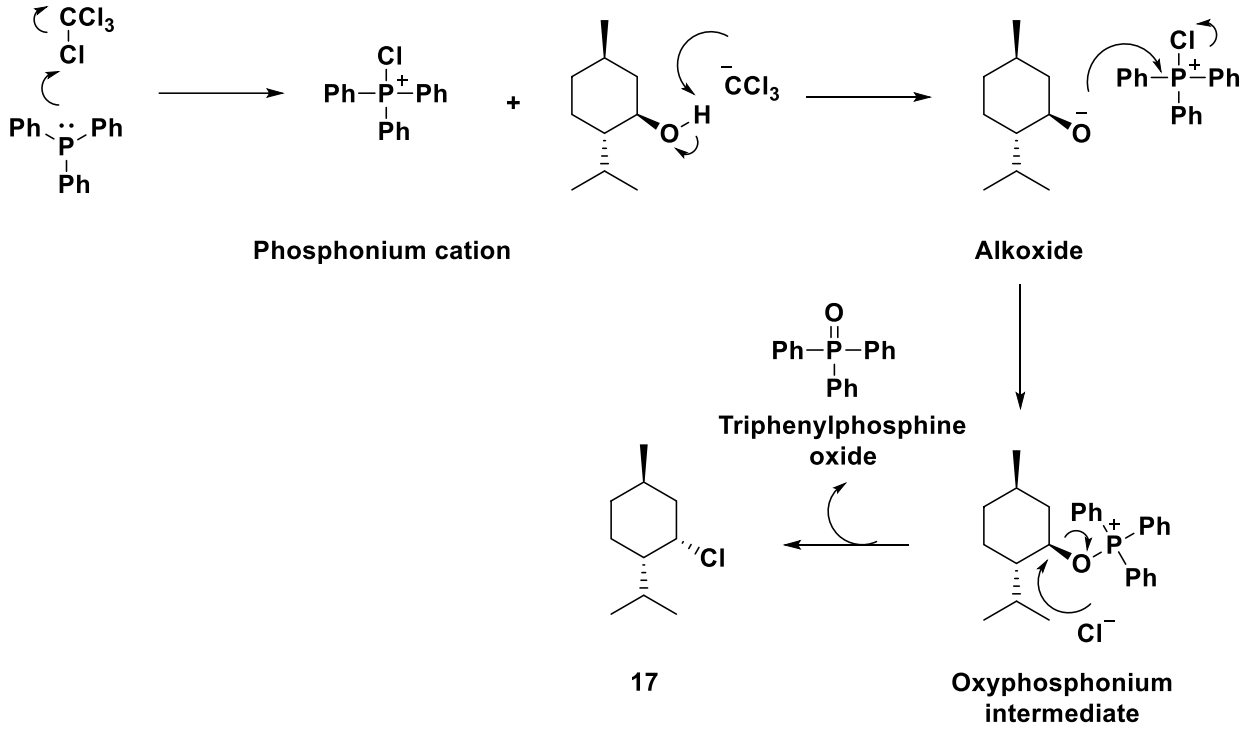

Scheme 3:34 Mechanism for Appel reaction applied to this specific system.[157,158]

NMR spectra 31 and 32, located in Appendix 1, were examined during the characterization of compound **17**. In the ^{1}H NMR spectrum, a multiplet was observed at 4.58 – 4.46 ppm which represented the proton of the carbon adjacent to the chloride atom. Furthermore, another multiplet was observed at 2.10 – 2.02 ppm which corresponded to the proton of the carbon attached to the isopropyl group. In the ^{13}C NMR spectrum, a slightly deshielded peak was seen at 63.58 ppm, which represented the carbon next to the chloride atom. In addition, two peaks appeared at 49.12 and 43.44 ppm, which corresponded to the carbon attached to the isopropyl group and the carbon in between the methyl substituent and the chloride substituent, respectively. As was the case for compound **15**, two separate peaks were seen for the two methyl groups of the isopropyl substituent on compound **17**. Literature did however also report two distinct peaks for this specific compound.[156]

All other proton and carbon atoms were noted, and the NMR spectroscopic data was in accordance with literature.[156]

The next step involved the attempted synthesis of the equatorial azide **18**, through a similar nucleophilic substitution that was used to obtain the axial azide **16**.

3.3.4. ATTEMPTED SYNTHESIS OF (1*S*,2*R*,4*R*)-2-AZIDO-1-ISOPROPYL-4-METHYLCYCLOHEXANE 18

The axial chloride **17** was subsequently reacted with sodium azide in dimethyl sulfoxide, as seen in Scheme 3:35. Unfortunately, the formation of the desired equatorial azide **18** was not observed under these conditions.

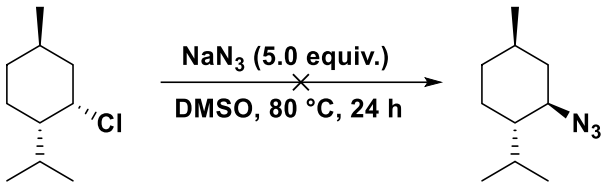

17 18

Scheme 3:35 Attempted synthesis of the equatorial azide 18.

The reaction conditions attempted for this conversion was identical to the conditions used during the S_N2 reaction to obtain the axial azide **16**. The only differences between this transformation and the successfully formed axial azide **16**, was the conformation of the carbon involved in the substitution reaction and the specific leaving group attached to this carbon atom. Although a chloride is considered to be a good leaving group, the approach of this S_N2 reaction might have been hindered by the specific conformation of compound **17**.

With these problems encountered during the synthesis of the equatorial azide **18**, and the time allocated to this project, it was decided to rather focus our attention on obtaining one of the triazole CBD analogues aimed for during the synthesis of Scaffold C. With one of these analogues in hand, biological results could indicate whether these compounds show any potential, and if continued investigation on this route would be recommended.

The final step for Scaffold C therefore involved a CuAAC reaction with the axial azide **16**.

3.3.5. SYNTHESIS OF 1-[(1*S*,2*S*,5*R*)-2-ISOPROPYL-5-METHYLCYCLOHEXYL]-4-PENTYL-1*H*-1,2,3-TRIAZOLE 19

The axial azide **16** was subsequently reacted with the chosen alkyne, 1-heptyne, under the optimized CuAAC reaction conditions as determined for Scaffold A (Scheme 3:36). As explained previously, it was assumed that the 1,4-regioisomer was obtained under the CuAAC reaction conditions due to overwhelming literature preference for this product; however, future two-dimensional NMR spectroscopy experiments are recommended for confirmation of this assumption. After standard work-up and purification by column chromatography, the pure 1,4-disubstituted triazole **19** was obtained in a rather disappointing yield of 21%.

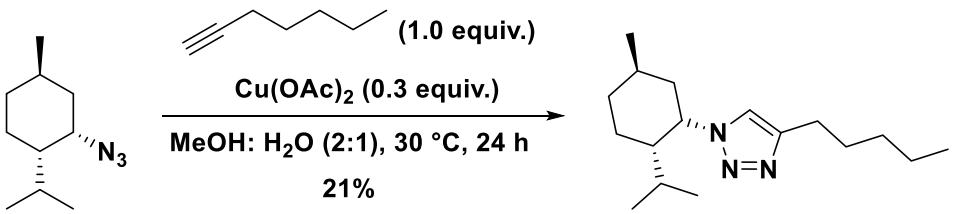

16 19

Scheme 3:36 CuAAC reaction to form the 1,4-disubstituted triazole 19.

This poor yield was once again due to incomplete consumption of both starting materials, which were successfully salvaged during the purification step. This low yield suggested that the optimised CuAAC reaction conditions, as based on the structures of Scaffold A, might not have been the ideal set of conditions for this system. Further optimization of the CuAAC reaction conditions for Scaffold C would therefore be recommended, but did not fall under the scope of this project due to a lack of time.

NMR spectra 33 and 34, located in Appendix 1, were used to characterize product **19**. In the ^{1}H NMR spectrum, a sharp singlet was observed in the aromatic region at 7.33 ppm which represented the proton of the unsubstituted carbon atom in the triazole ring. When comparing this spectrum to that of compounds **(±)-3** and **14**, the 1,4-disubstituted triazoles of Scaffold A and B, the chemical shift of this triazole ring proton appeared in a similar region. Furthermore, a multiplet was seen at 5.02 – 4.95 ppm which corresponded to the proton attached to the nitrogen atom (of the newly formed triazole ring). When comparing this spectrum to that of compound **16**, the corresponding azide, this peak shifted more downfield due to the ring current provided by the adjacent triazole ring.

In the ^{13}C NMR spectrum, one peak was observed at a high chemical shift value of 121.68 ppm. This peak represented the unsubstituted carbon atom of the triazole ring. When once again comparing this peak to the spectrum of compounds **(±)-3** and **14**, the 1,4-disubstituted triazoles of Scaffold A and B, the chemical shift of this unsubstituted carbon atom of the triazole ring was very similar. In the ^{13}C NMR spectrum, we would however expect to see another peak at an even higher chemical shift value corresponding to the substituted carbon atom of the triazole ring. The absence of this peak could once again be the result of an inadequate acquisition time during the NMR spectroscopy experiment based on the concentration of this specific NMR sample. A similar case was observed in the ^{13}C NMR spectrum of 1,4,5-disubstituted triazole **(±)-7** in Scaffold A, as this is a problem often encountered for quaternary carbons with no protons attached. Furthermore, in the ^{13}C NMR spectrum, a peak was seen at 58.97 ppm, which represented the carbon adjacent to the nitrogen atom (of the newly formed triazole ring). When comparing this spectrum to that of compound **16**, the corresponding azide, this peak shifted slightly downfield due to the ring current provided by the triazole ring. It was also interesting to note the two methyl groups of the isopropyl substituent of compound **19**. As already mentioned, although only one peak would be expected for these carbon atoms, two separate peaks were observed for all the precursors of this scaffold. The chemical shift values for these two carbon atoms were however much closer together than observed for compound **15** and **17**.

In addition, HRMS results also indicated the successful formation of this triazole CBD analogue **19**, see Mass Spectrum 7 in Appendix 1. The spectroscopic result obtained, 278.2600 amu, correlated well with the calculated value of 278.2596 amu. Considering the chirality of product **19**, further characterization will entail various optical measurements by way of spectroscopic methods such as

optical rotation and perhaps even circular dichroism spectroscopy; however, this was outside the scope of the current study.

During the synthesis of the compounds based on Scaffold C, a readily available starting material, (–)-menthol, was converted to the enantiomerically pure 1,4-disubstituted triazole **19** in only three steps. In addition, the synthesis of the corresponding enantiomer, as well as the two 1,5-disubstituted triazoles were set up for future completion.

CHAPTER 4
BIOLOGICAL EVALUATION

Two sets of the synthesized triazole CBD analogues were sent for biological tests to determine whether these compounds exhibit anti-cancer activity. The first set was sent to the Council for Scientific and Industrial Research (CSIR) in Pretoria, South Africa; and the second set was sent to the New Mexico Institute of Mining and Technology (NMT) in Socorro, the United States of America. The test conducted at NMT was done by the research group of Dr Snezna Rogelj. Please note that these biological tests were independently conducted at the two institutes mentioned, and that we were not involved in the testing procedures. The method used for each set, as well as the results obtained will be discussed separately.

4.1. BIOLOGICAL TEST CONDUCTED AT THE CSIR

This set of evaluations were done by Dr Kabamba B. (Alex) Alexandre and Dr Asongwe Lionel Tantoh from the CSIR in Pretoria. In preparation for these biological tests, the samples were exposed to MCF-7 cells (a breast cancer cell line) for four days. The detailed method is discussed below.

4.1.1. TESTING METHOD USED AT THE CSIR

The synthetic molecule array printing solution was prepared according to the method reported by Erfle and Pepperkok in 2005.[159] This process began by dispensing 5 µL of each sample into a 96 well plate, followed by the addition of 18 µL of the encapsulation mixture to the respective samples. The encapsulated compounds were then loaded from the 96 well plate, by capillary action using micro-fluidic filling plates, into 330 µm diameter elements. During this step, each encapsulated compound was loaded into a different element which was pre-mounted onto a printing plate. Microarray printing was subsequently performed with a custom-built printer. This was achieved by mounting the printing plates onto a custom-built Z axis movable head. An array of the individual compounds was then spotted from the printing plates onto a poly-L-Lysine (PLL) modified glass slip array using a 2.5 second contact time. This array printing process was done under a constant stream of humidified air. The printed array was then stored in an airtight desiccator in the absence of light. The next step involved the diffusion of the printed compounds into target cells. This was done by transferring the printed array glass slip from the desiccator into a tissue culture dish, followed by subsequent culture of MCF-7 breast cancer cells in the same dish. The MCF-7 cells were cultured in Dulbecco's Modified Eagle Medium (DMEM) containing 10% fetal bovine serum at a concentration of 1.5×10^6 cells / 10 mL. This was done over four days while keeping the temperature constant at 37 °C; and under a 5% carbon dioxide concentration to maintain a constant pH. These conditions were chosen to mimic the cell's natural environment. The printed array glass slip containing the MCF-7 cells was subsequently treated with immunofluorescence, mounted on a microtiter plate

dummy for imaging, and imaged under consecutive acquisitions with a point scanner confocal reader (Cytation 3 imaging reader) to provide the required microarray images. During the microarray acquisition with the imaging reader, three channels were used: the spots were imaged in the red channel (Sulforhodamine B, 568 nm), the actin cytoskeleton in the green channel (Phalloidin, 488 nm) and the DNA in the blue channel (DAPI, 408 nm).

4.1.2. RESULTS OBTAINED AGAINST THE MCF-7 CELL LINE

Two independent experiments were carried out according to the method described. Please note that the triazole CBD analogues of this project were tested with other samples sent from Stellenbosch University, along with various reference compounds. The figure below indicates the location on the compound array of the samples sent from Stellenbosch University, which were 24 in total. Out of the 24 samples, 7 compounds, marked on position 16-22, were the CBD triazole analogues generated as a result of this project (Figure 4:1 A). This figure further depicts the images obtained from the two independent experiments conducted on these samples (Figure 4:1 B).

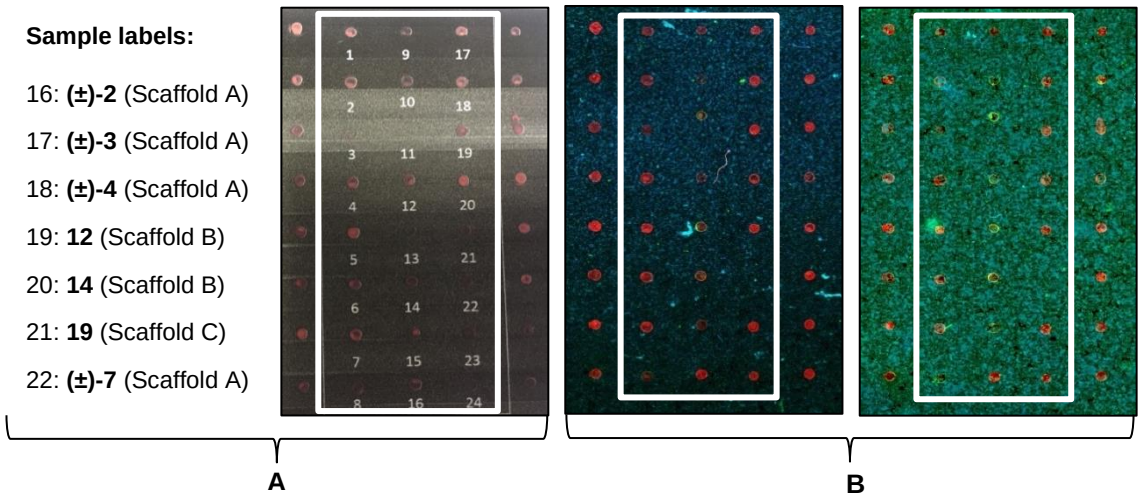

Figure 4:1 A: Location of compounds 16-22 on array; B: The two independent experiments.

A summary of the seven CBD analogues submitted for testing can be seen in Figure 4:2 below.

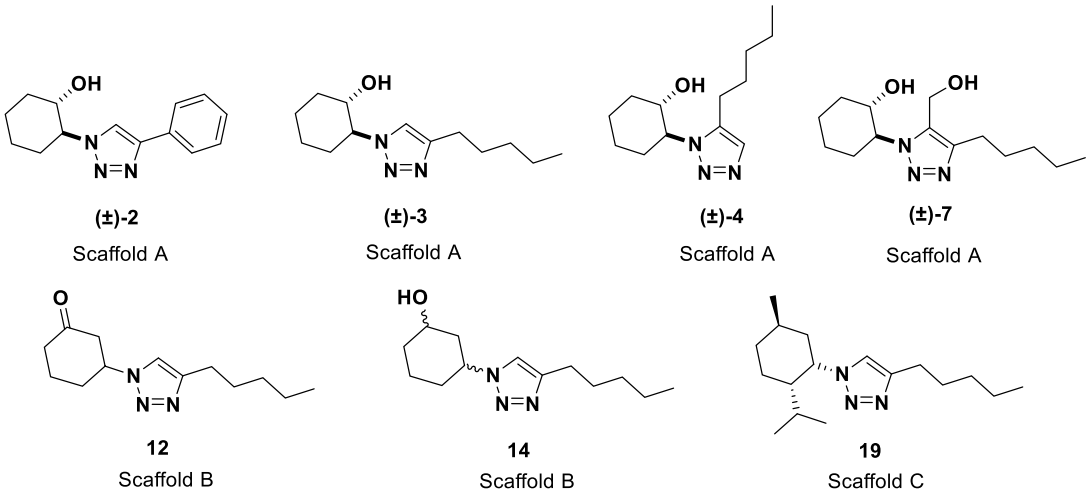

Figure 4:2 Structures of the seven compounds sent for testing.

The images (TIFF files) obtained from these two experiments were then processed using ImageJ v1.44 and Array-pro analyzer v6.3 software, and subsequently analyzed with Persomics and CellProfiler algorithms. In addition, data quantification was done using Microsoft Excel and the results are illustrated in Figure 4:3 below. The activity was measured relative to untreated MCF-7 cells, and subsequently quantified in terms of the percentage cell count normalized against the untreated MCF-7 cells. The final values as seen below resulted from averaging the two independent experiments that were conducted. The compounds pertaining to this project, are shown in blue, and some reference samples[3] with anticancer activity are shown in grey. All irrelevant samples were removed for simplification.

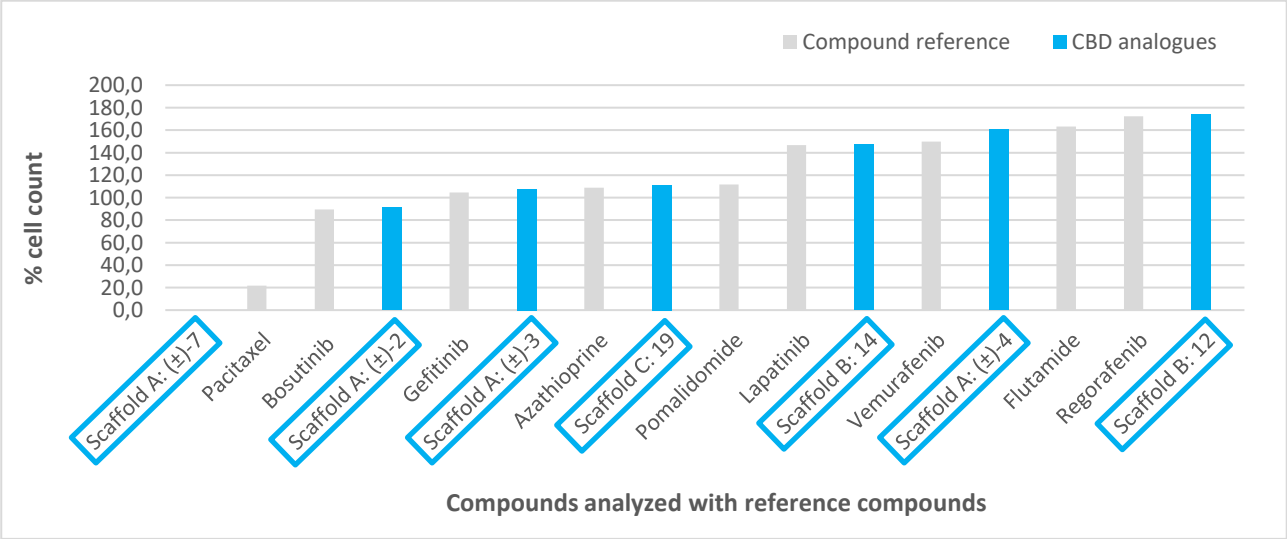

Figure 4:3 Graph representing the % cell count of the triazole CBD analogues and various reference samples.

Unfortunately, most of these analogues did not show any significant activity against the MCF-7 cell line. For most of the triazole CBD analogues the percentage cell count obtained was more than 100%. This indicates that these compounds did not inhibit the growth of the cancer cells, but promoted proliferation instead. Nevertheless, a speculative comparison was drawn between the structure of these analogues through interpretation of the graph illustrated in Figure 4:3. When comparing the triazole analogues associated with Scaffold A, the 1,4-disubstituted triazole analogue **(±)-3** had a lower % cell count than the 1,5-disubstituted triazole analogue **(±)-4**. Disappointingly, the 1,4,5-trisubstituted triazole analogue **(±)-7** was not detected (see position 22 in Figure 4:1 A), which means that the cells on this spot could not be counted. When further comparing the compounds for Scaffold B and Scaffold C to the compounds of Scaffold A, the ketone functionalized 1,4-disubstituted triazole analogue **12**, of Scaffold B, had the highest % cell count of all the analogues tested against the MCF-7 cells. However, the hydroxyl functionalized 1,4-disubstituted triazole

[3] Structures of these reference samples with anticancer activity are illustrated in Appendix 1.

analogue **14** provided a slightly lower % cell count compared to **12** and also had a lower % cell count than the 1,5-disubstituted triazole analogue **(±)-4**. In addition, the analogue associated with Scaffold C (**19**) containing the additional functional group on the cyclohexyl ring, had a lower % cell count than the compounds of Scaffold B and had a similar % cell count than **(±)-3**.

As previously mentioned, none of these results were particularly appealing, but to our surprise, the only compound which showed some potentially interesting activity against the MCF-7 cell line was the phenyl side chain triazole analogue **(±)-2** of Scaffold A. Although this compound was initially synthesized as a test compound for the triazole formation, this was the only compound with a % cell count below 100 (91.6%). If we consider the reference compounds used during this evaluation, it is interesting to note that compound **(±)-2** provided a better % cell count value than Gefitinib (a kinase inhibitor drug used in the treatment of certain breast cancers).[160] After interpreting these results, we can conclude that the replacement of the fatty acid-inspired tails (pentyl side chain) of our compounds with aromatic groups should rather be investigated in future CBD analogues.

This same set of compounds was then sent to NMT for additional biological tests.

4.2. BIOLOGICAL TEST CONDUCTED AT NMT

These evaluations were performed in Dr Snezna Rogelj's group at NMT by the following students, Maximo Santarosa, Danielle Turner and Shishir Acharya. During these biological tests, the samples were exposed to HeLa cells, and the anti-bacterial, anti-trypanosomal and anti-fungal toxicity of these seven compounds were assessed.

The anti-bacterial toxicity was determined through *in-vitro* screening of MRSA (Gram-positive), as well as *A. baumannii* (Gram-negative) bacterial cultures. The anti-fungal toxicity was also evaluated through *in-vitro* screening of a *C. albicans* yeast culture; and additionally, the anti-trypanosomal toxicity was investigated through *in-vitro* screening of a *T.cruzi* epimastigotes culture. The anti-bacterial, anti-fungal and anti-trypanosomal activity of the triazole CBD analogues was then assessed by using a tetrazolium dye (MTT) colorimetric assay. Unfortunately, during all three of these screenings no activity was observed below a concentration of 100 µM of the triazole CBD analogues. An additional assay was also performed to determine whether these compounds induce shedding of L-selection from human polymorphonuclear leukocytes **(**PMNs), which would indicate if these compounds have potential as an immunosuppressive. Unfortunately, no induction was observed from human neutrophils and lymphocytes.

The biological evaluation that was most of interest to us, was the anti-proliferative activity of these compounds against the HeLa cell line.

4.2.1. TESTING METHOD USED AT THE NMT

This process started with the trypsinization of the HeLa cell line. The resulting trypsinized cells were subsequently plated on a 96-well microtiter plate. Thereafter, the cells were cultured at 37 °C for 24 hours. The triazole CBD analogues were subsequently diluted to 100 mM in DMSO and added to the cultured cells at concentrations ranging from 0.004 to 100 µM. The next step involved a 48-hour incubation period in 200 µL of media. This was followed by the addition of 20 µL MTT reagent in serum free medium and an additional 2-hour incubation period. After the stipulated period, the media was removed and the newly formed formazan crystals were dissolved in 100 µL of DMSO. A plate reader was then used to measure the absorbance at 490 nm. Experiments were done in quadruplets.

4.2.1. RESULTS OBTAINED AGAINST THE HELA CELL LINE

Out of the seven compounds illustrated in Figure 4:2 that were sent for testing, only two had an IC_{50} value below 100 µM. The structures of these two compounds along with their determined IC_{50} values are illustrated in Figure 4:4.

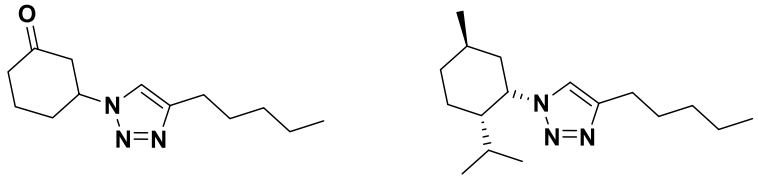

12
Scaffold B
IC_{50} = 74.3 µM

19
Scaffold C
IC_{50} = 95.3 µM

Figure 4:4 The two compounds that showed moderate activity against the HeLa cell line.

It was interesting to compare the results from the CSIR, during which these analogues where tested against MCF-7 cells, to the results obtained from NMT, where these analogues were tested against HeLa cells. The phenyl side chain triazole analogue **(±)-2** of Scaffold A was the only compound that showed activity against MCF-7 cells, but did not show any activity against the HeLa cells. In addition, the ketone functionalized 1,4-disubstituted triazole analogue **12** gave the least favourable result against MCF-7 cells, but showed the best activity against the HeLa cells with an IC_{50} value of 74.6 µM. Finally, the analogue of Scaffold C (**19**) provided moderate results against both cancer cell lines compared to the other analogues tested.

The complete absence of toxicity of these analogues below a concentration of 100 µM, as determined through the anti-bacterial, anti-trypanosomal and anti-fungal assays, is an initial indication that these compounds could be safe to use as potential drugs. Apart from the limitations of using a very small set of compounds for testing, the two sets of results obtained on different cancer cell lines can now be used to design new analogues with increased anti-cancer activity against the two cell lines that were tested. As a first step, the generation of more compounds should be a high priority – this will be important if further structure-activity relationships (SAR) are to be determined.

CHAPTER 5
CONCLUDING REMARKS

5.1. CONCLUSION

In conclusion, this research project focused on the synthesis of CBD analogues with potential anticancer activity, in which the core structure was modified with a triazole moiety. To this end, three different systems (Scaffold A, B, and C) were synthesized with the help of copper- and ruthenium-mediated click chemistry.

The general structure of these analogues was systematically altered, with each alteration bringing us closer to the structure of CBD. The three pharmacophoric groups of importance in the synthesis of Scaffold A, was the cyclohexyl ring, the cyclohexanol group and the fatty acid-inspired tail. Most analogues aimed for throughout this project were small molecules lacking any UV-active groups, making the tracking of reactions by TLC very difficult. For this reason, an initial 1,4-disubstituted 1,2,3-triazole compound was synthesized as a test reaction under Scaffold A, which contained an aromatic group, instead of the chosen lipophilic side-chain as mentioned above. This test reaction was conducted to monitor the triazole formation and the starting material consumption. After optimization of the copper- and ruthenium-mediated click reactions, the 1,4-, 1,5-, as well as the 1,4,5-polysubstituted 1,2,3-triazole analogues of Scaffold A containing the chosen lipophilic side-chain was successfully synthesized. The desired 1,4,5-trisubstituted 1,2,3-triazole analogue **(±)-7** was unfortunately obtained in a very low yield, and the selectivity of this reaction was not satisfactory. In this study, we attempted this synthesis with an internal alkyne containing a propargyl alcohol. The presence of this functionality is thought to provide the product with the propargyl alcohol in the 5-position on the triazole ring as major product, but in our hands, this was not the case. Although these two regioisomers were successfully separated from each other, the ruthenium-mediated click reaction with the chosen internal alkyne requires further investigation.

During the design of Scaffold B, the same three pharmacophoric groups were used as in Scaffold A. The alteration that was made was the position of the cyclohexanol group which was placed one atom further away from the triazole ring, to mimic the one cyclohexyl ring substituent on the structure of CBD. The synthesis of this system did however prove somewhat problematic, as neither the desired azide **11**, nor the 1,5-disubstituted 1,2,3-triazole CBD analogue **13**, could be isolated in a pure form. Nevertheless, the ketone functionalized 1,4-disubstituted 1,2,3-triazole CBD analogue **12** was successfully obtained by using the inseparable azide mixture, and this product was subsequently reduced to the desired hydroxyl functionalized 1,4-disubstituted 1,2,3-triazole CBD analogue **14**.

The general analogues designed for Scaffold C included an additional functional group on the cyclohexyl ring to mimic the second cyclohexyl ring substituent on the structure of CBD. (–)-Menthol

was chosen as a convenient starting material which inherently provided the desired functional groups while also introducing stereochemistry into the system. Two routes were set out which involved either a single or a double inversion of stereochemistry, thereby providing two diastereomeric triazole CBD analogues. Although the double inversion strategy was not successful in our hands, one 1,4-disubstituted 1,2,3-triazole CBD analogue, **19**, was successfully synthesized by making use of the optimised copper-mediated click reaction.

The analogues obtained were subsequently subjected to independent biological evaluations. Two sets of analogues were prepared and the anticancer activity was assessed against the MCF-7 cell line, as well as the HeLa cell line. None of the CBD triazole analogues of this study showed particularly appealing activity against the MCF-7 cell line. The 1,4,5-trisubstituted 1,2,3-triazole analogue **(±)-7** of Scaffold A did unfortunately not provide an anti-proliferation value, as it was not detected on the plate during this evaluation. The 1,5-disubstituted 1,2,3-triazole analogue of Scaffold A provided a higher % cell count than the 1,4-disubstituted 1,2,3-triazole analogue of Scaffold A, suggesting that the 1,5-regioisomers should not be further explored for these analogues. To our surprise, the only compound which showed some potentially interesting activity, with a cell count of 91.6%, was the test compound **(±)-2** which contained an aromatic group on the triazole ring. When considering the activity results obtained against the HeLa cell line, two compounds had an IC_{50} value below 100 µM. The compound which gave the most promising result, with an IC_{50} value of 74.3 µM, was the ketone functionalized analogue **12** of Scaffold B, the compound obtained before reduction to the final cyclohexanol analogue **14**. In addition, the biological results showed that Scaffold C is worth exploring, as the first analogue synthesized in Scaffold C, compound **19**, provided moderate activity against the Hela cell line.

These results provide valuable insight for the future design of triazole CBD analogues, as will be discussed in the next section.

5.2. FUTURE WORK

This section will systematically address improvements needed based on the conclusion, followed by additional suggestions for the future design of CBD analogues.

When first considering Scaffold A, the low yield and lack of selectivity obtained during the synthesis of the 1,4,5-trisubstituted 1,2,3-triazole analogue **(±)-7** must be addressed. An improved synthetic method is essential due to the inability to determine the anticancer activity of this analogue against the MCF-7 cell line during the course of the study. Obtaining these biological results will enable us to conclude whether the incorporation of the additional hydroxyl group onto the triazole ring is worth exploring in future triazole CBD analogues. Suggestions on how to improve the yield and selectivity for this analogue was provided in section 3.1.6, but a brief summery will be given here. One possibility is to use an internal alkyne containing a propargyl amine, as this functionality is known to

promote the formation of the regioisomer in which the propargyl group is in the 5-position on the triazole ring.[130] This route will however require additional steps to convert the amine into the desired hydroxyl group after the cycloaddition reaction. This could be achieved through an initial conversion to the primary amine which could subsequently be converted into the primary alcohol.[134,135] A second option would be to use an internal alkyne containing the desired propargyl alcohol, as well as an electron-withdrawing group, for instance a ketone, on the opposite side of the triple bond. Internal alkynes containing an electron-withdrawing group are known to promote the formation of the regioisomer with the electron-withdrawing group in the 4-position on the triazole ring.[130] This route would however also require an additional step to remove the ketone functionality through either a Clemmensen or a Wolff-Kishner reduction.[136] The general scheme for the processes which would be involved when using the proposed internal alkynes is re-illustrated in Scheme 5:1 below.

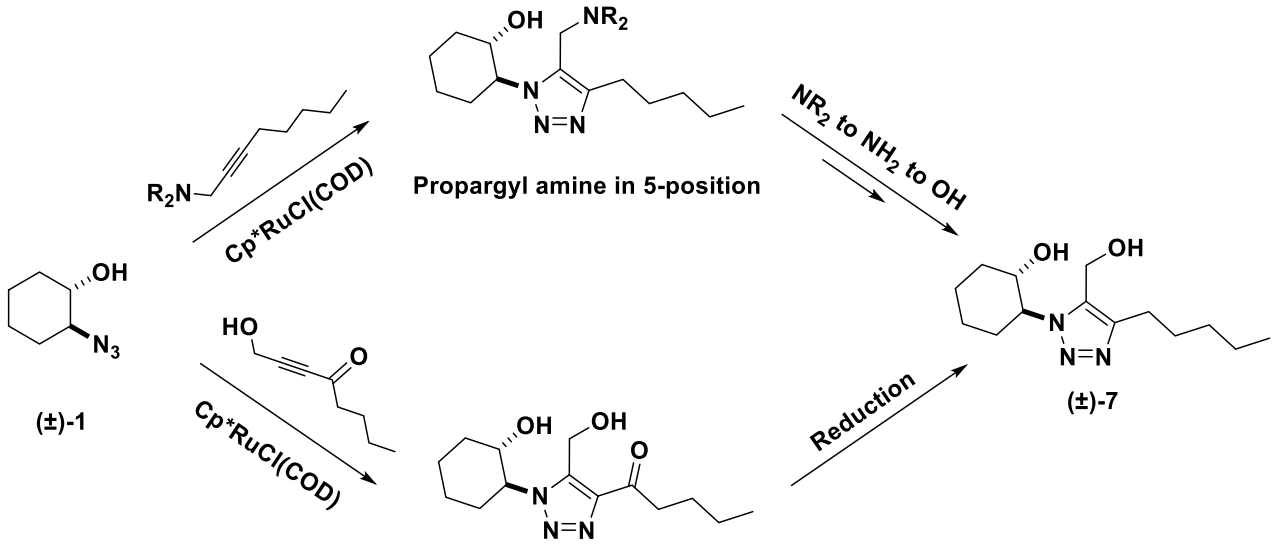

Scheme 5:1 Two options for improving the selectivity for the synthesis of (±)-7, using internal alkynes with either a propargyl amine or an electron-withdrawing group and a propargyl alcohol.

Upon writing-up, a more efficient route for the synthesis of the axial azide **16** of Scaffold C, obtained with a single inversion of stereochemistry, was revealed. By using this route, (–)-menthol can be converted into the axial azide **16** in only one step by using a derivation of the Mitsunobu reaction as depicted in Scheme 5:2.[161]

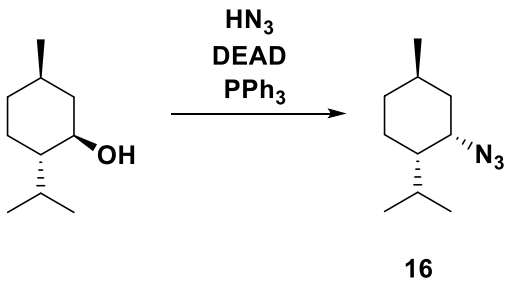

Scheme 5:2 Alternative route for the synthesis of the axial azide 16.

In order to obtain the diastereomer of analogue **19** synthesized in Scaffold C, the double inversion strategy must be revisited. As discussed in the results section, this approach might have been hindered by the specific chair conformation of the chlorinated (–)-menthol compound **17**. One could consider the incorporation of a better leaving group onto the structure of (–)-menthol, for instance a bromine atom, which could be achieved with the help of an Appel reaction using carbon tetrabromide. Alternatively, the synthesis of the brominated (–)-menthol compound with inversion of stereochemistry, could be obtained by subjecting (–)-menthol to a mesylation reaction, followed by a nucleophilic substitution reaction with lithium bromide. After optimization of the single and double inversion strategy of Scaffold C, these conditions could be directly applied to a different starting material, namely (+)-menthol. This additional scaffold would provide two analogues which would be enantiomers of the two diastereomers discussed above.

When considering the biological results, improved activity against the MCF-7 cell line could involve the replacement of the fatty acid-inspired tail with aromatic groups. For improved activity against the HeLa cell line, the intentional incorporation of a ketone functionality onto the cyclohexyl ring, without the additional reduction step should be considered. In addition, the results obtained from this project show that Scaffold C is worth exploring as the first analogue synthesized in Scaffold C showed moderate activity against the HeLa cell line.

Besides the suggestions made above, the design of future CBD analogues could include different heterocycles, apart from the 1,2,3-triazole moiety found at the core of the present analogues. A possible option would be to explore the formation of 3,5-disubstituted isoxazoles via a copper(I)-mediated cycloaddition of terminal alkynes with nitrile oxides. This step-wise cycloaddition sequence also proceeds via a copper(I) acetylides intermediate as seen in the CuAAC reactions.[106] The required nitrile oxide moiety could be obtained from the corresponding chlorinated aldoxime, as shown in Scheme 5:3.[162]

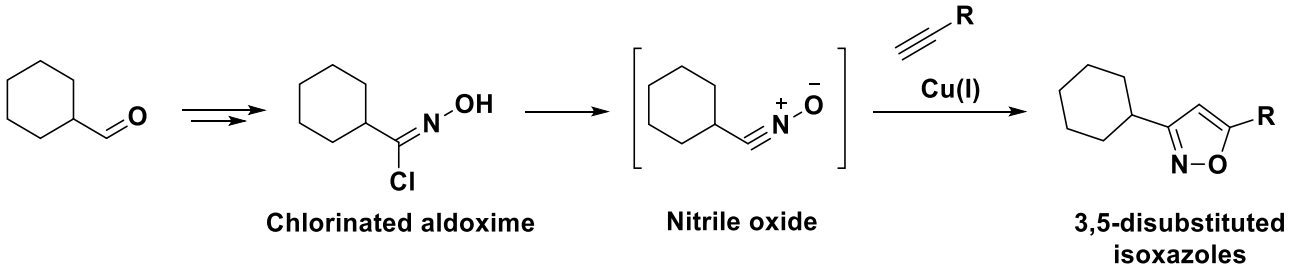

Scheme 5:3 General scheme that would be involved in the synthesis of 3,5-disubstituted isozoles.

Finally, the pharmacophoric groups of CBD could further be explored by wisely choosing readily available monoterpenes, similar to menthol, to be used as starting materials for the synthesis of novel analogues with improved functionalities on the cyclohexyl ring portion of the final analogues. Examples of monoterpenes that could be used include limonene, carvone, pinene and thymol.[163]

Figure 5:1 shows the structure of these possible starting materials, as well as the structure of CBD for comparison.

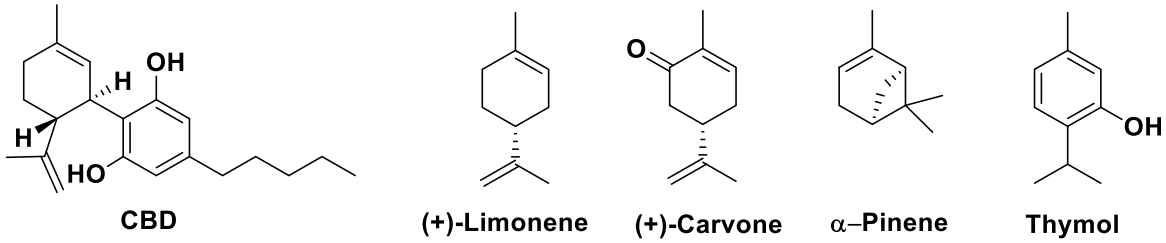

Figure 5:1 Comparison between the structure of CBD and suggested monoterpenes that can be used as starting materials when designing future CBD analogues.

The basic structure of limonene is similar to that of menthol with the exception of an additional double bond on the cyclohexyl ring. By using this methylcyclohexylidene, all the pharmacophoric groups found on the cyclohexyl ring of CBD could be incorporated into future analogues. Carvone could subsequently be explored as this could incorporate an additional carbonyl functionality onto the cyclohexyl ring of these analogues. The structure of pinene also contains the additional double bond on the cyclohexyl ring as seen in CBD. It could be interesting to see what effect the carbon bridge found in this bicyclic monoterpene might have on the anticancer activity of future analogues. The use of thymol, could also provide valuable insight on whether additional aromaticity on the outer structure would have any effect on the activity of these analogues.

In summary, this study produced a small series of CBD analogues by making use of the “click” approach. These compounds subsequently provided valuable information regarding the structure-activity relationships (SARs) relative to the MCF-7 and HeLa cell lines, thereby providing a solid foundation for the design of future heterocycle CBD analogues. As a final remark, it is recommended that the synthesis of novel analogues, based on the suggestions presented above, should be of high priority as this will provide access to much needed further SARs information.

CHAPTER 6
EXPERIMENTAL

6.1. GENERAL INFORMATION

Reaction glassware was dried by heating under a positive nitrogen pressure, or in an oven at 110 °C for two hours. Furthermore, standard Schlenk techniques were used when needed. Reaction mixtures were heated by placing the reaction flask in a paraffin oil bath, set to the correct temperature on a magnetic stirrer hot plate. Solvents were removed *in vacuo*, by using a rotary evaporator followed by the use of a high vacuum pump at ca. 0.08 mm Hg, to remove trace amounts of residual solvent.

All chemicals used in these experiments were purchased from Sigma Aldrich (Merck). Reaction solvents were dried over the appropriate drying agents and distilled under a positive nitrogen pressure. Tetrahydrofuran was distilled under nitrogen from sodium metal flakes, with benzophenone as an indicator. Dichloromethane and acetonitrile were distilled under nitrogen from calcium hydride, and ethanol was distilled from magnesium turnings and iodine. In addition, triethylamine was distilled under potassium hydroxide. Other reagents which required purification was purified according to standard procedures.

Solvents used for chromatography (ethyl acetate and hexane) were distilled by conventional distillation procedures. Thin layer chromatography (TLC) was performed using Macherey-Nagel™ Xtra SIL G Silica Layers on Alugram™ Aluminum Sheets. Visualization of the plates is usually achieved by using a 254 nm UV light; although during this project very few compounds proved to be UV-active. For this reason, various stains appropriate to the compounds, including iodine on silica or solutions of *p*-anisaldehyde, ninhydrin, potassium permanganate or cerium ammonium molybdate was used, followed by heating of the stained plate. Column chromatography was performed using Merck silica gel 60 (particle size 0.063-0.200 mm) and different combinations of ethyl acetate and hexane.

Nuclear magnetic resonance (NMR) spectra (^{1}H, ^{13}C) were either recorded on a 300 MHz Varian VNMRS (75 MHz for ^{13}C), a 400 MHz Varian Unity Inova (101 MHz for ^{13}C), or a 600 MHz Varian Unity Inova (150 MHz for ^{13}C). All spectra were obtained at 25 °C unless otherwise stated, and the NMR spectroscopy data was processed using MestReNova. Chemical shifts were recorded using the residual solvent peak or external reference (tetramethylsilane). Furthermore, chemical shifts (δ) are given in parts per million (ppm) and coupling constants (J-values) in Hertz (Hz). Mass spectrometry was performed on a Waters SYNAPT G2. Melting points were obtained using a Gallenkamp Melting Point Apparatus and are uncorrected.

6.2. SYNTHESIS OF SCAFFOLD A

6.2.1. SYNTHESIS OF (±)-*TRANS*-2-AZIDOCYCLOHEXAN-1-OL 1

A 50 mL two-neck round-bottom flask charged with NaN_3 (1.49 g, 22.9 mmol, 2.50 equiv.) was set up under reflux conditions. Distilled H_2O (4.6 mL) was added through the septum, and the flask was left to stir for 5 min at RT to allow the complete dissolution of NaN_3. Distilled acetone (4.6 mL) was subsequently added and the mixture was heated to 75 °C under reflux. Once heated, cyclohexene oxide (0.93 mL, 9.2 mmol, 1.0 equiv.) was slowly added by syringe and the reaction mixture was allowed to stir for 17 h at 75 °C. It is interesting to note that the reaction colour changed from colourless to a yellow-brown transparent solution during the course of the reaction. After complete consumption of the starting material (monitored by TLC), the acetone was removed under reduced pressure and the reaction residue was partitioned between distilled H_2O and EtOAc. The aqueous layer was then extracted with successive portions of EtOAc (3 × 100 mL). The combined organic layers were washed with brine (40 mL), dried over $MgSO_4$, filtered, and concentrated under reduced pressure. The resulting oily residue was purified by flash chromatography (Hexane: EtOAc, 95:5 – 90:10) to afford the pure 1,2-azido alcohol **(±)-1** as a light-yellow oil (1.23 g, 8.71 mmol, 95%).

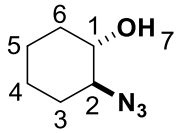

(±)-1

R_f = 0.31 (Hexane: EtOAc, 85:15). **IR (ATR, cm^{-1}):** 3365 (O-H str, br), 2935 (C-H str), 2861, 2089 (N=N=N str), 1451 (O-H bend), 1257 (C-N str), 1068, 991, 844. **^{1}H NMR (400 MHz, $CDCl_3$) δ** 3.36 – 3.30 (m, 1H, *H*$_1$), 3.15 – 3.09 (m, 1H, *H*$_2$), 2.48 (bs, 1H, O*H*$_7$), 2.00 – 1.93 (m, 2H), 1.70 – 1.64 (m, 2H), 1.31 – 1.17 (m). **^{13}C NMR (101 MHz, $CDCl_3$) δ** 73.46 (*C*$_1$), 66.98 (*C*$_2$), 33.13, 29.82, 24.14, 23.82.

Analytical data was in accordance with literature.[125]

6.2.2. SYNTHESIS OF (±)-*TRANS*-2-(4-PHENYL-1*H*-1,2,3-TRIAZOL-1-YL)CYCLOHEXAN-1-OL 2

A dry 50 mL two-neck round-bottom flask charged with copper(II) sulphate pentahydrate (42.4 mg, 0.170 mmol, 0.100 equiv.), and sodium ascorbate (337 mg, 1.70 mmol, 1.00 equiv.) was evacuated under high vacuum and placed under a N_2 atmosphere. Distilled H_2O (1.0 mL) was subsequently added and the flask was allowed to stir for 10 min, allowing the reduction of the Cu(II) species to the active Cu(I) species. During the reduction, a colour change was observed from a dark brown to a yellow colour. Thereafter, MeOH (2.0 mL) was added to the flask followed by the alkyne, phenylacetylene (0.174 g, 1.70 mmol, 1.00 equiv.). The reaction mixture was stirred for 10 min, followed by the addition of the azide, (±)-*trans*-2-azidocyclohexan-1-ol **(±)-1** (240 mg, 1.70 mmol,

1.00 equiv.), dissolved in MeOH (2 mL). The flask was then left to stir at 30 °C for 18 h. The MeOH was evaporated off under reduced pressure and the reaction residue was quenched with a saturated solution of NH_4Cl (15 mL). The aqueous layer was then repeatedly extracted with EtOAc (3 × 50 mL). The combined organic layers were washed with brine (20 mL), dried over $MgSO_4$, filtered, and concentrated under reduced pressure. The crude residue was washed with Hexane (10 mL) and purified by crystallization from a minimum amount of hot EtOAc. The resulting crystals was filtered and redissolved in a minimum amount of hot EtOAc and left to recrystallize. This provided the pure product **(±)-2** as a white solid (261 mg, 1.07 mmol, 63%).

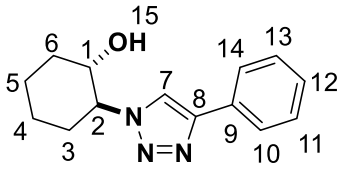

(±)-2

R_f = 0.19 (DCM: MeOH, 97:3). **MP** 160 – 162 °C. **^{1}H NMR (400 MHz, $CDCl_3$) δ** 7.76 (s, 1H, *H_7*), 7.73 – 7.68 (m, 2H, 2 × Ar*H*), 7.40 – 7.35 (m, 2H, 2 × Ar*H*), 7.33 – 7.27 (m, 1H, Ar*H*), 4.21 – 4.03 (m, 2H, *H_1* and *H_2*), 3.52 (bs, 1H, O*H_{15}*), 2.27 – 1.35 (m, 8H, 2 × *H_3* and 2 × *H_4* and 2 × *H_5* and 2 × *H_6*). **^{13}C NMR (101 MHz, $CDCl_3$) δ** 147.18 (*C_8*), 130.52, 128.91, 128.19, 125.68, 119.69 (*C_7*), 72.77 (*C_1*), 67.21 (*C_2*), 33.85, 31.73, 24.93, 24.18. **HRMS-TOF MS ES+: m/z $[M+H]^+$** calcd for $C_{14}H_{18}N_3O^+$: 244.1450; found 244.1452.

6.2.3. SYNTHESIS OF (±)-*TRANS*-2-(4-PENTYL-1*H*-1,2,3-TRIAZOL-1-YL)CYCLOHEXAN-1-OL 3

Optimization of the copper-catalyzed azide alkyne cycloaddition (CuAAC) reaction

The experimental details regarding each method explored for the optimization of the CuAAC reaction will be discussed in the sections below, followed by the characterization of compound **(±)-3**.

6.2.3.1. CUAAC WITH COPPER(I) SULPHATE PENTAHYDRATE

A dry 50 mL two-neck round-bottom flask containing copper(II) sulphate pentahydrate (106 mg, 0.425 mmol, 0.300 equiv.), sodium ascorbate (281 mg, 1.42 mmol, 1.00 equiv.) and distilled H_2O (1.0 mL) was evacuated under high vacuum and filled with N_2. The flask was left to stir for 10 min, allowing the reduction of the Cu(II) species to the active Cu(I) species. During the reduction, a colour change was observed from a dark brown to a yellow colour. Thereafter, MeOH (2 mL) was added to the flask followed by the alkyne, 1-heptyne (0.20 mL, 1.6 mmol, 1.1 equiv.). The reaction mixture was stirred for 10 min, followed by the addition of the azide, (±)-*trans*-2-azidocyclohexan-1-ol **(±)-1** (200 mg, 1.42 mmol, 1.00 equiv.), dissolved in MeOH (2 mL). The flask was then left to stir at 30 °C for 18 h. The MeOH was evaporated off under reduced pressure and the reaction residue was

quenched with saturated aqueous NH_4Cl (40 mL). The aqueous layer was then extracted with successive portions of EtOAc (3 × 70 mL). The combined organic layers were washed with brine (30 mL), dried over $MgSO_4$, filtered, and concentrated under reduced pressure. The crude product was purified by silica gel column chromatography (Hexane: EtOAc, 90:10 – 50:50) to obtain the pure product **(±)-3** as a white solid (265 mg, 1.12 mmol, 79%).

6.2.3.2. CuAAC with Copper(I) iodide

6.2.3.2.1. First approach with copper(I) iodide (DCM at RT)

A dry 50 mL two-neck round-bottom flask was covered with foil and charged with copper(I) iodide (80.9 mg, 0.425 mmol, 0.300 equiv.). The flask was then evacuated under high vacuum and placed under a N_2 atmosphere. Anhydrous DCM (3.7 mL) was added by syringe, followed by DIPEA (0.81 mL, 4.7 mmol, 3.3 equiv.), as well as the alkyne, 1-heptyne (0.20 mL, 1.6 mmol, 1.1 equiv.). The mixture was then left to stir at RT for 15 min, followed by the addition of the azide, (±)-*trans*-2-azidocyclohexan-1-ol **(±)-1** (200 mg, 1.42 mmol, 1.00 equiv.). The resulting solution was stirred in the dark at RT for 18 h. Thereafter, the solution was diluted with DCM (20 mL) and washed with a saturated NH_4Cl solution (40 mL). The layers were then separated, and the aqueous layer was extracted with consecutive portions of DCM (3 × 50 mL). The combined organic layers were then washed with brine (20 mL), dried over $MgSO_4$ and evaporated under reduced pressure. The crude product was purified by silica gel column chromatography (Hexane: EtOAc, 90:10 – 50:50) to obtain the pure product **(±)-3** as a white solid (130 mg, 0.548 mmol, 39%).

6.2.3.2.2. Second approach copper(I) iodide (DCM at 40 °C)

The copper(I) iodide-catalyzed click reaction, with DCM as the solvent, was then also attempted at a slightly elevated temperature of 40 °C, following the same procedure as above. The exact amounts used are as follows: Copper(I) iodide (74.8 mg, 0.393 mmol, 0.300 equiv.), DIPEA (0.75 mL, 4.3 mmol, 3.3 equiv.), the alkyne, 1-heptyne (0.19 mL, 1.4 mmol, 1.1 equiv.), and the azide, (±)-*trans*-2-azidocyclohexan-1-ol **(±)-1** (185 mg, 1.31 mmol, 1.00 equiv.) in anhydrous DCM (3.5 mL) at 40 °C for 18 h, in the absence of light. After purification by flash chromatography (Hexane: EtOAc, 90:10 – 50:50), the pure product **(±)-3** was obtained as a white solid (260 mg, 1.09 mmol, 83%).

6.2.3.2.3. Third approach with copper(I) iodide (MeCN at 65 °C)

In a final attend to optimize the copper(I)-iodide catalyzed click reaction, MeCN was used as the solvent, following the same procedure as above. The exact amounts used are as follows: Copper(I) iodide (80.9 mg, 0.425 mmol, 0.300 equiv.), DIPEA (0.81 mL, 4.7 mmol, 3.3 equiv.), the alkyne, 1-heptyne (0.20 mL, 1.6 mmol, 1.1 equiv.), and the azide, (±)-*trans*-2-azidocyclohexan-1-ol **(±)-1** (200 mg, 1.42 mmol, 1.00 equiv.) in MeCN (3.7 mL) at 65 °C for 18 h, in the dark. Thereafter, the MeCN was removed under reduced pressure, and the reaction residue was diluted with EtOAc (30 mL).

This organic layer was washed with saturated aqueous NH_4Cl (50 mL). The layers were separated and the aqueous layers was extracted with EtOAc (3 × 50 mL). The combined organic layers were washed with brine (40 mL), dried over $MgSO_4$ and the solvent was removed *in vacuo*. After purification by flash column chromatography over silica gel (Hexane: EtOAc, 90:10 – 50:50), the pure product **(±)-3** was obtained as a white solid (289 mg, 1.21 mmol, 86%).

6.2.3.3. CuAAC with Copper(II) acetate

Copper(II) acetate (772 mg, 0.425 mmol, 0.300 equiv.) and distilled H_2O (1.5 mL) was added into a dry 50 mL two-neck round-bottom flask and placed under a N_2 atmosphere. MeOH (3.0 mL) was added through the septum by syringe, followed by the alkyne, 1-heptyne (0.20 mL, 1.6 mmol, 1.1 equiv.). The mixture was left to stir for 10 min, and the azide (±)-*trans*-2-azidocyclohexan-1-ol **(±)-1** (200 mg, 1.42 mmol, 1.00 equiv.) was subsequently added to the flask. The reaction was allowed to stir at 30 °C for 18 h. After complete consumption of the starting materials (monitored by TLC), the MeOH was removed under reduced pressure, diluted with EtOAc (20 mL) and washed with a saturated NH_4Cl solution (50 mL). The aqueous layer was extracted with EtOAc (3 × 100 mL) and the combined organic layers were washed with brine (40 mL), dried over $MgSO_4$, filtered, and concentrated *in vacuo*. The crude product was purified by column chromatography (Hexane: EtOAc, 90:10 – 50:50) to obtain the pure product **(±)-3** as a white solid (300 mg, 1.26 mmol, 89%).

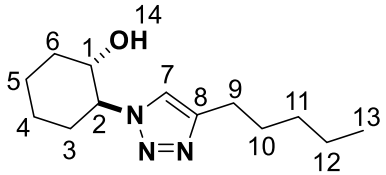

(±)-3

R_f = 0.33 (Hexane: EtOAc, 50:50). **MP** 54 – 56 °C. **^{1}H NMR (300 MHz, $CDCl_3$) δ** 7.28 (s, 1H, H_7), 4.17 (bs, 1H, OH_{14}), 4.09 – 3.95 (m, 2H, H_2 and H_1), 2.56 (t, ^3J = 7.4 Hz, 2H, 2 × H_9), 2.18 – 1.36 (m, 10H), 1.30 – 1.26 (m, 4H), 0.85 (t, ^3J = 6.9 Hz, 3H, 3 × H_{13}). **^{13}C NMR (75 MHz, $CDCl_3$) δ** 147.48 (C_8), 120.55 (C_7), 72.41 (C_1), 66.80 (C_2), 33.93, 31.78, 31.55, 29.06, 25.62, 24.86, 24.16, 22.46, 14.04 (C_{13}). **HRMS-TOF MS ES+: m/z [M+H]** calcd for $C_{13}H_{24}N_3O^+$: 238.1919; found 238.1920.

Analytical data was in accordance with literature.[121]

The CuAAC reaction with copper(II) acetate as the copper source gave the best result, and was the only method which did not require the addition of a reducing agent or stabilizing ligand, as was the case with the other two copper sources investigated. For this reason, this method was used throughout this project for all further CuAAC reactions.

6.2.4. SYNTHESIS OF (±)-*TRANS*-2-(5-PENTYL-1*H*-1,2,3-TRIAZOL-1-YL)CYCLOHEXAN-1-OL 4

Optimized ruthenium-catalyzed azide alkyne cycloaddition (RuAAC) reaction

A dry Schlenk tube was evacuated under high vacuum and placed under a N_2 atmosphere. Anhydrous dioxane (8.0 mL) was subsequently added via syringe and the solvent was degassed by five cycles of the freeze-pump-thaw technique. One of these cycles involved the evacuation of the tube under high vacuum, after which the Schlenk tube containing dioxane was placed into a liquid nitrogen container until the solvent was completely frozen. The tube was subsequently placed under high vacuum for 5 min, while still immersed in liquid nitrogen. Thereafter, the tube was placed in a beaker with lukewarm water and the solvent was allowed to slowly thaw. The Schlenk tube was then purged with N_2 gas for 5 min, followed by the addition of the catalyst Cp*RuCl(COD) (21.5 mg, 0.0567 mmol, 4 mol%). The Schlenk tube was once again purged with N_2 gas for 5 min before adding the alkyne, 1-heptyne (0.19 mL, 1.4 mmol, 1.0 equiv.) into the flask by syringe. After another round of N_2 purging, the azide (±)-*trans*-2-azidocyclohexan-1-ol **(±)-1** (200 mg, 1.42 mmol, 1.00 equiv.) was added under positive N_2 pressure. After a final N_2 purge, the reaction mixture was left to stir at 60 °C for 24 h. The reaction mixture was then wet loaded directly onto a silica gel column and purified by flash chromatography (Hexane: EtOAc, 90:10 – 50:50). This afforded the pure product **(±)-4** as a white solid (0.212 mg, 0.893 mmol, 63%).

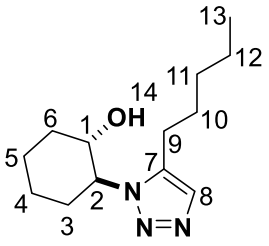

(±)-4

R_f = 0.26 (Hexane: EtOAc, 50:50). **MP** 122 – 124 °C. **^{1}H NMR (300 MHz, $CDCl_3$) δ** 7.39 (s, 1H, *H_8*), 4.33 (bs, 1H, O*H_{14}*), 3.94 – 3.85 (m, 1H, *H_1*), 2.72 – 2.54 (m, 3H, 2 × *H_9* and *H_2*), 2.23 – 1.42 (m, 10H, 2 × *H_3* and 2 × *H_4* and 2 × *H_5* and 2 × *H_6* and 2 × *H_{10}*), 1.40 – 1.35 (m, 4H), 0.91 (t, ^3J = 7.1 Hz, 3H, 3 × *H_{13}*). **^{13}C NMR (75 MHz, $CDCl_3$) δ** 138.24 (*C_7*), 131.82 (*C_8*), 72.47 (*C_1*), 64.36 (*C_2*), 33.95, 32.25, 31.48, 27.93, 25.18, 24.35, 23.24, 22.45, 14.07 (*C_{13}*). **HRMS-TOF MS ES+: m/z [M+H]** calcd for $C_{13}H_{24}N_3O^+$: 238.1919; found 238.1921.

6.2.5. SYNTHESIS OF INTERNAL ALKYNE, OCT-2-YN-1-OL 5

Dry THF (7.0 mL) was added into a 50 mL two-neck round-bottom flask under a constant N_2 flow, followed by 1-heptyne (0.95 mL, 7.3 mmol, 1.0 equiv.). This solution was then cooled down to −78 °C (acetone/dry ice bath). *n*-Butyllithium (1.9 M in Hexane, 3.9 mL, 7.3 mmol, 1.0 equiv.) was then added drop-wise. This mixture was then stirred for 1 h at −78 °C, after which time paraformaldehyde (229

mg, 7.64 mmol, 1.05 equiv.) was added to the flask. During the addition of paraformaldehyde, a white suspension was formed. The mixture was then allowed to stir for another 2 h at −78 °C. Thereafter, the reaction mixture was warmed up slowly and allowed to stir for 20 h at RT. After this time, the flask contained a yellow-green transparent solution. The reaction was then quenched with a saturated solution of NH_4Cl (40 mL) and the aqueous layer was repeatedly extracted with EtOAc (3 × 50 mL). The combined organic layers were washed with brine (30 mL), dried over $MgSO_4$ and filtered. The solvent was removed *in vacuo* to afford a crude oily residue which was subsequently purified by flash chromatography. (Hexane: EtOAc, 98:2 – 90:10). This afforded the pure internal alkyne **5** as a yellow-green oil (623 mg, 4.86 mmol, 67%).

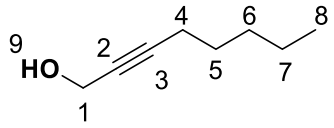

5

R_f = 0.57 (Hexane: EtOAc, 70:30). **^{1}H NMR (400 MHz, $CDCl_3$) δ** 4.24 (m, 2H, 2 × *H_1*), 2.23 – 2.16 (m, 2H, 2 × *H_4*), 1.80 – 1.77 (m, 1H, O*H_9*), 1.55 – 1.45 (m, 2H), 1.37 – 1.29 (m, 4H), 0.89 (t, *^3J* = 7.1 Hz, 3H, 3 × *H_8*). **^{13}C NMR (101 MHz, $CDCl_3$) δ** 86.73 (*C_2*), 78.40 (*C_3*), 51.49 (*C_1*), 31.16 (*C_4*), 28.42, 22.32, 18.82 and 14.07 (*C_8*).

Analytical data was in accordance with literature.[131]

6.2.6. SYNTHESIS OF (±)-*TRANS*-2-[4-(HYDROXYMETHYL)-5-PENTYL-1*H*-1,2,3-TRIAZOL-1-YL]CYCLOHEXAN-1-OL 6 AND (±)-*TRANS*-2-[5-(HYDROXYMETHYL)-4-PENTYL-1*H*-1,2,3-TRIAZOL-1-YL]CYCLOHEXAN-1-OL 7

A dry Schlenk tube was evacuated and filled with N_2 gas (3×). Anhydrous dioxane (8.0 mL) was then added by syringe and the solvent was degassed through five cycles of the freeze-pump-thaw technique, see section 6.4.2. The Schlenk tube was then purged with N_2 gas for 5 min, followed by the addition of the catalyst Cp*RuCl(COD) (21.5 mg, 0.0567 mmol, 4 mol%). The Schlenk tube was once again purged with N_2 gas for 5 min, before adding the alkyne, oct-2-yn-1-ol **5** (200 mg, 1.56 mmol, 1.10 equiv.), followed by another 5 min of N_2 purging. The azide, (±)-*trans*-2-azidocyclohexan-1-ol **(±)-1** (200 mg, 1.42 mmol, 1.00 equiv.) was then added under positive N_2 pressure and after a final N_2 purge, the reaction mixture was left to stir at 60 °C for 24 h. The reaction mixture was then wet loaded directly onto a silica gel column and purified by flash chromatography (Hexane: EtOAc, 90:10 – 50:50) to obtain compound **(±)-6** as a yellow-green solid (22.1 mg, 0.0827 mmol, 6%) and compound **(±)-7** as a yellow-green solid (20.9 mg, 0.0782 mmol, 6%).

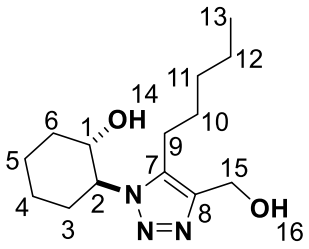

(±)-6

R_f = 0.08 (Hexane: EtOAc, 50:50) and 0.17 (Hexane: EtOAc, 0:100). **^{1}H NMR (300 MHz, $CDCl_3$) δ** 5.82 (bs, 1H, O*H*$_{16}$), 4.55 (s, 2H, 2 × *H*$_{15}$), 4.43 (bs, 1H, O*H*$_{14}$), 4.10 – 3.95 (m, 2H, *H*$_2$ and *H*$_1$), 2.59 – 2.42 (m, 2H, 2 × *H*$_9$), 2.37 – 1.39 (m,10H), 1.35 – 1.17 (m, 4H), 0.85 (t, ^3J = 6.9 Hz, 3H, 3 × *H*$_{13}$). **^{13}C NMR (75 MHz, $CDCl_3$) δ** 144.93 (*C*$_8$), 133.37 (*C*$_7$), 73.13 (*C*$_1$), 64.59 (*C*$_2$), 51.42 (*C*$_{15}$), 34.49, 31.54, 30.90, 29.72, 25.20, 24.57, 24.39, 22.50, 14.12 (*C*$_{13}$).

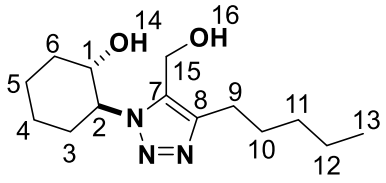

(±)-7

R_f = 0.19 (Hexane: EtOAc, 50:50) and 0.52 (Hexane: EtOAc, 0:100). **^{1}H NMR (300 MHz, $CDCl_3$) δ** 4.62 – 4.48 (m, 2H, 2 × *H*$_{15}$), 4.30 (bs, 1H, O*H*$_{14}$), 4.23 – 4.15 (m, 1H, *H*$_2$), 3.88 – 3.80 (m, 1H, *H*$_1$), 3.56 (bs, 1H, O*H*$_{16}$), 2.78 – 2.62 (m, 2H, 2 × *H*$_9$), 2.19 – 1.42 (m,10H), 1.34 – 1.29 (m, 4H), 0.88 (t, ^3J = 6.8 Hz, 3H, 3 × *H*$_{13}$). **^{13}C NMR (75 MHz, $CDCl_3$) δ** 136.46 (*C*$_7$ or *C*$_8$), 72.61 (*C*$_1$), 64.82 (*C*$_2$), 55.56 (*C*$_{15}$), 34.06, 32.12, 31.47, 29.07, 25.27, 24.36, 22.40, 22.36, 14.03 (*C*$_{13}$). **HRMS-TOF MS ES+: m/z [M+H]$^+$** calcd for $C_{14}H_{26}N_3O_2^+$: 268.2025; found 268.2037.

6.3. Synthesis of Scaffold B

6.3.1. Attempted synthesis of azide 11 in four steps

The starting material used to obtain the desired azide **11**, namely 2-cyclohexen-1-one is labeled as **11_{SM}**.

6.3.1.1. Synthesis of 2,3-epoxycyclohexanone, (7-oxabicyclo[4.1.0]heptan-2-one) 8

A dry 100 mL three-neck round-bottom flask was evacuated and placed under a N_2 atmosphere. MeOH (9.0 mL) was added into the flask via syringe, followed by 2-cyclohexen-1-one **11_{SM}** (0.91 mL, 9.4 mmol, 1.0 equiv.). This solution was then cooled to 0 °C by placing the flask in an ice bath. Thereafter, 30% hydrogen peroxide (4.8 mL, 47 mmol, 5.0 equiv.) was added through the septum by syringe, followed by 1 M NaOH (1.3 mL, 1.3 mmol, 0.14 equiv.). The reaction mixture was then allowed to stir under N_2 for 6 h, while maintaining the 0 °C environment. After this time, the MeOH

was removed under reduced pressure and the reaction residue was partitioned between H_2O (30 mL) and DCM (30 mL). The aqueous layer was then extracted with successive portions of DCM (3 × 100 mL). The combined organic layers were washed with 10% aqueous Na_2SO_3 and brine, dried over $MgSO_4$, filtered, and concentrated under reduced pressure. The resulting oily residue was purified by flash chromatography (Hexane: EtOAc, 97:3 – 90:10). This afforded the pure epoxide **8** as a colourless oil (0.691 g, 6.16 mmol, 66%).

However, a yield of 77% was obtained when doing this reaction on a smaller scale (2-cyclohexen-1-one = 0.200 g (0.22 mL)).

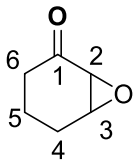

8

R_f = 0.25 (Hexane: EtOAc, 90:10). **^{1}H NMR (300 MHz, $CDCl_3$) δ** 3.53 – 3.50 (m, 1H, *H_3*), 3.13 (d, ^3J = 3.9 Hz, 1H, *H_2*), 2.45 (dt, ^2J = 8.2, ^3J = 4.4 Hz, 1H), 2.25 – 2.13 (m, 1H), 2.05 – 1.79 (m, 3H), 1.65 – 1.54 (m, 1H). **^{13}C NMR (75 MHz, $CDCl_3$) δ** 205.85 (*C_1*), 55.87, 55.04, 36.33, 22.80, 16.95.

Analytical data was in accordance with literature.[140]

6.3.1.2. SYNTHESIS OF 3-HYDROXYCYCLOHEXAN-1-ONE 9

A dry 50 mL two-neck round-bottom flask charged with diphenyl diselenide (1.80 g, 5.75 mmol, 1.50 equiv.) was evacuated and placed under a constant N_2 flow. EtOH (5.0 mL) was added through the septum by syringe and the flask was then left to stir for 5 min at 30 °C until the diphenyl diselenide was completely dissolved. At this point the solution had an orange colour. Sodium borohydride (0.435 g, 11.5 mmol, 3.00 equiv.) was then slowly added and the flask mixture was left to stir for 5 min at 30 °C to allow for the reduction of diphenyl diselenide. After the reduction, the colour changed to a light-yellow colour, indicating the presence of the active species, $BH_3PhSeNa$. Acetic acid (0.11 mL, 1.9 mmol, 0.50 equiv.) was then added to this flask containing the $BH_3PhSeNa$ species and this mixture was stirred for 5 min. In a separate 100 mL three-neck round-bottom flask, the epoxide, 2,3-epoxycyclohexanone (7-oxabicyclo[4.1.0]heptan-2-one) **8** (0.430 g, 3.84 mmol, 1.00 equiv.) was dissolved in EtOH (5.0 mL) and placed in an ice bath. The solution containing the $BH_3PhSeNa$ species was then slowly added to this cooled solution of the epoxide, 2**,**3-epoxycyclohexanone **8**. The reaction mixture was then left to stir for 4 h at 30 °C. The solution was then diluted with EtOAc (40 mL) and distilled H_2O (40 mL), the layers were separated and the aqueous layer was repeatedly extracted with EtOAc (3 × 100 mL). The combined organic layers were then washed with brine (40 mL), dried over $MgSO_4$, filtered, and concentrated under reduced pressure. The resulting oily residue was purified by flash chromatography (first eluted with Hexane: EtOAc, 95:5 to recover the diphenyl

diselenide (1.62 g, 5.19 mmol, 90% recovered), followed by a gradient elution of Hexane: EtOAc, 80:20 – 50:50). This afforded the pure β-hydroxy ketone **9** as a colourless oil (0.274 g, 2.40 mmol, 63%).

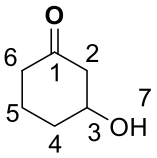

9

R_f = 0.25 (Hexane: EtOAc, 50:50). **^{1}H NMR (300 MHz, $CDCl_3$) δ** 4.18 – 4.10 (m, 1H, *H_3*), 3.09 (bs, 1H, O*H_7*), 2.59 (dd, *^2J* = 14.0, *^3J* = 4.2 Hz, 1H), 2.36 (dd, *^2J* = 14.0, *^3J* = 7.4 Hz, 1H), 2.27 (t, *^3J* = 6.7 Hz, 2H), 2.09 – 1.90 (m, 2H), 1.79 – 1.60 (m, 2H). **^{13}C NMR (75 MHz, $CDCl_3$) δ** 210.75 (*C_1*), 69.68 (*C_3*), 50.39, 40.98, 32.67, 20.72.

Analytical data was in accordance with literature.[140,146]

6.3.1.3. ATTEMPTED SYNTHESIS OF 3-OXOCYCLOHEXYL METHANESULFONATE 10

A solution of 3-hydroxycyclohexan-1-one **9** (0.210 g, 1.84 mmol 1.00 equiv.) in anhydrous DCM (7 mL) was added into a 50 mL two-neck round-bottom flask set up under inert conditions. Thereafter, Et_3N (0.51 mL, 3.7 mmol, 2.0 equiv.) was added by syringe and the solution was left to stir for 5 min. Methanesulfonyl chloride (0.27 mL, 3.5 mmol, 1.9 equiv.) was subsequently added through the septum and the mixture was left to stir for 2 h at RT. Although literature suggests full consumption of the starting material after 1 h, in our hands this was not the case. When monitoring the reaction by TLC, some starting material was still detected after stirring for 2 h at RT. As a result, the reaction mixture was then heated to 30 °C and stirred for another 2 h, after which time, TLC showed complete conversion to the product. Thereafter, distilled H_2O (20 mL) was added, the layers were separated and the aqueous layer was extracted with successive portions of DCM (3 × 50 mL). The combined organic layers were then washed with brine (30 mL), dried over $MgSO_4$, filtered, and concentrated *in vacuo*. However, we were surprised to find the reaction flask practically empty after concentration of the crude residue.

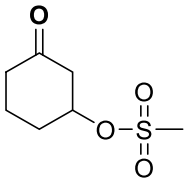

10

6.3.2. SYNTHESIS OF AZIDE 11 IN ONE STEP

6.3.2.1. SYNTHESIS OF 3-AZIDOCYCLOHEXAN-1-ONE 11

Three different methods were explored for this conversion. In the next section, the experimental procedure for each method will be discussed separately and the characterization of **11** will follow.

6.3.2.1.1. First attempted synthesis of 3-azidocyclohexan-1-one 11 (NaN_3)

A two-neck round-bottom flask charged with NaN_3 (0.812 g, 12.5 mmol, 4.00 equiv.) was evacuated and filled with N_2 gas. Distilled H_2O (2.0 mL) was then added to the flask via syringe and the flask was stirred for 10 min to allow the complete dissolution of NaN_3. Glacial acetic acid (0.71 mL, 13 mmol, 4.0 equiv.) was subsequently added and the mixture was stirred for 30 min at RT. After this time, the mixture became a light transparent orange-brown colour. Thereafter, Et_3N (0.087 mL, 0.62 mmol, 0.20 equiv.) was added through the septum, followed by cyclohex-2-en-1-one (**11_{SM}**) (0.30 mL, 3.1 mmol, 1.0 equiv.). After the addition of cyclohex-2-en-1-one (**11_{SM}**) the mixture changed into a light-orange milky colour. The reaction mixture was left to stir at 30 °C for 24 h. After this time, the reaction mixture was a brown suspension.

The R_f values of the starting material, cyclohex-2-en-1-one (**11_{SM}**) and the desired product, 3-azidocyclohexan-1-one **11** was extremely similar, irrespective of the mobile phase used. This made it very difficult to say for certain whether all the starting material was consumed during the course of the reaction. To compensate for this, the reaction time was significantly increased compared to the prescribed time in literature, but it could still not be said with certainty that the reaction was complete. In literature, the pure azido ketone was obtained within 6 h, without any further purification; but in our hands, some starting material was still present even after running the reaction for 24 h. After experimenting with different TLC stains, as well as various combinations of stains, we found that by staining the TLC plate with 10% PPh_3 in DCM, followed by immediate staining with Ninhidrin, the formation of an azide functionality could selectively be detected on the TLC plate.

The reaction was then worked up after 24 h by adding saturated $NaHCO_3$ (20 mL) to the flask, followed by repeated extraction with EtOAc (3 × 50 mL). The combined organic layers were then washed with brine (30 mL), dried over $MgSO_4$, filtered, and concentrated under reduced pressure. After various purification attempts, the pure product, 3-azidocyclohexan-1-one **11**, could unfortunately not be separated from the unreacted starting material, cyclohex-2-en-1-one (**11_{SM}**). The same reaction was also attempted with pyridine as a base instead of Et_3N, but the same problem was encountered.

A second procedure which required $TMSN_3$, along with a polystyrene-supported ammonium fluoride catalyst, namely Amberlite IRA900F, under solvent free conditions, was then investigated.

6.3.2.1.2. Second attempted synthesis of 3-azidocyclohexan-1-one 11 (Amberlite IRA900N_3)

A 50 mL two-neck round-bottom flask charged with Amberlite IRA900F (88.0 mg, 0.263 mmol, 0.250 equiv.) was evacuated and set up under inert conditions. By using a syringe, cyclohex-2-en-1-one (**11$_{SM}$**) (0.11 mL, 1.1 mmol, 1.0 equiv.) was added to the flask, followed by $TMSN_3$ (0.21 mL, 1.6 mmol, 1.5 equiv.). The reaction mixture was left to stir at 30 °C for 18 h. Thereafter, the flask was diluted with EtOAc (20 mL), and the catalyst was recovered by filtration. The organic solvent was then evaporated under vacuum.

This procedure gave the same problem as explained in the first attempted synthesis of 3-azidocyclohexan-1-one **11**, in which residual starting material, cyclohex-2-en-1-one (**11$_{SM}$**) remained present even after a prolonged reaction time. When taking in to account the conversion and purification problems already explained, as well as the cost associated with the Amberlite IRA900F catalyst, a third procedure for this conversion was explored.

6.3.2.1.3. Third attempted synthesis of 3-azidocyclohexan-1-one 11 ($TMSN_3$)

Anhydrous DCM (2.1 mL) was added into a dry two-neck round-bottom flask set up under a N_2 atmosphere. By making use of a syringe, $TMSN_3$ (1.4 mL, 10 mmol, 5.0 equiv.) was then added through the septum, followed by glacial acetic acid (0.60 mL, 10 mmol, 5.0 equiv.). The mixture was left to stir for 20 min, during which the colour of the solution changed from colourless to a milky white colour. Thereafter, cyclohex-2-en-1-one (**11$_{SM}$**) (0.21 mL, 2.1 mmol, 1.0 equiv.) was added by syringe, followed by Et_3N (0.058 mL, 0.42 mmol, 0.20 equiv.). The reaction mixture was left to stir over the weekend at RT and after this time the flask contained a dark brown solution.

In the literature procedure, the crude reaction mixture was directly applied to a silica plug and eluted with a solution of Hexane: EtOAc, 55:45. During various attempts to obtain the pure product, the DCM was removed by evaporation and the crude mixture was dry loaded onto the column. Purification was attempted with varying gradients of Hexane: EtOAc, 95:5 – 50:50. Even under these varied purification conditions, it was still not possible to separate the desired product, azidocyclohexan-1-one **11** from the unreacted starting material, cyclohex-2-en-1-one (**11$_{SM}$**).

Evaluation by way of NMR spectroscopy showed a 5:1 ratio of product, 3-azidocyclohexan-1-one **11** to residual starting material, cyclohex-2-en-1-one (**11$_{SM}$**) under these conditions.

Please note that the following NMR assignment has a slightly different style compared to the previous assignments in this document. This is due to the residual inseparable starting material present in this sample. It is important to keep in mind that the desired product is in a 5 to 1 ratio with the residual starting material. This means that while one proton of **11** will accurately integrate for 1H, one proton of **11$_{SM}$** will only integrate for 0.2H.

To explain the style used, the first assignment of the ^{1}H NMR assignment will act as an example. The first different seen in the assignment is the style in which the integration is given. The '1H' refers to the number of protons responsible for this peak, while the integration given in brackets as '∫=0.2H' refers to the accurate integration obtained from the NMR spectrum due to the product to starting material ratio, as explained above.

The second difference seen in this style is the compound number given after the atom assignment. For example, $H_{3(\mathbf{11SM})}$ means this peak resulted from the proton atom number 3 of the residual starting material, compound **11$_{SM}$**.

5:1 Ratio

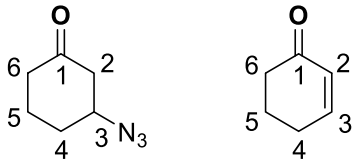

11 **11$_{SM}$**

R$_f$ (11) = 0.44 (Hexane: EtOAc, 80:20), **R$_f$ (11$_{SM}$)** = 0.44 (Hexane: EtOAc, 80:20).
R$_f$ (11) = 0.68 (Hexane: EtOAc, 50:50). **R$_f$ (11$_{SM}$)** = 0.70 (Hexane: EtOAc, 50:50).
R$_f$ (11) = 0.61 (Hexane: EtOAc, 25:75). **R$_f$ (11$_{SM}$)** = 0.68 (Hexane: EtOAc, 25:75).

^{1}H NMR (400 MHz, CDCl$_3$) δ 6.99 – 6.95 (m, 1H(∫=0.2H), $H_{3(\mathbf{11SM})}$), 6.01 – 5.97 (m, 1H(∫=0.2H), $H_{2(\mathbf{11SM})}$), 3.90 – 3.84 (m, 1H, $H_{3(\mathbf{11})}$), 2.62 (dd, ^{3}J = 14.3, ^{4}J = 4.6 Hz, 1H, $H_{2a(\mathbf{11})}$), 2.43 – 2.30 (m, 7H(∫=3.8H), 2 × $H_{6(\mathbf{11SM})}$ and 2 × $H_{6(\mathbf{11})}$ and 2 × $H_{4(\mathbf{11SM})}$ and $H_{2b(\mathbf{11})}$), 2.10 – 2.01 (m, 4H(∫=2.4H), 2 × $H_{5(\mathbf{11SM})}$ and $H_{5b(\mathbf{11})}$ and $H_{4a(\mathbf{11})}$), 1.84 – 1.66 (m, 2H, $H_{5a(\mathbf{11})}$ and $H_{4b(\mathbf{11})}$). **^{13}C NMR (101 MHz, CDCl$_3$) δ** 207.55 ($C_{1(\mathbf{11})}$), 199.78 ($C_{1(\mathbf{11SM})}$), 150.74 ($C_{3(\mathbf{11SM})}$), 129.97 ($C_{2(\mathbf{11SM})}$), 59.61 ($C_{3(\mathbf{11})}$), 46.66 ($C_{2(\mathbf{11})}$), 40.75 ($C_{6(\mathbf{11})}$), 38.17 ($C_{6(\mathbf{11SM})}$), 29.87 ($C_{4(\mathbf{11})}$), 25.74 ($C_{4(\mathbf{11SM})}$), 22.80 ($C_{5(\mathbf{11SM})}$), 21.47 ($C_{5(\mathbf{11})}$).

Analytical data was in accordance with literature.[151,152]

Because the conversion from cyclohex-2-en-1-one (**11$_{SM}$**) into 3-azidocyclohexan-1-one **11** could not be quantified due to the purification problems encountered; it was decided that the inseparable 3-azidocyclohexan-1-one **11** mixture would be would be used directly in the next step. This is possible because the residual 2-cyclohexen-1-one would not interfere with the following step, as it has no functionalities that could be utilized in the click reaction.

6.3.3. SYNTHESIS OF 3-(4-PENTYL-1*H*-1,2,3-TRIAZOL-1-YL)CYCLOHEXAN-1-ONE 12

Due to the problems encountered during the purification of the desired azide **11**, the inseparable azide mixture from two of the azidation methods discussed above was directly used for the copper-mediated click reaction using the optimized conditions.

6.3.3.1. FIRST SYNTHESIS OF 3-(4-PENTYL-1*H*-1,2,3-TRIAZOL-1-YL)CYCLOHEXAN-1-ONE 12

A two-neck round-bottom flask charged with NaN_3 (0.812 g, 12.5 mmol, 4.00 equiv.) was evacuated and filled with N_2 gas. Distilled H_2O (2.0 mL) was then added to the flask via syringe and the flask was stirred to allow all NaN_3 to dissolve. Glacial acetic acid (0.71 mL, 13 mmol, 4.0 equiv.) was subsequently added and the mixture was stirred for 30 min. After this time, the mixture became a light transparent orange-brown colour. Thereafter, Et_3N (0.22 mL, 1.6 mmol, 0.50 equiv.) was added through the septum, followed by cyclohex-2-en-1-one (0.30 mL, 3.1 mmol, 1.0 equiv.). After the addition of cyclohex-2-en-1-one, the mixture changed into a light-orange milky colour. The reaction mixture was left to stir for 24 h at 30 °C. After this time, the reaction mixture was a brown suspension. The mixture was quenched with $NaHCO_3$ (25 mL) and repeatedly extracted with EtOAc (3 × 70 mL). The combined organic layers were then washed with NH_4Cl (20 mL) and brine (20 mL), dried over $MgSO_4$, filtered, and concentrated under reduced pressure, to obtain the crude intermediate, 3-azidocyclohexan-1-one **11** as a brown oil. The inseparable mixture was then directly used in the copper-mediated click reaction. Copper(II) acetate (170 mg, 0.936 mmol, 0.300 equiv.) was added into a two-neck round-bottom flask, followed by distilled H_2O (2.0 mL). The flask was then evacuated under high vacuum, and placed under a N_2 atmosphere. MeOH (2.0 mL) was then added into the flask, followed by the alkyne 1-heptyne (0.41 mL, 3.1 mmol, 1.0 equiv.). The flask was allowed to stir for 10 min. The crude azide, 3-azidocyclohexan-1-one **11**, dissolved in MeOH (2.0 mL) was subsequently added into the flask via syringe and the reaction mixture was left to stir for 24 h at 30 °C. Upon completion (monitored by TLC), the MeOH was removed under reduced pressure, diluted with EtOAc (20 mL) and washed with a saturated NH_4Cl solution (50 mL). The aqueous layer was extracted with EtOAc (3 × 100 mL) and the combined organic layers were washed with brine, dried over $MgSO_4$, filtered, and concentrated *in vacuo*. The crude product was purified by column chromatography (Hexane: EtOAc, 90:10 – 50:50) to obtain the pure product **12** as a white solid (0.260 mg, 1.10 mmol, 35%, yield over two steps, based on cyclohex-2-en-1-one).

6.3.3.2. SECOND SYNTHESIS OF 3-(4-PENTYL-1*H*-1,2,3-TRIAZOL-1-YL)CYCLOHEXAN-1-ONE 12

Anhydrous DCM (3.2 mL) was added into a dry two-neck round-bottom flask set up under a N_2 atmosphere. By making use of a syringe, $TMSN_3$ (2.1 mL, 16 mmol, 5.0 equiv.) was then added through the septum followed by glacial acetic acid (0.90 mL, 16 mmol, 5.0 equiv.). The mixture was left to stir for 20 min, during which time the colour of the solution changed from colourless to a milky white colour. Thereafter, cyclohex-2-en-1-one (0.30 mL, 3.1 mmol, 1.0 equiv.) was added by syringe followed by Et_3N (0.087 mL, 0.62 mmol, 0.20 equiv.), and the reaction mixture was left to stir for 24 h at RT. After this time, the flask contained a dark brown solution. The reaction mixture was concentrated under reduced pressure to obtain the crude intermediate 3-azidocyclohexan-1-one **11** as a brown oil. The crude azide, 3-azidocyclohexan-1-one **11** was then directly used in the CuAAC

reaction. Copper(II) acetate (170 mg, 0.936 mmol, 0.300 equiv.) was added into a two-neck round-bottom flask, followed by distilled H_2O (2.0 mL). The flask was then evacuated under high vacuum, and placed under a nitrogen atmosphere. MeOH (2.0 mL) was then added into the flask, followed by the alkyne, 1-heptyne (0.41 mL, 3.1 mmol, 1.0 equiv.). The flask was then allowed to stir for 10 min allowing coordination of the alkyne to the copper catalyst. The crude azide, 3-azidocyclohexan-1-one **11**, dissolved in MeOH (2.0 mL), was subsequently added into the flask via syringe and the reaction mixture was then left to stir for 24 h at 30 °C. Upon completion, the MeOH was removed under reduced pressure, diluted with EtOAc (20 mL) and washed with a saturated NH_4Cl solution (50 mL). The aqueous layer was extracted with EtOAc (3 × 100 mL) and the combined organic layers were washed with brine (50 mL), dried over $MgSO_4$, filtered, and concentrated *in vacuo*. The crude product was purified by column chromatography (Hexane: EtOAc, 90:10 – 50:50) to obtain the pure product **12** as a white solid (0.280 mg, 1.19 mmol, 38%, yield over two steps, based on cyclohex-2-en-1-one).

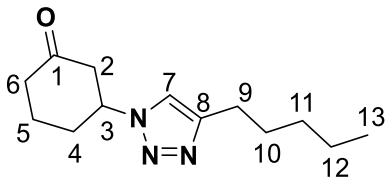

12

R_f = 0.39 (Hexane: EtOAc, 50:50). **MP** 51 – 53 °C. **^{1}H NMR (300 MHz, $CDCl_3$) δ** 7.27 (s, 1H, *H_7*), 4.83 – 4.73 (m, 1H, *H_3*), 3.03 – 2.65 (m, 4H, 2 × *H_2* and 2 × *H_6*), 2.55 – 1.61 (m, 8H), 1.42 – 1.27 (m, 4H), 0.89 (t, ^3J = 7.0 Hz, 3H, 3 × *H_{13}*). **^{13}C NMR (75 MHz, $CDCl_3$) δ** 206.82 (*C_1*), 148.58 (*C_8*), 119.12 (*C_7*), 58.74 (*C_3*), 47.59 (*C_2*), 40.69 (*C_6*), 31.90, 31.61, 29.26 (*C_4*), 25.81, 22.55, 21.88 (*C_5*), 14.14 (*C_{13}*). **HRMS-TOF MS ES+: m/z [M+H]** calcd for $C_{13}H_{22}N_3O^+$: 236.1763; found 236.1768.

6.3.4. SYNTHESIS OF 3-(5-PENTYL-1*H*-1,2,3-TRIAZOL-1-YL)CYCLOHEXAN-1-ONE 13

A two-neck round-bottom flask charged with NaN_3 (0.812 g, 12.5 mmol, 4.00 equiv.) was evacuated and filled with N_2. Distilled H_2O (2.0 mL) was then added to the flask via syringe and the flask was stirred for 10 min to allow all NaN_3 to dissolve. Glacial acetic acid (0.71 mL, 13 mmol, 4.0 equiv.) was subsequently added and the mixture was stirred for 30 min. After this time, the mixture became a light transparent orange-brown colour. Next, by Et_3N (0.22 mL, 1.6 mmol, 0.50 equiv.) was added through the septum, followed by 2-cyclohexen-1-one (0.30 mL, 3.1 mmol, 1.0 equiv.). After the addition of 2-cyclohexen-1-one, the mixture changed into a light-orange milky colour. The reaction mixture was left to stir for 24 h at 30 °C. After this time, the reaction mixture was a brown suspension. The reaction mixture was quenched with $NaHCO_3$ (50 mL) and extracted with EtOAc (3 × 100 mL). The combined organic layers were then washed with NH_4Cl (40 mL) and brine (40 mL), dried over $MgSO_4$, filtered, and concentrated under reduced pressure to obtain the crude azidocyclohexan-1-one **11** as a brown oil. The crude product **11** was then directly used in the RuAAC reaction. A dry

Schlenk tube was evacuated under high vacuum and placed under a nitrogen atmosphere. Anhydrous dioxane (8.0 mL) was then added to this Schlenk tube by syringe. The solvent was then degassed by 5 cycles of the freeze-pump-thaw technique. The Schlenk tube was then purged with N_2 gas for 5 min, followed by the addition of the catalyst Cp*RuCl(COD) (47.4 mg, 0.125 mmol, 4 mol%) under inert conditions. The tube was once again purged with N_2 gas for 5 min before adding the alkyne, 1-heptyne (0.41 mL, 3.1 mmol, 1.0 equiv.) into the flask by syringe. After another round of N_2 purging, the crude azide, azidocyclohexan-1-one **11** was added under positive N_2 pressure. After a final N_2 purge, the reaction mixture was left to stir at 60 °C for 24 h. The reaction mixture was then wet loaded directly onto a silica gel column and purified by flash column chromatography over silica gel (Hexane: EtOAc, 90:10 – 50:50). Under these conditions, we recovered a substantial amount of the crude azide, azidocyclohexan-1-one **11** (0.164 g, 1.18 mmol, 38%, based on the theoretical yield of **11** before the click reaction) and obtained the desired 1,5-disubstituted product **13** in a 2 to 1 ratio with the 1,4-disubstituted product **12**, as determined by way of NMR evaluation, (0.0383 g, 0.163 mmol, 5%, combined yield of **13** and **12** in a 2:1 ratio).

NMR spectra 23 and 24, found in Appendix 1, were used to characterize these two products **12** and **13**. The numbered structures of **12** and **13** are depicted in Figure 3:4. These atom numbers will be referred to during the NMR spectroscopy discussion below.

Please note that the NMR assignment below is once again given in a different style. The style used is the same as explained in section 6.3.2.1.3. The desired product **13** is present in a 2 to 1 ratio with the regioisomer **12**, meaning that while one proton of **13** will accurately integrate for 1H, one proton of **12** will only integrate for 0.5H. Although this style was already explained, a brief explanation will be given here:

The second peak (7.27 ppm) of the ^{1}H NMR assignment will act as an example. The ‘1H’ refers to the number of protons responsible for this peak, while the integration given in brackets as ‘∫=0.5H’ refers to the accurate integration obtained from the NMR spectrum due to the ratio of the two products, as explained above. In addition, the compound number is given after the atom assignment, in this case, $H_{7(\mathbf{12})}$ means this peak resulted from the proton atom number 7 of compound **12**.

1:2 Ratio

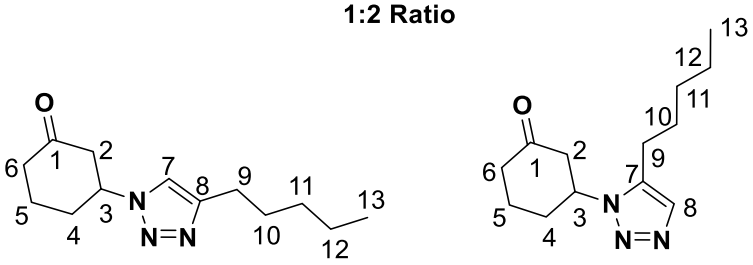

12 **13**

R_f = 0.37 (Hexane: EtOAc, 50:50). **^{1}H NMR (400 MHz, $CDCl_3$) δ** 7.45 (s, 1H, $H_{8(13)}$), 7.27 (s, 1H(∫=0.5H), $H_{7(12)}$), 4.83 – 4.73 (m, 1H(∫=0.5H), $H_{3(12)}$), 4.52 – 4.42 (m, 1H, $H_{3(13)}$), 3.24 – 2.67 (m, 6H(∫=4H), 2 × $H_{6(13)}$ and 2 × $H_{2(12)}$ and 2 × $H_{6(12)}$), 2.61 – 2.56 (m, 2H, 2 × $H_{2(13)}$), 2.51 – 1.61 (m,16H(∫=12H)), 1.38 – 1.31 (m, 8H(∫=6H)), 0.90 (m, 6H(∫=4.5H), 3 × $H_{13(12)}$ and 3 × $H_{13(13)}$). **^{13}C NMR (101 MHz, $CDCl_3$) δ** 207.16 ($C_{1(13)}$), 206.85 ($C_{1(12)}$), 148.56 ($C_{8(12)}$), 136.46 ($C_{7(13)}$), 132.12 ($C_{8(13)}$), 119.13 ($C_{7(12)}$), 58.74 ($C_{3(12)}$), 55.99 ($C_{3(13)}$), 47.85 ($C_{2(13)}$), 47.56 ($C_{2(12)}$), 40.68 ($C_{6(12)}$), 40.58 ($C_{6(13)}$), 31.87, 31.71, 31.60, 31.41, 29.24 ($C_{4(12)}$), 28.05 ($C_{4(13)}$), 25.78, 23.14, 22.54, 22.41, 22.13 ($C_{5(13)}$), 21.86 ($C_{5(12)}$), 14.13 ($C_{13(12)}$), 14.02 ($C_{13(13)}$). **HRMS-TOF MS ES+: m/z [M+H]** calcd for $C_{13}H_{22}N_3O^+$: 236.1763; found 236.1770.

6.3.5. SYNTHESIS OF 3-(4-PENTYL-1*H*-1,2,3-TRIAZOL-1-YL)CYCLOHEXAN-1-OL 14

Anhydrous THF (4.0 mL) was added into a 50 mL two-neck round-bottom flask charged with $LiAlH_4$ (0.100 g, 2.64 mmol, 3.00 equiv.) under a constant N_2 flow. The click product **12** (0.207 g, 0.879 mmol, 1.00 equiv.) dissolved in an additional amount of THF (6.0 mL) was added to the flask containing the $LiAlH_4$ solution. The reaction mixture was heated to 60 °C (oil-bath) under reflux for 1 h. Thereafter the oil bath was removed and the flask was allowed to cool while stirring for an additional 1 h. At this point, the reaction mixture was grey in colour. Upon completion, the mixture was quenched with distilled H_2O (15 mL). The H_2O was added drop-wise to dampen the resulting vigorous reaction. During the quenching process, the colour of the reaction mixture changed from grey to white. The aqueous solution was subsequently extracted with successive portions of EtOAc (3 × 60 mL). The combined organic layers were washed with brine (30 mL), dried over $MgSO_4$, filtered and concentrated *in vacuo*. The crude mixture was then purified by silica gel column chromatography (Hexane: DCM, 90:10 – 50:50) to obtain the pure product **14** as a white solid (0.183 g, 0.771 mmol, 88%).

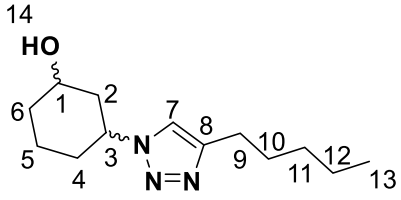

14

R_f = 0.27 (Hexane: EtOAc, 50:50). **^{1}H NMR (300 MHz, cdcl$_3$) δ** 7.27 (s, 1H, *H_7*), 4.52 – 4.40 (m, 1H, *H_3*), 3.86 – 3.73 (m, 1H, *H_1*), 2.75 – 2.41 (m, 4H, incl. O*H_{14}*), 2.20 – 2.06 (m, 2H), 1.98 – 1.90 (m, 1H), 1.82 – 1.29 (m, 10H), 0.88 (t, ^3J = 7.0 Hz, 3H, 3 × *H_{13}*).**^{13}C NMR (75 MHz, CDCl$_3$) δ** 148.32 (*C_8*), 118.39 (*C_7*), 68.97 (*C_1*), 58.11 (*C_3*), 42.17 (*C_2*), 34.56 (*C_6*), 32.75, 31.60, 29.26 (*C_4*), 25.82, 22.54, 21.88 (*C_5*), 14.12 (*C_{13}*).

6.4. Synthesis of Scaffold C

6.4.1. Synthesis of (1*R*,2*S*,5*R*)-2-isopropyl-5-methylcyclohexyl methanesulfonate 15

A 50 mL two-neck round-bottom flask loaded with (1*R*,2*S*,5*R*)-2-Isopropyl-5-methylcyclohexanol, (–)-menthol (0.562 g, 3.60 mmol, 1.00 equiv.) was evacuated and set up under inert conditions. Anhydrous DCM (8.0 mL) was added by syringe, followed by triethylamine (0.60 mL, 4.3 mmol, 1.2 equiv.) and the flask was cooled to 0 °C (ice-bath). While maintaining the temperature at 0 °C, methanesulfonyl chloride (0.34 mL, 4.3 mmol, 1.2 equiv.) was added slowly through the septum. The flask was then removed from the ice-bath and allowed to warm up to RT, and stirred for 3 h. During the addition of methanesulfonyl chloride, the reaction mixture formed a white precipitate and upon completion the flask contained a yellow precipitate. After the specified reaction time, the reaction residue was partitioned between distilled H_2O (30 mL) and DCM (30 mL). The layers were separated and the aqueous layer was extracted with consecutive portions of DCM (3 × 100 mL). The combined organic layers were washed with brine, dried over $MgSO_4$, filtered and concentrated under reduced pressure. After purification by silica gel column chromatography (Hexane: DCM, 90:10 – 50:50), the pure product **15** was obtained as a colourless oil (0.754 g, 3.22 mmol, 89%).

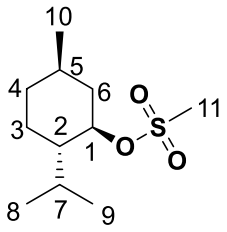

15

R_f = 0.46 (Hexane: EtOAc, 90:10). **^{1}H NMR (300 MHz, CDCl$_3$) δ** 4.55 (td, ^3J = 10.9, 4.6 Hz, 1H, *H_1*), 3.00 (s, 3H, 3 × *H_{11}*), 2.30 – 2.23 (m, 1H), 2.14 – 2.00 (m, 1H), 1.76 – 1.64 (m, 2H), 1.47 – 1.37 (m, 2H), 1.32 – 1.21 (m, 1H), 1.13 – 0.99 (m, 1H), 0.93 (dd at 0.93, ^3J = 6.7, ^4J =2.5 Hz, 6H, 3 × *H_8* and 3 × *H_9*), 0.91 – 0.85 (m, 1H, *H_{3a}*), 0.83 (d, ^3J = 7.0 Hz, 3H, 3 × *H_{10}*). **^{13}C NMR (75 MHz, CDCl$_3$) δ** 83.55 (C_1), 47.59, 42.39, 39.26, 33.92, 31.80, 25.96, 23.26, 22.00, 20.96, 15.84.

Analytical data was in accordance with literature.[156]

6.4.2. SYNTHESIS OF (1*S*,2*S*,4*R*)-2-AZIDO-1-ISOPROPYL-4-METHYLCYCLOHEXANE 16

A 50 mL two-necked round-bottom flask charged with (1*R*,2*S*,5*R*)-2-isopropyl-5-methylcyclohexyl methanesulfonate **15** (0.204 g, 0.871 mmol, 1.00 equiv.) was evacuated and filled with N_2. Anhydrous DMSO (4.0 mL) was then added through the septum, followed by sodium azide (0.283 g, 4.35 mmol, 5.00 equiv.). The reaction mixture was then heated to 80 °C (oil-bath) and the flask was allowed to stir for 24 h under inert conditions. Upon complete consumption of the starting material (monitored by TLC), the reaction residue was decanted into a beaker of cold water (30 mL), and the aqueous layer was extracted with successive portions of EtOAc (3 x 70 mL). The combined organic layers were washed with cold water (3 x) and then with brine, dried over $MgSO_4$, filtered and concentrated *in vacuo*. The residue was purified by flash chromatography (Hexane: EtOAc, 90:10). This afforded the pure product **16** as a light-yellow oil (0.0642 g, 0.354 mmol, 41%).

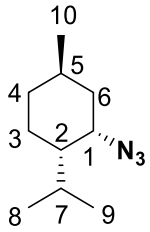

16

R_f = 0.85 (Hexane: EtOAc, 90:10). **^{1}H NMR (300 MHz, $CDCl_3$) δ** 3.99 – 3.96 (m, 1H, H_1), 2.05 – 1.97 (m, 1H, H_2), 1.77 – 1.10 (m, 7H), 1.01 – 0.80 (m, 4H), 0.89 (d, ^3J = 6.7 Hz, 6H, 3 × H_8 and 3 × H_9). **^{13}C NMR (75 MHz, $CDCl_3$) δ** 60.69 (C_1), 47.51 (C_2), 39.08, 34.99, 29.64, 26.67, 25.04, 22.32, 21.05, 20.82.

Analytical data was in accordance with literature.[156]

6.4.3. SYNTHESIS OF (1*S*,2*S*,4*R*)-2-CHLORO-1-ISOPROPYL-4-METHYLCYCLOHEXANE 17

A two-neck 50 mL round-bottom flask was setup under inert conditions and (1*R*,2*S*,5*R*)-2-Isopropyl-5-methylcyclohexanol, (-)-menthol (0.316 g, 2.02 mmol, 1.00 equiv.), as well as triphenylphosphine (1.06 g, 4.04 mmol, 2.00 equiv.) was added under constant N_2 flow. CCl_4 (2.5 mL) was then added through the septum and the reaction flask was heated to 80 °C under reflux for 16 h. After cooling to RT, hexane (100 mL) was added, and the white precipitate of triphenylphosphine oxide was removed by filtration. The filtrate was then cooled and the newly precipitated triphenylphosphine oxide was removed by filtration. The solvent was removed under reduced pressure, and purified by flash column chromatography (Hexane: EtOAc, 90:10). This afforded the pure product **17** as a colourless oil (0.160 g, 0.916 mmol, 45%).

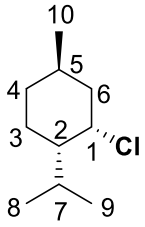

17

R_f = 0.87 (Hexane: EtOAc, 95:5). **^{1}H NMR (300 MHz, $CDCl_3$) δ** 4.58 – 4.46 (m, 1H, H_1), 2.10 – 2.02 (m, 1H, H_2), 2.00 – 0.99 (m, 7H), 0.96 – 0.90 (m, 7H), 0.88 (d, ^3J = 7.0 Hz, 3H, 3 × H_{10}). **^{13}C NMR (75 MHz, $CDCl_3$) δ** 63.58 (C_1), 49.12 (C_2), 43.44, 34.99, 30.21, 26.03, 24.42, 22.03, 20.94, 20.33.

Analytical data was in accordance with literature.[156]

6.4.4. Attempted synthesis of (1*S*,2*R*,4*R*)-2-azido-1-isopropyl-4-methylcyclohexane 18

A 50 mL two-necked round-bottom flask was charged with (1*S*,2*S*,4*R*)-2-chloro-1-isopropyl-4-methylcyclohexane **17** (0.150 g, 0.859 mmol, 1.00 equiv.) and placed under an inert atmosphere. Anhydrous DMSO (4.0 mL) was then added by syringe, followed by sodium azide (0.279 g, 4.29 mmol, 5.00 equiv.). The reaction mixture was then heated to 80 °C (oil-bath) and the flask was allowed to stir for 24 h under inert conditions. Unfortunately, under these conditions, no conversion was observed by TLC. The reaction residue was decanted into a beaker of cold water (30 mL), and the aqueous layer was extracted with DCM (3 x 70 mL). The combined organic layers were washed with brine, dried over $MgSO_4$, filtered and concentrated *in vacuo* to recover the starting material **17**.

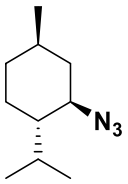

18

6.4.5. Synthesis of 1-[(1*S*,2*S*,5*R*)-2-isopropyl-5-methylcyclohexyl]-4-pentyl-1*H*-1,2,3-triazole 19

Copper(II) acetate (19.3 mg, 0.106 mmol, 0.300 equiv.) was added into a two-neck round-bottom flask, followed by distilled H_2O (1.0 mL). The flask was then evacuated under high vacuum, and placed under a N_2 atmosphere. MeOH (1.0 mL) was then added to the flask via syringe, followed by the alkyne, 1-heptyne (0.047 mL, 0.35 mmol, 1.0 equiv.). The flask was then allowed to stir for 10 min. The azide, (1*S*,2*S*,4*R*)-2-azido-1-isopropyl-4-methylcyclohexane **16** (64.2 mg, 0.354 mmol, 1.00 equiv.), dissolved in MeOH (1 mL) was subsequently added into the flask via syringe and the reaction mixture was then left to stir for 24 h at 30 °C. Upon completion (monitored by TLC), the

MeOH was removed under reduced pressure, diluted with EtOAc (20 mL) and washed with a saturated NH_4Cl solution (50 mL). The aqueous layer was extracted with EtOAc (3 × 100 mL) and the combined organic layers were washed with brine, dried over $MgSO_4$, filtered and concentrated *in vacuo*. The crude product was purified by column chromatography (Hexane: EtOAc, 90:10 – 50:50) to obtain the pure product **19** as a white solid (20.9 mg, 0.0753 mmol, 21%)

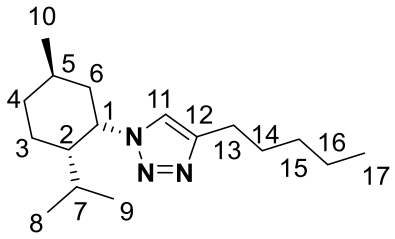

19

R_f = 0.25 (Hexane: EtOAc, 50:50). **MP** 85 – 87 °C. **^{1}H NMR (300 MHz, $CDCl_3$) δ** 7.33 (s, 1H, H_{11}), 5.02 – 4.95 (m, 1H, H_1), 2.70 (t, ^3J = 7.8, 2H, 2 × H_{13}), 1.97 – 1.30 (m, 14H), 0.93 – 0.81 (m, 10H), 0.77 (d, ^3J = 6.6 Hz, 3H, 3 × H_{17}). **^{13}C NMR (75 MHz, $CDCl_3$) δ** 121.68 (C_{11}), 58.97 (C_1), 46.88 (C_2), 41.02, 34.83, 31.69, 29.31, 29.28, 26.61, 25.83, 25.17, 22.57, 22.46, 21.29, 20.66, 14.19 (C_{17}). **HRMS-TOF MS ES+: m/z [M+H]** calcd for $C_{17}H_{32}N_3^+$: 278.2596; found 278.2600.

APPENDIX 1

NUCLEAR MAGNETIC RESONANCE SPECTROSCOPY RESULTS

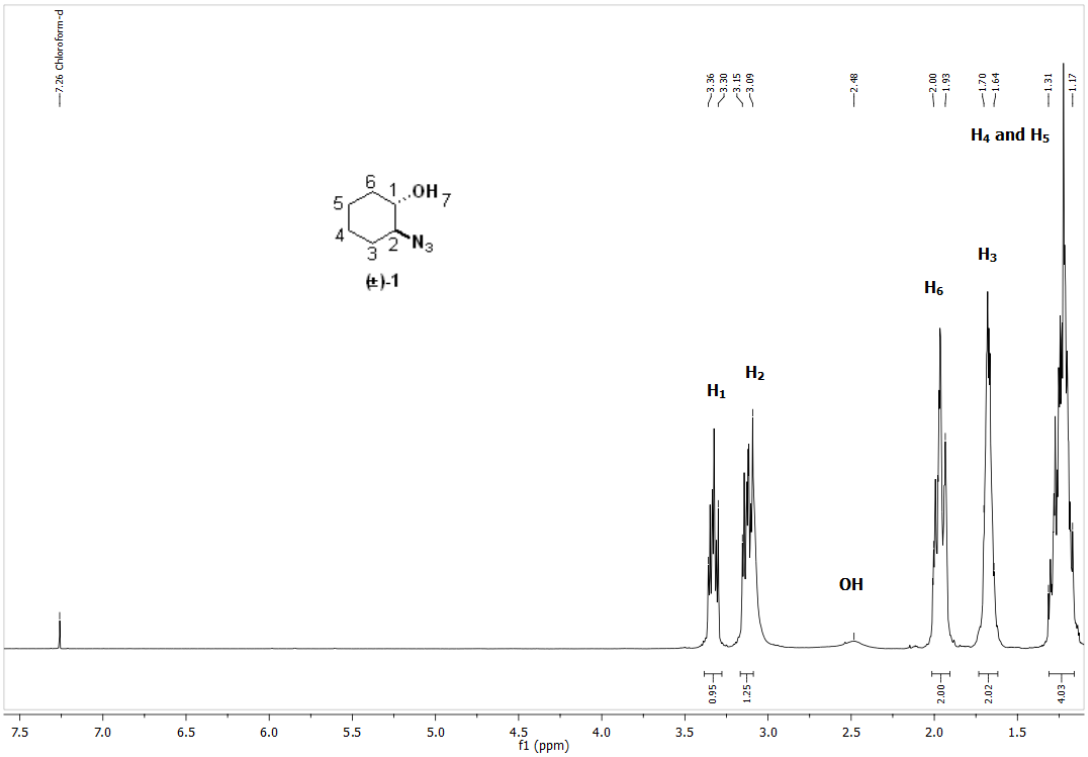

CBD NMR Spectrum 1 ^{1}H NMR spectrum of (±)-*trans*-2-azidocyclohexan-1-ol 1.

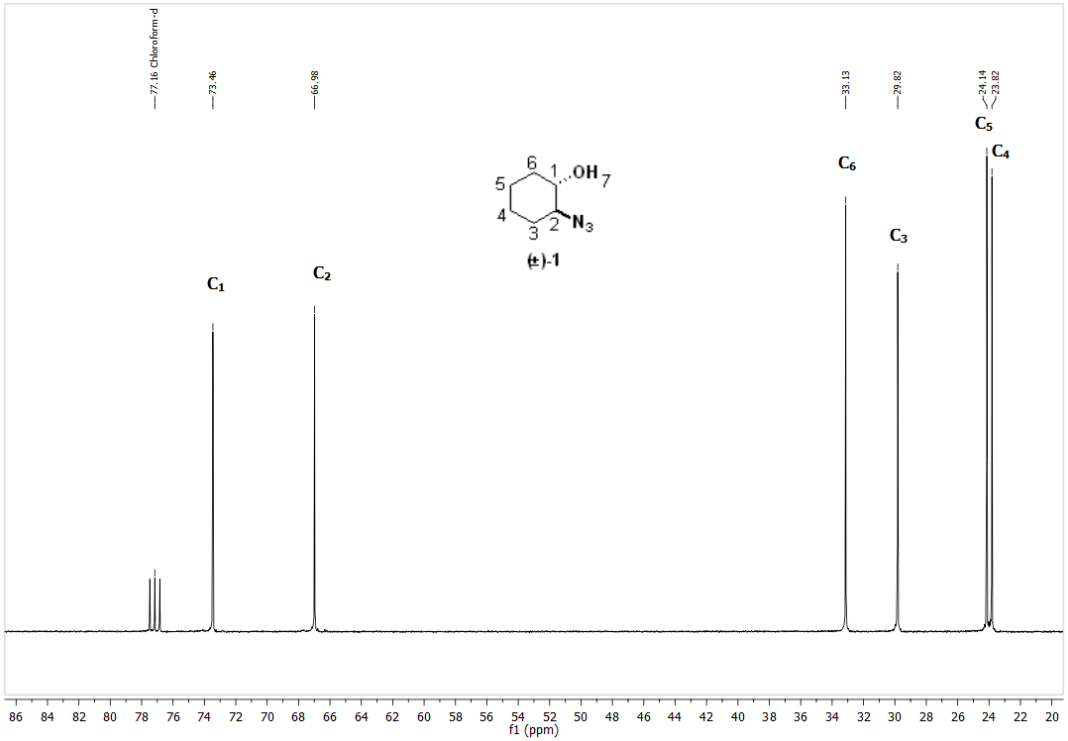

CBD NMR Spectrum 2 ^{13}C NMR spectrum of (±)-*trans*-2-azidocyclohexan-1-ol 1.

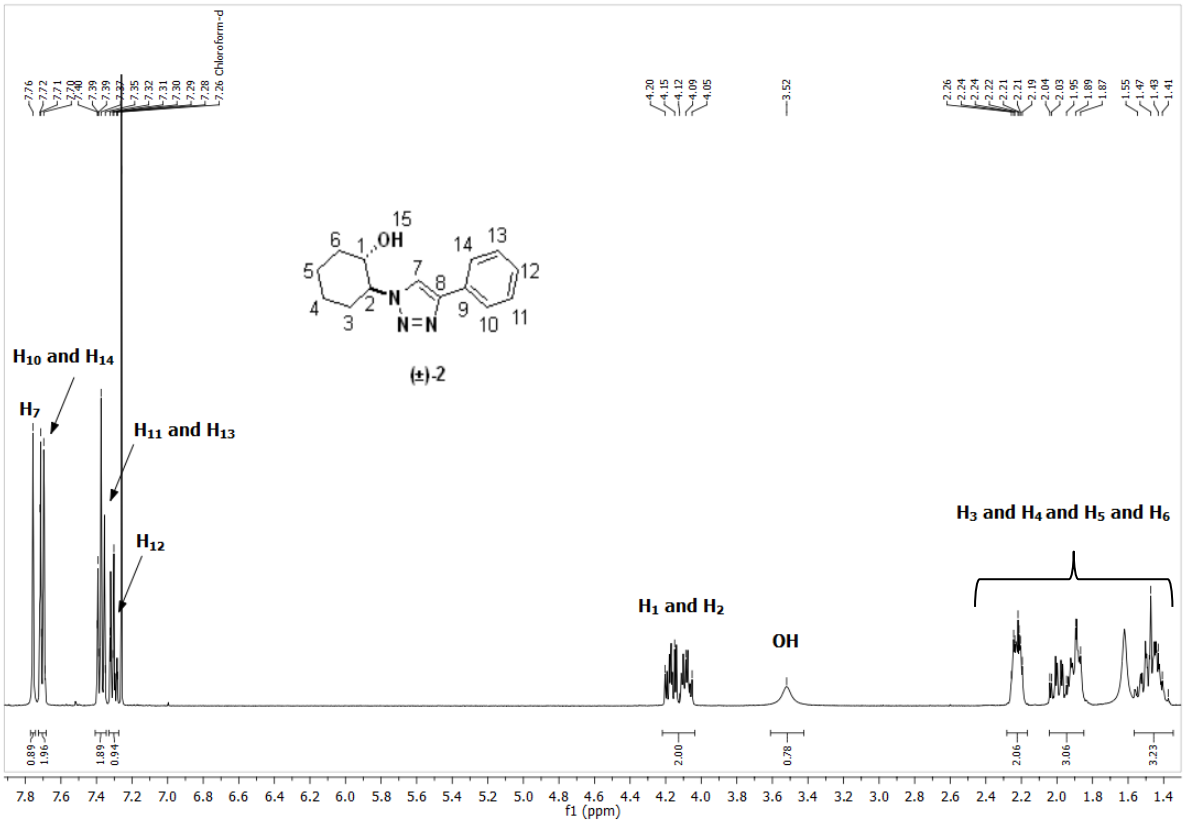

CBD NMR Spectrum 3 **^{1}H NMR spectrum of (±)-*trans*-2-(4-phenyl-1*H*-1,2,3-triazol-1-yl)cyclohexan-1-ol 2.**

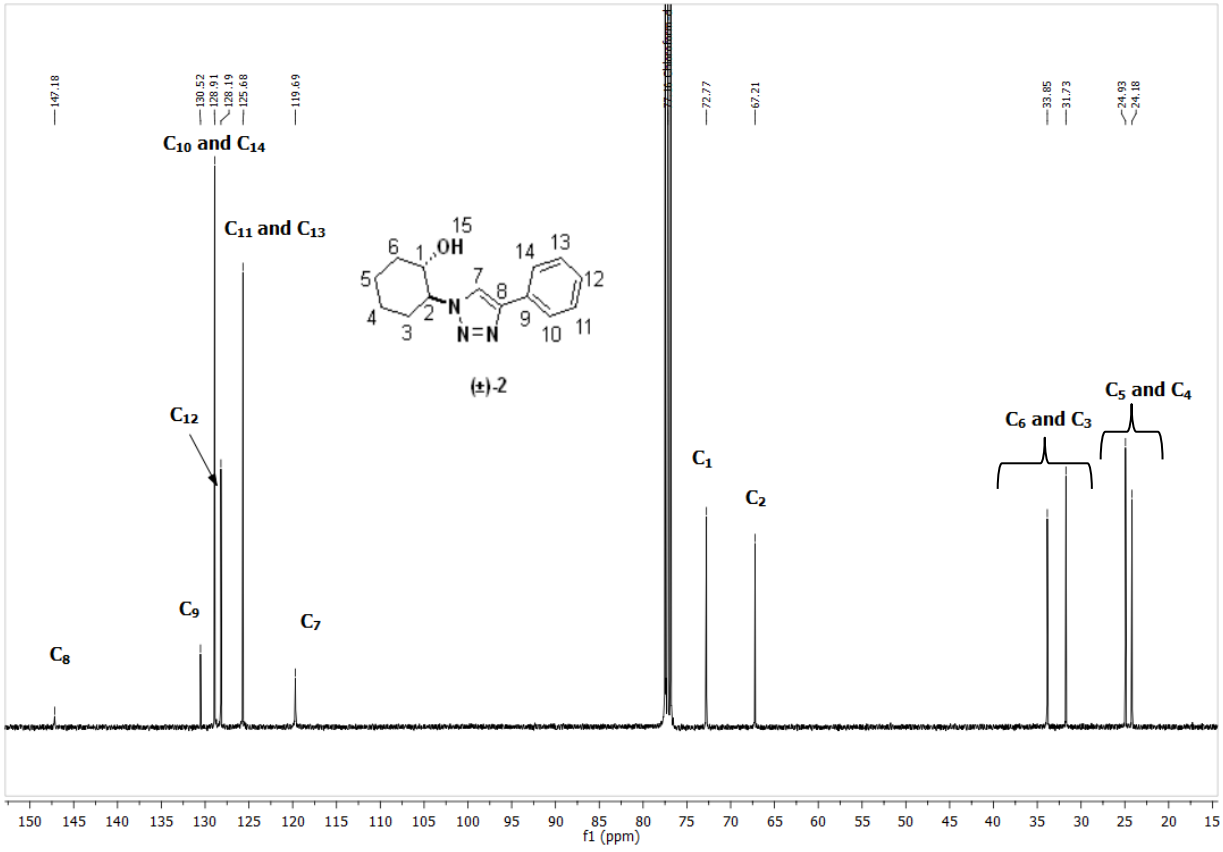

CBD NMR Spectrum 4 **^{13}C NMR spectrum of (±)-*trans*-2-(4-phenyl-1*H*-1,2,3-triazol-1-yl)cyclohexan-1-ol 2.**

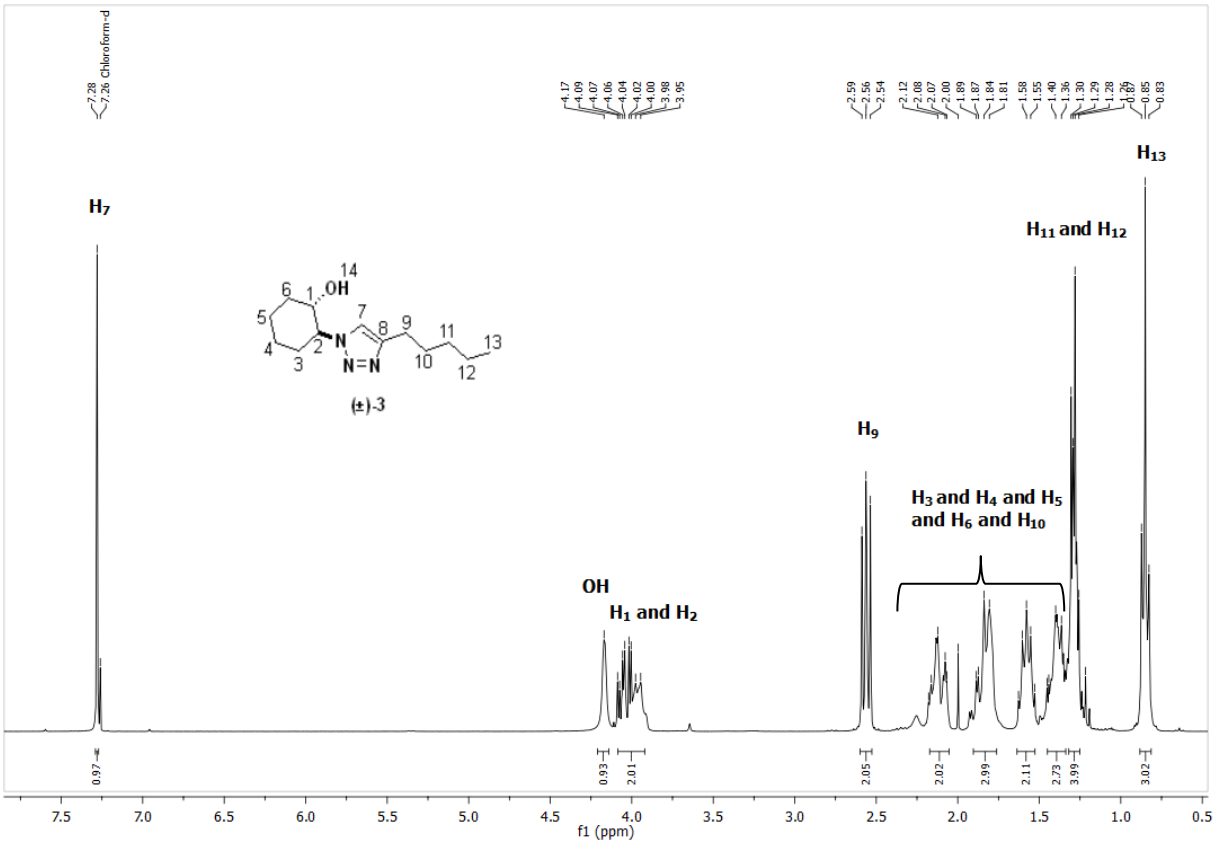

CBD NMR Spectrum 5 ^{1}H NMR spectrum of (±)-*trans*-2-(4-pentyl-1*H*-1,2,3-triazol-1-yl)cyclohexan-1-ol 3.

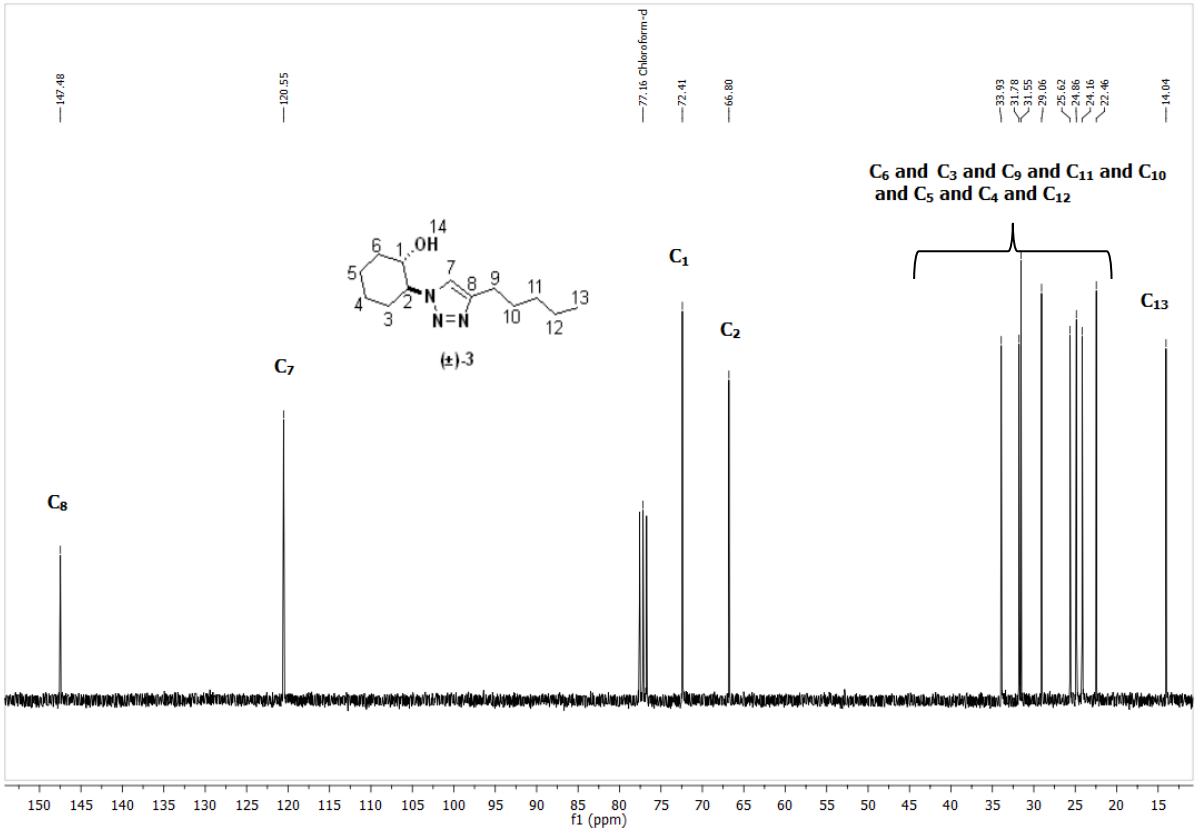

CBD NMR Spectrum 6 ^{13}C NMR spectrum of (±)-*trans*-2-(4-pentyl-1*H*-1,2,3-triazol-1-yl)cyclohexan-1-ol 3.

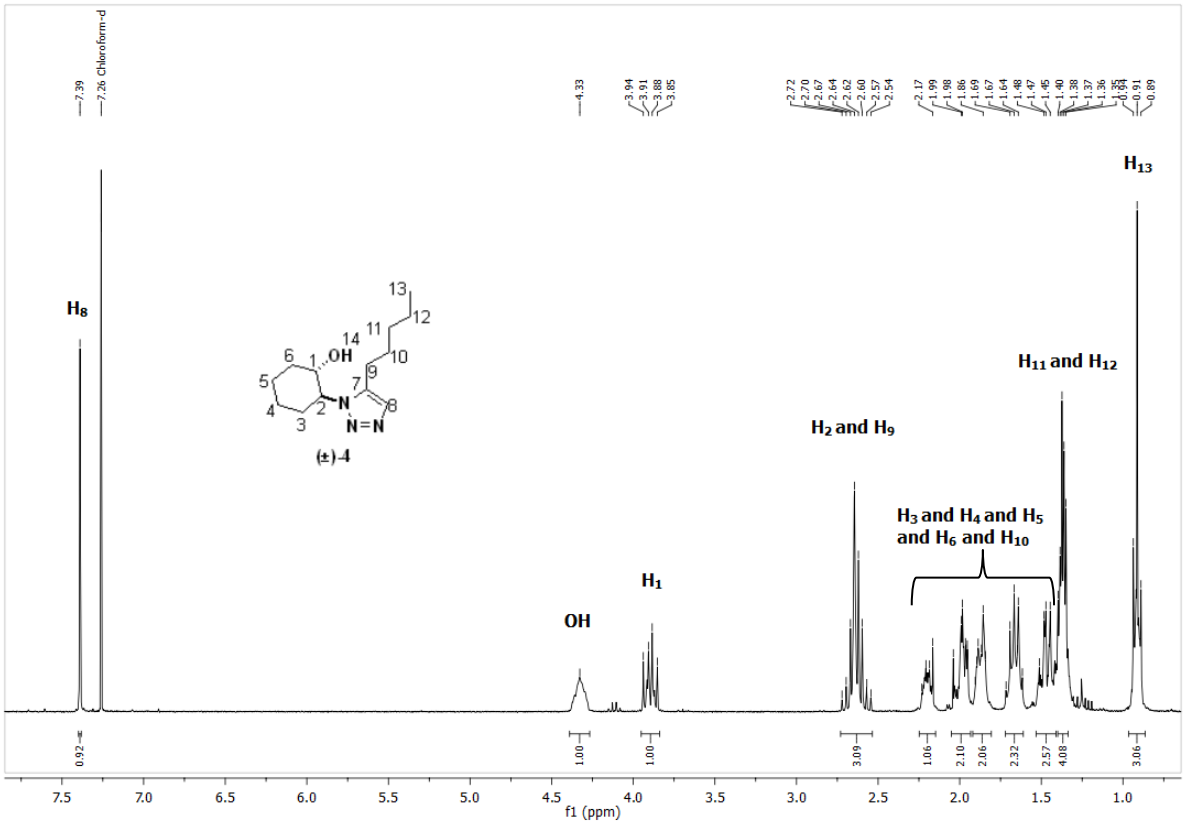

CBD NMR Spectrum 7 **^{1}H NMR spectrum of (±)-*trans*-2-(5-pentyl-1*H*-1,2,3-triazol-1-yl)cyclohexan-1-ol 4.**

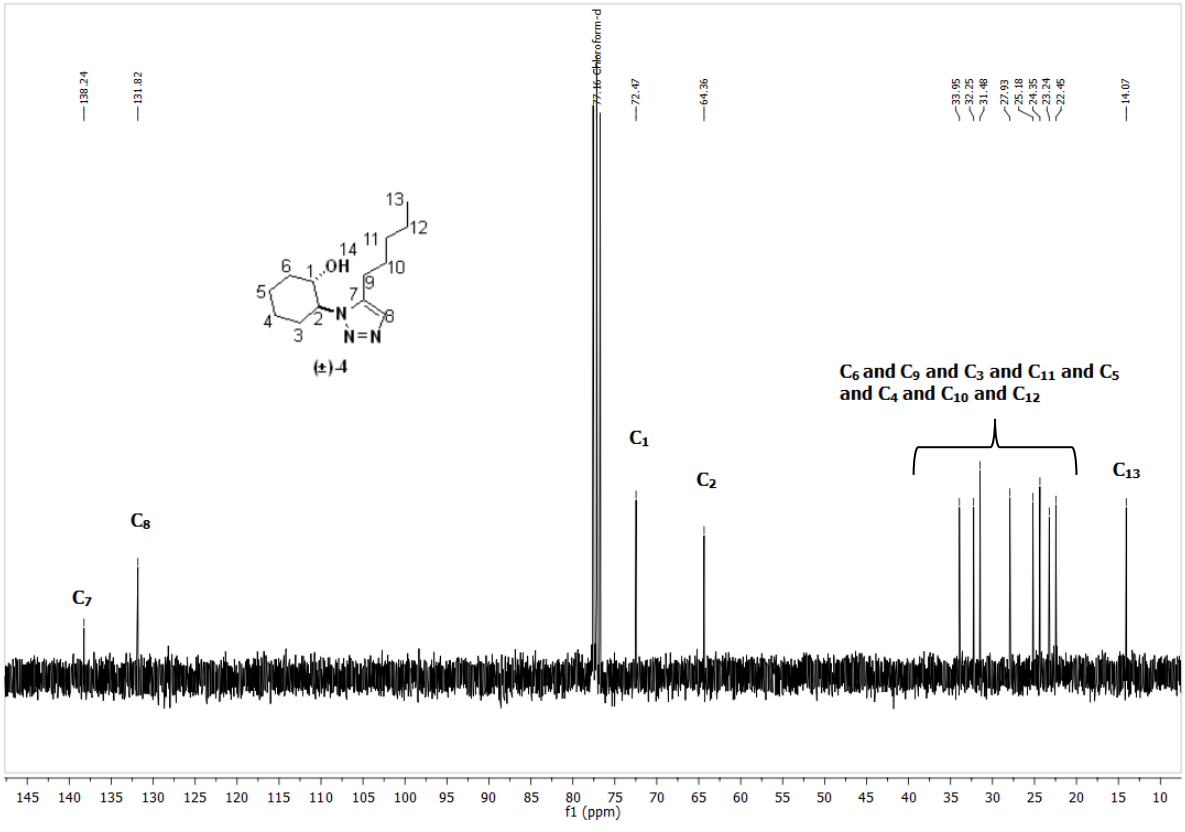

CBD NMR Spectrum 8 **^{13}C NMR spectrum of (±)-*trans*-2-(5-pentyl-1*H*-1,2,3-triazol-1-yl)cyclohexan-1-ol 4.**

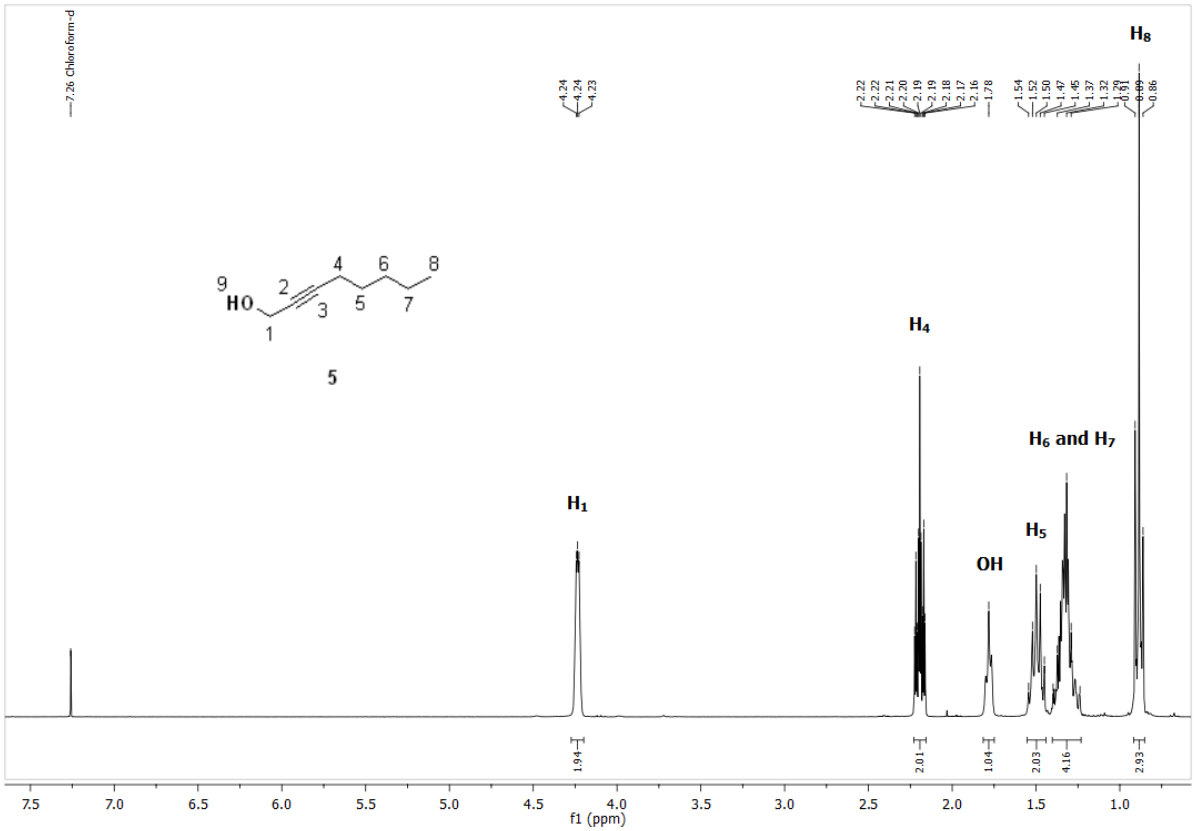

5

CBD NMR Spectrum 9 ^{1}H NMR spectrum of internal alkyne, oct-2-yn-1-ol 5.

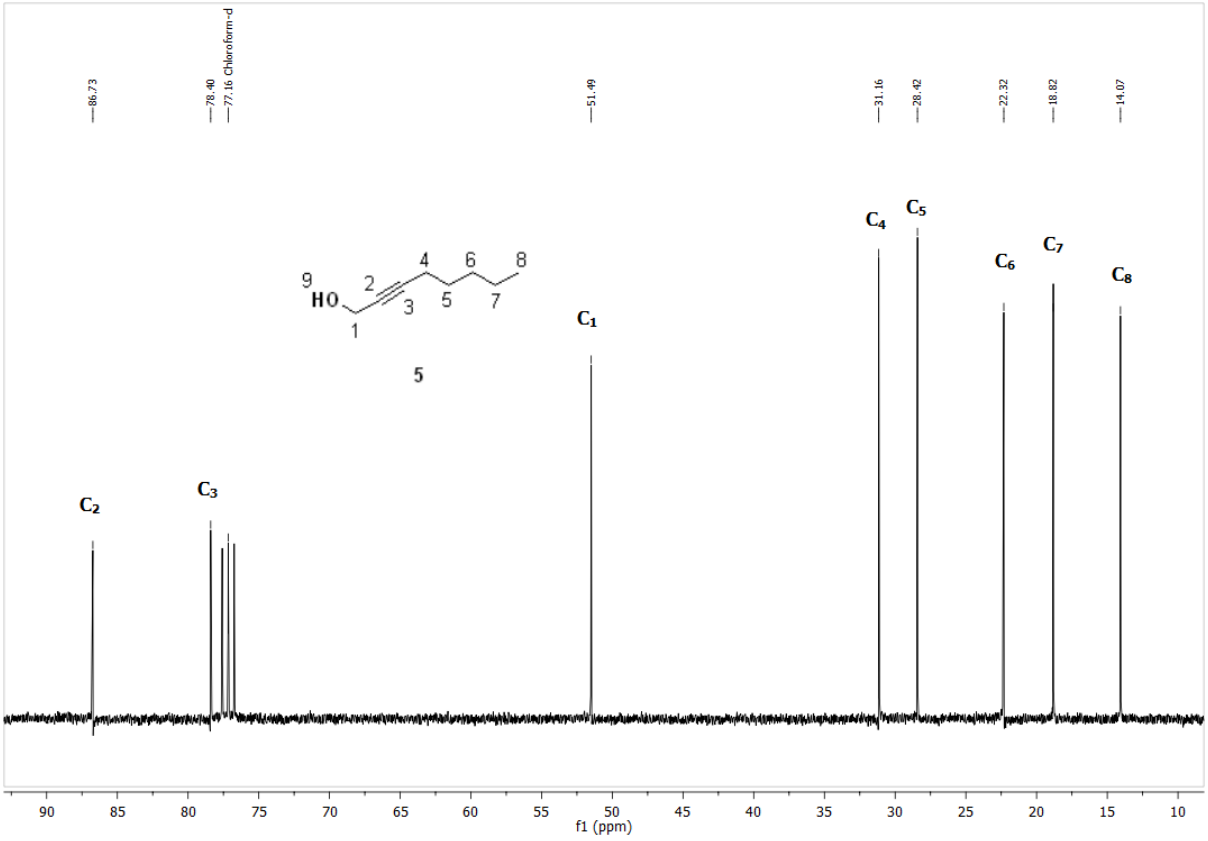

5

CBD NMR Spectrum 10 ^{13}C NMR spectrum of internal alkyne, oct-2-yn-1-ol 5.

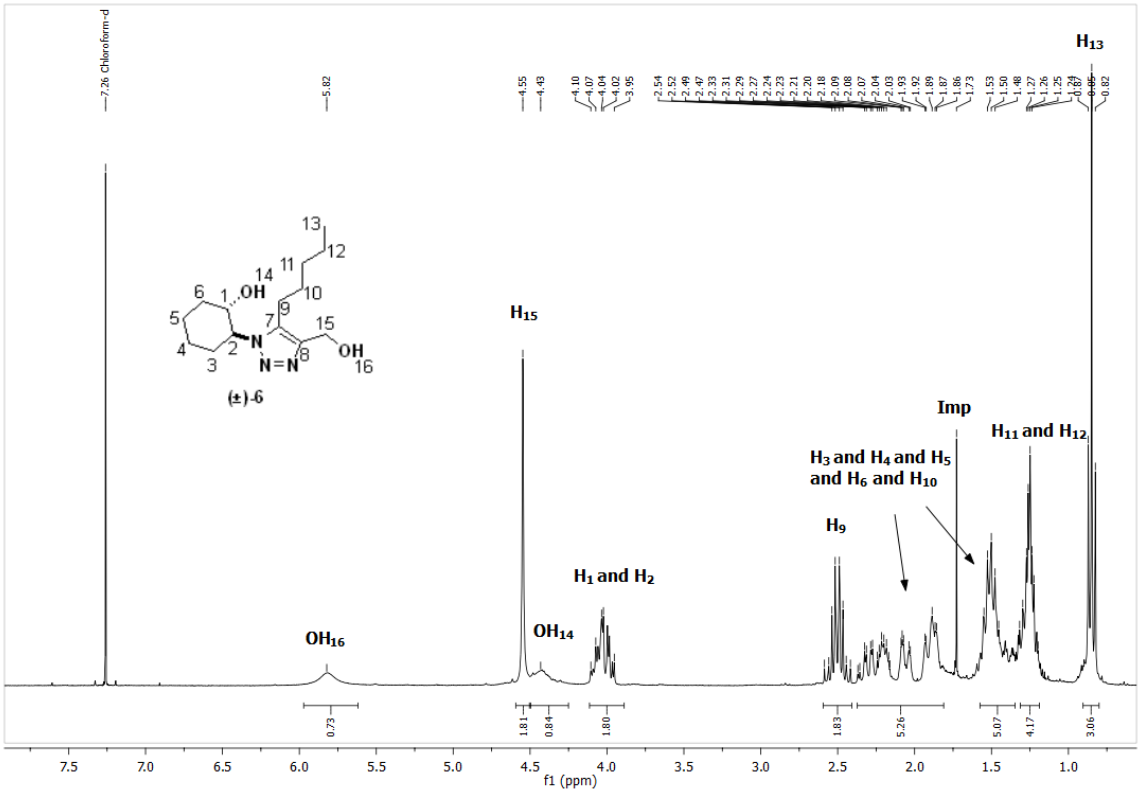

CBD NMR Spectrum 11 **^{1}H NMR spectrum of (±)-*trans*-2-[4-(hydroxymethyl)-5-pentyl-1*H*-1,2,3-triazol-1-yl]cyclohexan-1-ol 6.**

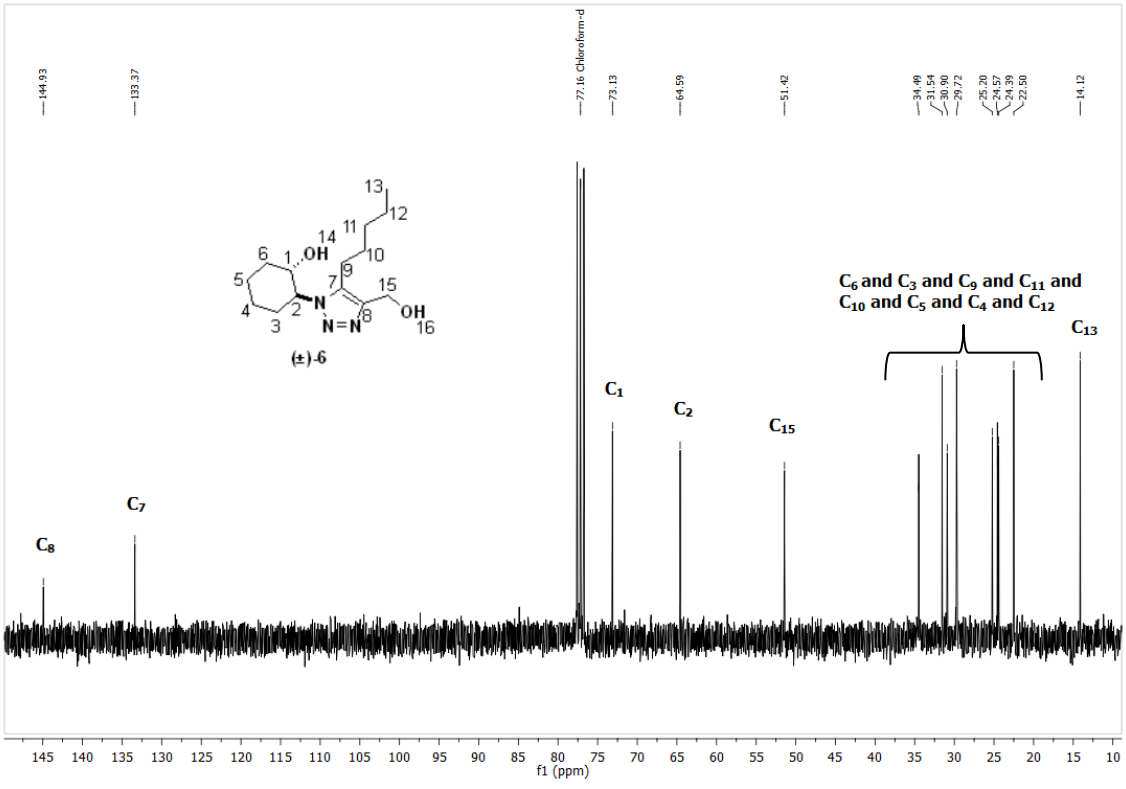

CBD NMR Spectrum 12 **^{13}C NMR spectrum of (±)-*trans*-2-[4-(hydroxymethyl)-5-pentyl-1*H*-1,2,3-triazol-1-yl]cyclohexan-1-ol 6.**

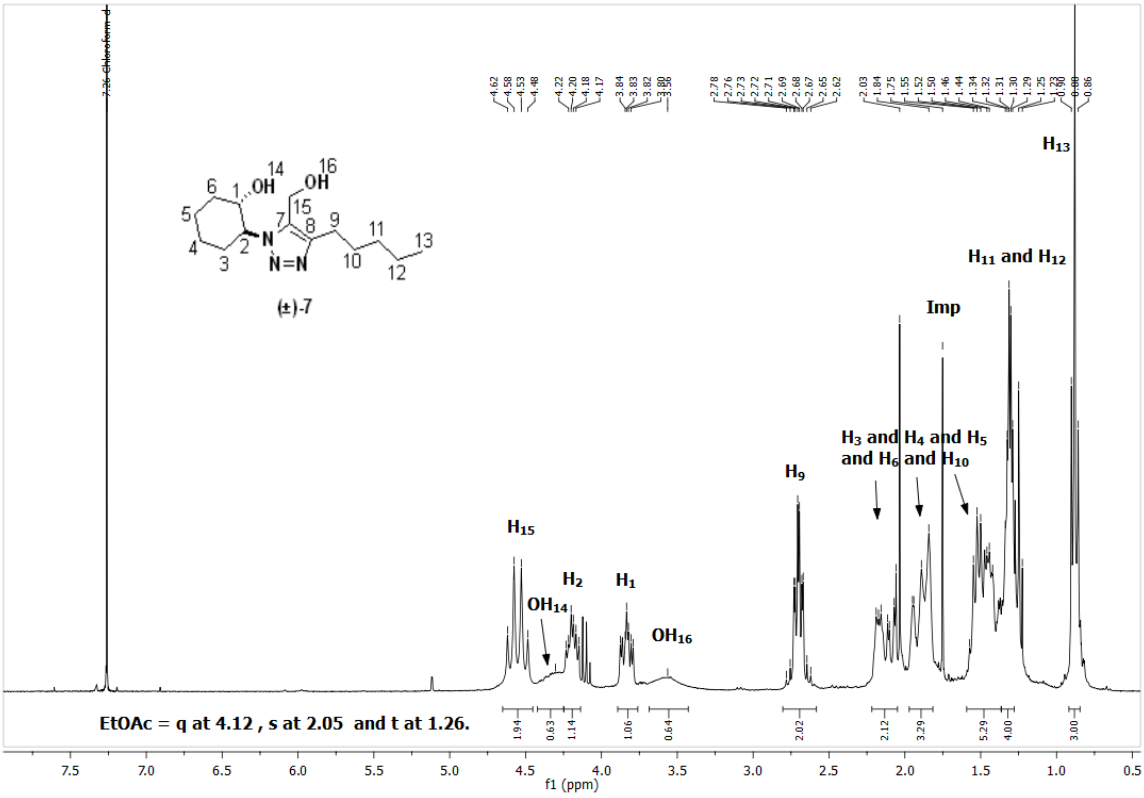

CBD NMR Spectrum 13 **^{1}H NMR spectrum of (±)-*trans*-2-[5-(hydroxymethyl)-4-pentyl-1*H*-1,2,3-triazol-1-yl]cyclohexan-1-ol 7.**

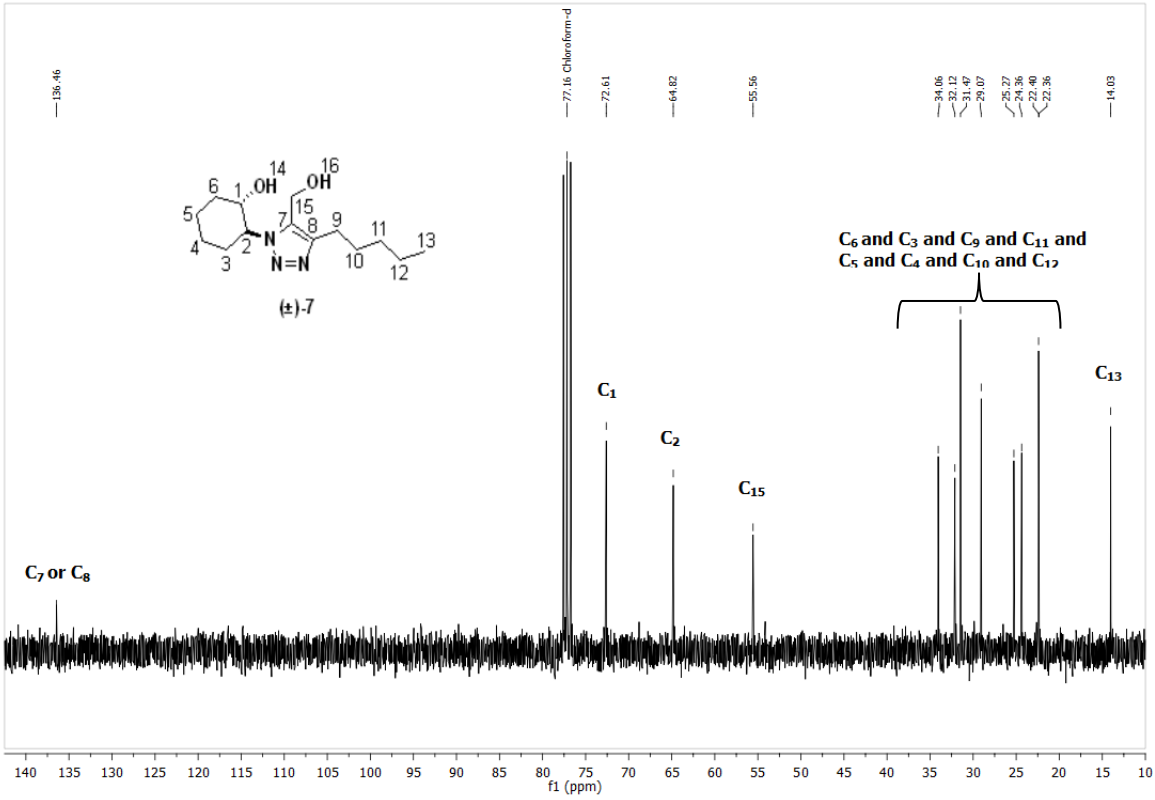

CBD NMR Spectrum 14 **^{13}C NMR spectrum of (±)-*trans*-2-[5-(hydroxymethyl)-4-pentyl-1*H*-1,2,3-triazol-1-yl]cyclohexan-1-ol 7.**

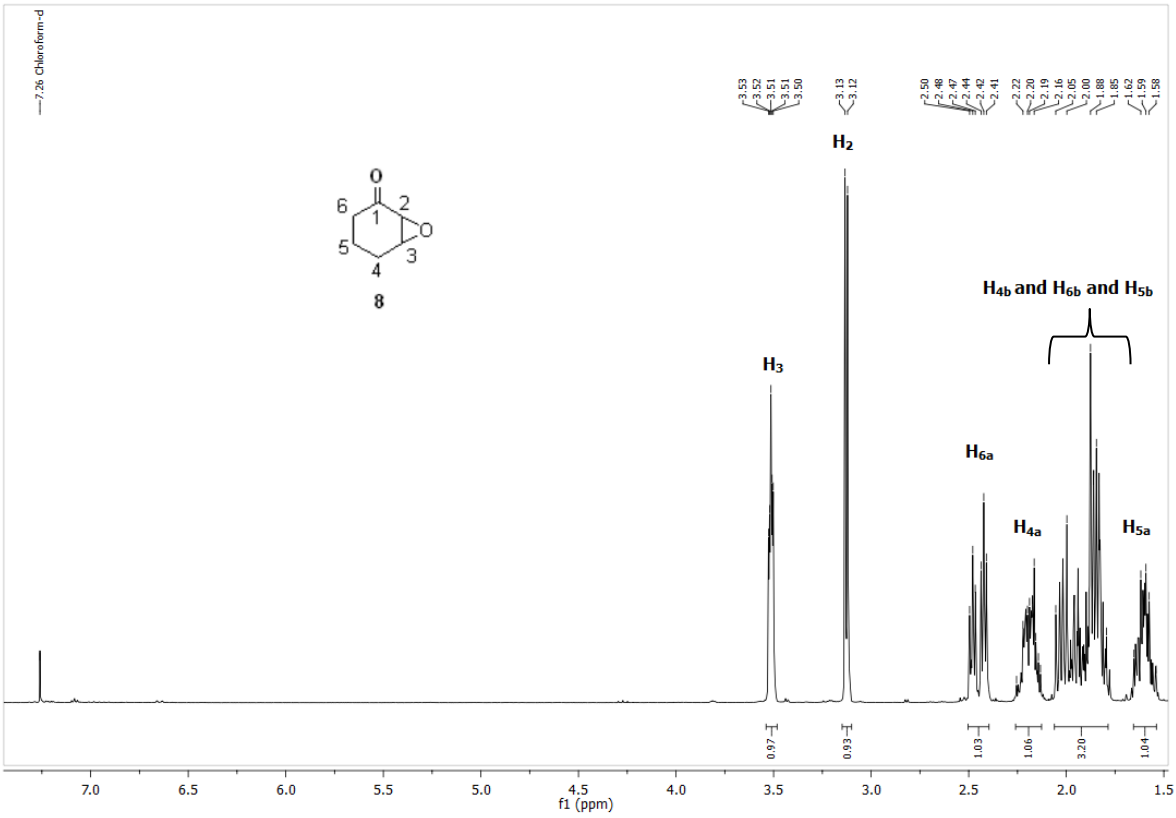

CBD NMR Spectrum 15 ^{1}**H NMR spectrum of 2,3-epoxycyclohexanone, (7-oxabicyclo[4.1.0]heptan-2-one) 8.**

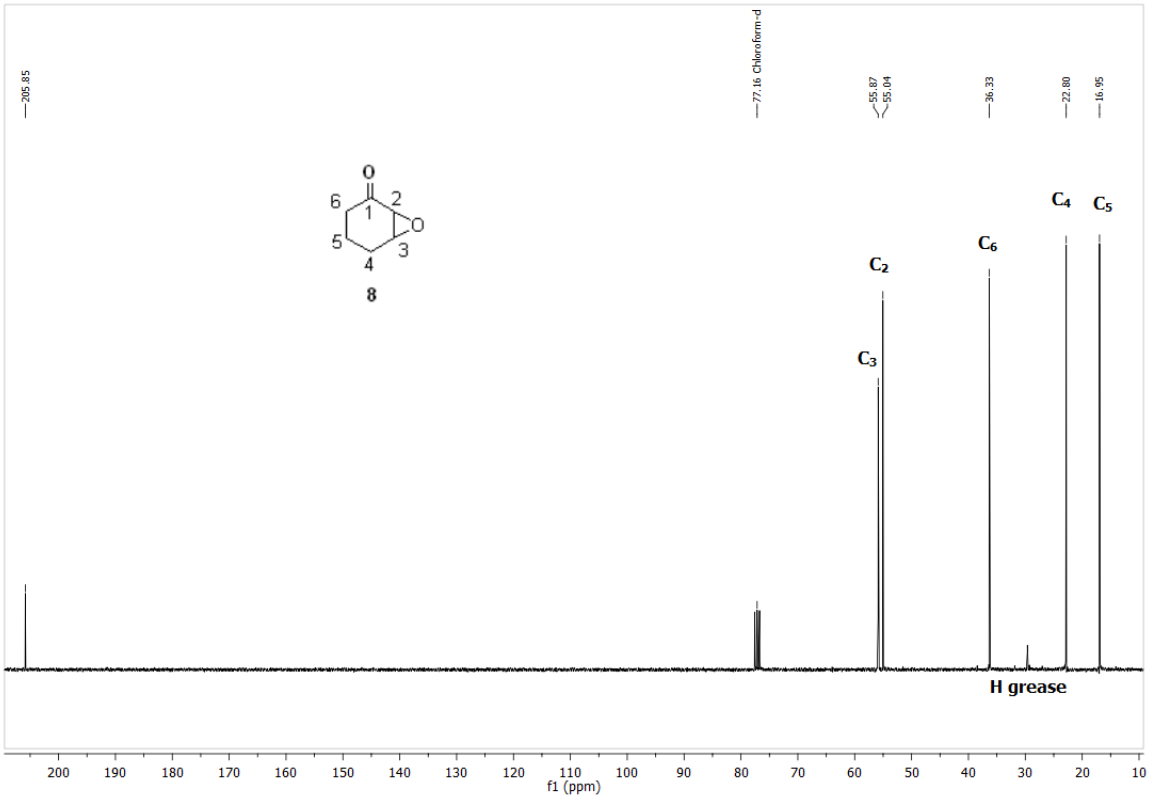

CBD NMR Spectrum 16 ^{13}**C NMR spectrum of 2,3-epoxycyclohexanone, (7-oxabicyclo[4.1.0]heptan-2-one) 8.**

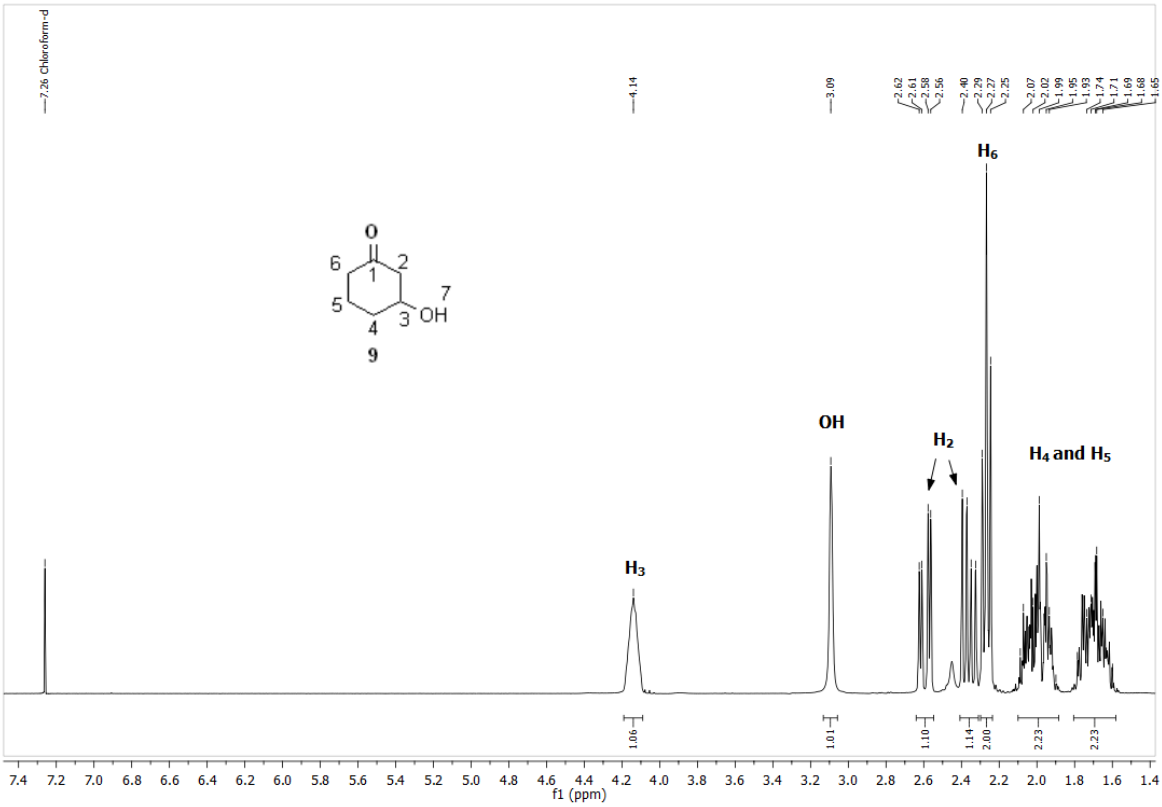

NMR Spectrum 17 ^{1}H NMR spectrum of 3-hydroxycyclohexan-1-one 9.

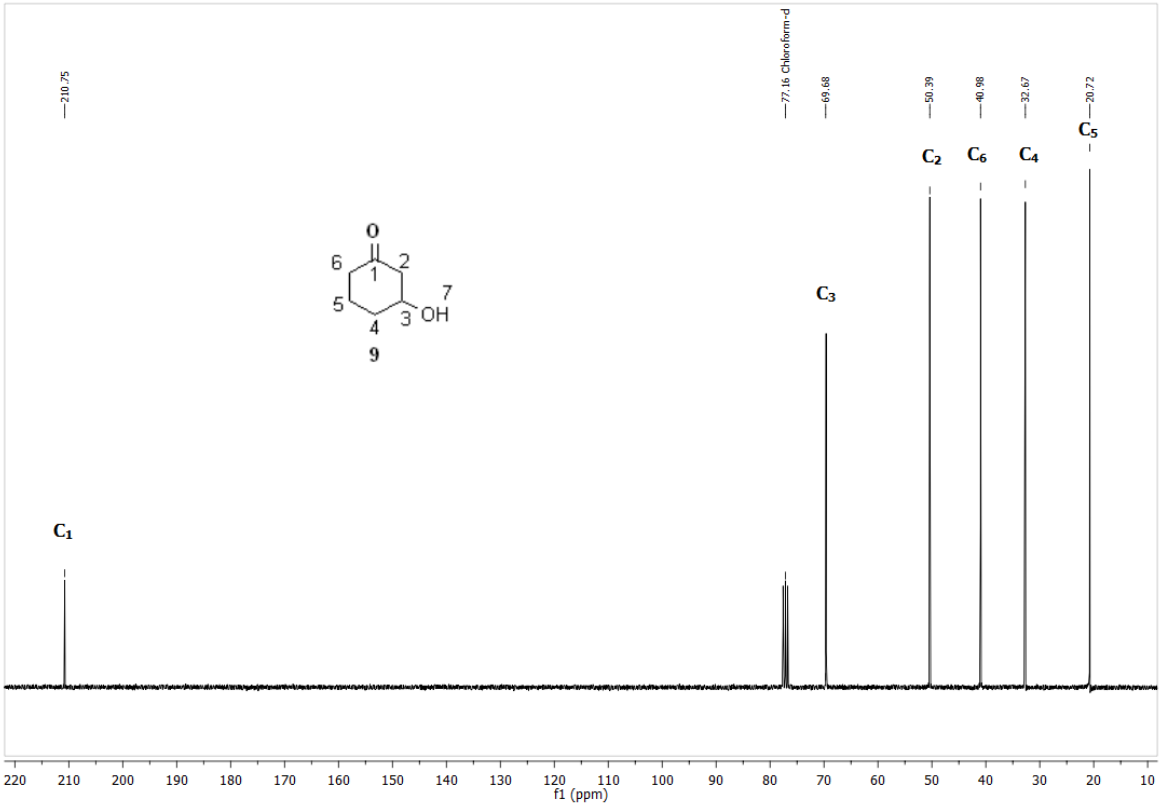

CBD NMR Spectrum 18 ^{13}C NMR spectrum of 3-hydroxycyclohexan-1-one 9.

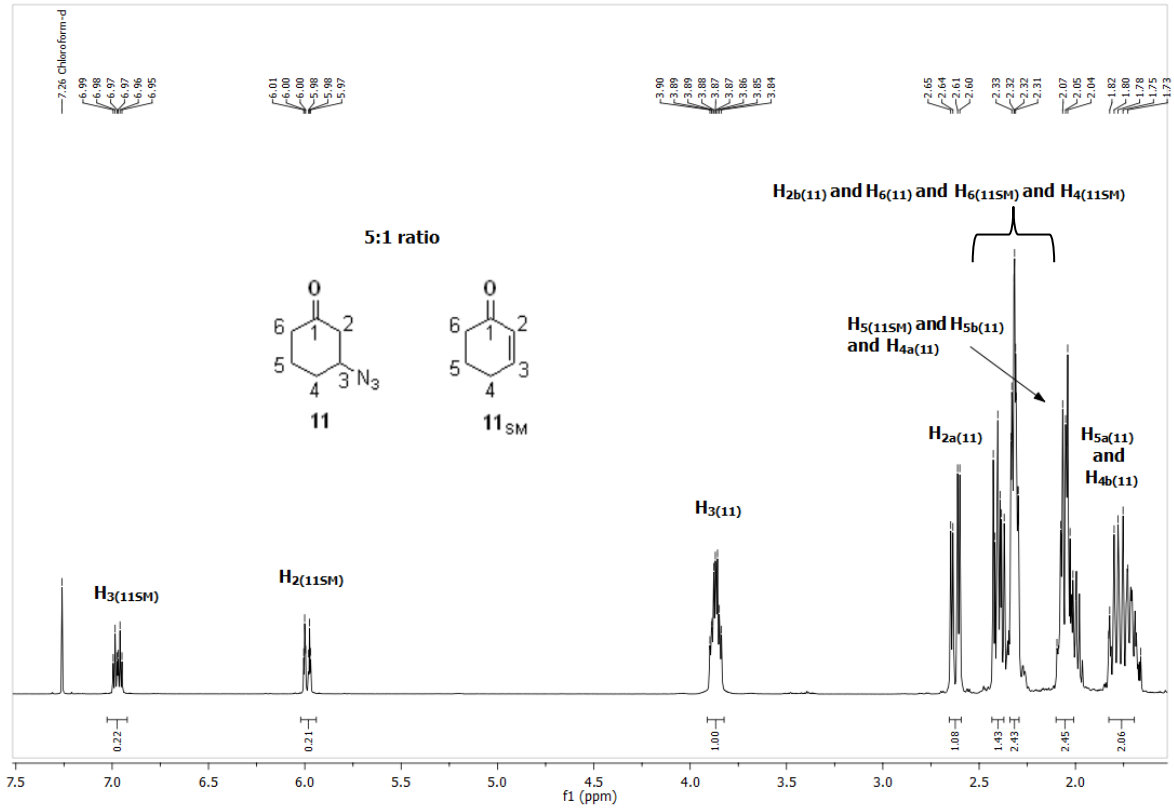

CBD NMR Spectrum 19 Crude ^{1}H NMR spectrum of 3-azidocyclohexan-1-one 11 with residual cyclohex-2-en-1-one (11_{SM}) in a 5:1 ratio.

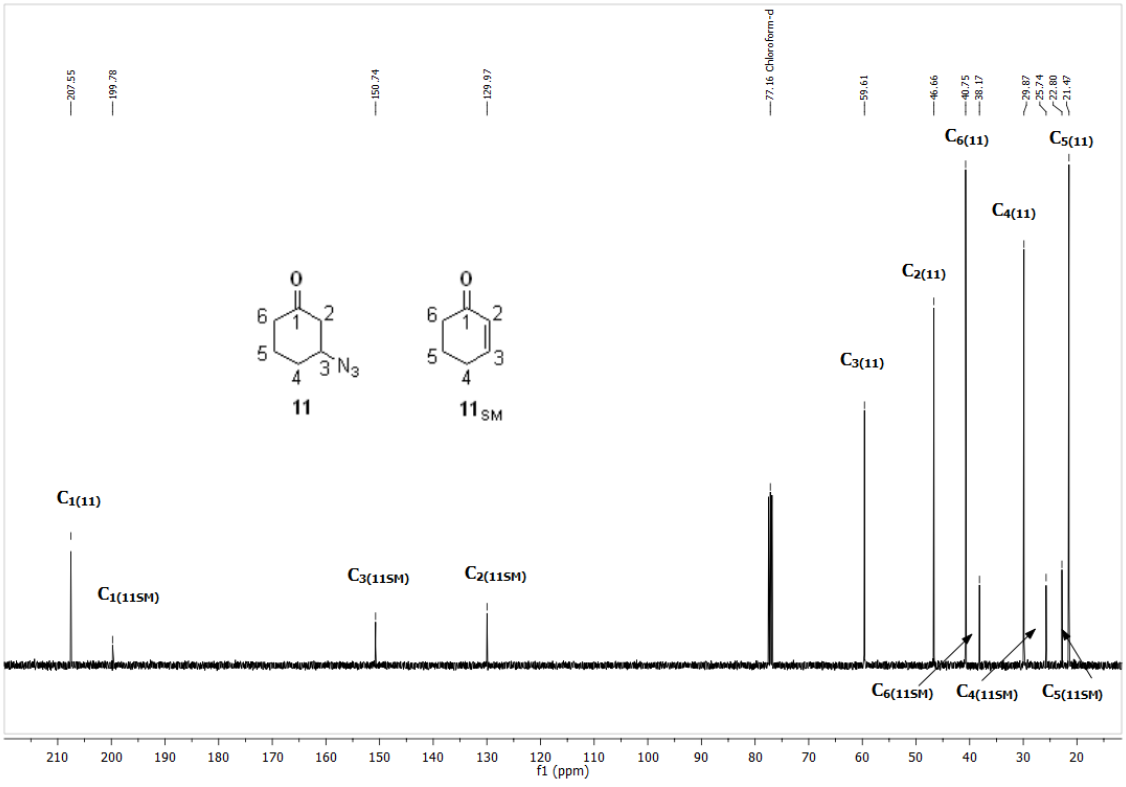

CBD NMR Spectrum 20 Crude ^{13}C NMR spectrum of 3-azidocyclohexan-1-one 11 with residual cyclohex-2-en-1-one (11_{SM}) in a 5:1 ratio.

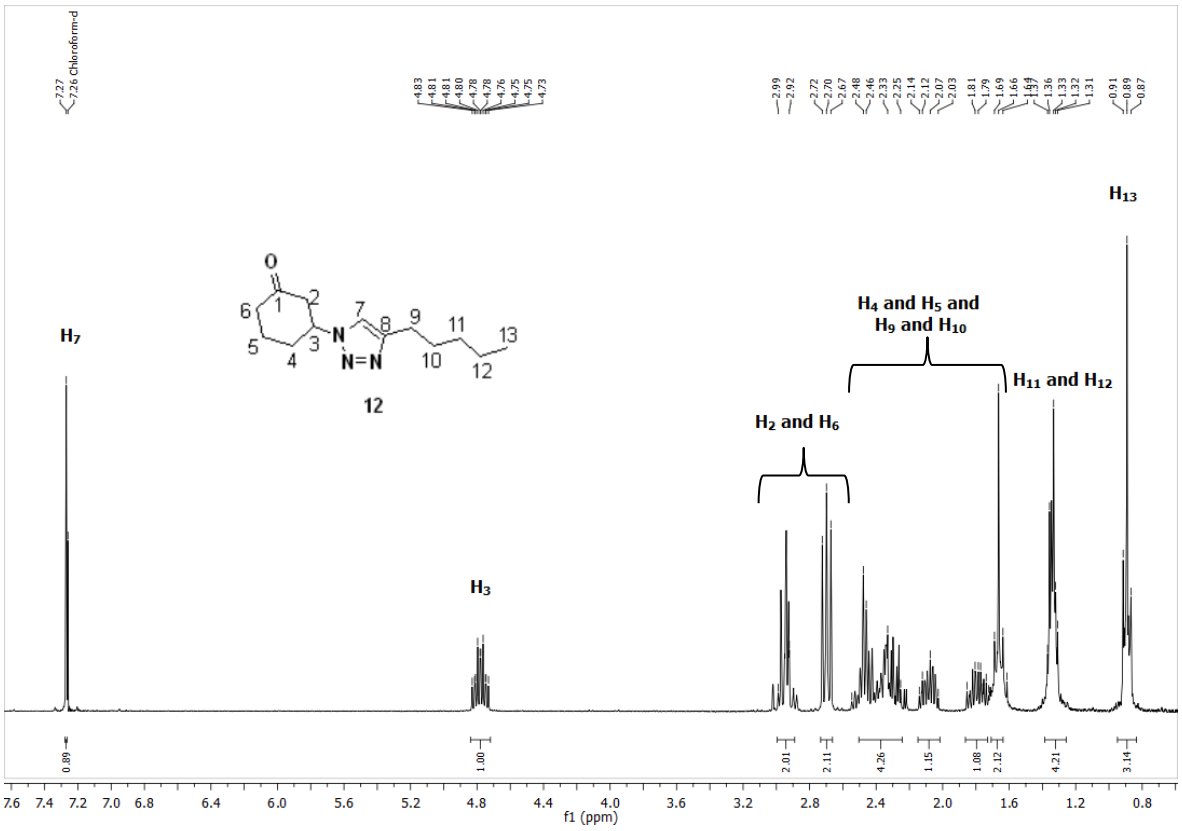

CBD NMR Spectrum 21 **^{1}H NMR spectrum of 3-(4-pentyl-1*H*-1,2,3-triazol-1-yl)cyclohexan-1-one 12.**

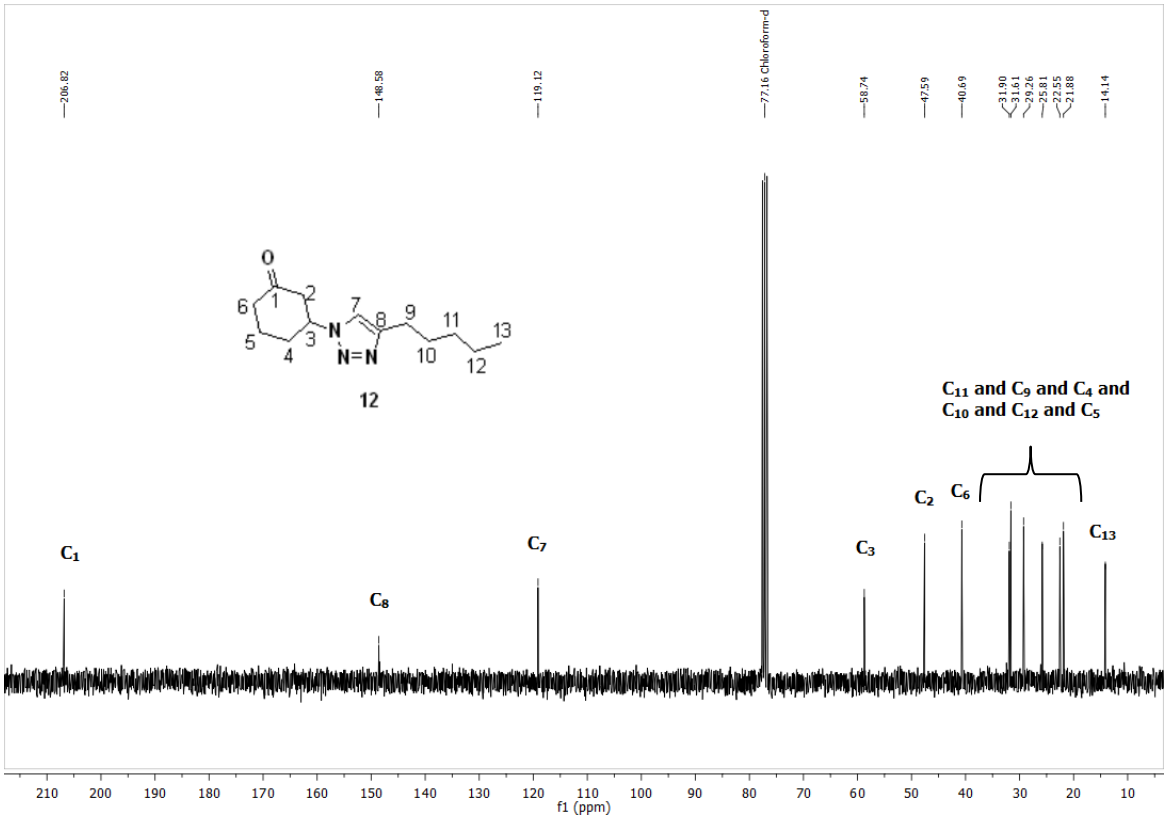

CBD NMR Spectrum 22 **^{13}C NMR spectrum of spectrum of 3-(4-pentyl-1*H*-1,2,3-triazol-1-yl)cyclohexan-1-one 12.**

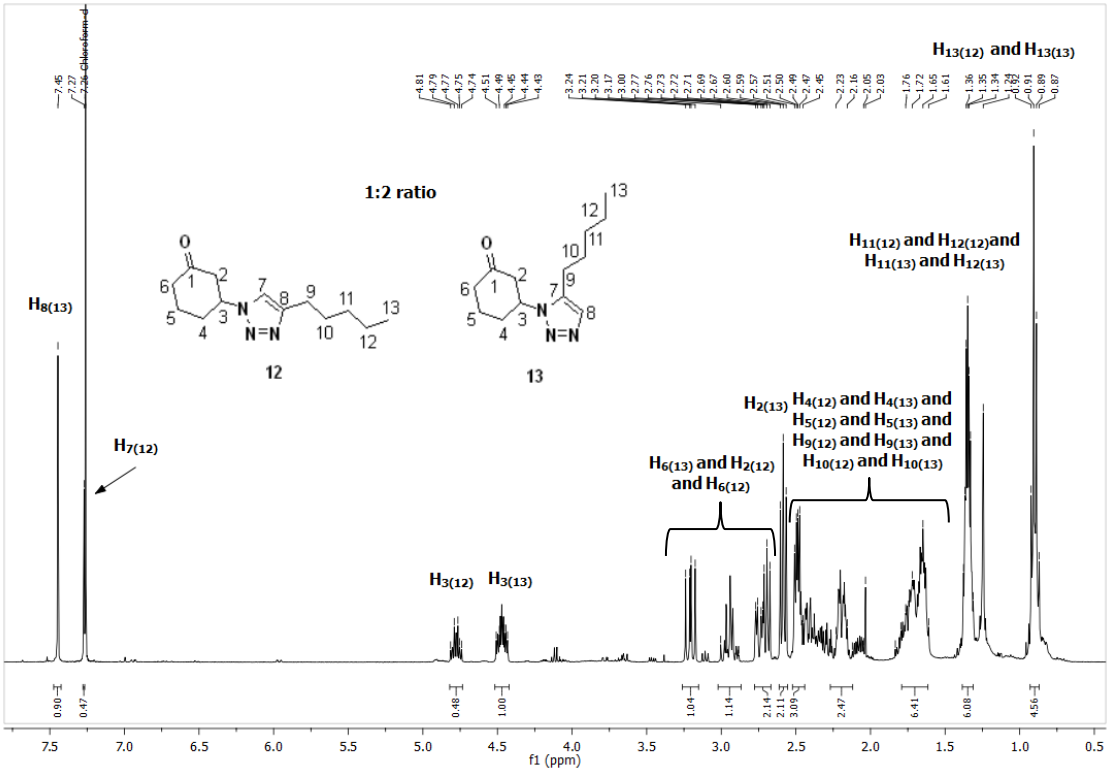

CBD NMR Spectrum 23 ^{1}H NMR spectrum of 3-(5-pentyl-1*H*-1,2,3-triazol-1-yl)cyclohexan-1-one 13 in a 2:1 mixture with 3-(4-pentyl-1*H*-1,2,3-triazol-1-yl)cyclohexan-1-one 12.

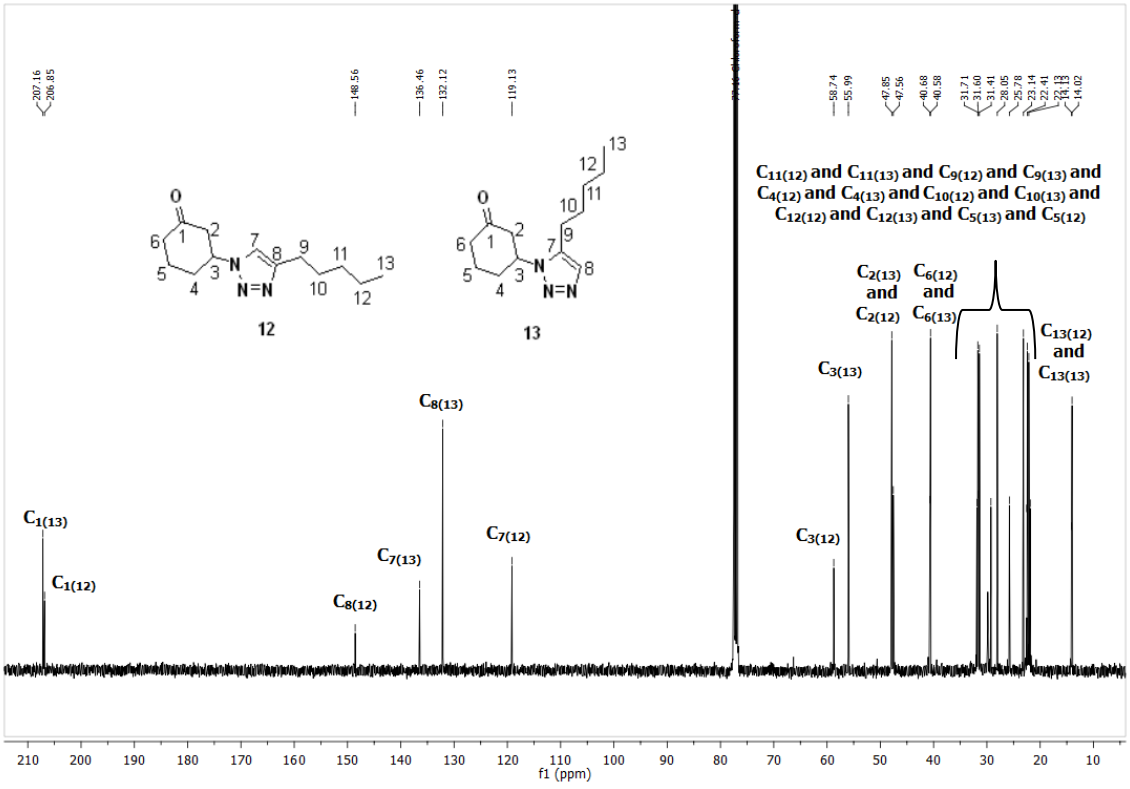

CBD NMR Spectrum 24 ^{13}C NMR spectrum of 3-(5-pentyl-1*H*-1,2,3-triazol-1-yl)cyclohexan-1-one 13 in a 2:1 mixture with 3-(4-pentyl-1*H*-1,2,3-triazol-1-yl)cyclohexan-1-one 12.

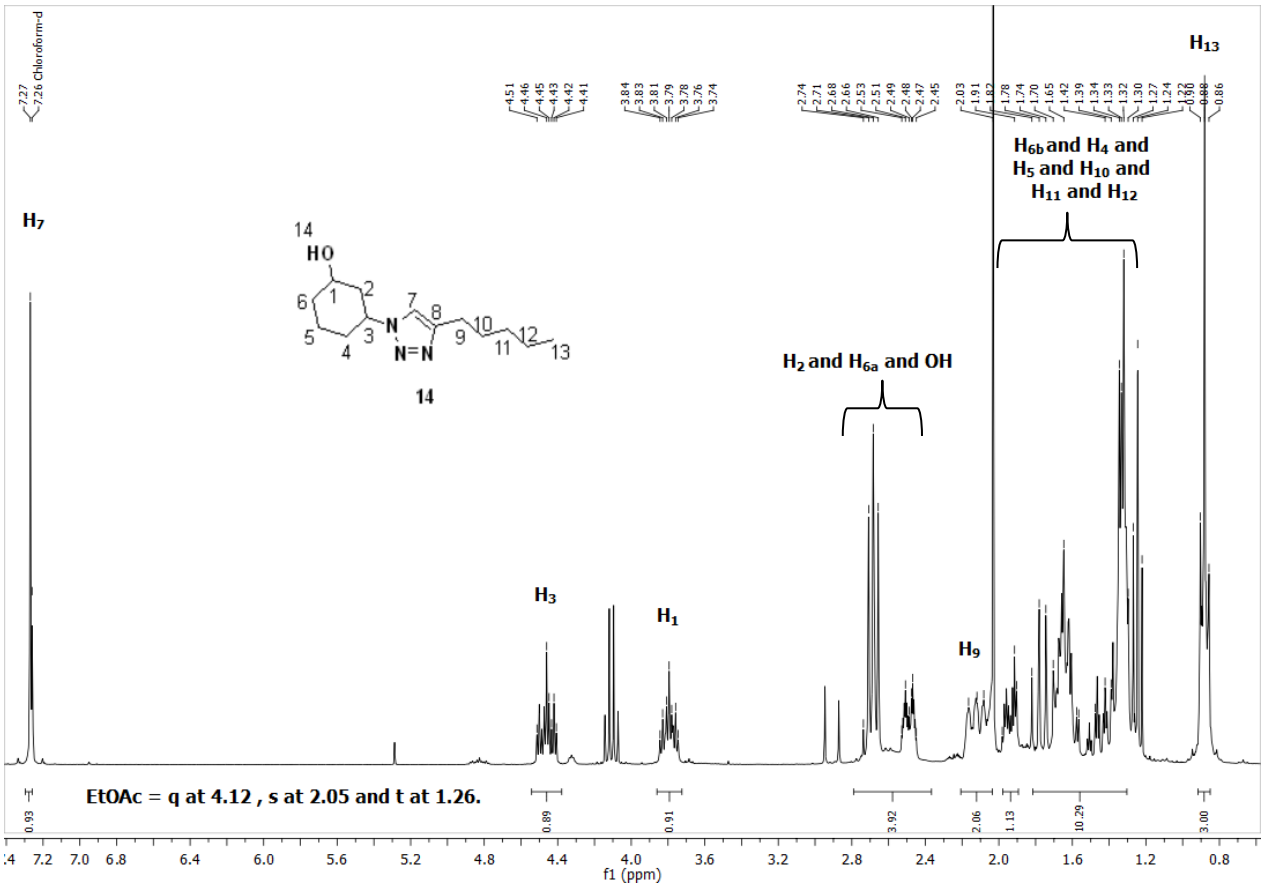

CBD NMR Spectrum 25 **^{1}H NMR spectrum of 3-(4-pentyl-1*H*-1,2,3-triazol-1-yl)cyclohexan-1-ol 14.**

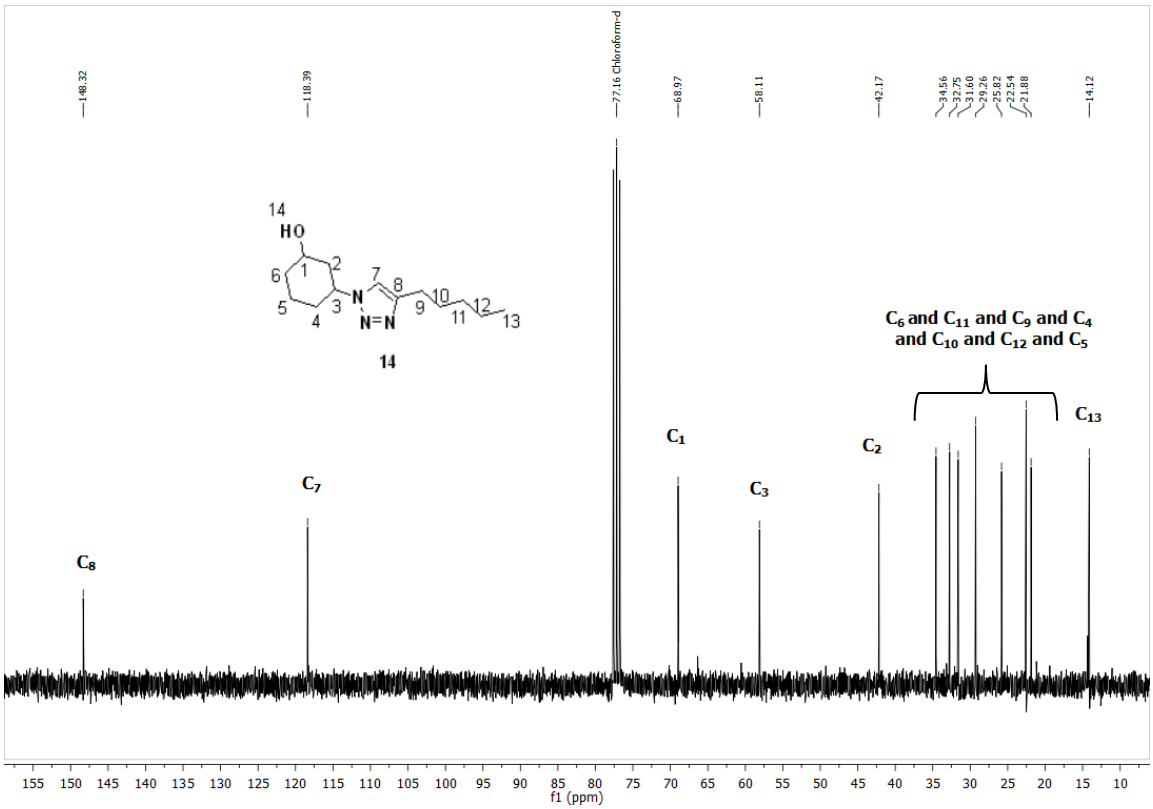

CBD NMR Spectrum 26 **^{13}C NMR spectrum of 3-(4-pentyl-1*H*-1,2,3-triazol-1-yl)cyclohexan-1-ol 14.**

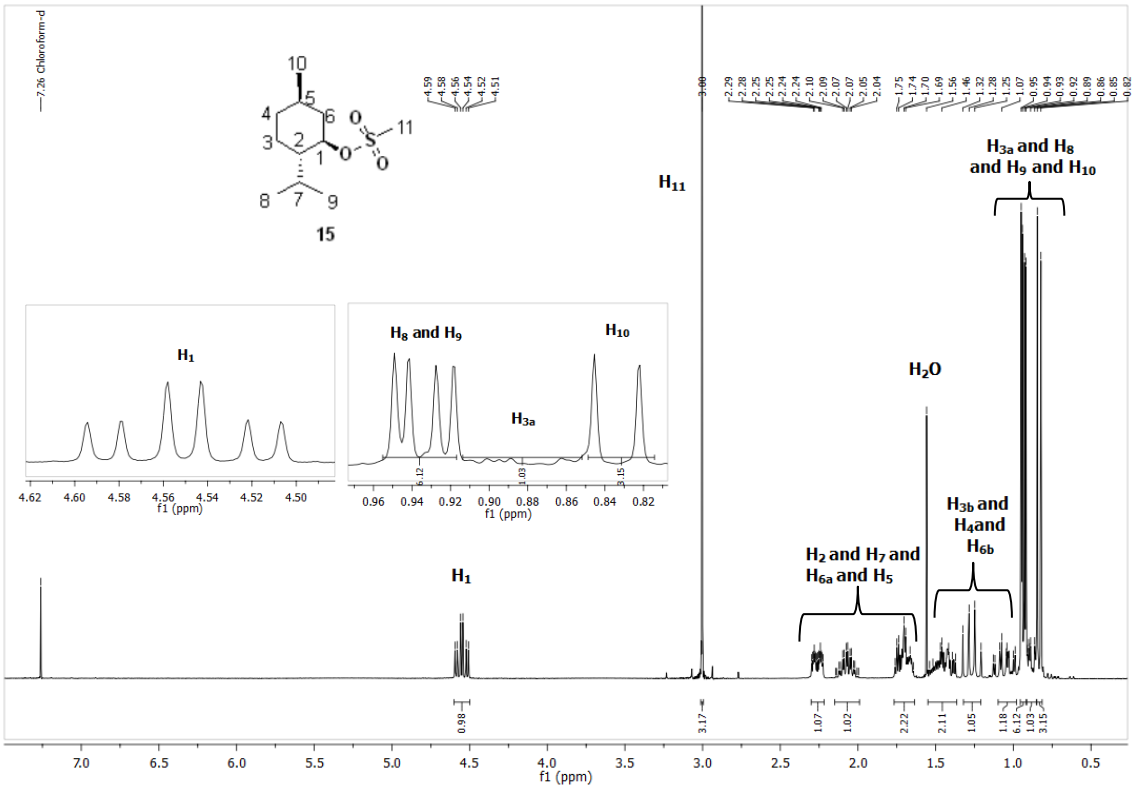

CBD NMR Spectrum 27 **^{1}H NMR spectrum of (1*R*,2*S*,5*R*)-2-isopropyl-5-methylcyclohexyl methanesulfonate 15.**

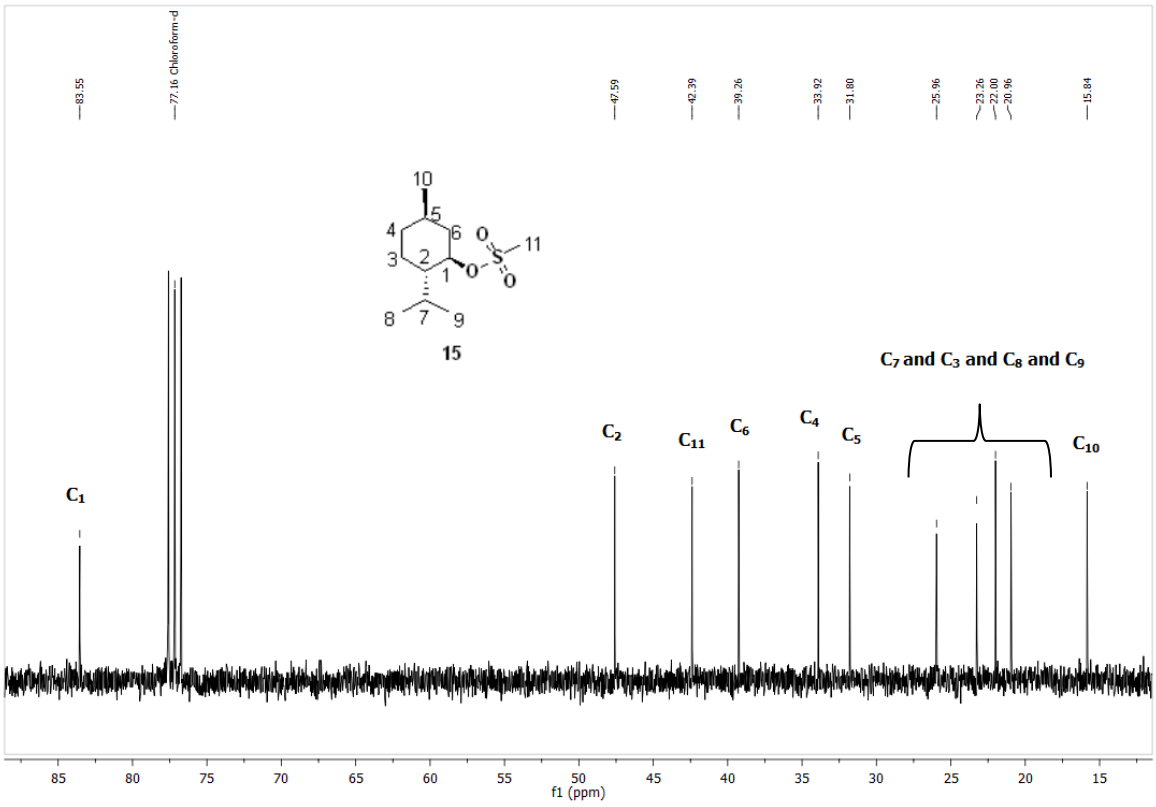

CBD NMR Spectrum 28 **^{13}C NMR spectrum of (1*R*,2*S*,5*R*)-2-isopropyl-5-methylcyclohexyl methanesulfonate 15.**

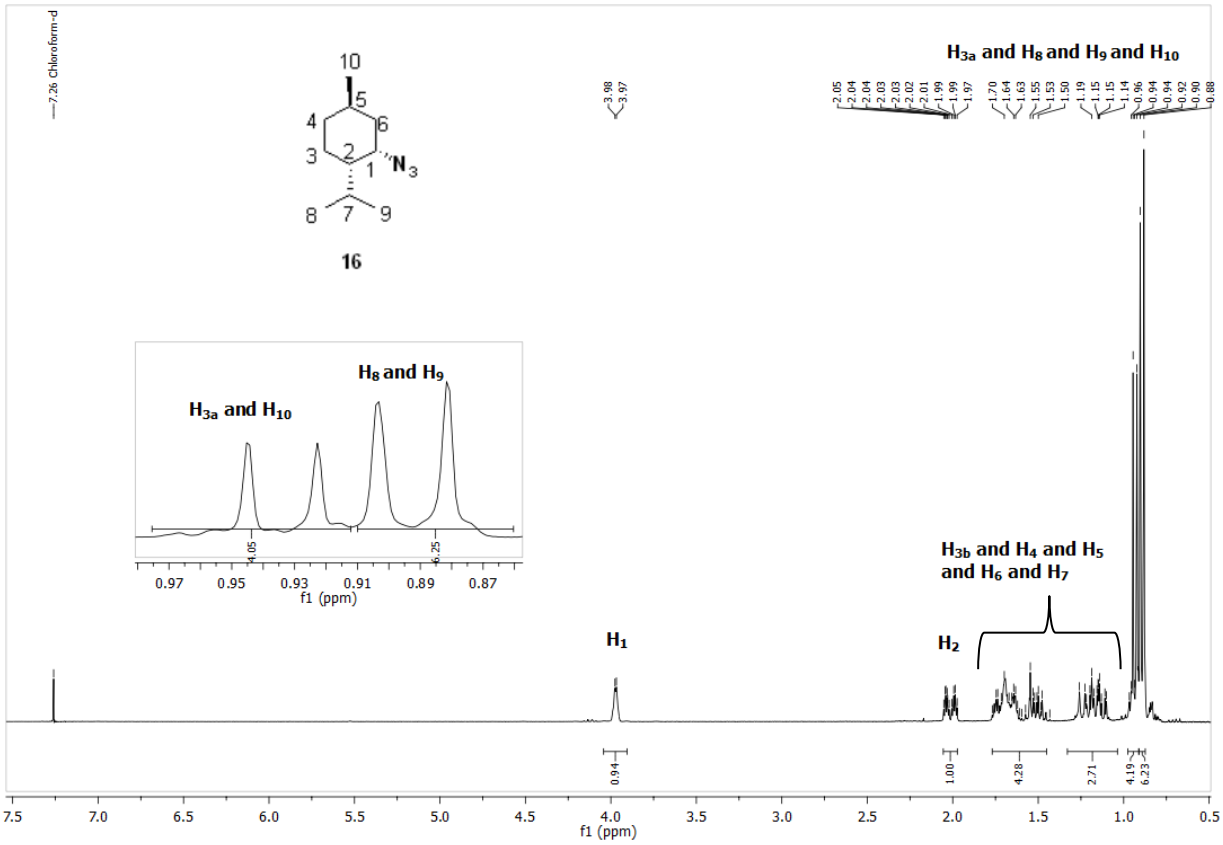

CBD NMR Spectrum 29 **^{1}H NMR spectrum of (1*S*,2*S*,4*R*)-2-azido-1-isopropyl-4-methylcyclohexane 16.**

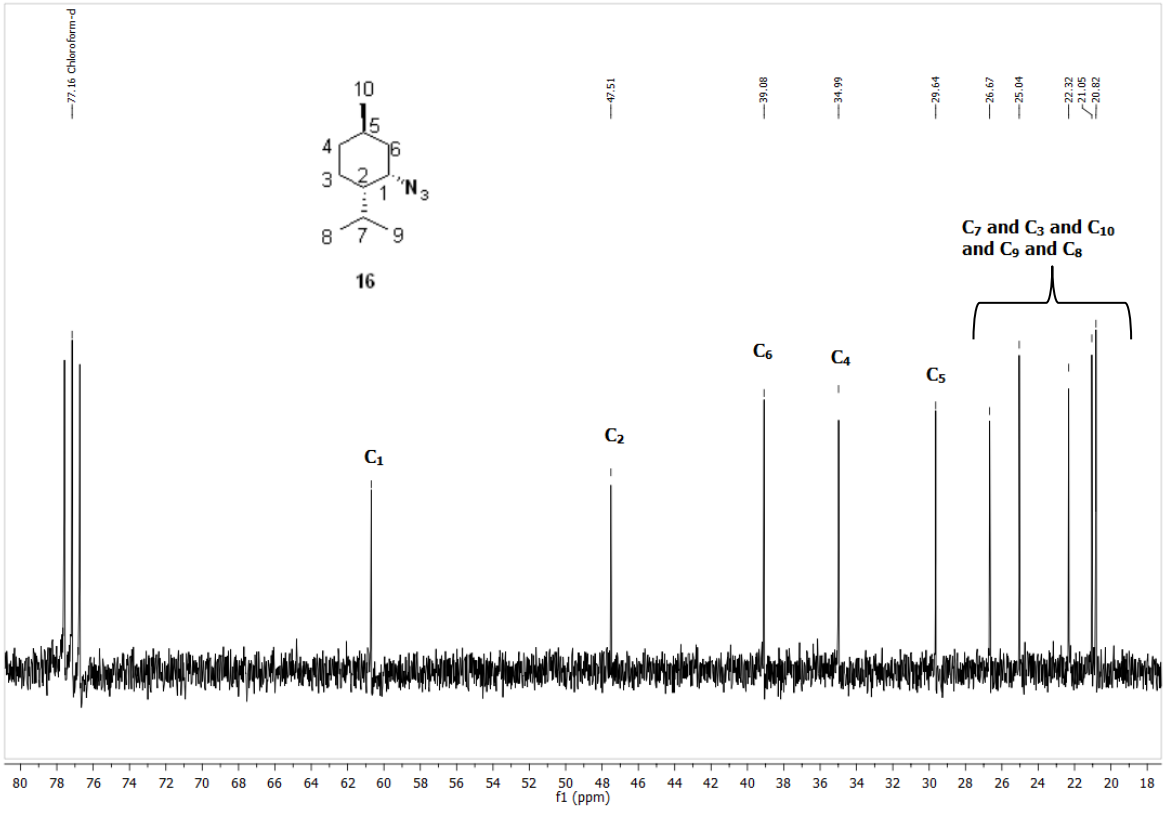

CBD NMR Spectrum 30 **^{13}C NMR spectrum of (1*S*,2*S*,4*R*)-2-azido-1-isopropyl-4-methylcyclohexane 16.**

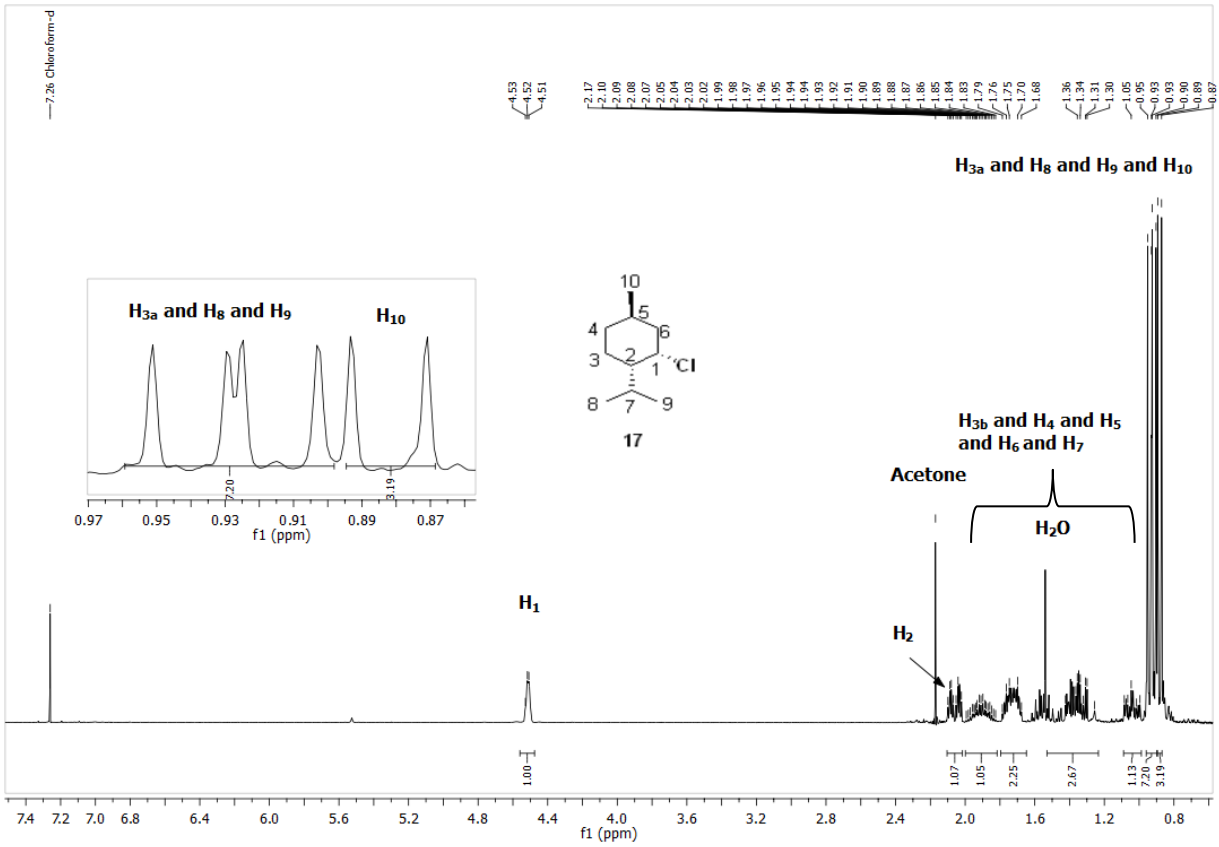

CBD NMR Spectrum 31 ^{1}**H NMR spectrum of (1*S*,2*S*,4*R*)-2-chloro-1-isopropyl-4-methylcyclohexane 17.**

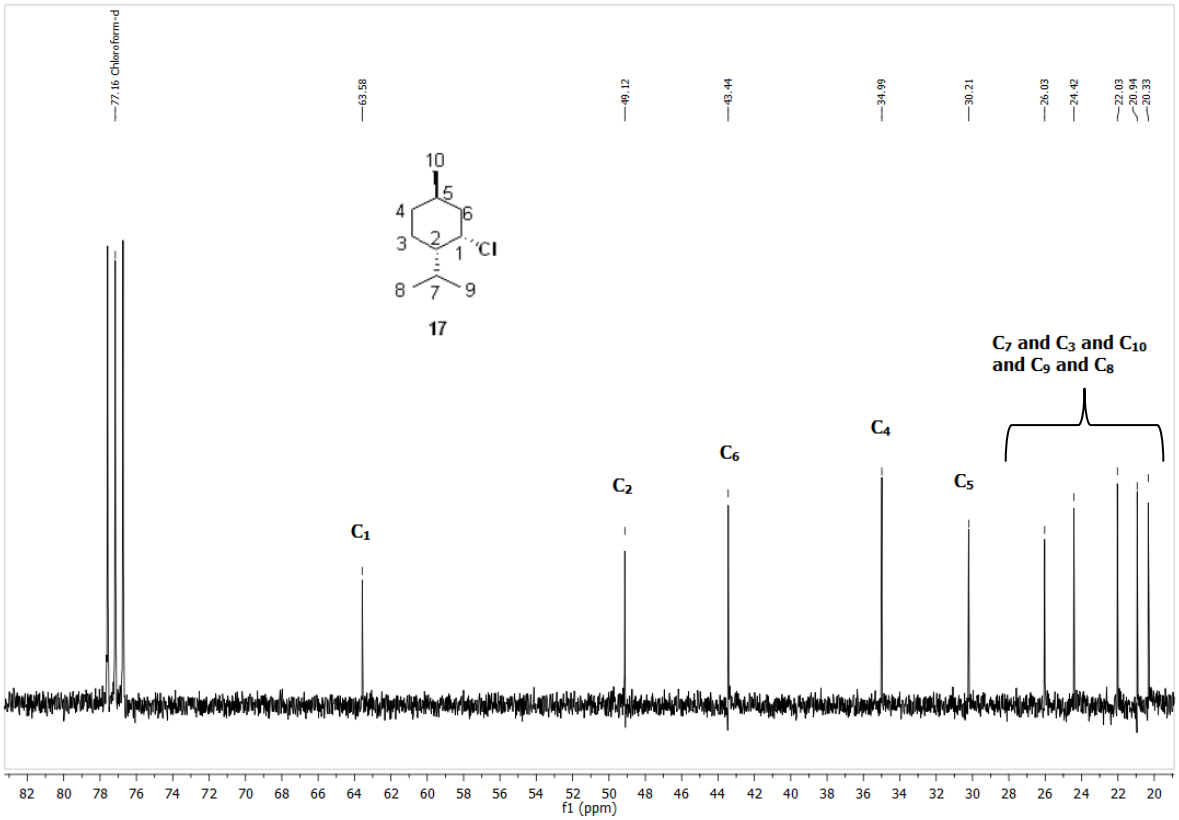

CBD NMR Spectrum 32 ^{13}**C NMR spectrum of (1*S*,2*S*,4*R*)-2-chloro-1-isopropyl-4-methylcyclohexane 17.**

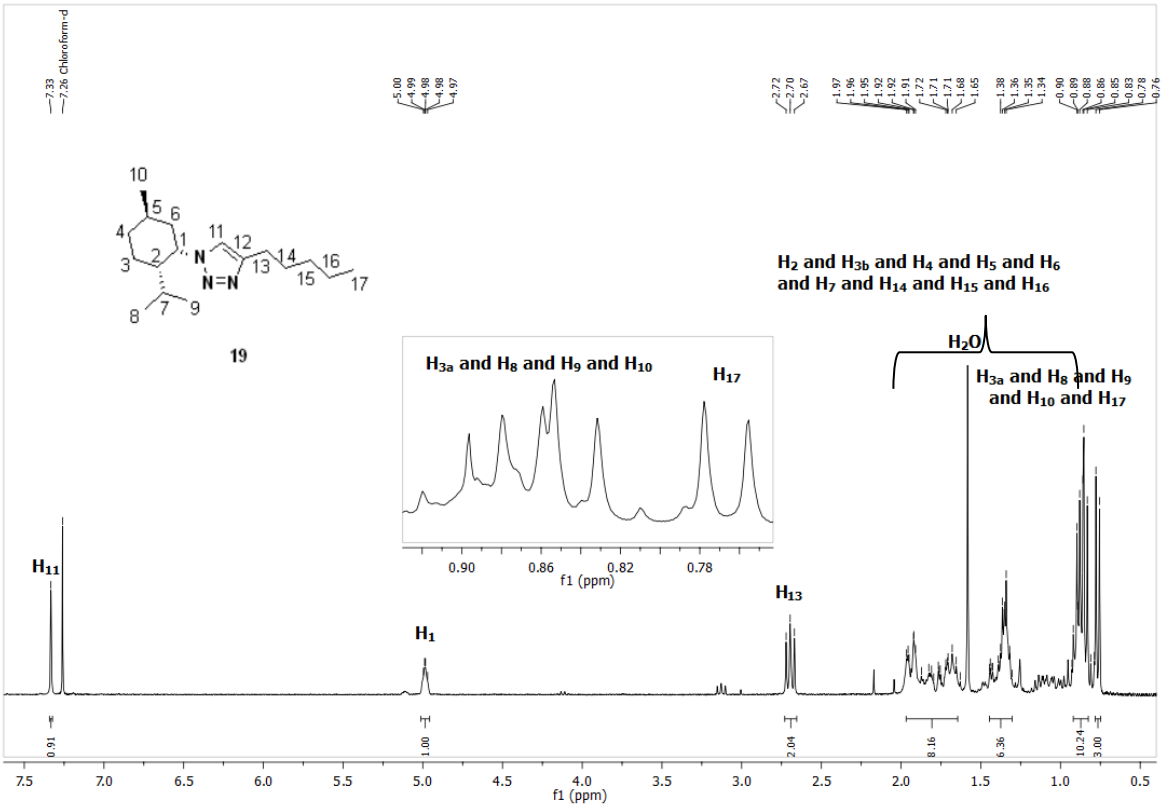

CBD NMR Spectrum 33 **^{1}H NMR spectrum of 1-[(1*S*,2*S*,5*R*)-2-isopropyl-5-methylcyclohexyl]-4-pentyl-1*H*-1,2,3-triazole 19.**

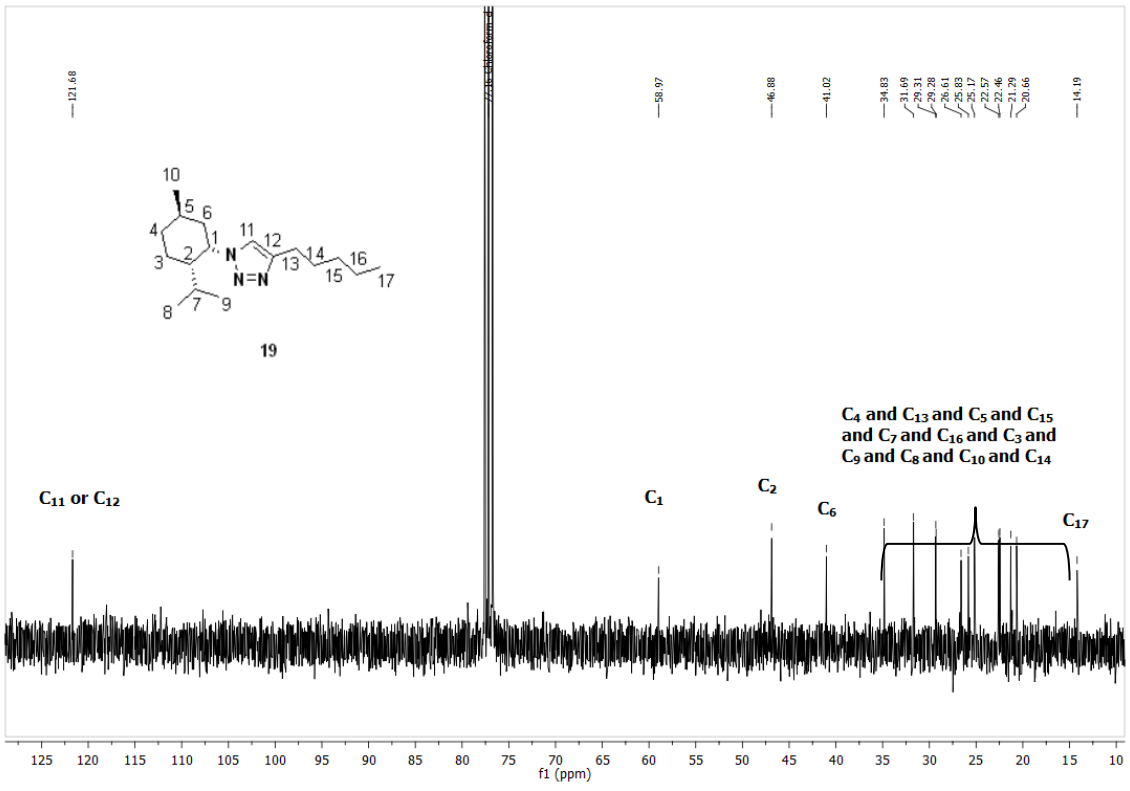

CBD NMR Spectrum 34 **^{13}C NMR spectrum of 1-[(1*S*,2*S*,5*R*)-2-isopropyl-5-methylcyclohexyl]-4-pentyl-1*H*-1,2,3-triazole 19.**

HIGH-RESOLUTION MASS SPECTROMETRY RESULTS

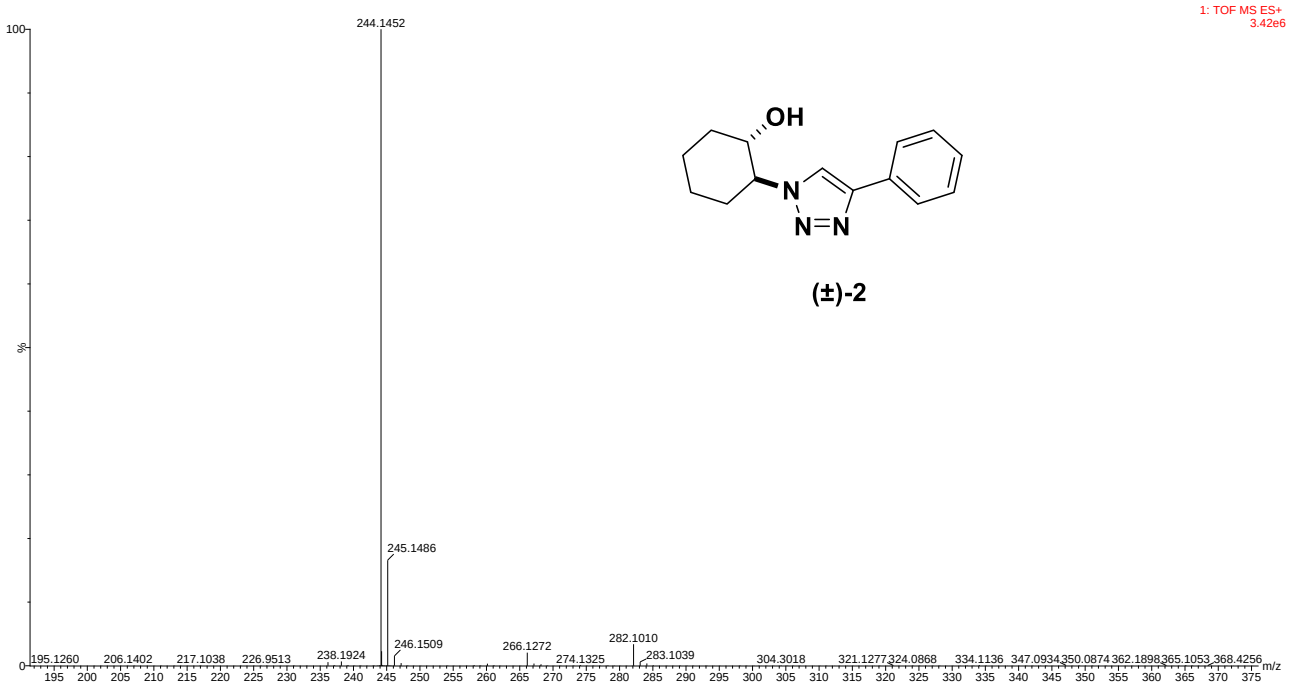

(±)-2

CBD Mass Spectrum 1 HRMS of (±)-*trans*-2-(4-phenyl-1*H*-1,2,3-triazol-1-yl)cyclohexan-1-ol 2.

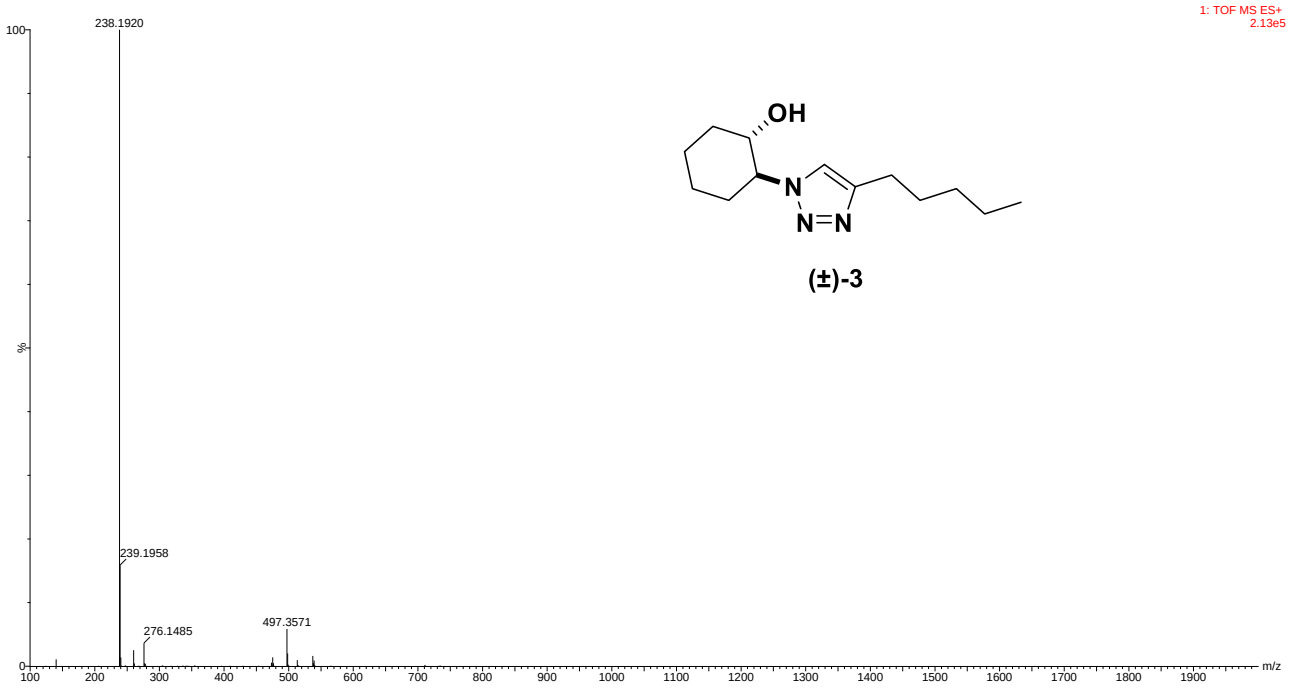

(±)-3

CBD Mass Spectrum 2 HRMS of (±)-*trans*-2-(4-pentyl-1*H*-1,2,3-triazol-1-yl)cyclohexan-1-ol 3.

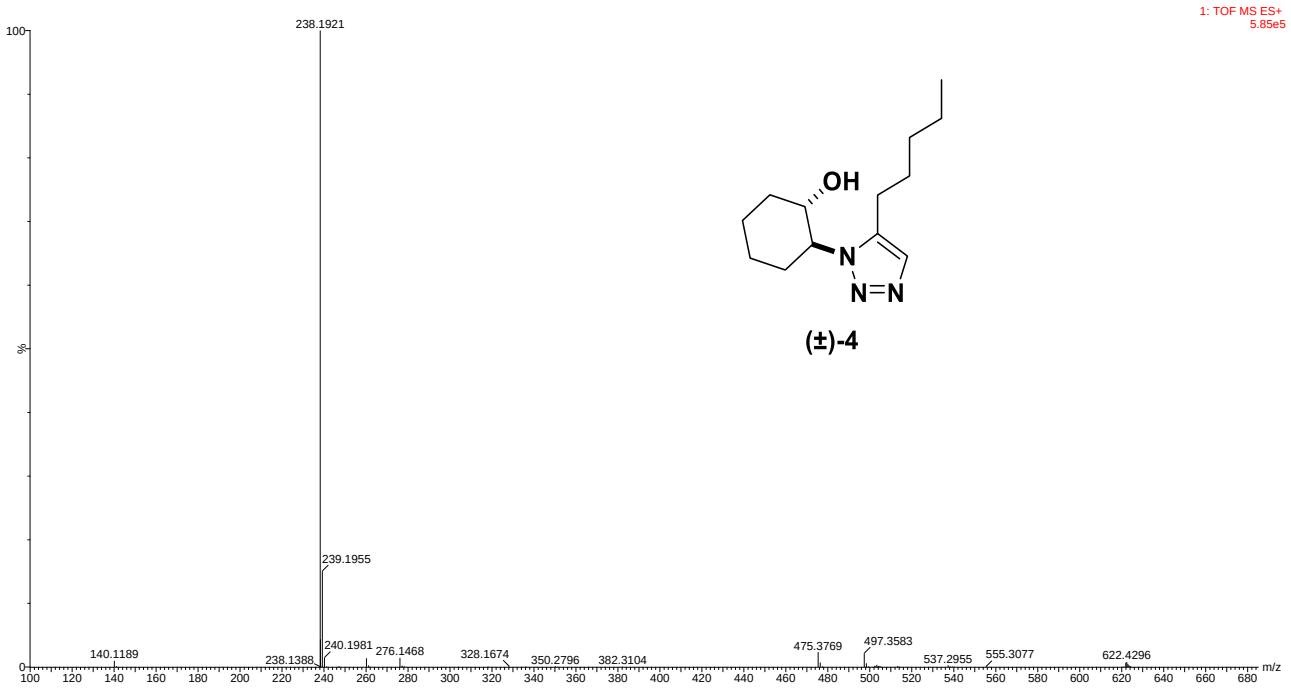

CBD Mass Spectrum 3 HRMS of (±)-*trans*-2-(5-pentyl-1*H*-1,2,3-triazol-1-yl)cyclohexan-1-ol 4.

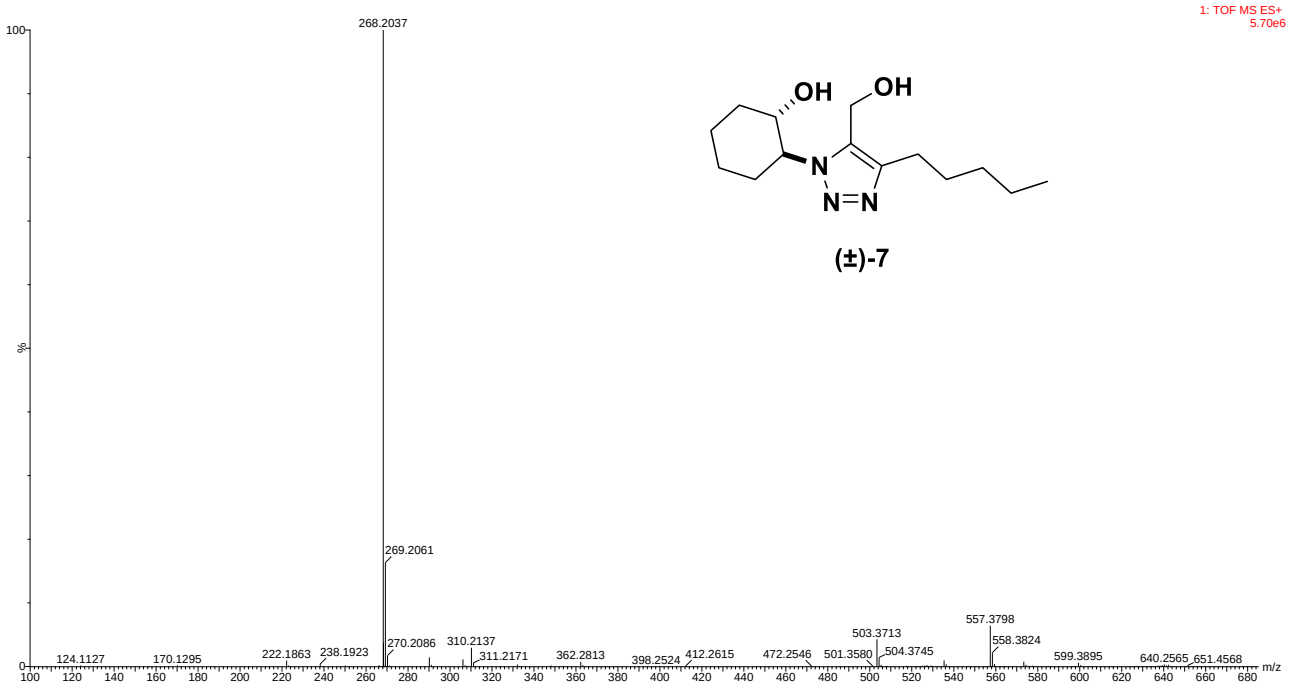

CBD Mass Spectrum 4 HRMS of (±)-*trans*-2-[5-(hydroxymethyl)-4-pentyl-1*H*-1,2,3-triazol-1-yl]cyclohexan-1-ol 7.

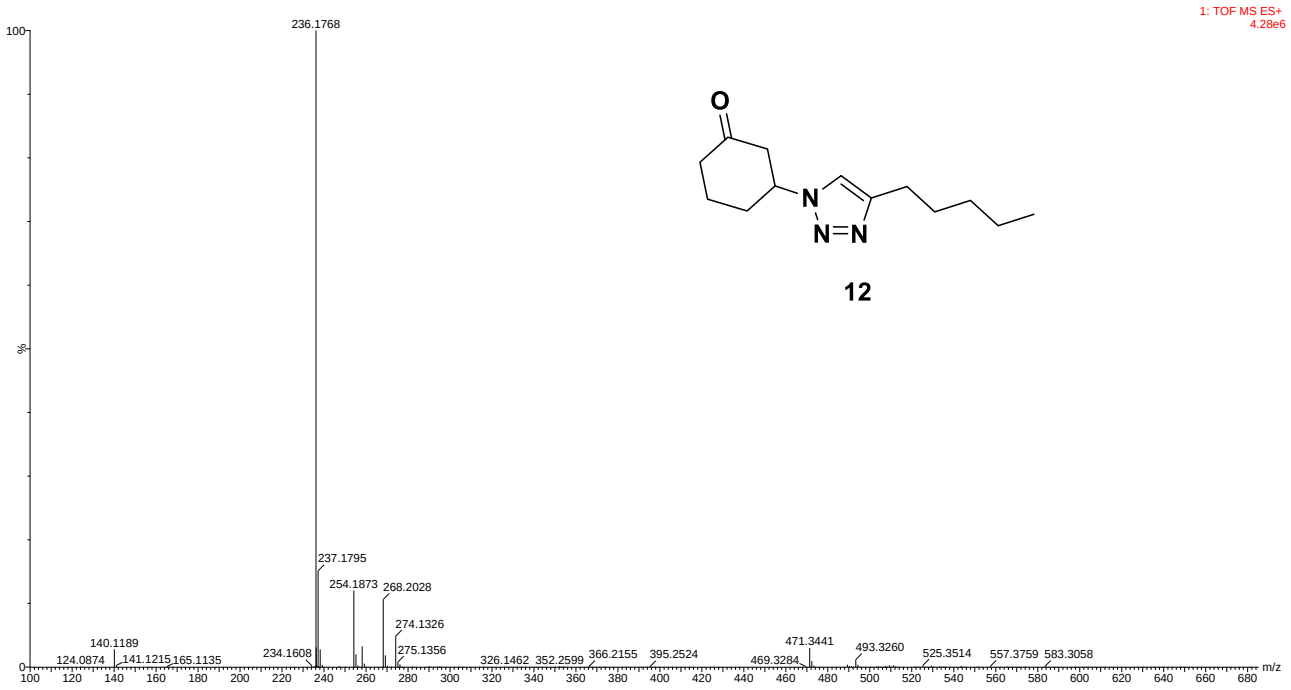

12

CBD Mass Spectrum 5 HRMS of 3-(4-pentyl-1*H*-1,2,3-triazol-1-yl)cyclohexan-1-one 12.

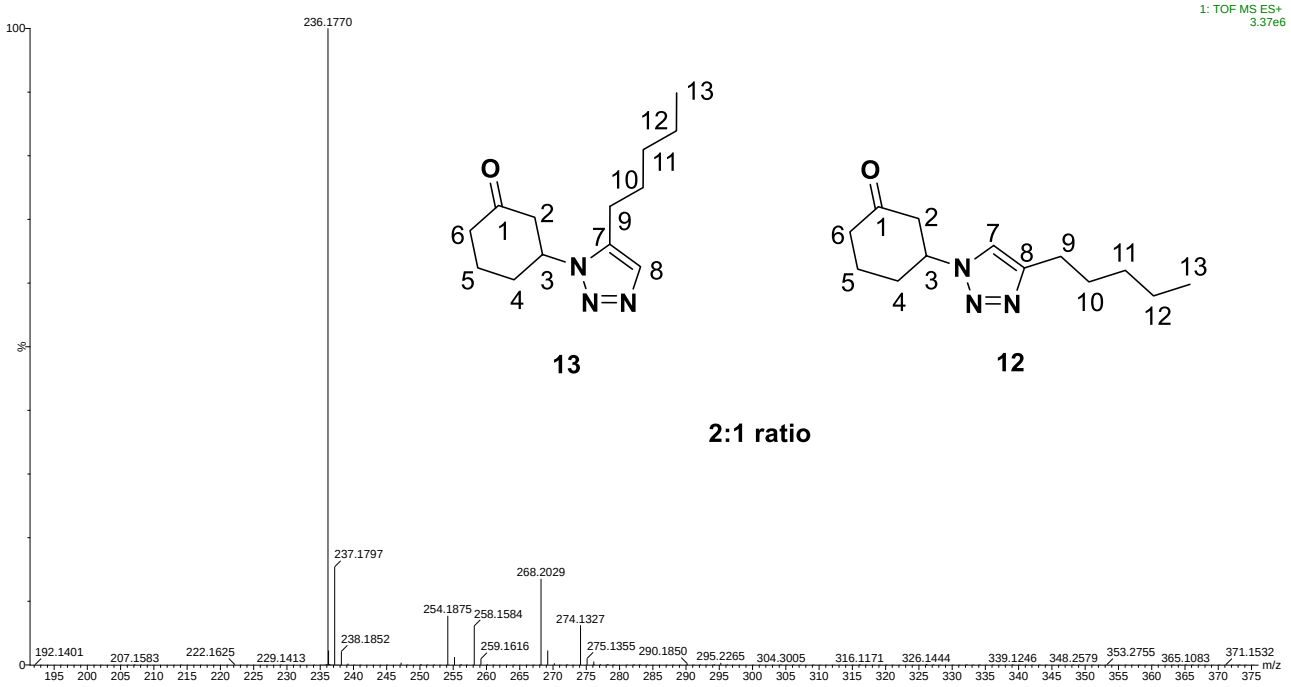

13 **12**

2:1 ratio

CBD Mass Spectrum 6 HRMS of 3-(5-pentyl-1*H*-1,2,3-triazol-1-yl)cyclohexan-1-one 13 in a 2:1 mixture with 3-(4-pentyl-1*H*-1,2,3-triazol-1-yl)cyclohexan-1-one 12.

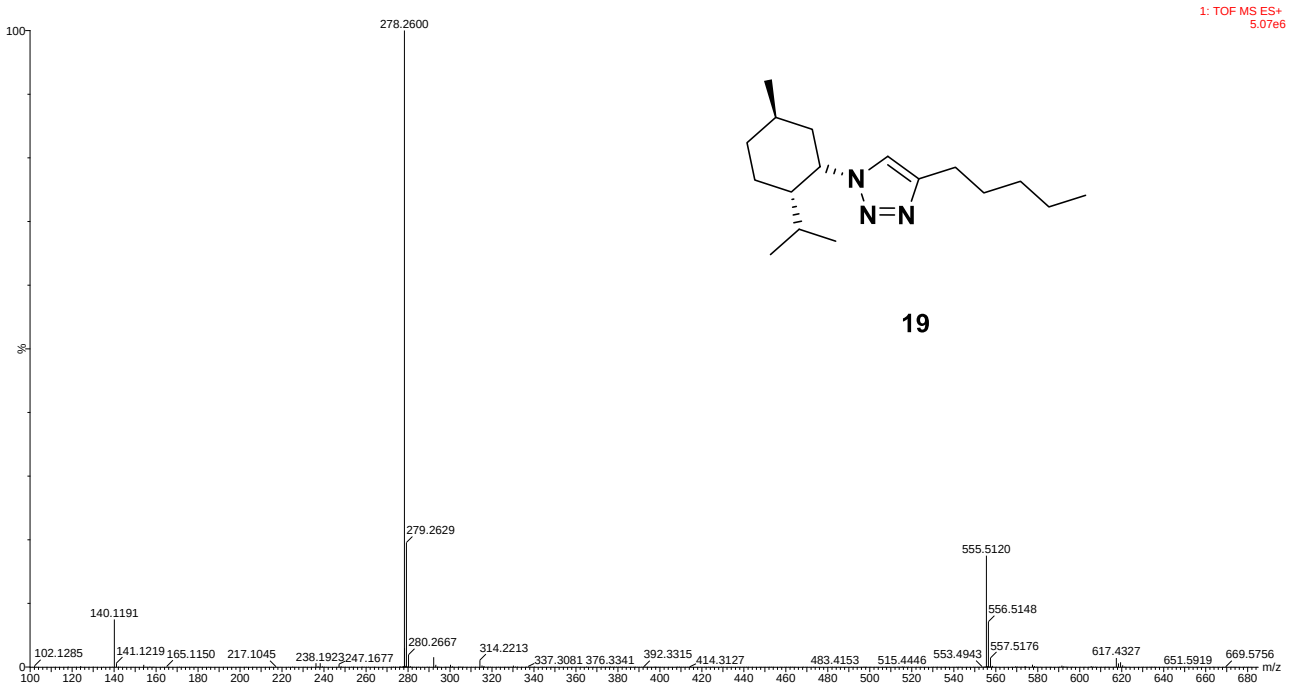

19

CBD Mass Spectrum HRMS of 7 1-[(1*S*,2*S*,5*R*)-2-isopropyl-5-methylcyclohexyl]-4-pentyl-1*H*-1,2,3-triazole 19.

STRUCTURES OF REFERENCE COMPOUNDS WITH ANTICANCER ACTIVITY

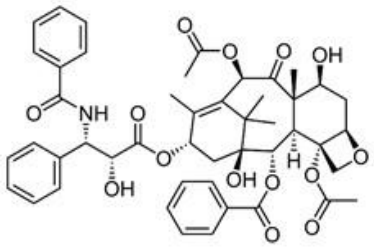

Pacitaxel

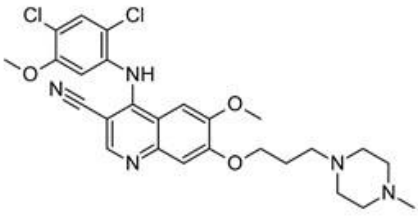

Bosutinib

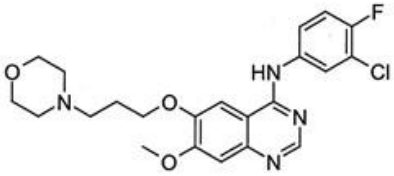

Gefitinib

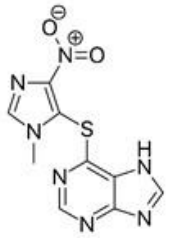

Azathioprine

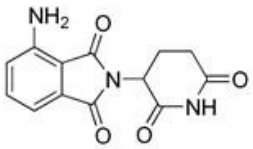

Pomalidomide

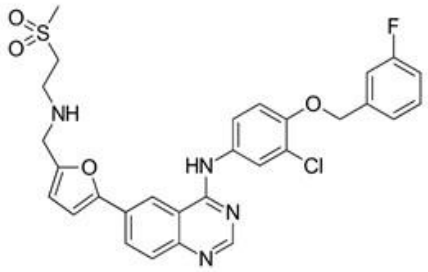

Lapatinib

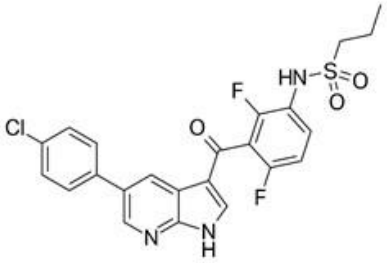

Vemurafenib

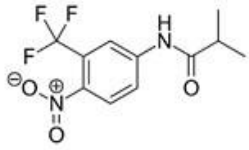

Flutamide

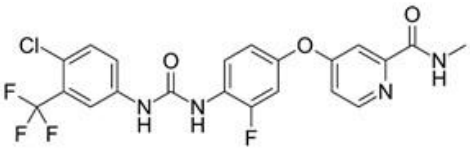

Regorafenib

TRANSITION BETWEEN THE TRIAZOLE CBD ANALOGUES PROJECT AND THE SUBSTITUTED CPP PROJECT

The focus of the next four chapters of this dissertation, as well as the Appendix (labeled as Appendix 2) following these chapters, is on a second research project completely separate from the triazole CBD analogue project discussed above. The research of this project was conducted at the Justus Liebig University in Giessen, Germany, in the research group of Prof. Dr Hermann A. Wegner.

Compound numbering and NMR spectra[4] numbering was restarted at 1 - to illustrate the complete division between these two projects.[5]

[4] For this project, ^{13}C NMR spectra were not obtained for compounds previously reported in literature.
[5] The room temperature in the laboratory in which this project was conducted was regulated and kept constant at 20 °C.

SYNTHESIS OF SUBSTITUTED CYCLOPARAPHENYLENES (CPPS)

CHAPTER 7
INTRODUCTION AND AIM OF CPP PROJECT

7.1. MACROCYCLES AND THEIR APPLICATIONS

Macrocycles have been defined by Marsault *et al.* as compounds that contain one or more cyclic units and consists of at least 12 atoms.[164] These molecules have interesting structures and properties which is why the synthesis of macrocycles is considered as a fascinating field of research. There are four general strategies available for macrocyclization, namely, cyclo-oligomerization, intramolecular cyclization, bimolecular coupling (dimerization), and template synthesis; however, all of these methods have certain drawbacks.

One field in which macrocycles are widely used is pharmaceutical drug therapy. When comparing macrocycles with their acyclic analogues, it is clear that the conformation of macrocycles is significantly more restricted. This structural characteristic gives macrocycles the benefit of being more soluble, having better oral bioavailability, possessing improved target binding, while also being more biologically stable than their acyclic analogues.[165] One macrocyclic compound which is currently being used in targeted drug therapy, is called Telomestatin (Figure 7:1) - this molecule acts as an inhibitor for the telomerase activity of cancer cells.[166]

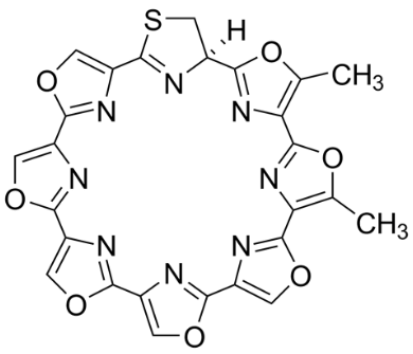

Figure 7:1 Structure of Telomestatin.[166]

Another field in which macrocycles have attracted significant attention is in supramolecular chemistry, due to their catalytic and redox properties, as well as the host-guest interactions of these macrocycles. The host-guest interactions of certain macrocycles, such as calixarenes and crown ethers have already been investigated.[167] Some unique macrocycles have also been investigated for their potential as building blocks for carbon nanotubes.

7.2. CARBON NANOTUBES

Carbon nanotubes (CNTs) are an allotrope of carbon with unique hollow cylindrical nanostructures. The study and synthesis of carbon nanotubes is still a developing field as the first reported observation of CNTs only occurred in 1991 by Iijima.[168]

These molecules have unique electrical transport properties, unusual mechanical properties, extraordinary strength and act as efficient heat conductors. When considering all these properties, CNTs can be used in many different applications including energy storage, electronics and in drug delivery systems. Many different methods have been reported for the synthesis of CNTs but the chiral-selective synthesis of CNTs is still under investigation.

One strategy for synthesizing CNTs with a specific chirality is to focus on the organic synthesis of CNT segments and using these molecules as building blocks for CNTs (Figure 7:*2*).[169]

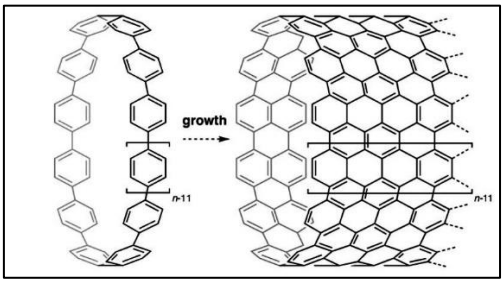

Figure 7:2 CNT "sidewall segment" as building block for CNTs.[169]

7.2.1. CNT SEGMENTS

"Carbon nanorings" are macrocycles that can be obtained from "slicing" CNTs perpendicular to the main axis. These macrocycles represent the sidewall segment of CNTs with a specific chirality.[170] Macrocycles that can now be identified as CNT armchair segments have attracted the attention of several chemists long before the discovery of CNTs, due to their remarkable symmetry and interesting properties. Thus far, a wide variety of armchair CNT segments have been synthesized including cycloparaphenylenes (CPPs), all-Z-benzannulenes and tetradehydrodianthracenes (TDDAs) (Figure 7:3).[170] For the purpose of this project, only the CPPs will be discussed in more detail.

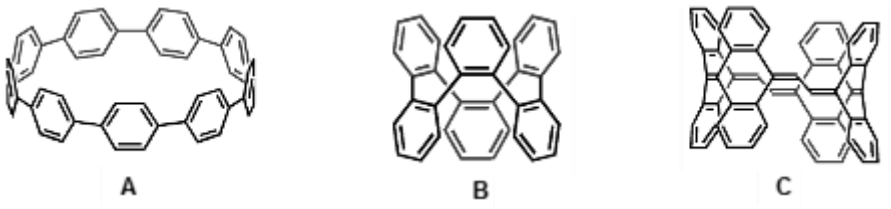

Figure 7:3 Selected armchair CNT segments (A: CPP; B: Benzannulenes; C: TDDA).[170]

7.2.1.1. CYCLOPARAPHENYLENES

Cycloparaphenylenes (CPPs) are macrocycles which consist of benzene rings connected through *para*-linkages, and these macrocycles represent the shortest sidewall segment of carbon nanotube structures. The long-awaited selective synthesis of single-walled carbon nanotubes (SWNTs) could therefore be achieved by using CPPs as a building block.[171]

Although the synthesis of CPPs have been investigated since the early 1930s, the first successful synthesis was only achieved in 2008 by Jasti *et al.*[172] The reason for this long struggle is due to the high strain energy that must be overcome to form these macrocycles. Jasti *et al.* addressed this problem by designing a route which involved an unstrained macrocyclic precursor, which meant that full conjugation would only be introduced in the final step (Scheme 7:1). In this synthesis, a curved diodo-building block was prepared from 1,4-benzoquinone and 1,4-diiodobenzene, followed by a borylation reaction to provide the curved borylated building block. The next step involved a Suzuki cross-coupling reaction between these two curved building blocks to obtain three macrocycles of different sizes. As mentioned above, the final step introduced full conjugation into the system through a reductive aromatization of these three macrocycles with lithium naphthalenide (LiNaph) to obtain three different CPP macrocycles, [9]CPP, [12]CPP, and [18]CPP.

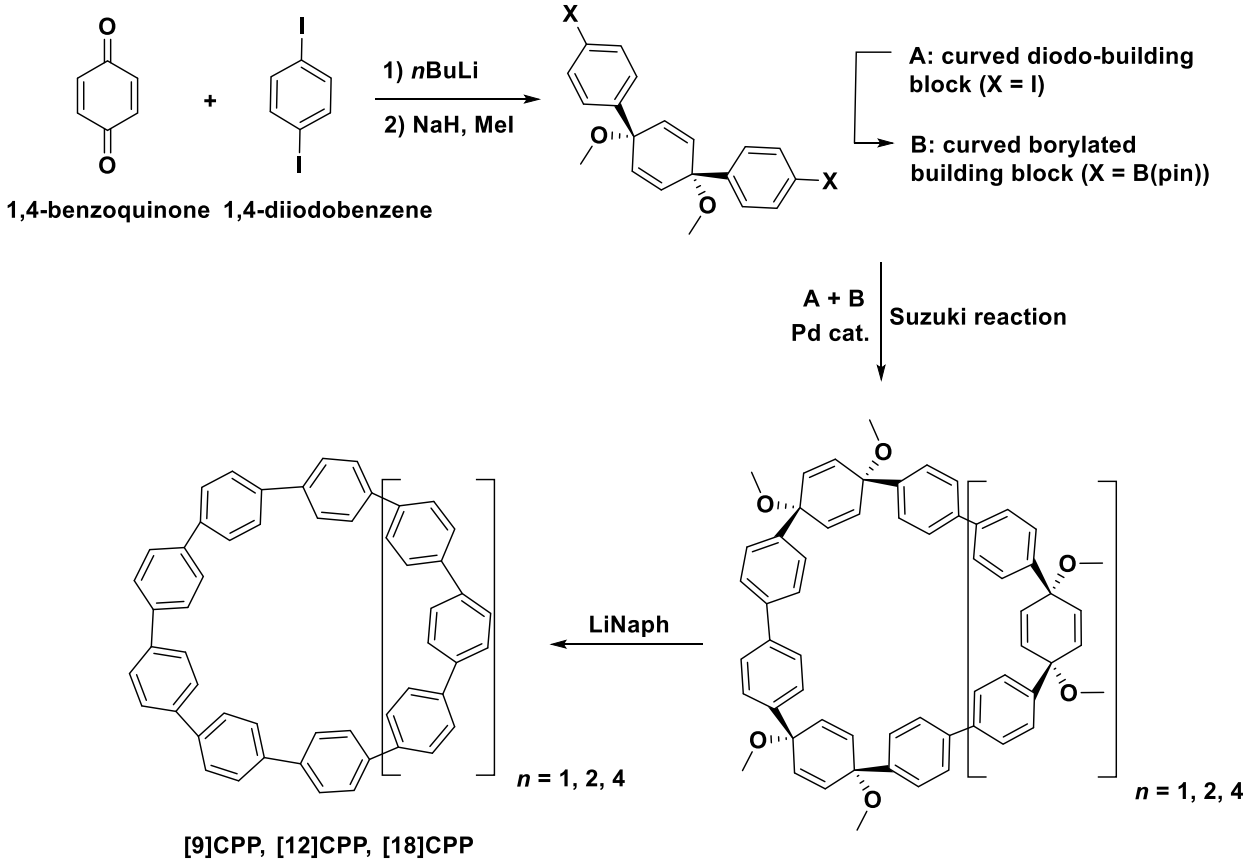

Scheme 7:1 The first successful synthesis of CPPs.[170]

A few months later, Itami and co-workers reported the first size-selective synthesis of CPP (Scheme 7:2).[173] In this synthesis, a L-shaped diodo-building block was prepared from 1,4-cyclohexanedione and 1,4-diiodobenzene. This L-shaped diodo-building block was then transformed into a MOM-protected L-shaped diodo-compound and an L-shaped borylated compound, respectively. These two compounds were then subjected to a palladium-catalyzed cross-coupling reaction to provide the C-shaped non-macrocyclic compound with two iodine's at the ends of the chain. This C-shaped molecule was then coupled to the original L-shaped borylated compound to obtain the non-conjugated macrocycle and the final step involved an aromatization reaction to finally get access to [12]CPP.

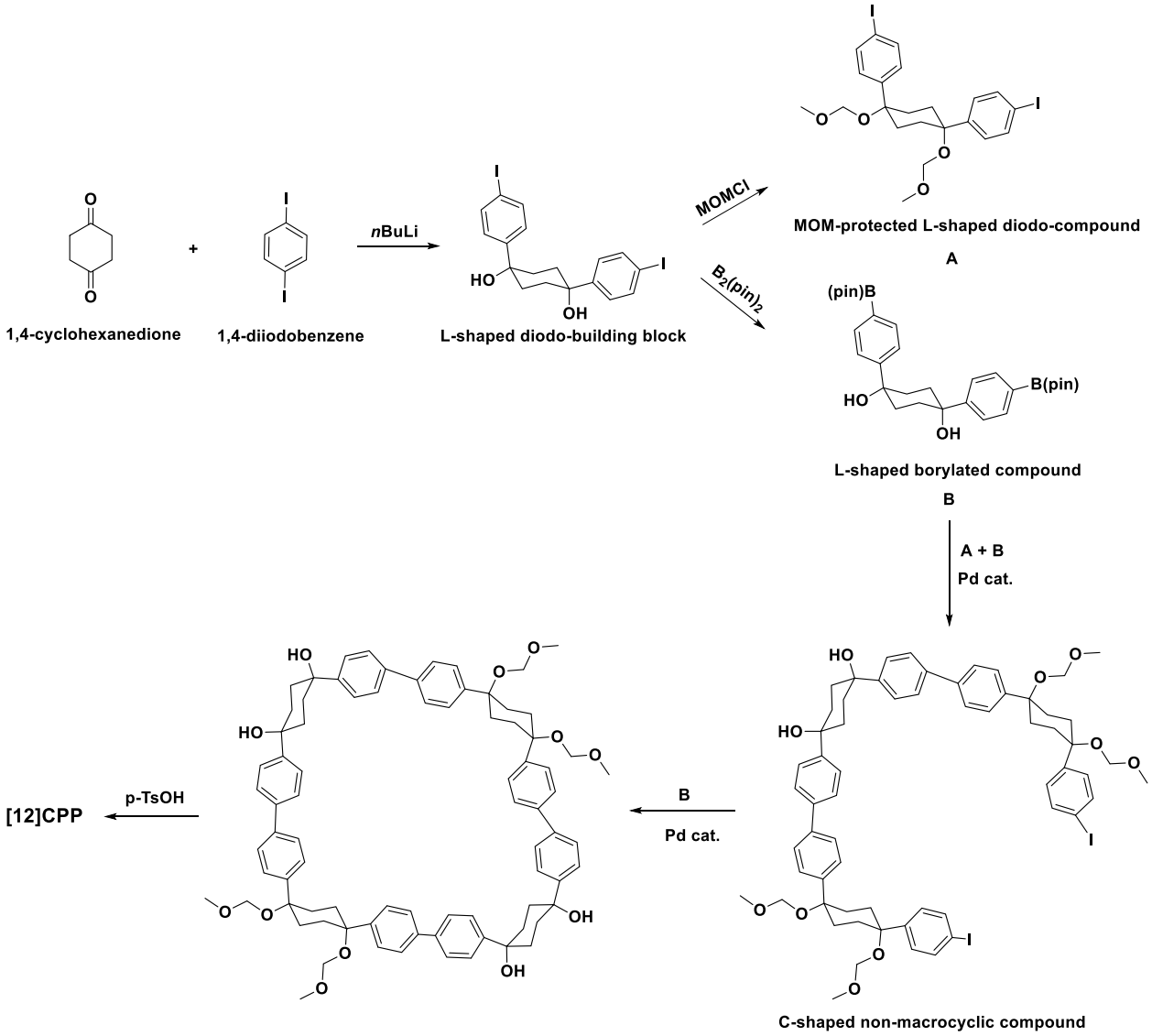

Scheme 7:2 First successful size selective synthesis of CPP.[173]

Although this route provided the desired CPP macrocycle size selectively, several steps were required to obtain the final compound. Itami and co-workers therefore focused on producing [7] – [16]CPPs in less steps. The success of this endeavor provided access to size dependent properties of specific CPPs, as well as their host–guest behaviour.[169]

After the successful synthesis of classical CPP macrocycles, the search for novel CPPs with different substituents began, as it became clear that this would lead to novel complex macrocycles with interesting properties and applications.

7.2.1.2. SUBSTITUTED CPPS

By incorporating functionalities onto the CPP structure, their applications can be significantly expanded. These expanded applications include new host−guest possibilities, possible use in chemosensors and nanoporous materials, as well as the option of connecting these CPP macrocycles to various surfaces. Nevertheless, the synthesis of substituted CPPs is notably more challenging then the unsubstituted CPP macrocycles.

A number of substituted CPPs have been successfully synthesized, including heteroatomic, acene-containing, polycyclic, as well as phenyl- and aryl-substituted CPPs (Figure 7:4).[174]

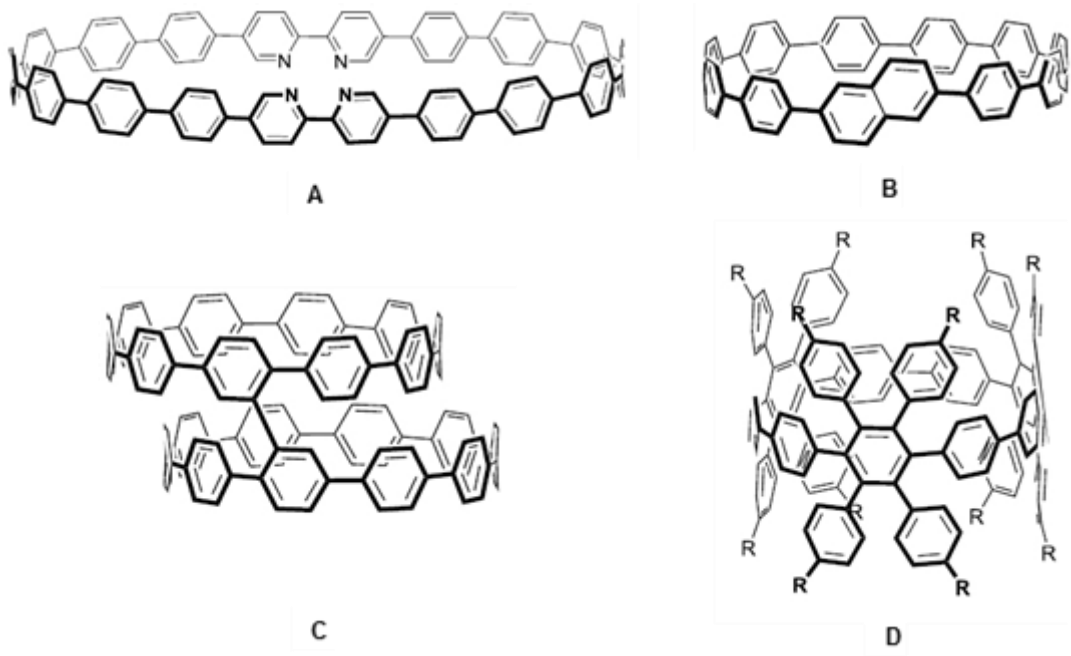

Figure 7:4 Examples of substituted CPPs.[174]

A previous study conducted in the research group of Prof. Dr Hermann A. Wegner, focused on the development of a strategy to obtain novel heteroatomic aryl-substituted [8]CPPs (Scheme 7:3).[175] These CPP molecules were synthesized from the same MOM-protected L-shaped diodo-compound as used by Itami and co-workers in their first size selective synthesis as illustrated in Scheme 7:2.[173] This L-shaped building block was coupled with a protected diyne, followed by the removal of the protecting group. The resulting product was subsequently subjected to a macrocyclization reaction. The final two steps of this synthesis involved a [2+2+2] cycloaddition reaction, followed by an aromatization reaction.

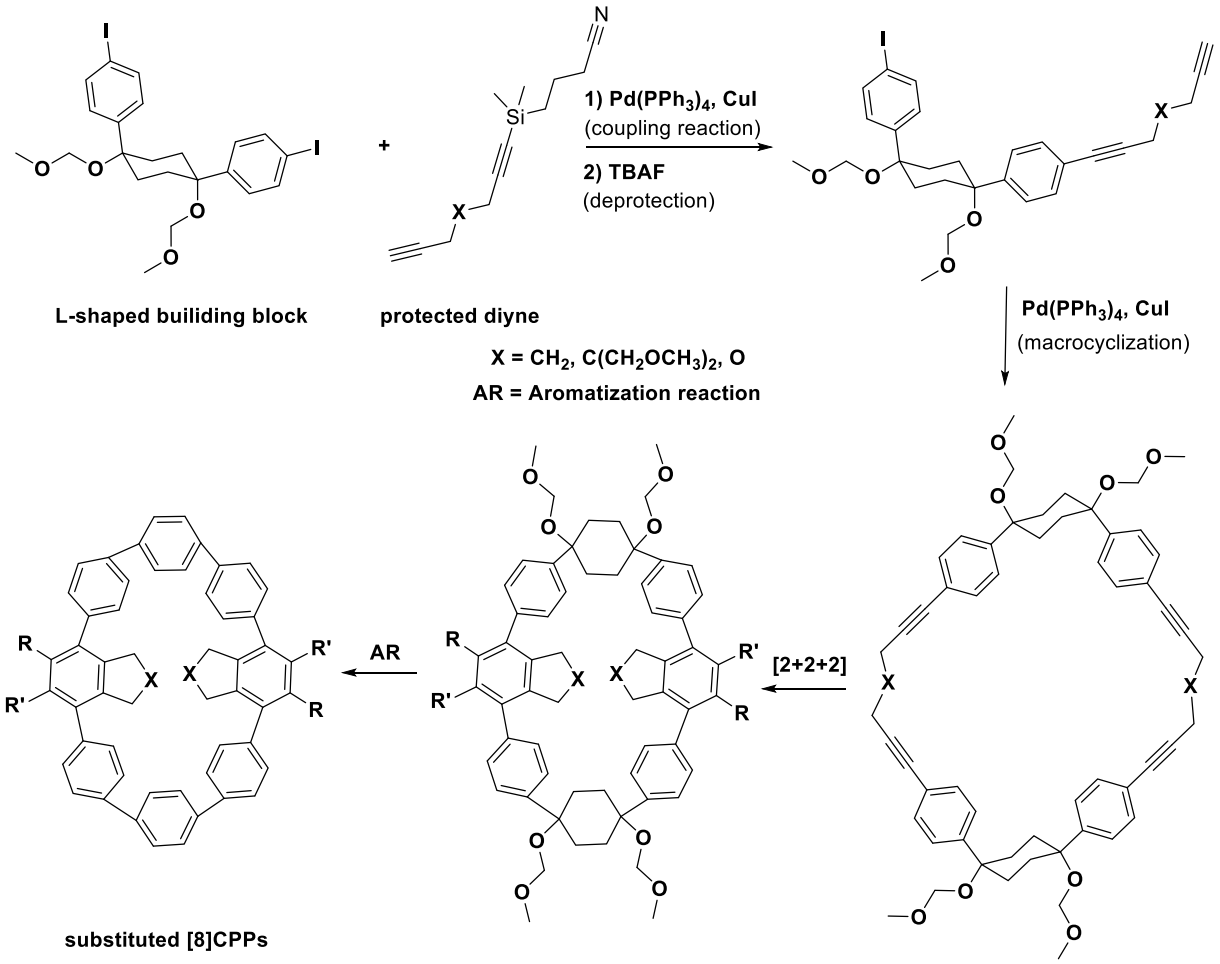

Scheme 7:3 Previous strategy for substituted [8]CPPs in the research group of Prof. Dr Wegner.[175]

The drawback of the method illustrated in Scheme 7:3, is that the protected diyne, as well as the L-shaped unit, must be synthesized separately, which means that the "X" atom in the protected diyne unit cannot be transformed into a different functional group during the synthesis. Incorporating different heteroatoms or halogens into the CPP structure is therefore not possible when using this strategy.

7.3. AIM AND OBJECTIVES

7.3.1. CPP LINKER SYSTEM

In this project, a unique strategy will be explored for the synthesis of substituted [8]CPPs, in which the substituents can easily be transformed into other functional group such as alcohols, thiols, or halogens throughout the synthesis. The envisioned synthetic route towards these substituted [8]CPPs is depicted in Scheme 7:4. The same MOM-protected L-shaped building block, containing two iodobenzenes, will be subjected to a series of reactions which include a Sonogashira coupling reaction, a macrocyclization reaction, a [2+2+2] cycloaddition reaction and finally an aromatization reaction, of which the final two steps are established reactions for this system. The aim is thus to

transform the “X” atom from an alcohol into a bromine atom and subsequently into a sulfur atom, before the macrocyclization step, which will give the option to either produce the oxygen- or sulfur-containing CPP macrocycle at will.

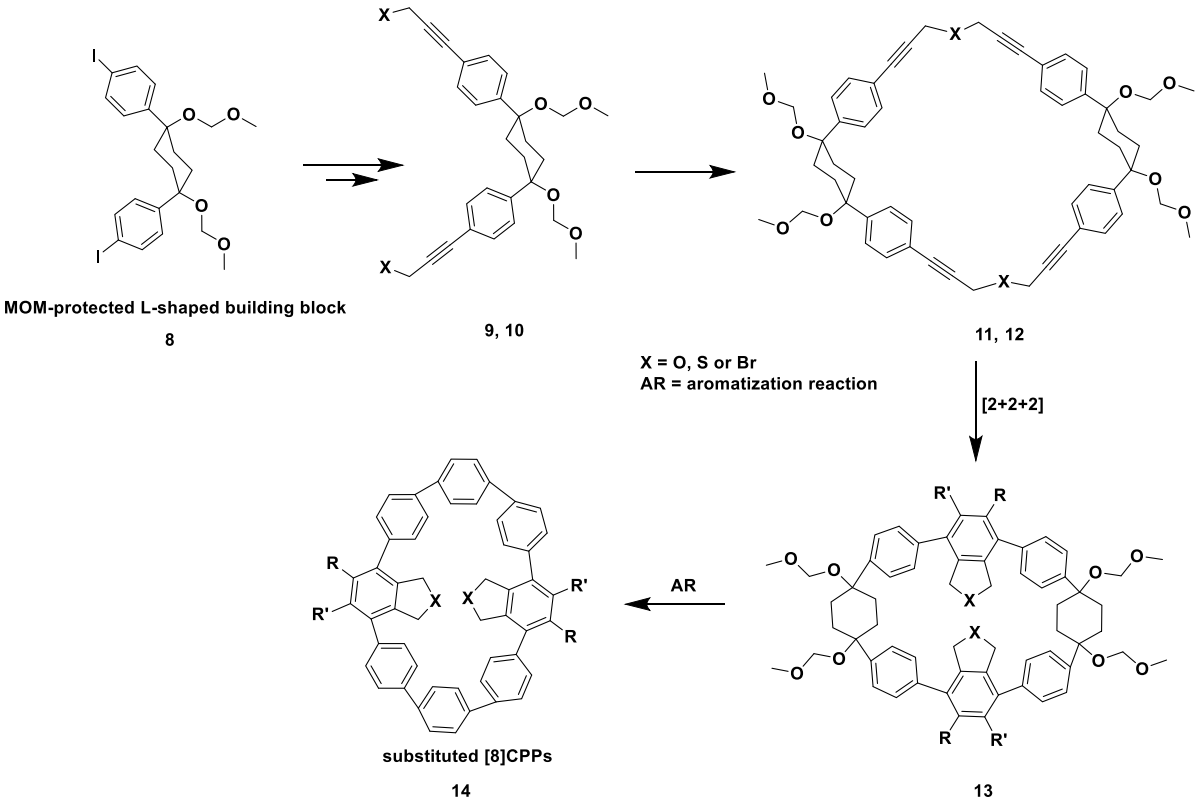

Scheme 7:4 Envisioned strategy for the synthesis of new substituted CPPs.

7.3.2. LINEAR TEST SYSTEM

A linear test system with a similar backbone structure to the substituted CPPs (Scheme 7:5), will first be explored in this study. The aim is to use this linear test system to investigate the synthetic route for the formation of the thioether functionality starting from iodobenzene. With the thioether **5** in hand, the [2+2+2] cycloaddition reaction could also be explored on this test system; however, this step has previously been optimized in the research group of Prof. Dr Wegner.[176] The most important aspect of the synthesis of the linear test system is to find the optimum route for the formation of the thioether functionality. This synthesis will include a Sonogashira coupling reaction, an Appel reaction or similar reactions leading to the same transformation, as well as a nucleophilic substitution reaction. After optimization of this route, the applicable reactions will directly be applied to the CPP linker system to gain access to the sulfur-containing CPP macrocycle.

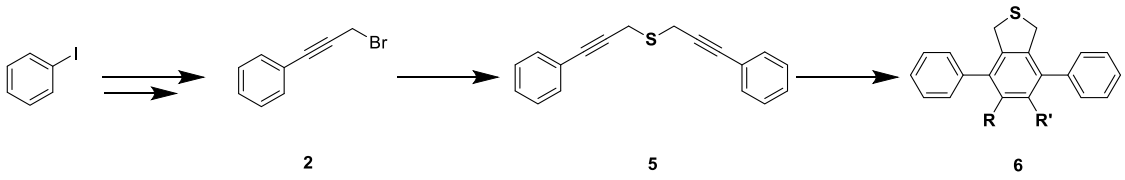

Scheme 7:5 Envisioned strategy for the linear test system.

CHAPTER 8
RESULTS AND DISCUSSION

8.1. SYNTHESIS OF THE LINEAR TEST SYSTEM

8.1.1. SYNTHESIS OF 3-PHENYLPROP-2-YN-1-OL 1

The synthesis of the linear test system started with a Sonogashira cross-coupling reaction as illustrated in Scheme 8:1.[177] Only catalytic amounts of bis(triphenylphosphine)palladium(II)dichloride and copper(I)iodide were needed to successfully couple iodobenzene and propargyl alcohol to obtain the resulting propargylic alcohol **1** in a high yield of 90%.

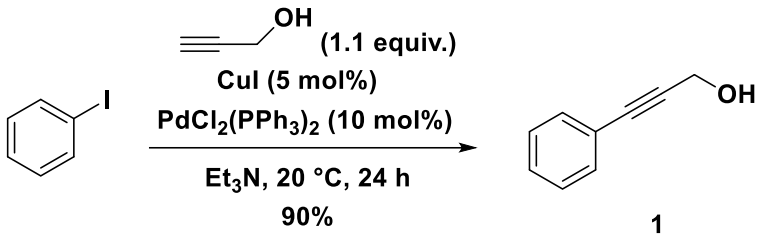

Scheme 8:1 Sonogashira coupling reaction for 1 in the linear test system.

NMR spectra 1 and 2 in Appendix 2 were used to characterize this compound. In the ^{1}H NMR spectrum, a peak was seen at 4.48 ppm which represented the protons attached to the carbon adjacent to the hydroxyl group. In addition, a broad singlet was observed at 2.81 ppm which corresponded to the proton of the hydroxyl group. In the ^{13}C NMR spectrum, two peaks were seen at around 86 ppm which corresponded to the two carbon atoms of the triple bond. Another noteworthy peak appeared at 51.47 ppm which was assigned to the carbon adjacent to the hydroxyl group. This carbon appeared at a higher chemical shift value than normally expected for methylene groups, due to the magnetic anisotropy caused by the adjacent triple bond, as well as the electronegativity of the nearby hydroxyl group. All other proton and carbon atoms were accounted for and the chemical shift values were in accordance with literature.[177]

The currently accepted mechanism for the co-catalyzed Sonogashira cross-coupling reaction applied to this specific system is illustrated in Scheme 8:2.[178] This mechanism is thought to involve two independent catalytic cycles. The palladium cycle started with an oxidative addition of iodobenzene to the palladium catalyst, while the next step in the palladium cycle linked up with the copper cycle. This rate determining step is a transmetalation from the copper acetylide formed via the copper cycle employing triethylamine. The final step involves a reductive elimination which regenerated the palladium catalyst and produced the desired product **1**.[178]

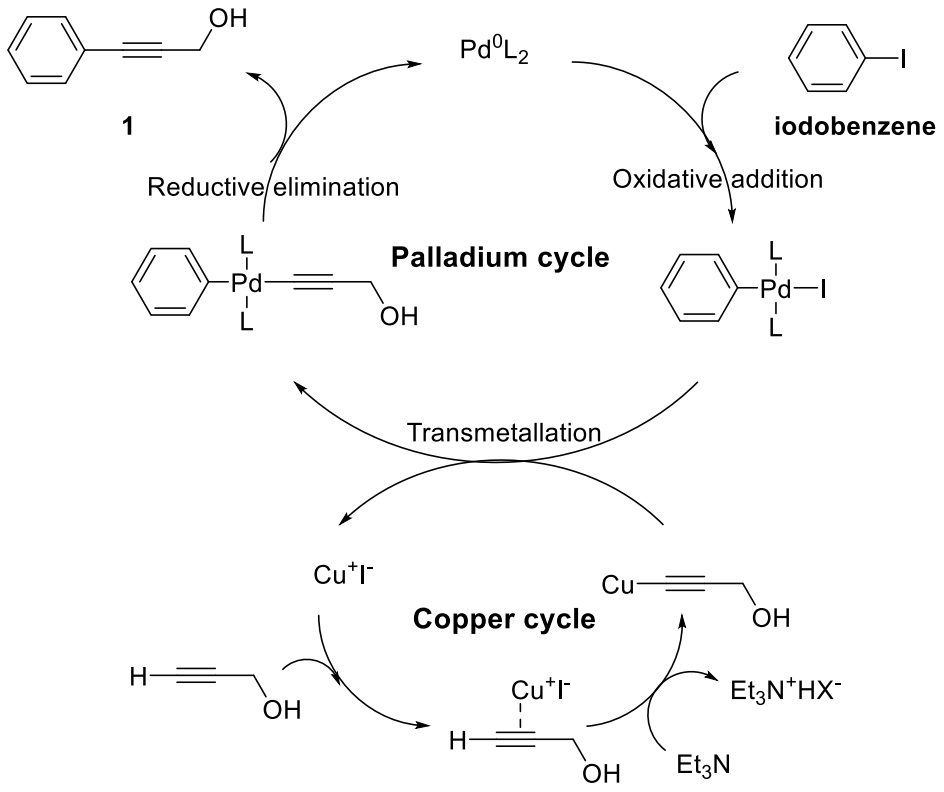

Scheme 8:2 Mechanism for the co-catalyzed Sonogashira cross-coupling reaction.[178]

This reaction proceeded smoothly at room temperature, and in a subsequent attempt the reaction time was shortened without having any effect on the yield. With an optimized procedure in hand, this Sonogashira coupling reaction could be directly applied to the synthesis of the strained CPP linker system.

The subsequent reaction focused on converting this alcohol group into a functionality that could act as a good leaving group.

8.1.2. SYNTHESIS OF (3-BROMOPROP-1-YN-1-YL)BENZENE 2

In the next step, the propargylic alcohol **1** was transformed into the corresponding propargylic bromide **2** by means of an Appel reaction (Scheme 8:3).[177] This transformation involved reacting the alcohol **1** with carbon tetrabromide in the presence of triphenylphosphine. Please note that the mechanism for the Appel reaction was already provided in Section 3.3.3. during the discussion of the main project of this dissertation. The only difference between these two examples is the carbon tetrahalide reagent used for this transformation. The same mechanism as seen in Scheme 3:34 could therefore be consulted for the mechanistic aspects of this reaction. Although the desired product was successfully isolated after purification by column chromatography, the yield was not satisfactory as it did not exceed 60%, even after several attempts.

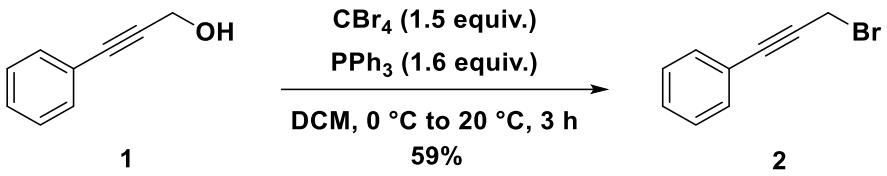

Scheme 8:3 Appel reaction for 2 in the linear test system.

Keeping in mind that these reactions need to be applied to the synthesis of the more strained CPP linker system, a different set of reaction conditions were then investigated for this transformation due to the moderate yield obtained with the Appel reaction. The characterization of compound **2** will follow after the discussion of the second method used for this conversion.

8.1.3. Alternative synthesis of (3-bromoprop-1-yn-1-yl)benzene 2

An alternative method for this functional group manipulation was then explored in which the alcohol **1** was initially transformed into a mesylate, which subsequently underwent a nucleophilic substitution reaction with lithium bromide (Scheme 8:4).[179] After standard work-up and purification, product **2** was obtained in a good yield of 78%, which was a significant improvement compared to the yield obtained when using the Appel reaction conditions.

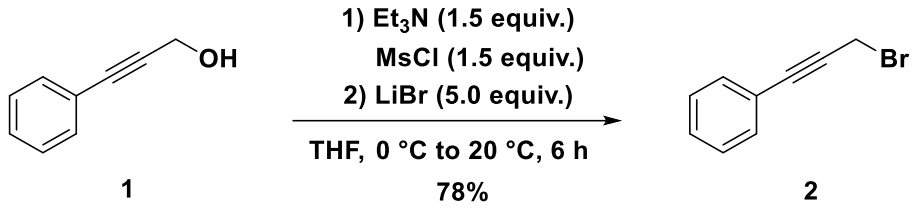

Scheme 8:4 Alternative method for 2 via mesylate intermediate in the linear test system.

NMR spectrum 3 in Appendix 2 was used to characterize this compound. A peak was observed at 4.17 ppm which represented the protons attached to the carbon next to the bromine atom. This peak moved more upfield in comparison to the corresponding peak for the propargylic alcohol **1**. This could be explained by the less electronegative nature of the bromine atom compared to the oxygen atom, which caused this proton to appear more shielded in the spectrum of compound **2**. The disappearance of the broad singlet at 2.81 ppm which corresponded to the proton of the hydroxyl group of **1** further confirmed the successful formation of the desired product **2**. All other proton atoms were accounted for, and the NMR spectroscopic data was consistent with values provided in literature.[177]

This optimized procedure could also be directly applied to the synthesis of the strained CPP linker system. The synthetic route set out for the thioether functionality **5** required the formation of the corresponding propargylic thiol **4**.

8.1.4. ATTEMPTED SYNTHESIS OF 3-PHENYLPROP-2-YNE-1-THIOL 4

The next transformation therefore involved the conversion of a halide (in this case the propargylic bromide) into the deprotected thiol in one step. This transformation required both the formation of the thioacetate **3** followed by a deacetylation to obtained the desired product **4**. It was reported that the deprotected thiol **4** should be obtained under the reaction conditions depicted in Scheme 8:5, but in our hands only the thioacetate **3** was observed.[180]

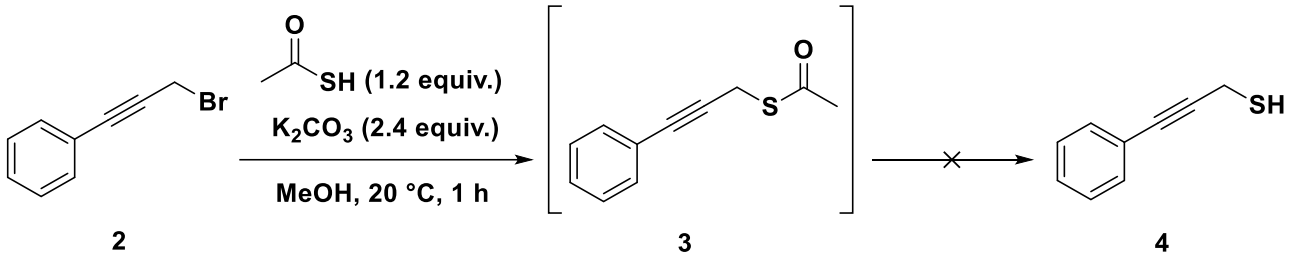

Scheme 8:5 Attempted synthesis of 4 in the linear test system.

With the difficulties encountered with the direct conversion of the propargylic bromide **2** into the deprotected thiol **4**, the synthetic strategy was slightly altered to a route which included the intentional synthesis of compound **3**. With the reaction conditions illustrated in Scheme 8:5, two compounds were observed as determined by TLC, and subsequent onsite GC-MS analysis confirmed the presence of the thioacetate **3** along with an unidentified by-product. Due to the formation of this unwanted side-product under these conditions, an additional set of reaction conditions were investigated for the synthesis of the thioacetate **3**. The characterization of product **3** will follow after the discussion of the second method used for this conversion.

8.1.5. SYNTHESIS OF S-(3-PHENYLPROP-2-YN-1-YL) ETHANETHIOATE 3

The propargylic thioacetate **3** could also be obtained from the alcohol **1** by using a Mitsunobu reaction with thioacetic acid in the presence of triphenylphosphine and diethyl azodicarboxylate (DEAD) as can be seen in Scheme 8:6.[181] Unfortunately, this method also led to a variety of side products, as determined by TLC. After removal of the solvent and a challenging purification process by means of column chromatography, the pure thioacetate **3** was obtained in a low yield of 34%.

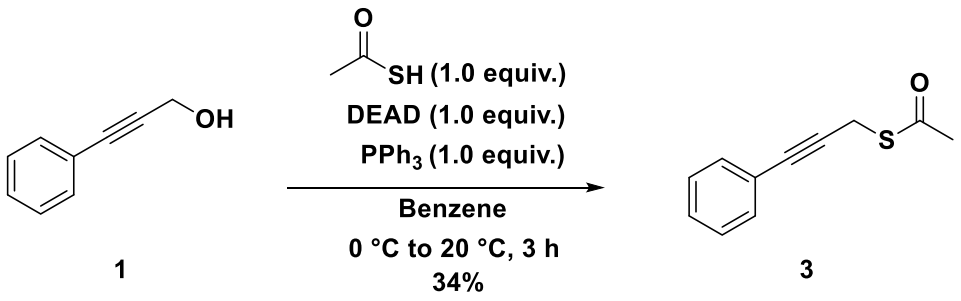

Scheme 8:6 Intentional synthesis of 3 in the linear test system (Mitsunobu reaction).

The proposed mechanism for the Mitsunobu reaction as applied to this specific system is depicted in Scheme 8:7.[182] This process started with the nucleophilic attack of triphenylphosphine onto the nitrogen-nitrogen double bond of DEAD and the resulting betaine intermediate was then protonated through an interaction with thioacetic acid. Subsequent addition of the propargylic alcohol **1** led to the formation of a hydrazide compound along with an oxyphosphonium intermediate. A final nucleophilic substitution reaction with the deprotonated thioacetic acid provided the thioacetate **3** along with triphenylphosphine oxide as by-product.[182]

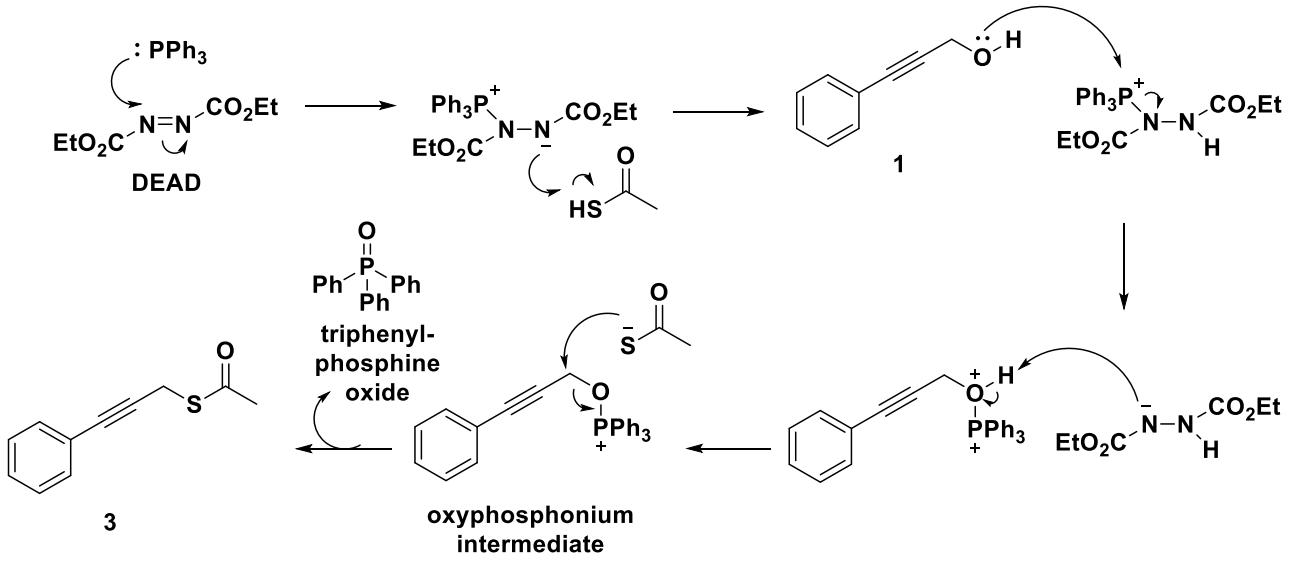

Scheme 8:7 Proposed mechanism for the Mitsunobu reaction.[182]

NMR spectrum 4 located in Appendix 2 was used to characterize this compound. A peak was seen at 3.90 ppm which represented the protons attached to the carbon next to the sulfur atom. This peak moved even more upfield in comparison to the corresponding peak for the propargylic bromide **2**, and this could once again be explained by the electronegativity difference of the adjacent atom as the electronegativity of bromine is slightly larger than that of sulfur. An additional peak also appeared at 2.39 ppm which represented the protons of the methyl carbon introduced by the acetate group.

The next step involved the transformation of the thioacetate **3** into the desired thioether functionality **5**. The crude thioacetate **3** obtained during the attempted synthesis of the free thiol **4** was used in the initial attempt to determine whether this would be a viable route to explore before using the thioacetate **3** isolated after the Mitsunobu procedure.

8.1.6. First attempted synthesis of bis(3-phenylprop-2-yn-1-yl)sulfane 5

A procedure was then attempted which involved the *in situ* cleavage of the acetal moiety of the thioacetate **3** with potassium hydroxide in methanol, followed by an alkylation of the resulting propargylic thiol **4** with the propargylic bromide **2** to potentially form the linear sulfide **5** (Scheme

8:8).[181] GC-MS analysis confirmed the presence of the propargylic thiol **4,** but unfortunately no alkylation reaction took place with the bromide **2**.

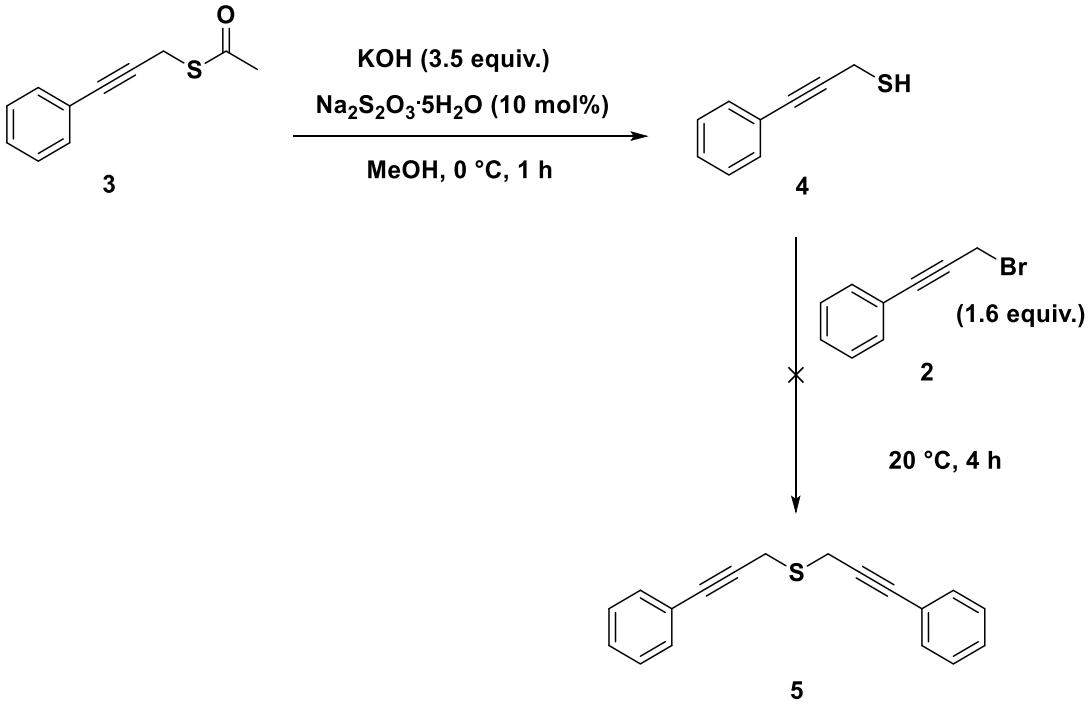

Scheme 8:8 Deacetylation and first attempted formation of the linear sulfide 5 in the linear test system.

Due to the problems encountered in obtaining the free thiol **4** and the subsequent low yield obtained for the thioacetate **3**, as well as the unsuccessful formation of the sulfide **5**, three alternative routes were investigated. The three additional routes explored for the synthesis of the linear sulfide **5**, did not involve the formation of the propargylic thiol **4**, which meant that two steps would be eliminated from the synthesis of the linear sulfide **5**.

8.1.7. SECOND ATTEMPTED SYNTHESIS OF BIS(3-PHENYLPROP-2-YN-1-YL)SULFANE 5

The second attempt at synthesizing the linear sulfide **5** was a coupling reaction in which the propargylic bromide **2** was reacted with sodium sulfide in methanol. Unfortunately, this route was also unsuccessful and only starting material was recovered (Scheme 8:9).[181]

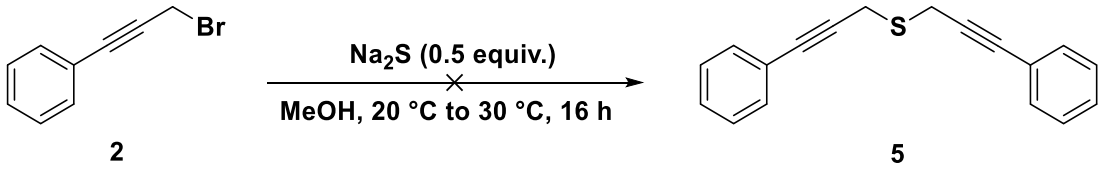

Scheme 8:9 Second attempted formation of linear sulfide 5 in the linear test system.

8.1.8. SUCCESSFUL SYNTHESIS OF BIS(3-PHENYLPROP-2-YN-1-YL)SULFANE 5

For the third attempt at synthesizing the linear sulfide **5** two different methods were combined. The alcohol **1** was initially transformed into a mesylate, which was subsequently reacted with sodium

sulfide (Scheme 8:10).[179,181] This method finally provided the linear sulfide **5**, but unfortunately a variety of side products were also formed which led to a very low yield of 28%.

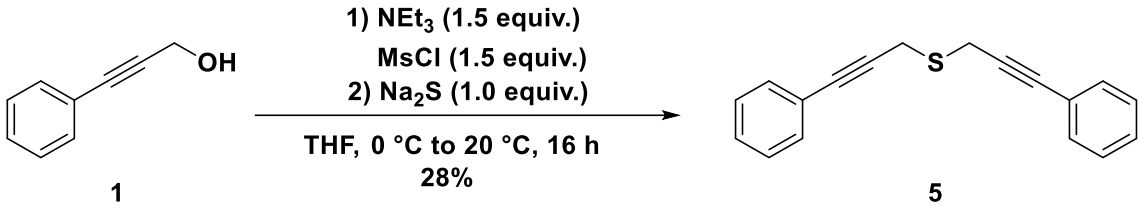

Scheme 8:10 First successful formation of linear sulfide 5 in the linear test system.

Characterization of compound 5 was achieved by studying NMR spectrum 5 in Appendix 2. A peak was observed at 3.72 ppm which represented the protons attached to the two carbon atoms adjacent to the sulfur atom. A significant difference was seen in the chemical shift values of these protons to the alcohol **1**. Due to the less electronegative nature of the sulfur atom, these protons appeared more shielded for **5** than in the corresponding alcohol. Also note the absence of a peak representing a methyl group which confirmed that this product was not the mesylate intermediate formed during this reaction. The calculated molar mass also corresponded with the molar mass determined by GC-MS. All other proton atoms were accounted for, and were in accordance with previously reported spectral data.[179]

8.1.9. Alternative synthesis of bis(3-phenylprop-2-yn-1-yl)sulfane 5

An alternative method for the synthesis of the linear sulfide **5** was then explored in which the propargylic bromide **2** underwent treatment with sodium sulfide in a solvent mixture of tetrahydrofuran and water, under phase transfer conditions (Scheme 8:11).[179] After standard work-up and purification by column chromatography, product **5** was obtained in a yield of 58%. Although the yield of this reaction was still not ideal, it was a significant improvement based on the yield obtained with the method shown in Scheme 8:10. When considering all the problems encountered while trying to obtain this thioether **5**, we were satisfied with this result.

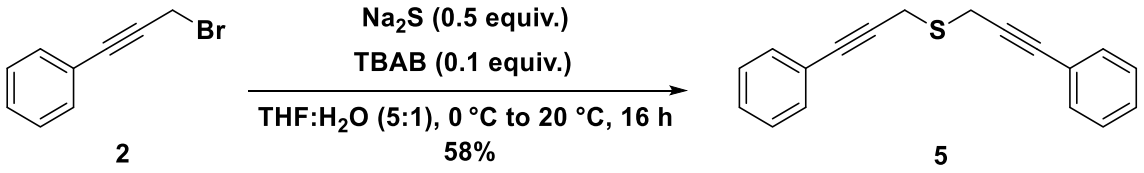

Scheme 8:11 Alternative method for formation of linear sulfide 5 in the linear test system.

As previously mentioned, the aim of this section was to explore the synthesis of the thioether functionality and to find reactions which could directly be applied to the more strained CPP linker system. However, with the linear thioether **5** in hand, a final reaction was attempted for this system in the hopes of obtaining the sulfur-containing linear *para*-phenylene **6**.

8.1.10. ATTEMPTED SYNTHESIS OF 5-ETHYL-4,7-DIPHENYL-6-PROPYL-1,3-DIHYDROBENZO[C]THIOPHENE 6

The final step for the linear test system was to subject the linear sulfide **5** to a [2+2+2] cycloaddition reaction by using Wilkinson's catalyst in a mixture of isopropyl alcohol and tetrahydrofuran under microwave irradiation (Scheme 8:12).[183] The monoyne chosen was hept-3-yne as a previous study had shown that it is a good substrate for systems similar to this test system.[176]

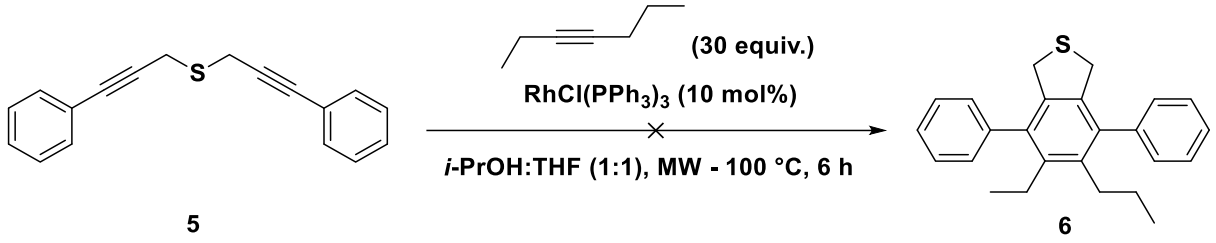

Scheme 8:12 Attempted [2+2+2] cycloaddition in the linear test system.

Unfortunately, the microwave vial exploded during this attempt. The [2+2+2] cycloaddition reaction has previously been investigated in the research group of Prof. Dr Wegner and optimum conditions for this cycloaddition have already been determined for similar linear systems.[176] Therefore, by keeping in mind the time limit associated with this project, it was decided to rather focus on the synthesis of the CPP linker system.

The process involved in the synthesis of the linear test system was very useful as it provided successful methods for the Sonogashira coupling reaction, the bromination reaction, as well as the formation of the thioether functionality which could all be directly applied to the synthesis of the CPP linker system.

8.2. SYNTHESIS OF THE CPP LINKER SYSTEM

8.2.1. SYNTHESIS OF THE L-SHAPED BUILDING BLOCK, 1,4-BIS(4-IODOPHENYL)CYCLOHEXANE-1,4-DIOL 7

The first step in the synthesis of the CPP linker system involved the formation of the L-shaped building block **7** from 1,4-diiodobenzene and 1,4-cyclohexanedione (Scheme 8:13).[171] The two-fold addition of the 4-iodophenyllithium compound (prepared from 1,4-diiodobenzene and *n*BuLi) to 1,4-cyclohexanedione provided the desired product **7** in a yield of 24% after purification by re-crystallization.

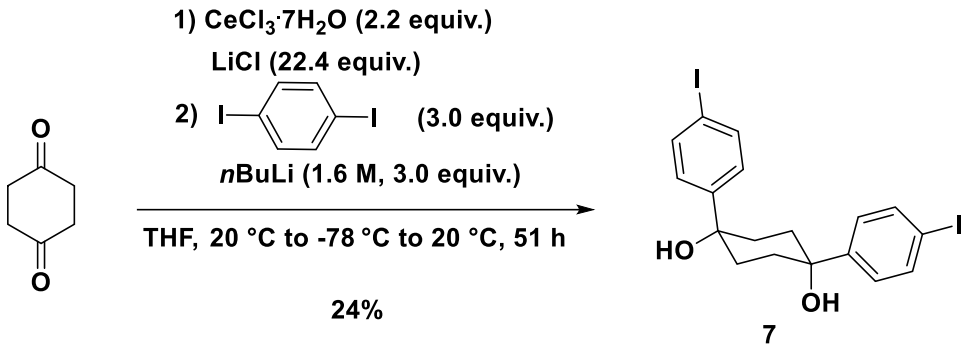

Scheme 8:13 Synthesis of L-shaped building block 7 in the CPP linker system.

The formation of both the mono-addition product and the *trans*-isomer, was suppressed through coordination of the 1,4-cyclohexanedione to the $CeCl_3$•$(LiCl)_2$ complex. This L-shaped curvature is essential as it pre-organizes the building block in a conformation that facilitates the subsequent macrocyclization. The yield could still be further improved as some problems were encountered during the transfer of the 4-iodophenyllithium species to the 1,4-cyclohexanedione solution by means of cannulation. NMR spectrum 6 in Appendix 2 was used to characterize this compound. In terms of evidence, the two protons of the hydroxyl groups were seen as a broad signal at 1.69 ppm and all 8 protons of the cyclohexane ring appeared as a multiplet at 2.10 – 2.02 ppm. All other proton atoms were accounted for and the NMR spectroscopic data was in agreement with literature.[169]

8.2.2. Synthesis of 1,4-bis(4-iodophenyl)-1,4-bis(methoxymethoxy)cyclohexane 8

A subsequent protection with chloromethyl methyl ether (MOMCl) provided the MOM-protected diiodide **8** in a good yield of 71% as depicted in Scheme 8:14.[171] The MOM-protecting group was chosen as it is known to enhance the solubility of the subsequent products based on this building block, thus facilitating their handling and purification.[171]

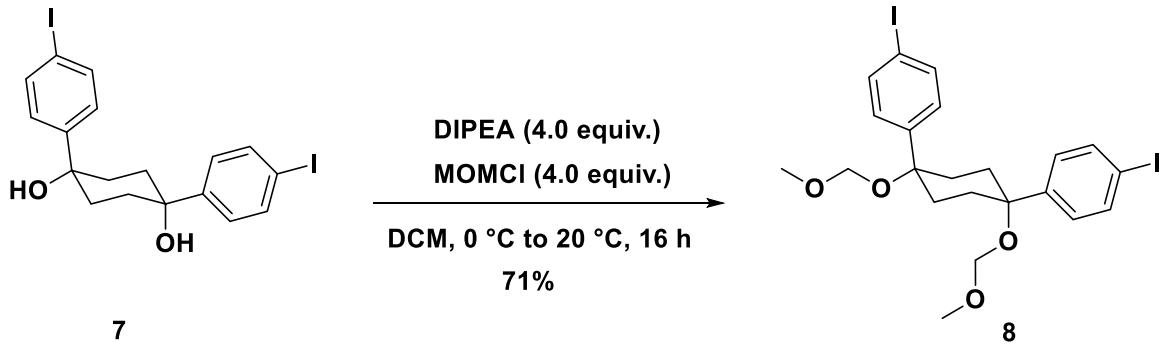

Scheme 8:14 Synthesis of the MOM-protected diiodide 8 in the CPP linker system.

NMR spectrum 7 in Appendix 2 was studied during the characterization of this compound. The two protons of the hydroxyl groups seen in the spectrum of compound **7** disappeared, but all 8 protons of the cyclohexane ring could still be seen as a multiplet at 2.28- 2.01 ppm. Two additional peaks

were also observed, one at 3.39 ppm corresponding to the two methyl carbons of the MOM-protecting group and one peak at 4.41 ppm corresponding to the two bridged carbons between the oxygen atoms of the MOM-protecting group.

All other proton atoms were noted and the chemical shift values were in accordance with previously reported spectra.[171]

8.2.3. Synthesis of 3,3'-{[1,4-bis(methoxymethoxy)cyclohexane-1,4-diyl]bis(4,1-phenylene)}bis(prop-2-yn-1-ol) 9

In the next step, the diol **9** was synthesized by means of a Sonogashira cross-coupling reaction between the MOM-protected diiodide **8** and propargyl alcohol (Scheme 8:15), in the presence of bis(triphenylphosphine)palladium(II) dichloride and copper iodide in triethylamine.[177] The yield of this reaction was comparable to the Sonogashira coupling reaction in the linear test system.

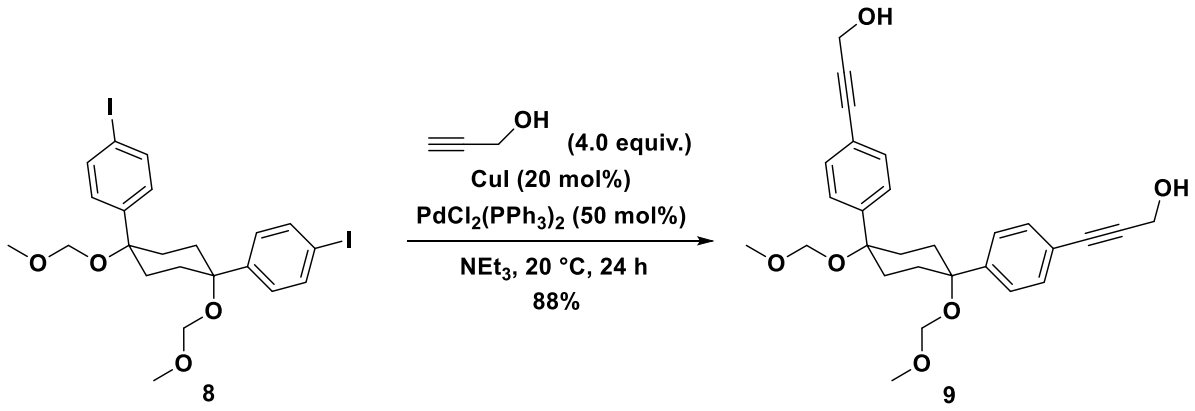

Scheme 8:15 Synthesis of diol 9 through a Sonogashira coupling reaction in the CPP linker system.

NMR spectrum 8 located in Appendix 2 was used to characterize this compound. Two additional peaks were present in comparison to the spectrum of compound **8**. A peak was observed at 1.62 ppm which represented the two hydroxyl groups, while the other peak, which corresponded to the protons attached to the carbon next to the hydroxyl group, appeared at 4.49 ppm. All other proton atoms were accounted for and the chemical shift values were in accordance with literature.[177]

8.2.4. Synthesis of 1,4-bis[4-(3-bromoprop-1-yn-1-yl)phenyl]-1,4-bis(methoxymethoxy)cyclohexane 10

The next reaction involved a functional group transformation from the diol **9** to the dibromo compound **10**. As shown in the linear test system, two methods were available for this transformation; however, the method shown in Scheme 8:16 was chosen because it led to a higher yield than the Appel reaction in the linear test system.[179] The diol **9** was initially transformed into the mesylated compound which subsequently underwent a nucleophilic substitution reaction with lithium bromide.

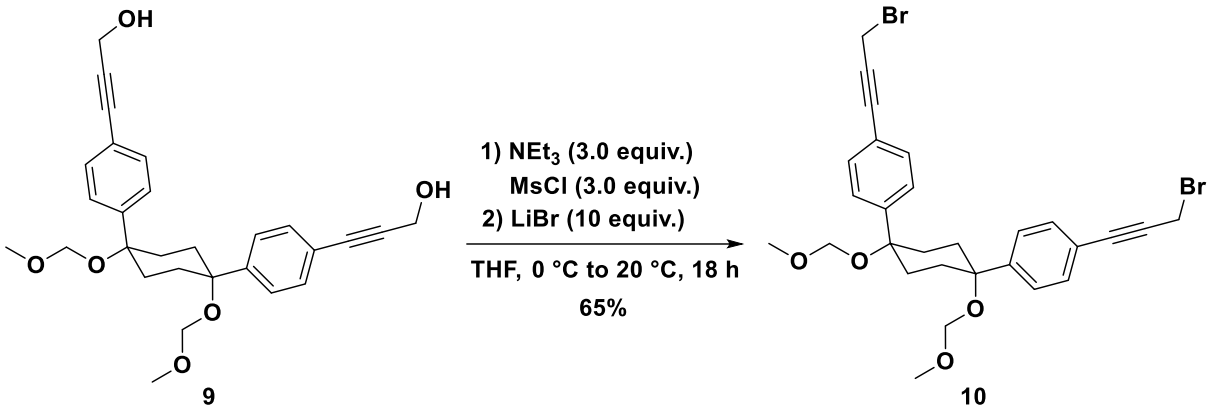

Scheme 8:16 Synthesis of dibromo 10 in the CPP linker system.

NMR spectrum 9 in Appendix 2 was used to characterize this compound. A peak was seen at 4.15 ppm which represented the protons attached to the carbon adjacent to the bromine atom. Similar to the linear test system, this peak moved more upfield in comparison to the corresponding peak for the propargylic alcohol **9** due to the fact that the oxygen atom was more electronegative than the bromine atom causing these protons of **10** to appear more shielded.

The biggest challenge in the synthesis of CPPs is the formation of the macrocycle which usually contains high levels of intrinsic ring strain, mostly resulting from the connection of benzene rings in the *para*-positions. The macrocyclization step is usually reported in very low yields and often requires high dilution to counteract the reduction of entropy.

As shown in Section 7.2.1.2, the oxygen-containing MOM-protected macrocycle and resulting substituted CPP compounds were already access in a previous study in the research group of Prof. Dr Hermann Wegner by using a different strategy than designed in this project. This project was therefore focused on designing a method which could provide access to the thioether functionality and the corresponding sulfur-containing substituted [8]CPP macrocycle, which could also allow access different functional groups instead of the thioether linker. To this end, the synthesis of the oxygen-containing MOM-protected macrocycle **11** was subsequently explored.

8.2.5. ATTEMPTED SYNTHESIS OF THE OXYGEN-CONTAINING MOM-PROTECTED MACROCYCLE 11

The macrocyclization was attempted between the diol **9** and dibromo **10** in the presence of the sodium hydride in the hope that the nucleophilic substitution reaction would take place to form the ether linkages (Scheme 8:17) and provide macrocycle **11**.[184] Unfortunately, under these conditions, formation of the macrocycle was not observed.

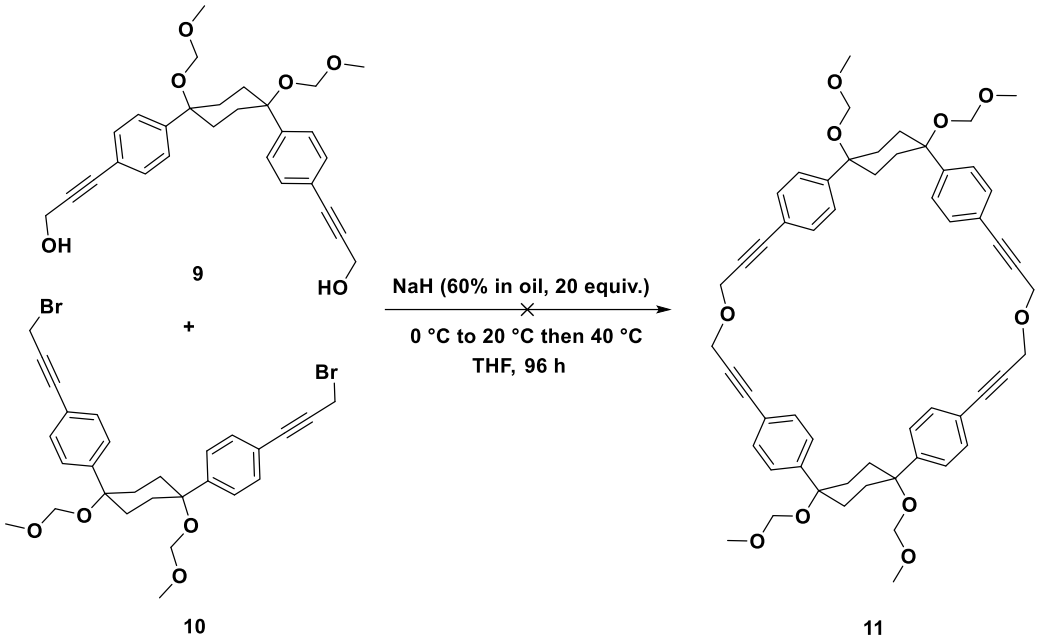

Scheme 8:17 Attempted synthesis of oxygen-containing macrocycle 11 in the CPP linker system.

As the synthesis of the oxygen-containing MOM-protected macrocycle was not the main purpose of this study, eyes were set on the synthesis of the sulfur-containing MOM-protected macrocycle.

8.2.6. SYNTHESIS OF THE SULFUR-CONTAINING MOM-PROTECTED MACROCYCLE 12

In a first trial to extend the synthetic strategy, the synthesis of the thioether linkage was attempted. The method developed for the linear test system was used to provide - what we believe to be - the thioether containing macrocycle in a low yield of 2%. In this event, the dibromo compound **10** was treated with sodium sulfide in a mixture of tetrahydrofuran and water under phase transfer conditions (Scheme 8:18).[179]

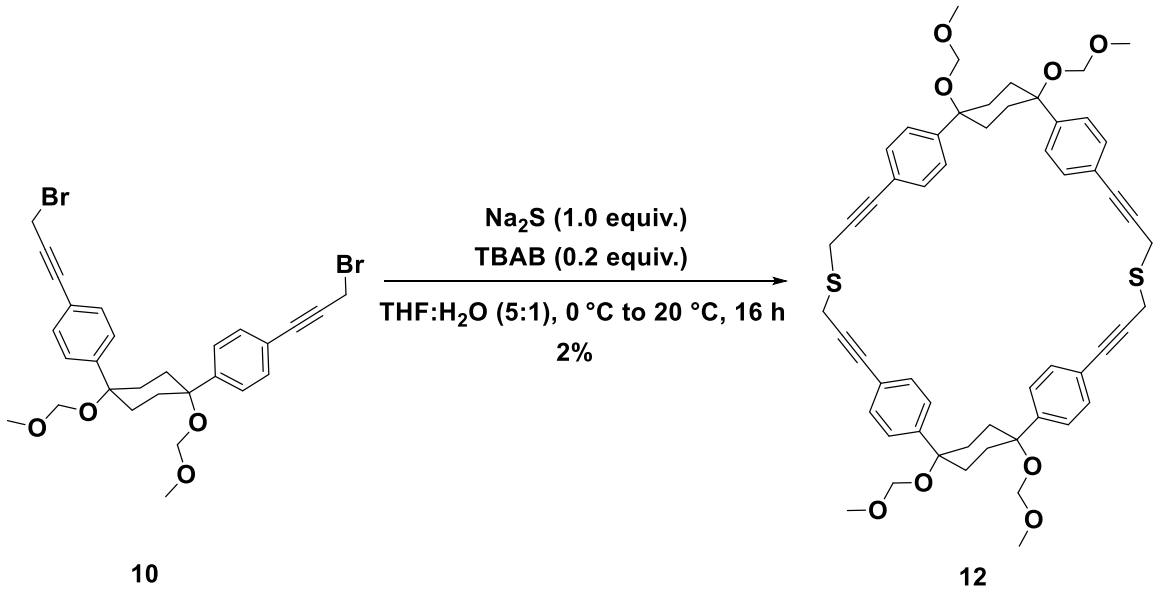

Scheme 8:18 Synthesis of sulfur-containing macrocycle 12 in the CPP linker system.

Note that the NMR assignment of this compound is given with caution. A tentative assignment has been made based on the NMR spectra at hand, the spectra of the precursors, as well as the spectra of the oxygen-containing MOM-protected macrocycle previously synthesized in this group, as already mentioned. For a more accurate assignment or to confirm the assignment made in this document, additional NMR experiments must be conducted. It should be considered to obtain the heteronuclear single-quantum correlation spectroscopy (HSQC) spectrum, as well as the homonuclear correlation spectroscopy (COSY) spectrum. These two experiments will provide information on the proton-carbon coupling between directly attached proton and carbon nuclei, as well as the proton-proton coupling between adjacent proton nuclei, respectively. An additional one-dimensional NMR experiment that might also be of interest is the attached proton test (APT). This experiment will indicate which of these carbons are quaternary or methylene carbons and which of these carbon atoms are methane or methyl carbons. These experiments were not conducted during the scope of this study, as only 18.7 mg (2%) of compound **12** was obtained, and the time allocated to this project and the exchange period had come to an end.

NMR spectra 10 and 11 in Appendix 2 were studied during the characterization of this compound. An important peak was observed at 3.70 ppm in the ^{1}H NMR spectrum. This peak represented the protons attached to the four carbon atoms next to the two sulfur atoms. This chemical shift was identical to the chemical shift of the corresponding protons for the thioether compound **5** in the linear test system. The structure of the sulfur-containing macrocycle **12** and the thioether compound **5** synthesized in the linear test system indication the relative atoms mentioned above is illustrated below:

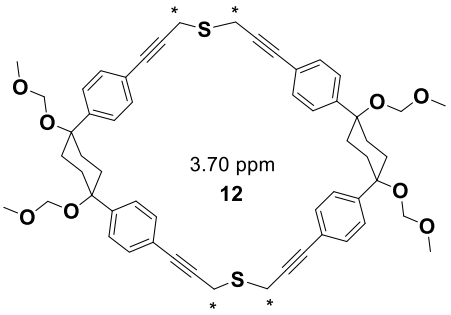

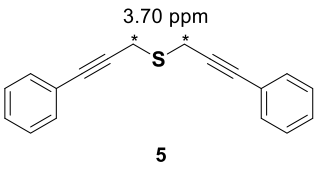

Unfortunately, an accurate molar mass could not be determined for this compound, even when using electron spray ionization and atmospheric pressure ionization. These results are essential for the complete characterization of this macrocycle. However, the NMR spectra strongly suggested that the desired sulfur-containing macrocycle was formed. Due to the time limit associated with this study and the exchange period in Germany, this project could unfortunately not be explored further; however, this is an ongoing research project in the group of Prof. Dr Wegner. It should be considered of high importance to synthesize this sulfur-containing MOM-protected macrocycle with an improved yield so that the following steps could be investigated for the synthesis of the sulfur-containing substituted [8]CPP.

CHAPTER 9
CONCLUDING REMARKS

9.1. CONCLUSION

In conclusion, a successful method for the synthesis of the thioether functionality has been developed throughout this project by means of a linear test system. The test system was very useful as it provided successful methods for the Sonogashira coupling reaction and the bromination reaction, as well as the formation of the thioether functionality which could all be directly applied to the synthesis of the CPP linker system. A successful method for the [2+2+2] cycloaddition reaction has been developed during a previous project for systems very similar to this linear test system. Nevertheless, the [2+2+2] cycloaddition reaction still needs to be tested on the linear test system (containing the thioether functionality) before it can be applied to the CPP linker system.

When considering the CPP linker system, a successful route was developed to obtain the dibromo-linker compound **10**. With this compound in hand, new exciting opportunities will come to light as this project progresses as this compound could provide the option of effortlessly transforming the substituents throughout the synthesis of future substituted CPPs. The dibromo-linker compound was subsequently used to gain access to the sulfur-containing MOM-protected macrocycle **12** by making use of the method developed in the linear test system. The novel sulfur-containing substituted [8]CPP macrocycle can now be obtain in only a few well-established steps.

9.2. FUTURE WORK

Once a successful method for the formation of the oxygen-containing MOM-protected macrocycle has also been determined, the [2+2+2] cycloaddition will be performed on both macrocycles to introduce the substituents into the macrocyclic structure (Scheme 9:1).[175]

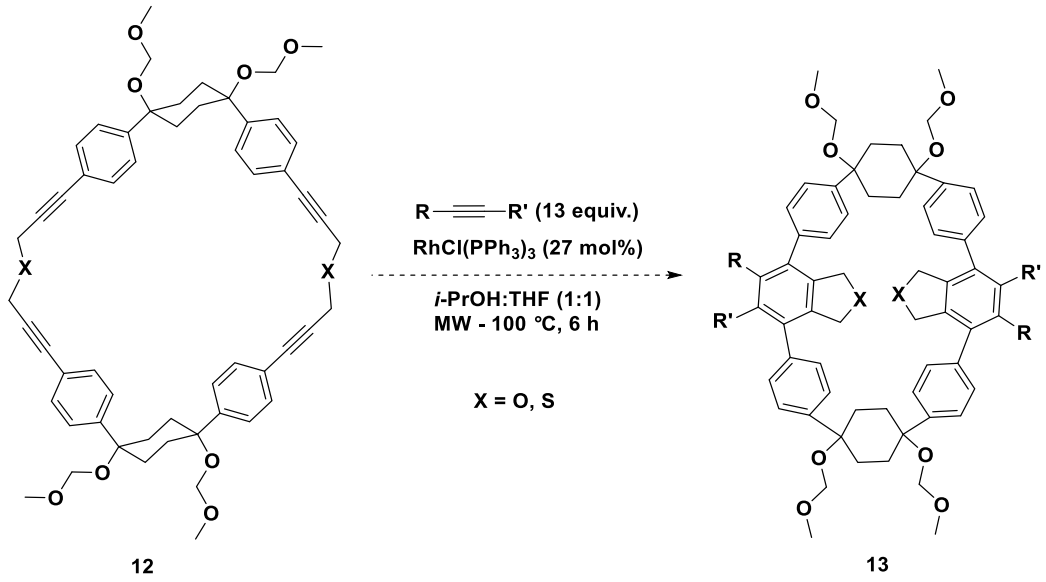

Scheme 9:1 The [2+2+2] cycloaddition reaction using Wilkinson's catalyst in the CPP linker system.

Finally, the substituted CPPs will be obtained through an aromatization reaction (Scheme 9:2).[175] Up to now, only very low yields have been reported for this step due to the high strain energy that must be overcome.

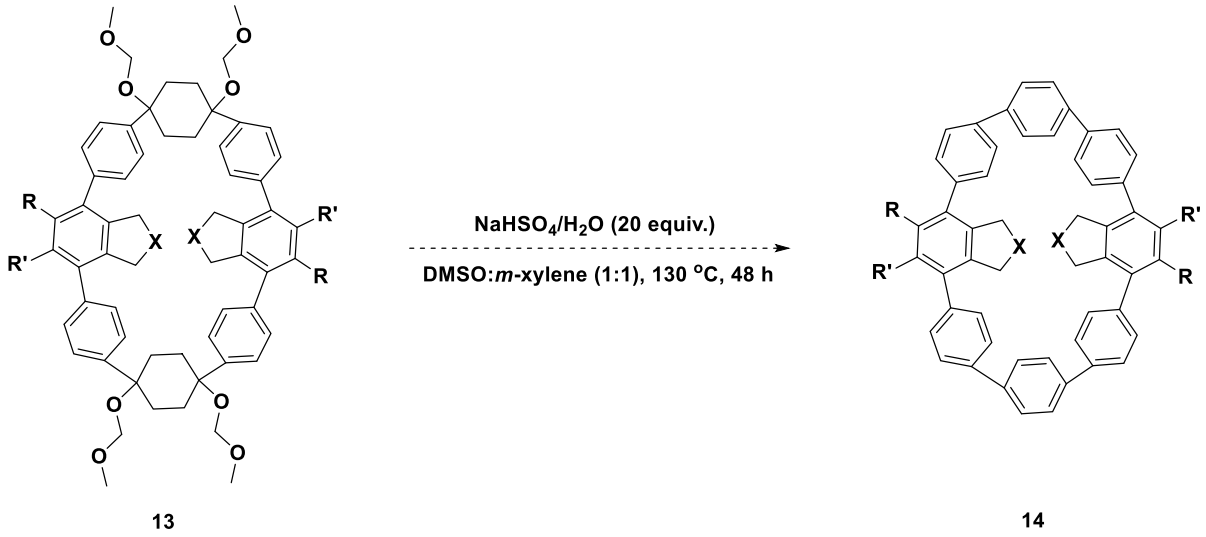

13 14

Scheme 9:2 Deprotection- elimination and Aromatization in the CPP linker system.

These substituted CPPs can then be subjected to further functionalizations in which the substituents can be transformed, and undergo further directed functionalizations onto the neighbouring unsubstituted benzene rings (Scheme 9:3).

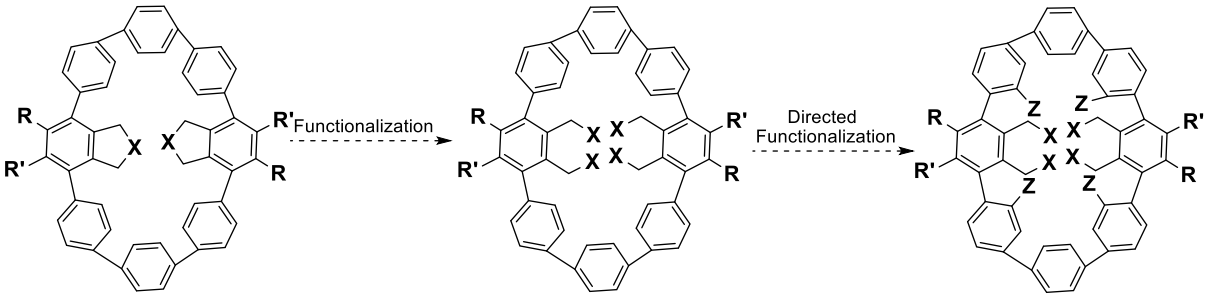

15 16 17

Scheme 9:3 Post-functionalizations of substituted CPPs.

The incorporation of functionalities at this late stage of the synthesis will lead to more creative new CPP-based structures which will further broaden the application range. Further work can also focus on determining the properties of these substituted CPPs, developing a synthetic strategy towards longer fragments of carbon nanotubes, and examining possible applications of these CPPs in nanoporous materials.

CHAPTER 10
EXPERIMENTAL

10.1. GENERAL INFORMATION

Reaction glassware was dried by heating under a positive nitrogen pressure, or in an oven at 110 °C for two hours. Reaction mixtures were heated by placing the reaction flask in a paraffin oil bath, set to the correct temperature on a magnetic stirrer hot plate. Solvents were removed *in vacuo*, by using a rotary evaporator followed by the use of a high vacuum pump at ca. 0.08 mm Hg, to remove trace amounts of residual solvent.

All chemicals used in these experiments were purchased from Sigma Aldrich (Merck), Acros, TCI Europe, or Alfa Aesar. Anhydrous solvents were dried with a solvent purification system (MBRAUN MB-SPS-800) or purchased directly (with crown cap vails over molecular sieves) for small scale reactions. Other reagents which required purification was purified according to standard procedures.

Air and/or moisture sensitive reactions were set up in a nitrogen-filled MBRAUN UNIlab glove box.

Thin layer chromatography (TLC) was performed using Macherey-Nagel™ POLYGRAM SIL G=UV254 Sheets. Visualization of the plates were achieved by using a 254 nm UV light; along with staining the compounds with appropriate stains, followed by heating of the stained plate. Column chromatography was performed using Macherey-Nagel™ silica gel 60 (particle size 0.063-0.200 mm) using different ratios of ethyl acetate and cyclohexane.

NMR spectra (^{1}H, ^{13}C) were either recorded on a Bruker Avance II 400 MHz (AV 400) (101 MHz for ^{13}C). All spectra were obtained at 25 °C unless otherwise stated, and the NMR spectroscopy data was processed using MestReNova. Chemical shifts were recorded using the residual solvent peak or external reference. Furthermore, chemical shifts (δ) are given in parts per million (ppm) and J-values in Hertz (Hz).

10.2. SYNTHESIS OF THE LINEAR TEST SYSTEM

10.2.1. SYNTHESIS OF 3-PHENYLPROP-2-YN-1-OL 1

Freshly distilled triethylamine (50 mL) was added into a 100 mL three-neck round-bottom flask under a N_2 atmosphere. Copper(I)iodide (4.0 mg, 0.021 mmol, 0.0050 equiv.) was subsequently added, followed by Bis(triphenylphosphine)palladium(II) dichloride (30 mg, 0.042 mmol, 0.010 equiv.). By making use of a syringe, iodobenzene (0.47 mL, 4.2 mmol, 1.0 equiv.) was then added through the septum. The resulting solution was then stirred and propargyl alcohol (0.27 mL, 4.6 mmol, 1.1 equiv.) was added drop-wise. During the addition of the propargyl alcohol, the colour of the reaction mixture changed from colourless to a light yellow colour. After allowing the mixture to stir for 1 h the colour changed to a milky light yellow colour. The reaction mixture was then stirred for 24 h at RT. The

crude product was then partitioned between ammonium chloride and EtOAc and the aqueous phase was then extracted with EtOAc (3 × 100 mL). The combined organic layers were then washed with brine, dried over $MgSO_4$, filtered and concentrated under reduced pressure. The resulting oily residue was purified by flash chromatography (Cyclohexane: EtOAc, 95:5 – 80:20). This afforded the pure propargylic alcohol **1** as a yellow brown oil (0.50 g, 3.8 mmol, 90%)

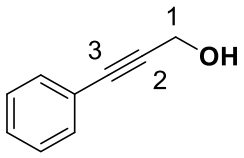

1

R_f = 0.39 (Cyclohexane: EtOAc, 80:20). **^{1}H NMR (400 MHz, $CDCl_3$) δ** 7.44 – 7.41 (m, 2H, Ar*H*), 7.33 – 7.22 (m, 3H, Ar*H*), 4.48 (s, 2H, 2 × H_1), 2.81 (bs, 1H, *OH*). **^{13}C NMR (101 MHz, $CDCl_3$) δ** 131.72 (Ar*C*), 128.50 (Ar*C*), 128.35 (Ar*C*), 122.60 (Ar*C*), 87.38 (C_2), 85.61 (C_3), 51.47 (C_1). **GC-MS: *m/z*** calculated: 132; found 132.

Analytical data was in accordance with previously reported spectra.[177]

10.2.2. SYNTHESIS OF (3-BROMOPROP-1-YN-1-YL)BENZENE 2

10.2.2.1. FIRST SYNTHESIS OF (3-BROMOPROP-1-YN-1-YL)BENZENE 2

Dry DCM (15 mL) was added into a 100 mL three-neck round-bottom flask under a constant N_2 flow. The Sonogashira coupling product **1** (489 mg, 3.70 mmol, 1.00 equiv.) was then added through the septum via syringe, followed by the addition of carbon tetrabromide (1.86 g, 5.55 mmol, 1.50 equiv.). The reaction mixture was then cooled to 0 °C and triphenylphosphine (1.50 g, 5.74 mmol, 1.55 equiv.) was added slowly. During the addition of the triphenylphosphine, the colourless solution initially turned into light yellow solution and then the mixture became a dark orange colour. The reaction was then allowed to warm to RT and stirred for 3 h. Within 5 min of stirring, the solution turned into a dark brown colour and after 3 h the solution was a light orange colour. After this time, EtOH (2.5 mL) was added and the reaction was stirred for an additional 20 min. Thereafter, the solvent was removed under reduced pressure and the product was purified by flash chromatography (Wet loaded with DCM, 100% cyclohexane). This afforded the pure propargylic bromide **2** as a yellow oil (262 mg, 1.34 mmol, 59%).

An alternative method was subsequently explored for this transformation. This second method will be discussed below, followed by the characterization of compound **2**.

10.2.2.2. ALTERNATIVE SYNTHESIS OF (3-BROMOPROP-1-YN-1-YL)BENZENE 2

An ice-cooled solution of the Sonogashira coupling product **1** (252 mg, 1.91 mmol, 1.00 equiv.) and triethylamine (0.40 mL, 2.9 mmol, 1.5 equiv.) in THF (10 mL) was prepared in a 100 mL three-neck

round-bottom flask. Methanesulfonyl chloride (0.22 mL, 2.9 mmol, 1.5 equiv.) dissolved in THF (5 mL) was then added dropwise. This mixture was allowed to stir for 20 min to allow the formation of the mesylate compound. Thereafter, lithium bromide (838 mg, 9.55 mmol, 5.00 equiv.) was added while the solution was kept at 0 °C. The mixture was then stirred for 6 h at RT, after which it was poured into distilled H_2O, extracted with DCM (3 × 100 mL), washed with brine, dried over $MgSO_4$, filtered and concentrated under reduced pressure. The resulting oily residue was purified by flash chromatography (100% cyclohexane). This afforded the pure propargylic bromide **2** as a yellow oil (291 mg, 1.49 mmol, 78%).

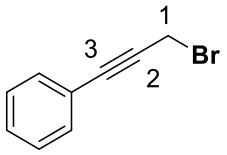

2

R_f = 0.44 (100% cyclohexane). **^{1}H NMR (400 MHz, $CDCl_3$) δ** 7.47 – 7.42 (m, 2H, Ar*H*), 7.35 – 7.31 (m, 3H, Ar*H*), 4.17 (s, 2H, 2 × H_1). **GC-MS: *m/z*** calculated: 194; found 194.

Analytical data was in accordance with literature.[177,179]

10.2.3. Synthesis of S-(3-phenylprop-2-yn-1-yl) ethanethioate 3

10.2.3.1. First Synthesis of S-(3-phenylprop-2-yn-1-yl) ethanethioate 3

The propargylic bromide **2** (103 mg, 0.526 mmol, 1.00 equiv.) dissolved in dry MeOH (4 mL) was added into a 50 mL two-neck round-bottom flask under a N_2 atmosphere. Thioacetic acid (0.050 mL, 0.63 mmol, 1.2 equiv.) was then added via syringe, followed by the addition of potassium carbonate (87.2 mg, 0.631 mmol, 1.20 equiv.). The solution was then left to stir for 0.5 h, and then a second portion of potassium carbonate (87.2 mg, 0.631 mmol, 1.20 equiv.) was added and the reaction was left to stir for another 0.5 h. After this time the solution was neutralized with 1 M HCl (approximately 1 mL) and extracted with DCM (3 × 100 mL). The combined organic layers were washed with brine, dried over $MgSO_4$, filtered and concentrated under reduced pressure. TLC analysis showed the presence of two products. GC-MS confirmed that the one product was the thioacetate **3** but the second product could not be identified. This crude mixture was used directly in the first attempt at the synthesis of the thioether compound **5**.

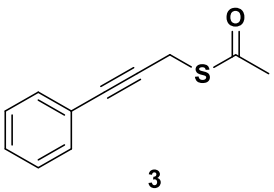

3

10.2.3.2. ALTERNATIVE SYNTHESIS OF S-(3-PHENYLPROP-2-YN-1-YL) ETHANETHIOATE 3

Dry benzene (5 mL) was added into a 50 mL two-neck round-bottom flask under inert conditions, followed by DEAD (722 mg, 4.02 mmol, 1.00 equiv.). In a separate 100 mL three-neck round-bottom flask, dry benzene (25 mL) was added, followed by triphenylphosphine (1.05 g, 4.02 mmol, 1.00 equiv.) and the 100 mL flask was cooled to 0 °C. The DEAD solution was then added to this cooled triphenylphosphine solution. The solution of DEAD in benzene was an orange colour but when added to the triphenylphosphine solution, the mixture became red after 10 min of stirring. The resulting red mixture was then left to stir at 0 °C for 20 min. In a separate 50 mL two-neck round-bottom flask, dry benzene (5 mL) was added followed by the propargylic alcohol **1** (531 mg, 4.02 mmol, 1.00 equiv.) and thioacetic acid (312 mg, 4.02 mmol, 1.00 equiv.). This mixture was also cooled down to 0 °C and then added to the red solution in one portion. The mixture was left to stir for 2.5 h after which time the solvent was removed under reduced pressure. After stirring the reaction mixture for 2.5 h, it was a red-orange colour. Flash chromatography was then attempted (cyclohexane: EtOAc, 95:5 – 90:10) but the fractions co-eluted. Only part of the clean thioacetate **3** was isolated as a yellow oil (262 mg, 1.38 mmol, 34%).

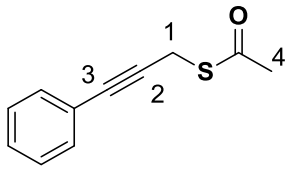

3

R_f = 0.50 (cyclohexane: EtOAc, 90:10). **^{1}H NMR (400 MHz, $CDCl_3$) δ** 7.43 – 7.38 (m, 2H, Ar*H*), 7.30 – 7.28 (m, 3H, Ar*H*), 3.90 (s, 2H, 2 × H_1), 2.39 (s, 3H, 3 × H_4). **GC-MS: *m/z*** calculated: 190; found 190.

Analytical data was in accordance with previously reported spectra.[181]

10.2.4. SYNTHESIS OF BIS(3-PHENYLPROP-2-YN-1-YL)SULFANE 5

10.2.4.1. FIRST ATTEMPTED SYNTHESIS OF BIS(3-PHENYLPROP-2-YN-1-YL)SULFANE 5

The crude mixture obtained during the first synthesis of the thioacetate from the bromide **2** (103 mg, 0.530 mmol, 1.00 equiv.) was used to produce the free thiol **4** and subsequently attempt the synthesis of the thioether **5**. Dry MeOH (8 mL) was added into a 50 mL round-bottom flask containing the crude mixture with the thioacetate **3** (98.4 mg, 0.517 mmol, 1.00 equiv.). Potassium hydroxide (102.6 mg, 1.83 mmol, 3.45 equiv.) was then added followed by sodium thiosulfate (8.18 mg, 0.0517 mmol, 0.100 equiv.). The solution was then stirred for 1 h at 0 °C (after this time TLC analysis showed complete conversion of the thioacetate **3** to the free thiol **4**). Thereafter, the bromide **2** (159 mg, 0.815 mmol, 1.58 equiv.) was dissolved in 2 mL of dry MeOH and added dropwise to the thiol mixture. The solution was then stirred for another 3 h at RT. The solution was then partitioned

between H_2O and EtOAc and the aqueous layer was then extracted with EtOAc (3 × 50 mL). The combined organic layers were washed with brine, dried over $MgSO_4$, filtered and concentrated over reduced pressure.

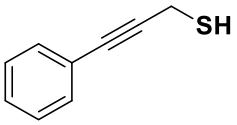

4

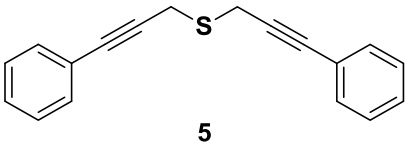

5

A crude NMR showed a mixture of products and GC-MS analysis confirmed the presence of two products, namely the free thiol **4** and an unidentified compound. No reaction took place between the free thiol and the bromide compound **2** to form the thioether **5**. This mixture was not purified as other options were available for the synthesis of the thioether **5**.

10.2.4.2. SECOND ATTEMPTED SYNTHESIS OF BIS(3-PHENYLPROP-2-YN-1-YL)SULFANE 5

Anhydrous MeOH (3 mL) was added into a 50 mL two-neck round-bottom flask under a N_2 atmosphere. Subsequently, sodium sulfide (35.1 mg, 0.445 mmol, 0.500 equiv.) was added followed by the bromide **2** (174 mg, 0.890 mmol, 1.00 equiv.) dissolved in 2 mL of dry MeOH. The reaction was allowed to stir at RT for 2 h (as situated in literature but after this time only starting material was detected). The temperature was then raised to 30 °C and stirred for another 14 h. The solution was partitioned between H_2O and EtOAc and then the aqueous layer was extracted with EtOAc (3 × 50 mL). The combined organic layers were then washed with brine, dried over $MgSO_4$, filtered and concentrated under reduced pressure. Only 36 mg (21%) of the bromide starting material was recovered and none of the thioether **5** was formed during this reaction.

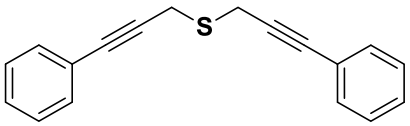

5

10.2.4.3. SUCCESSFUL SYNTHESIS OF BIS(3-PHENYLPROP-2-YN-1-YL)SULFANE 5

The alcohol **1** (225 mg, 1.70 mmol, 1.00 equiv.) resulting from the Sonogashira coupling reaction was added into a 100 mL three-neck round-bottom flask in Dry THF (10 mL) followed by triethylamine (0.35 mL, 2.6 mmol, 1.5 equiv.). This solution was then cooled to 0 °C. Thereafter, methanesulfonyl chloride (292 mg, 2.55 mmol, 1.50 equiv.) dissolved in 1 mL of THF was added and the mixture was left to stir for 20 minutes to allow the formation of the mesylate compound. Sodium sulfide (134 mg, 1.70 mmol, 1.00 equiv.) was then added to the solution and the mixture was stirred at RT for 16 h. The reaction mixture was then poured into H_2O and extracted with DCM (3 × 100 mL), washed with brine, dried over $MgSO_4$, filtered and concentrated under reduced pressure.

The resulting oily residue was purified by flash chromatography (Cyclohexane: EtOAc, 100:0 – 98:2). This afforded the pure product **5** as a yellow solid (72.7 mg, 0.278 mmol, 28%).

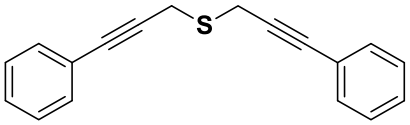

5

An additional method was explored for the synthesis of this thioether functionality and will be discussed below followed by the characterization of **5**.

10.2.4.4. ALTERNATIVE SYNTHESIS OF BIS(3-PHENYLPROP-2-YN-1-YL)SULFANE 5

The bromide **2** (285 mg, 1.46 mmol, 1.00 equiv.) was taken into a THF/H_2O mixture (10 mL: 2 mL). This solution was then cooled down to 0 °C and then TBAB (47.5 mg, 0.146 mmol, 0.100 equiv.) was added followed by sodium sulfide (57.5 mg, 0.730 mmol, 0.500 equiv.). This mixture was stirred at RT for 3 h. After this time, a significant amount of **2** was still detected by TLC and GC-MC analyses which prompt us to heat the solution to 30 °C while stirring for an additional 1 h. When starting material was still detected after this attempt, the reaction mixture was heated to 40 °C and stirred for another 1 h, followed by the addition of another portion of sodium sulfide (57.5 mg, 0.730 mmol, 0.500 equiv.). This mixture was then allowed to stir at 40 °C for 11 h. The mixture was poured into H_2O and extracted with DCM (3 × 100 mL), washed with brine, dried over $MgSO_4$, filtered and concentrated under reduced pressure. The resulting oily residue was purified by flash chromatography (Cyclohexane: EtOAc, 100:0 – 95:5). This afforded the pure product **5** as a yellow solid (152 mg, 0.579 mmol, 58%).

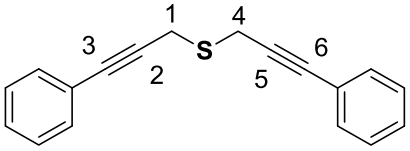

5

R_f = 0.58 (Cyclohexane: EtOAc, 90:10). **^{1}H NMR (400 MHz, $CDCl_3$) δ** 7.47 – 7.41 (m, 4H, Ar*H*), 7.33 – 7.28 (m, 6H, Ar*H*), 3.72 (s, 4H, 2 × H_1 *and* 2 × H_4). **GC-MS: *m/z*** calculated: 262; found 262.

Analytical data was in accordance with previously reported spectra.[179]

10.2.5. ATTEMPTED SYNTHESIS OF THE SULFUR-CONTAINING LINEAR *PARA*-PHENYLENE, 5-ETHYL-4,7-DIPHENYL-6-PROPYL-1,3-DIHYDROBENZO[C]THIOPHENE 6

The thioether **5** (50.1 mg, 0.191 mmol, 1.00 equiv.) was added into a 35 mL microwave vial equipped with a magnetic stirrer bar followed by 2-propanol (5 mL) and anhydrous THF (5 mL). This solution was then degassed by bubbling N_2 through for 15 min. Thereafter, hept-3-yne (568 mg, 5.73 mmol, 30.0 equiv.) was added followed by Wilkinson's catalyst, $RhCl(PPh_3)_3$, (17.7 mg, 0.0191 mmol, 0.100

equiv.). The flask was then place in the microwave reactor at 100 °C for 6 h. Unfortunately, the microwave vial exploded during this reaction. The work up would have involved quenching with $NaHCO_3$ and extracting the mixture with DCM. The mixture would then have been washed with brine, dried over $MgSO_4$, filtered and concentrated under reduced pressure.

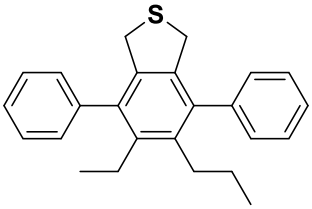

6

The [2+2+2] cycloaddition reaction has previously been investigated in the research group of Prof. Dr Wegner and optimum conditions for this cycloaddition have already been determined for similar linear systems.[176] Therefore, by keeping in mind the time limit associated with this project, it was decided to rather focus on the synthesis of the CPP linker system.

10.3. SYNTHESIS OF THE CPP LINKER SYSTEM

10.3.1. SYNTHESIS OF THE L-SHAPED BUILDING BLOCK, 1,4-BIS(4-IODOPHENYL)CYCLOHEXANE-1,4-DIOL 7

$CeCl_3$*$7H_2O$ (8.35 g, 22.2 mmol, 2.20 equiv.) and LiCl (9.58 g, 226 mmol, 22.0 equiv.) were added into a 500 mL three-neck round-bottom flask. The flask was heated to 150 °C under vacuum. Thereafter, the flask was left to cool to RT and dry THF (110 mL) was then added. The suspension was stirred for 16 h at RT. Dry THF (10 mL) was then added into a dry Schleck-tube under N_2 followed by 1,4-cyclohexanedione (1.14 g, 10.1 mmol, 1.00 equiv.). After the 1,4-cyclohexanedione was completely dissolved, this solution was added to the 500 mL round-bottom flask. The $CeCl_3$-LiCl suspension, after stirring 16 h, was a white suspension. When adding 1,4-cyclohexanedione the colour of the suspension change to an off-yellow colour. The resulting solution was stirred for 2.5 h at RT and cooled down to −78 °C afterwards (acetone/ liquid N_2 bath). This suspension started to freeze. The round-bottom flask was then removed out of the acetone/liquid N_2 bath and allowed to heat slightly and thaw. Then, an extra 18 mL of THF was added to the suspension. Dry THF (60 mL) was then added into a dry 100 mL three-neck round-bottom flask under N_2 atmosphere followed by 1,4-diiodobenzene (10.2 g, 30.3 mmol, 3.00 equiv.). This solution was then also cooled down to −78 °C. *n*-Butyllithium (1.6 M in Hexane, 21 mL, 34 mmol, 3.4 equiv.) was then added dropwise. During the addition of *n*-Butyllithium an extra 6 mL of dry THF was added because the solution started to freeze. The diiodobenzene solution turned into a bright yellow colour during the addition of *n*-Butyllithium. This solution was then left to stir at −78 °C for 0.5 h. This solution was then transferred to the prepared suspension via transfer cannula (additional THF had to be added to the 1,4-diiodobenzene solution during the transfer). During the transfer process of

the diiodobenzene solution to the cyclohexanedione solution, the colour changed from an off-yellow (as indicated previously) to a light orange-brown colour. Not everything was transferred, next time add THF at the end and transfer with a needle at RT to prevent the mixture from freezing. Afterwards the stirring was continued from 17 h. Reaction was quenched with saturated NH_4Cl at this point. The mixture was then passed through celite and rinsed with EtOAc and the filtrate was concentrated under reduced pressure. After adding H_2O (300 mL) and EtOAc (400 mL) the organic phase was separated and the aqueous phase was extracted with EtOAc (3 × 300 mL). The combined organic layers were dried over $MgSO_4$, filtered and concentrated under reduced pressure. The product was recrystallized in chloroform to afford the pure L-shaped building block **7** as an off-white (light pink) solid (1.23 g, 2.36 mmol, 24%).

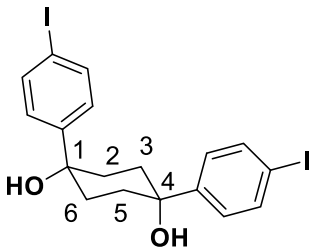

7

^{1}H NMR (400 MHz, $CDCl_3$) δ 7.70 – 7.65 (m, 4H, Ar*H*), 7.24 – 7.19 (m, 4H, Ar*H*), 2.06 (s, 8H, 2 × *H_2 and* 2 × *H_3 and* 2 × *H_5 and* 2 × *H_6*), 1.69 (bs, 2H, 2 × *OH*).

Analytical data was in accordance with literature.[169]

10.3.2. Synthesis of 1,4-bis(4-iodophenyl)-1,4-bis(methoxymethoxy)cyclohexane 8

Dry DCM (15 mL) was added into a 50 mL three-neck round-bottom flask under N_2 atmosphere followed by the L-shaped building block **7** (1.23 g, 2.36 mmol, 1.00 equiv.). To this suspension, *N,N*-diisopropylethylamine (1.6 mL, 9.4 mmol, 4.0 equiv.) was added and subsequently, MOMCl (0.76 mL, 9.4 mmol, 4.0 equiv.) was added dropwise. The suspension of the L-shaped building block **7** in DCM was a light pink solution. After the addition of the base, the colour of the suspension changed to a white colour. MOMCl reacted vigorously so the flask was placed in an ice bath during the addition. After the addition of MOMCl, the reaction was stirred at RT for 30 min and then the mixture was no longer a suspension. The solution was now a transparent yellow-brown colour. This mixture was then left to stir for 16 h at RT. Thereafter, NH_4Cl (80 mL) was added and the mixture was extracted with DCM (3 x 100 mL). The combined organic layers were washed with brine, dried over $MgSO_4$ and concentrated under reduced pressure. The resulting residue was purified by flash chromatography (cyclohexane: EtOAc, 90:10 – 80:20). This afforded the pure MOM-protected diiodo-compound **8** as a white solid (1.01 g, 1.66 mmol, 71%).

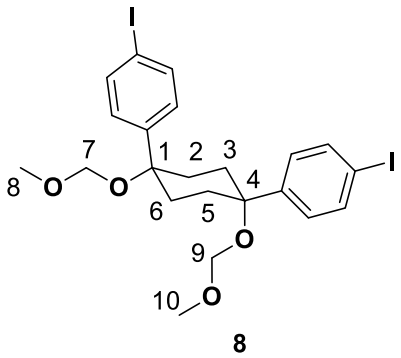

8

R_f = 0.62 (cyclohexane: EtOAc, 70:30). **^{1}H NMR (400 MHz, $CDCl_3$) δ** 7.66 – 7.64 (m, 4H, Ar*H*), 7.17 – 7.15 (m, 4H, Ar*H*), 4.41 (s, 4H, 2 × H_7 *and* 2 × H_9), 3.39 (s, 6H, 2 × H_8 *and* 2 × H_{10}), 2.28 – 2.01 (2 × H_2 *and* 2 × H_3 *and* 2 × H_5 *and* 2 × H_6).

Analytical data was in accordance with previously reported spectra.[171]

10.3.3. Synthesis of 3,3'-{[1,4-bis(methoxymethoxy)cyclohexane-1,4-diyl]bis(4,1-phenylene)}bis(prop-2-yn-1-ol) 9

Freshly distilled triethylamine (45 mL) was added into a 100 mL three-neck round-bottom flask under N_2 atmosphere. Copper(I)iodide (9.1 mg, 0.048mmol, 0.040 equiv.) was then added followed by bis(triphenylphosphine)palladium(II)-dichloride (51 mg, 0.071 mmol, 0.060 equiv.). After the addition of the palladium catalyst the colour of the solution turned into a yellow colour. The MOM-protected diiodo-compound **8** (720 mg, 1.2 mmol, 1.0 equiv.) was then added with a syringe via the septum. The resulting solution was then stirred and propargyl alcohol (0.28 mL, 4.8 mmol, 4.0 equiv.) was added drop-wise. During the addition of propargyl alcohol the yellow solution turned into an orange-brown suspension. After leaving the mixture to stir for 1 h the colour changed again to a light brown solution. The reaction mixture was then stirred for 23 h under inert atmosphere at RT. The crude product was partitioned between ammonium chloride and EtOAc. The aqueous phase was then extracted with EtOAc (3 × 200 mL). The combined organic layers were then washed with brine, dried over $MgSO_4$, filtered and concentrated under reduced pressure. The resulting residue was purified by flash chromatography (cyclohexane: EtOAc, 70:30 – 30:70). This afforded the pure product **9** as a yellow solid (420 mg, 0.89 mmol, 88%).

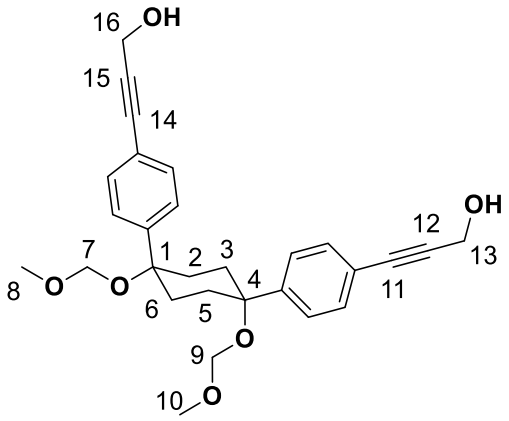

9

R_f = 0.19 (cyclohexane: EtOAc, 50:50). **^{1}H NMR (400 MHz, $CDCl_3$) δ** 7.39 – 7.36 (m, 8H, Ar*H*), 4.49 (s, 4H, 2 × H_{13} *and* 2 × H_{16}), 4.41 (s, 4H, 2 × H_7 *and* 2 × H_9), 3.39 (s, 6H, 2 × H_8 *and* 2 × H_{10}), 2.39 – 1.90 (m, 8H, 2 × H_2 *and* 2 × H_3 *and* 2 × H_5 *and* 2 × H_6), 1.62 (s, 2H, 2 × *OH*).

Analytical data was in accordance with literature.[177]

10.3.4. Synthesis of 1,4-bis[4-(3-bromoprop-1-yn-1-yl)phenyl]-1,4-bis(methoxymethoxy)cyclohexane 10

An ice-cooled solution of the Sonogashira coupling product **9** (197 mg, 0.424 mmol, 1.00 equiv.) and triethylamine (0.18 mL, 1.3 mmol, 3.0 equiv.) in THF (10 mL) was prepared in a three-neck round-bottom flask. Methanesulfonyl chloride (0.010 mL, 1.3 mmol, 3.0 equiv.) dissolved in THF (1 mL) was then added dropwise. This mixture was then allowed to stir for 20 min to allow the formation of the mesylate compound. Thereafter, lithium bromide (372 mg, 4.24 mmol, 10.0 equiv.) was added while the solution was kept at 0 °C. The mixture was then stirred for 17 h at RT. It was then poured into H_2O (40 mL), extracted with DCM (3 × 100 mL), washed with brine, dried over $MgSO_4$, filtered and concentrated under reduced pressure. The resulting residue was purified by flash chromatography (cyclohexane: EtOAc, 95:5 – 70:30). This afforded the pure product **10** as a white solid (163 mg, 0.276 mmol, 65%).

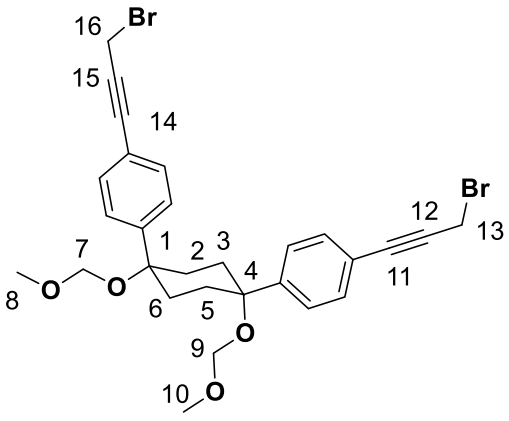

10

R_f = 0.67 (cyclohexane: EtOAc, 50:50). **^{1}H NMR (400 MHz, $CDCl_3$) δ** 7.43 – 7.36 (m, 8H, Ar*H*), 4.41 (s, 4H, 2 × *H_7 and* 2 × *H_9*), 4.15 (s, 4H, 2 × *H_{13} and* 2 × *H_{16}*), 3.39 (s, 6H, 2 × *H_8 and* 2 × *H_{10}*), 2.29 – 2.05 (m, 8H, 2 × *H_2 and* 2 × *H_3 and* 2 × *H_5 and* 2 × *H_6*).

10.3.5. ATTEMPTED SYNTHESIS OF THE OXYGEN-CONTAINING MOM-PROTECTED MACROCYCLE 11

At 0 °C, to a suspension of sodium hydride (60% in mineral oil, 13.6 mg, 0.339 mmol, 4.00 equiv.) in THF (100 mL) was added a solution of the diol-compound **9** (39.3 mg, 0.0847 mmol, 1.00 equiv.) and the dibromo-compound **10** (50.0 mg, 0.085 mmol, 1.00 equiv.) in THF (10 mL). The reaction mixture was then allowed to warm up to RT and stirred for 16 h. The mixture was finally quenched with saturated ammonium chloride and extracted with EtOAc. The combined organic layers were washed with brine, dried over $MgSO_4$, filtered and concentrated under vacuum. A crude NMR showed only the presence of the two starting materials, so the crude mixture was dissolved in THF (125 mL), cooled to 0 °C and sodium hydride (60% in mineral oil, 27.1 mg, 0.678 mmol, 8.00 equiv.) was added. The mixture was then allowed to warm to RT. After 1 h there was no indication that the reaction was taking place after examination by TLC so another portion of sodium hydride (60% in mineral oil, 27.1 mg, 0.678 mmol, 8.00 equiv.) was added. The reaction was then left to stir for 16 h and the next morning it was heated up to 30 °C and stirred for another 16 h. Then, another portion of sodium hydride (60% in mineral oil, 13.6 mg, 0.339 mmol, 4.00 equiv.) was added and the mixture was heated up to 40 °C and left to stir over the weekend. The mixture was finally quenched with saturated NH_4Cl (15 mL) and extracted with EtOAc (3 × 50 mL). The combined organic layers were washed with brine, dried over $MgSO_4$, filtered and concentrated under reduced pressure. A crude NMR was then compared to that in literature but there was no prove of the formation of the macrocycle.

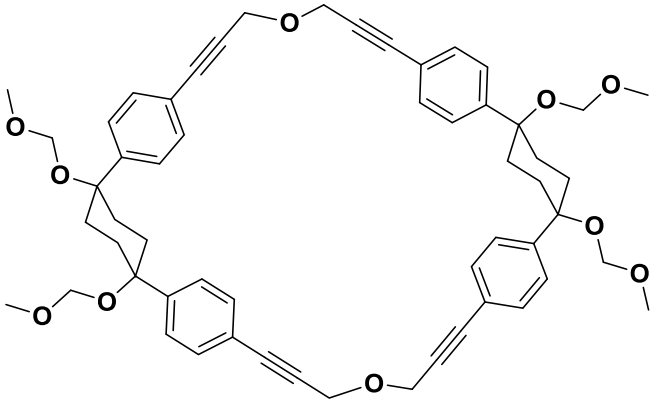

11

10.3.6. SYNTHESIS OF THE SULFUR-CONTAINING MOM-PROTECTED MACROCYCLE 12

The dibromo-compound **10** (116 mg, 0.197 mmol, 1.00 equiv.) was added to a mixture of THF/H_2O (90 mL:18 mL, solvent ratio of 5:1). This solution was then cooled down to 0 °C and then TBAB, (12.8 mg, 0.0394 mmol, 0.200 equiv.) was added, followed by sodium sulfide (15.5 mg, 0.197 mmol, 1.00 equiv.). The reaction was then stirred at RT for 16 h. The solvent was then evaporated and the mixture was poured into H_2O and extracted with DCM (3 × 200 mL), washed with brine, dried over $MgSO_4$, filtered and concentrated under reduced pressure. The resulting residue was purified by flash chromatography (cyclohexane: EtOAc, 95:5 – 70:30). This afforded the pure product **12** as an off-white solid (18.7 mg, 0.579 mmol, 2%).

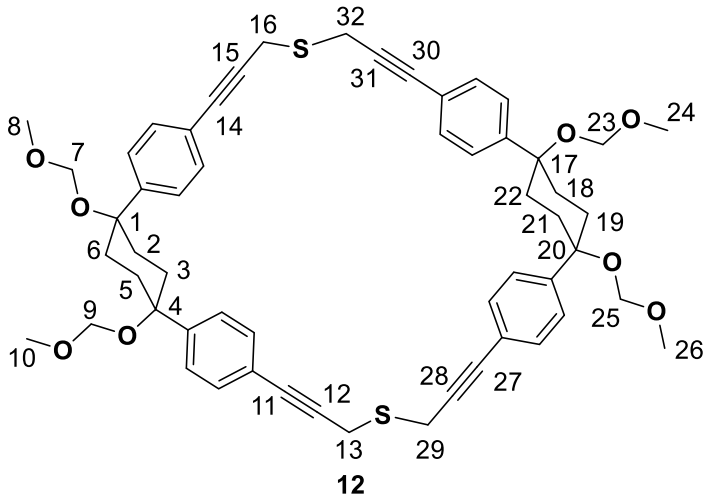

12

Note that the NMR assignment of this compound is given with caution. A tentative assignment has been made based on the NMR spectra at hand, the spectra of the precursors, as well as the spectra of the oxygen-containing MOM-protected macrocycle previously synthesized in this group. For a more accurate assignment or to confirm the assignment made in this document, additional NMR experiments must be conducted. After several attempts, HRMS results could not be determined for this compound – this should be of high importance to complete characterization of this macrocycle.

R_f = 0.38 (Cyclohexane: EtOAc, 70:30). **^{1}H NMR (400 MHz, $CDCl_3$) δ** 7.36 (m, 16H, Ar*H*), 4.44 (s, 8H, 2 × H_7 and 2 × H_9 and 2 × H_{23} and 2 × H_{25}), 3.70 (s, 8H, 2 × H_{13} and 2 × H_{16} and 2 × H_{29} and 2 × H_{32}), 3.39 (s, 12H, 3 × H_8 and 3 × H_{10} and 3 × H_{24} and 3 × H_{26}), 2.27- 2.04 (m, 16H, 2 × H_2 and 2 × H_3 and 2 × H_5 and 2 × H_6 and 2 × H_{18} and 2 × H_{19} and 2 × H_{21} and 2 × H_{22}). **^{13}C NMR (101 MHz, $CDCl_3$) δ** 131.92 (16 × ArH-*C*), 126.87 (4 × Ar*C*), 122.27 (4 × Ar*C*), 92.37 (C_{11} and C_{14} and C_{27} and C_{30}), 84.75 (C_{12} and C_{15} and C_{28} and C_{31}), 83.49 (C_7 and C_9 and C_{23} and C_{35}), 78.18 (C_{13} and C_{16} and C_{29} and C_{32}), 56.15 (C_8 and C_{10} and C_{24} and C_{26}), 33.01 (C_1 and C_4 and C_{17} and C_{20}), 19.89 (C_2 and C_3 and C_5 and C_6 and C_{18} and C_{19} and C_{21} and C_{22}).

APPENDIX 2

NUCLEAR MAGNETIC RESONANCE SPECTROSCOPY RESULTS

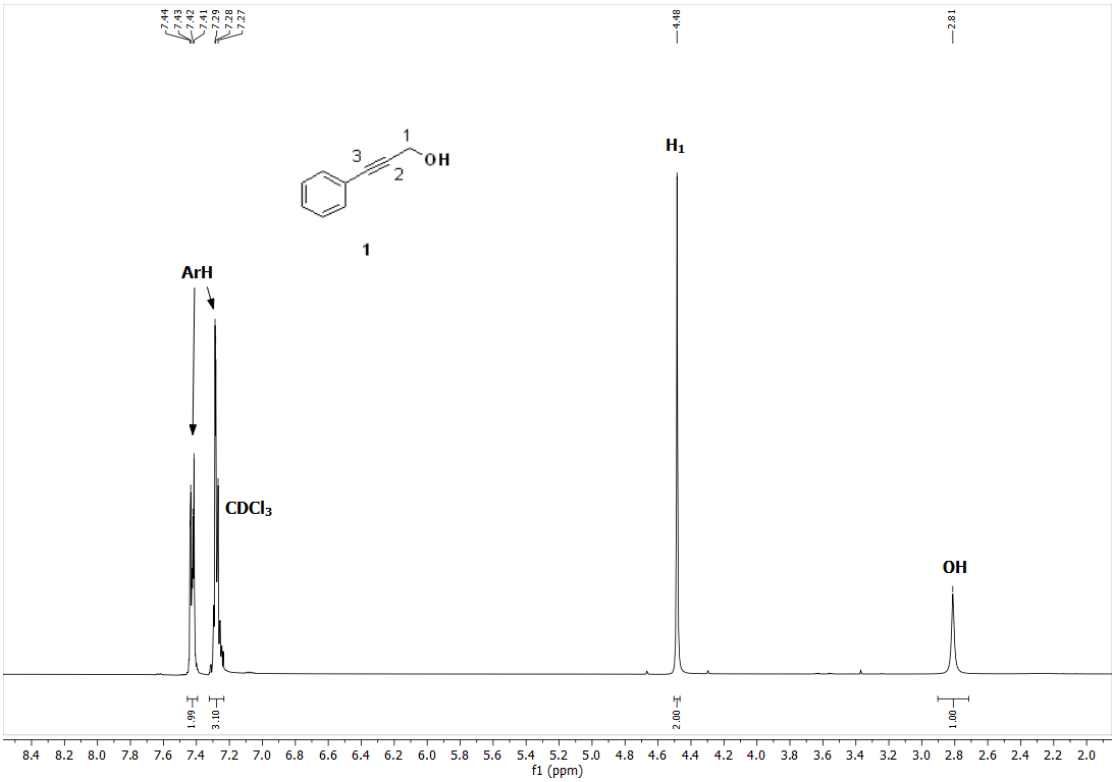

CPP NMR Spectrum 1 ^{1}H NMR spectrum of 3-phenylprop-2-yn-1-ol 1.

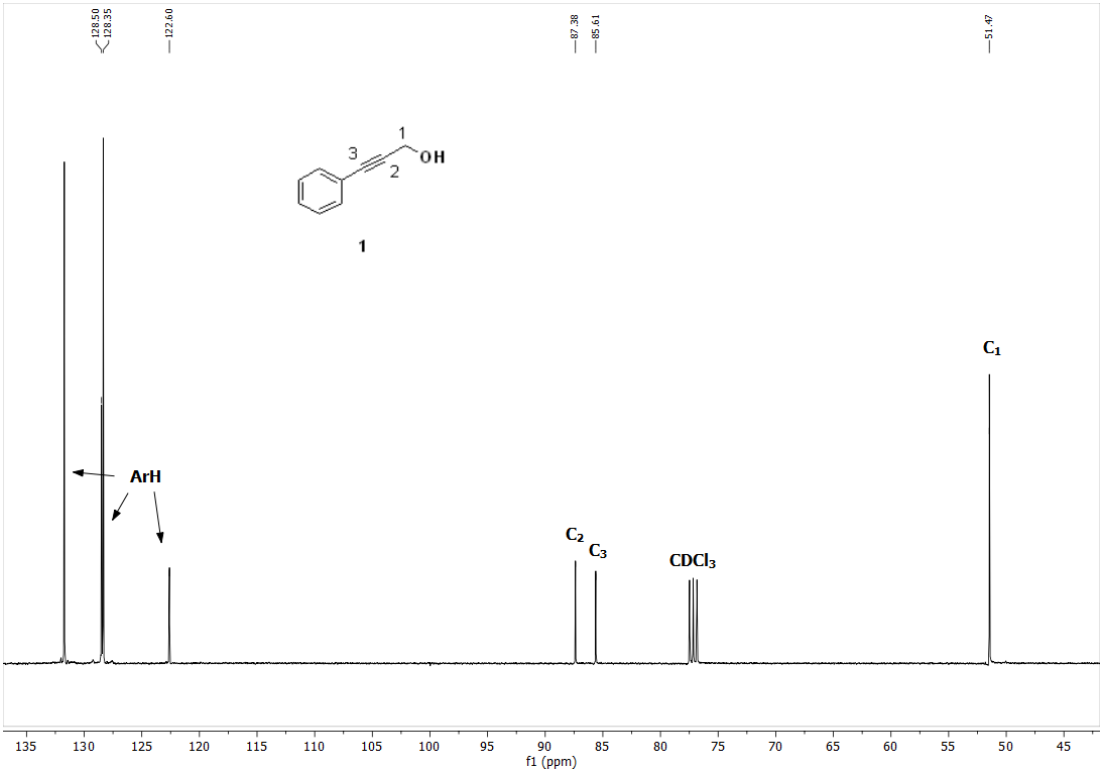

CPP NMR Spectrum 2 ^{13}C NMR spectrum of 3-phenylprop-2-yn-1-ol 1.

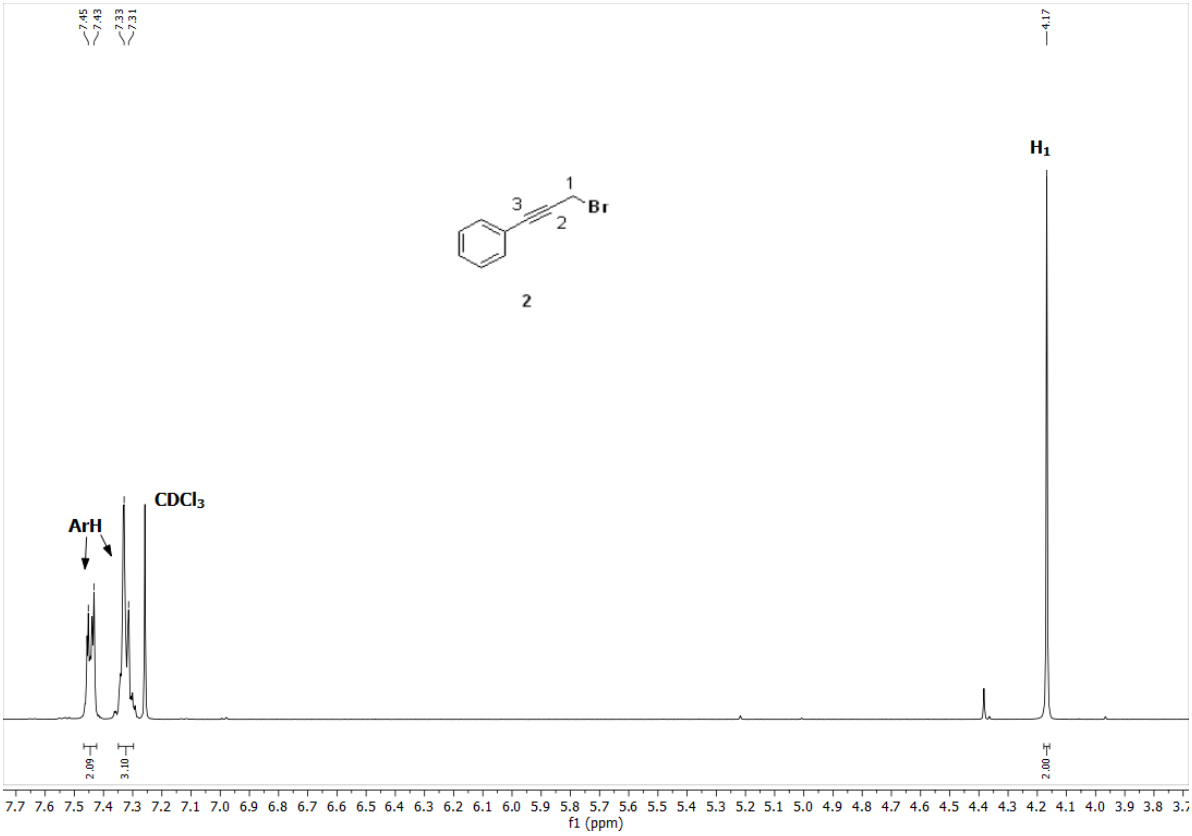

CPP NMR Spectrum 3 ^{1}H NMR spectrum of (3-bromoprop-1-yn-1-yl)benzene 2.

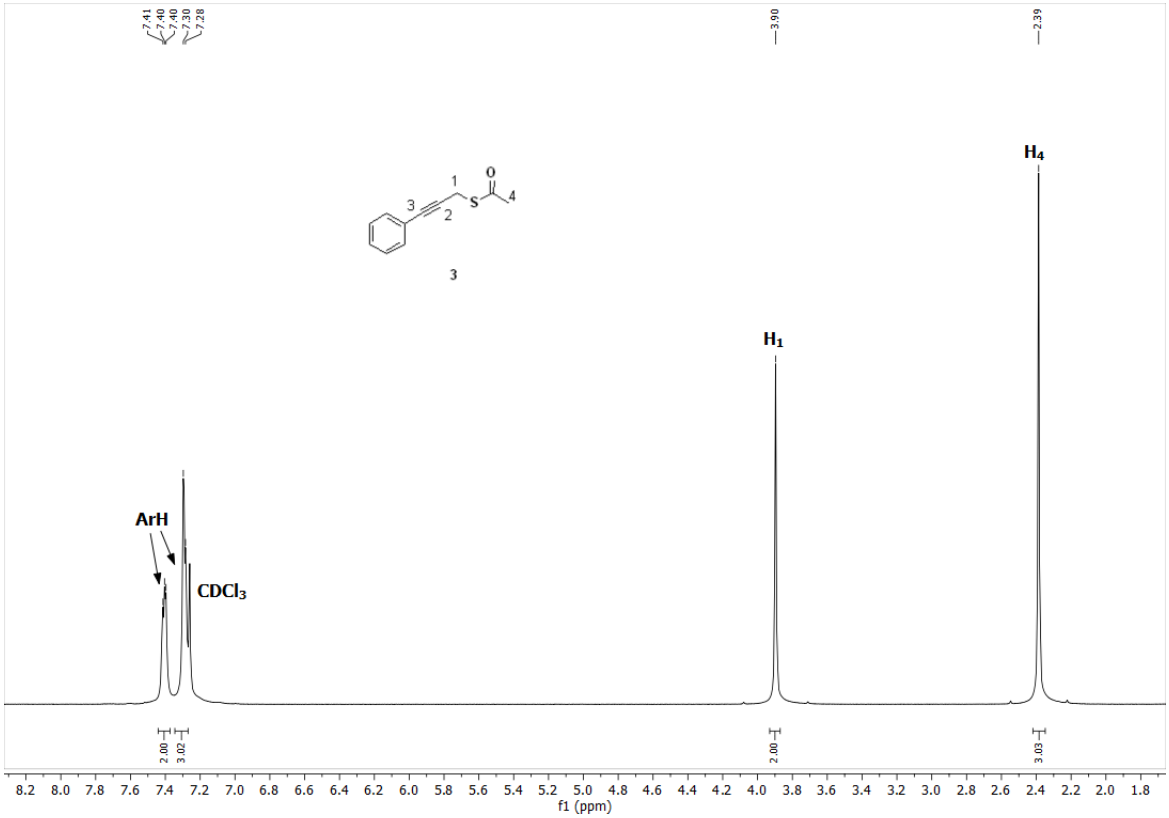

CPP NMR Spectrum 4 ^{1}H NMR spectrum of S-(3-phenylprop-2-yn-1-yl) ethanethioate 3.

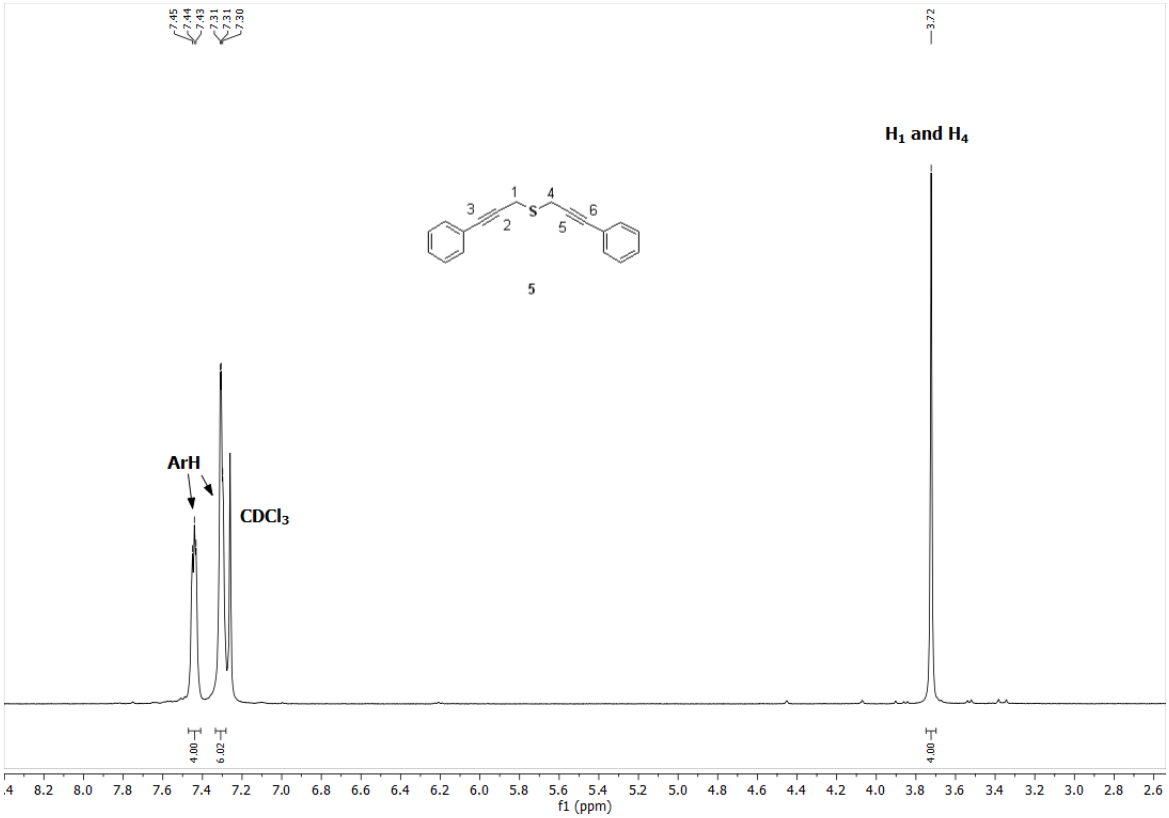

CPP NMR Spectrum 5 ^{1}**H NMR spectrum of bis(3-phenylprop-2-yn-1-yl)sulfane 5.**

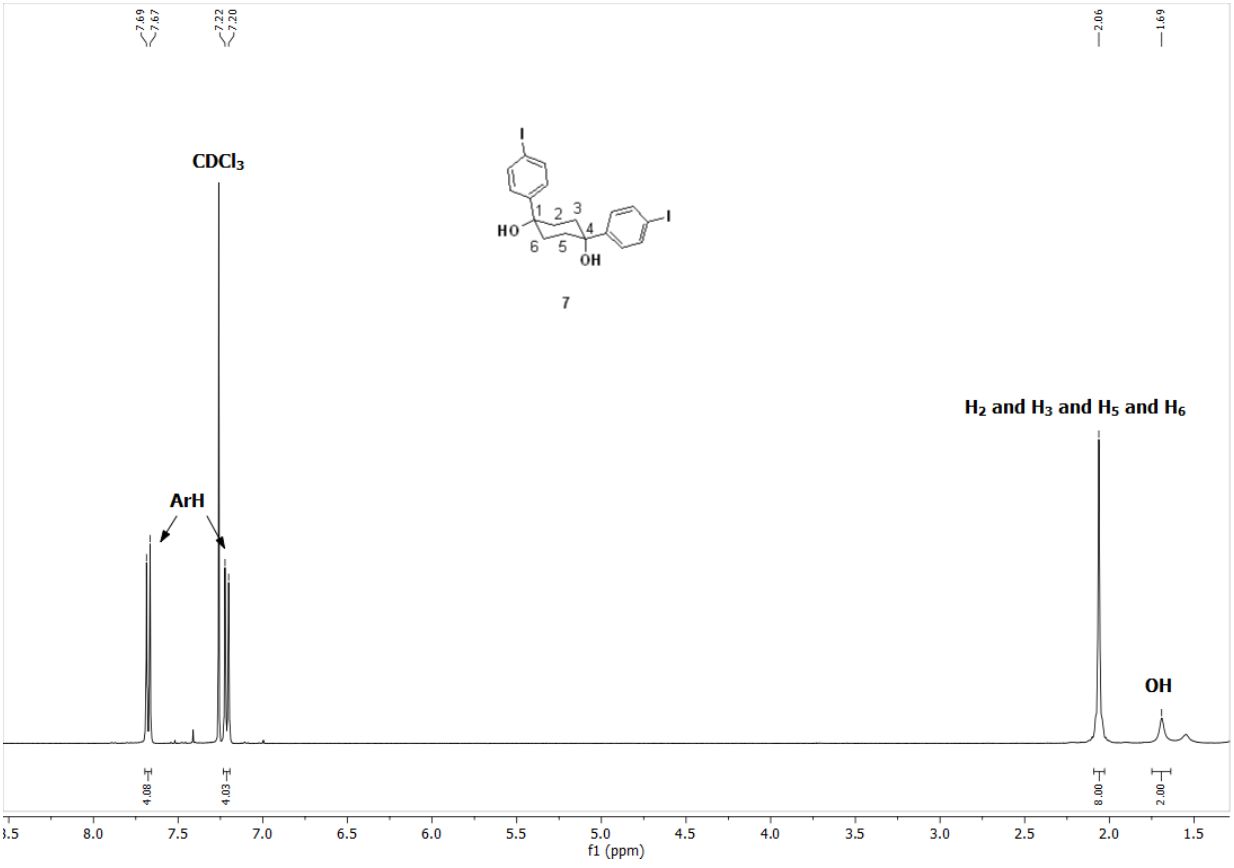

CPP NMR Spectrum 6 ^{1}**H NMR spectrum of 1,4-bis(4-iodophenyl)cyclohexane-1,4-diol 7.**

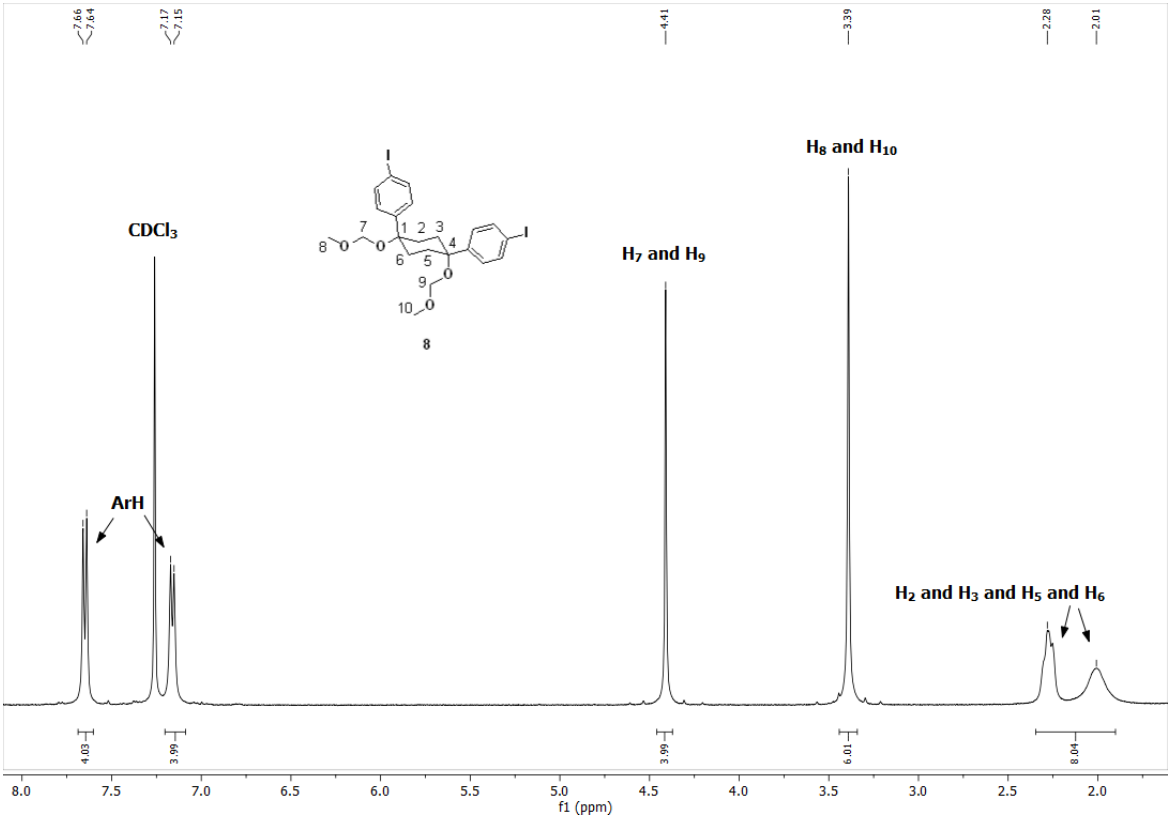

CPP NMR Spectrum 7 ^{1}H NMR spectrum of 1,4-bis(4-iodophenyl)-1,4-bis(methoxymethoxy)cyclohexane 8.

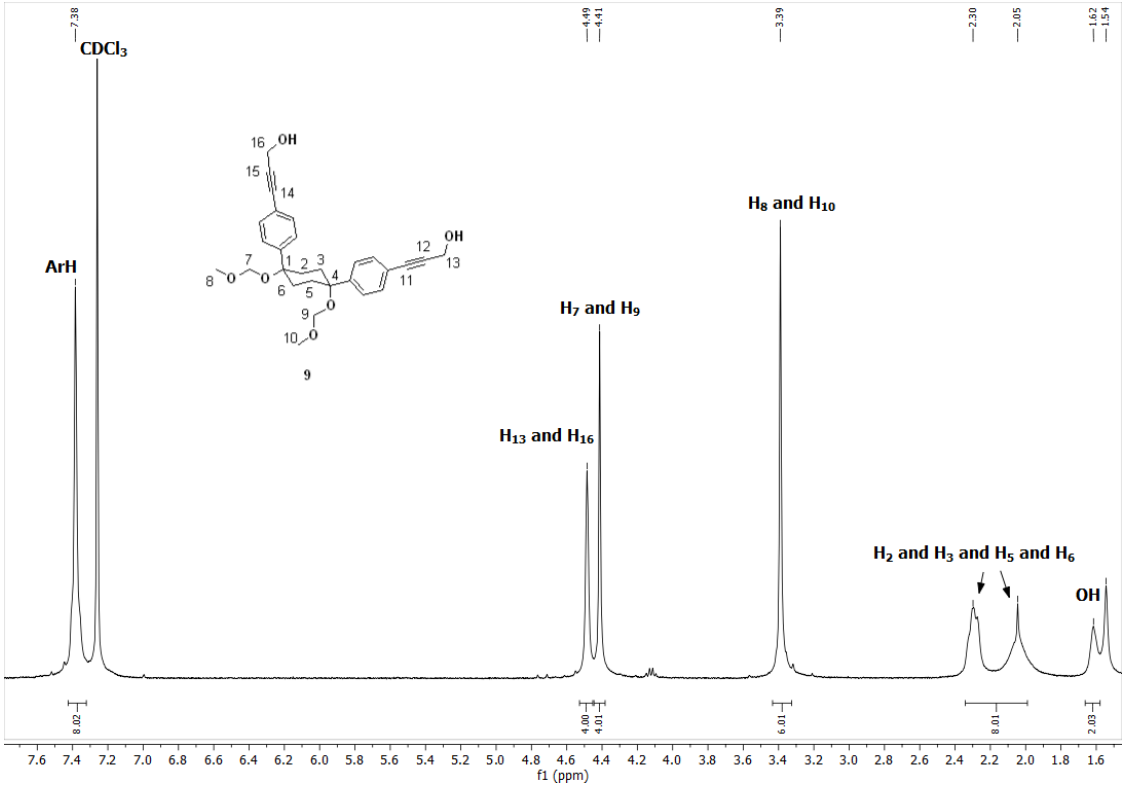

CPP NMR Spectrum 8 ^{1}H NMR spectrum of 3,3'-{[1,4-bis(methoxymethoxy)cyclohexane-1,4-diyl]bis(4,1-phenylene)}bis(prop-2-yn-1-ol) 9.

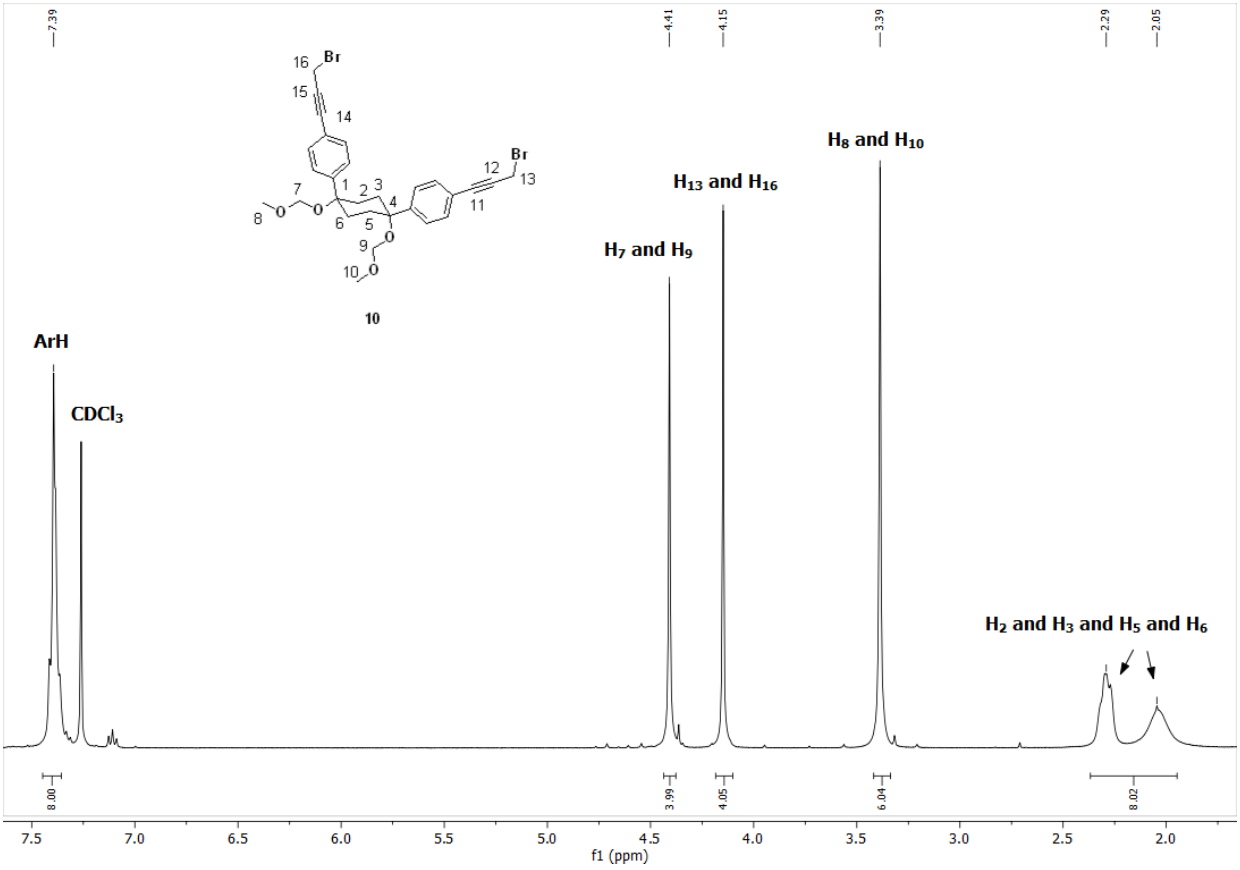

CPP NMR Spectrum 9 ^{1}H NMR spectrum of 1,4-bis[4-(3-bromoprop-1-yn-1-yl)phenyl]-1,4-bis(methoxymethoxy)cyclohexane 10

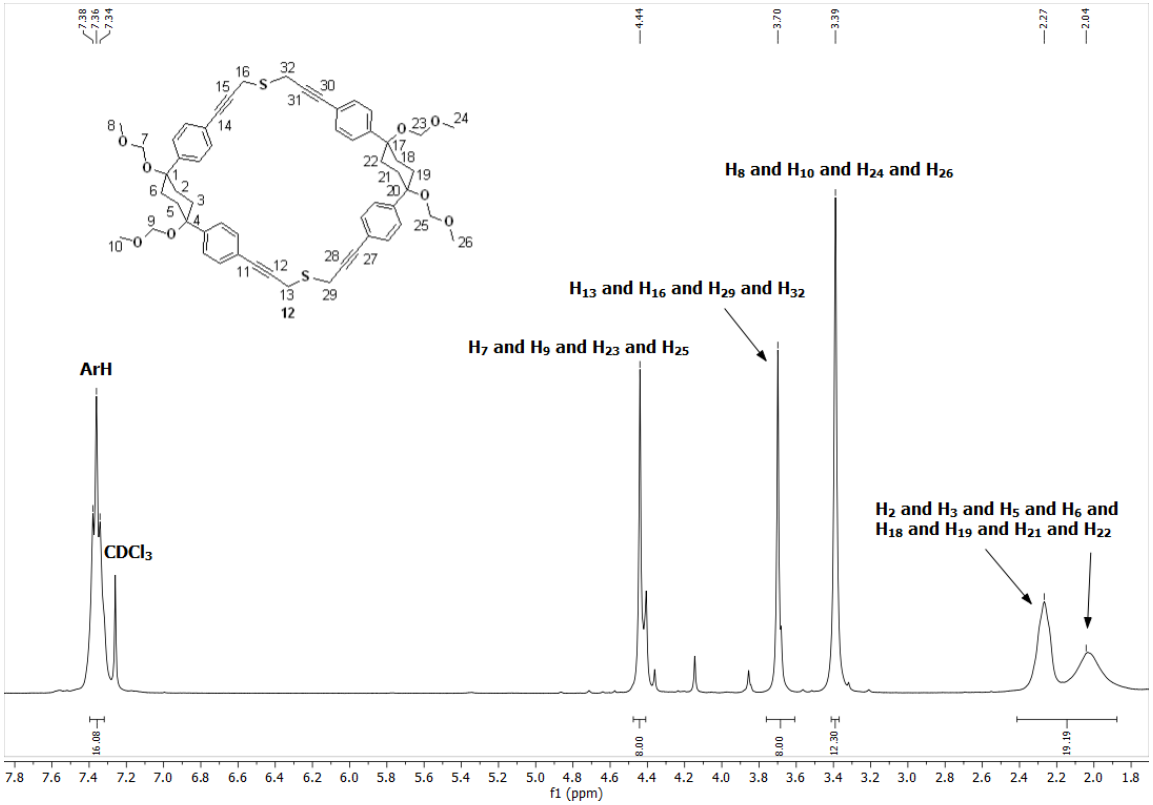

CPP NMR Spectrum 10 ^{1}H NMR spectrum of the sulfur-containing mom-protected macrocycle 12.

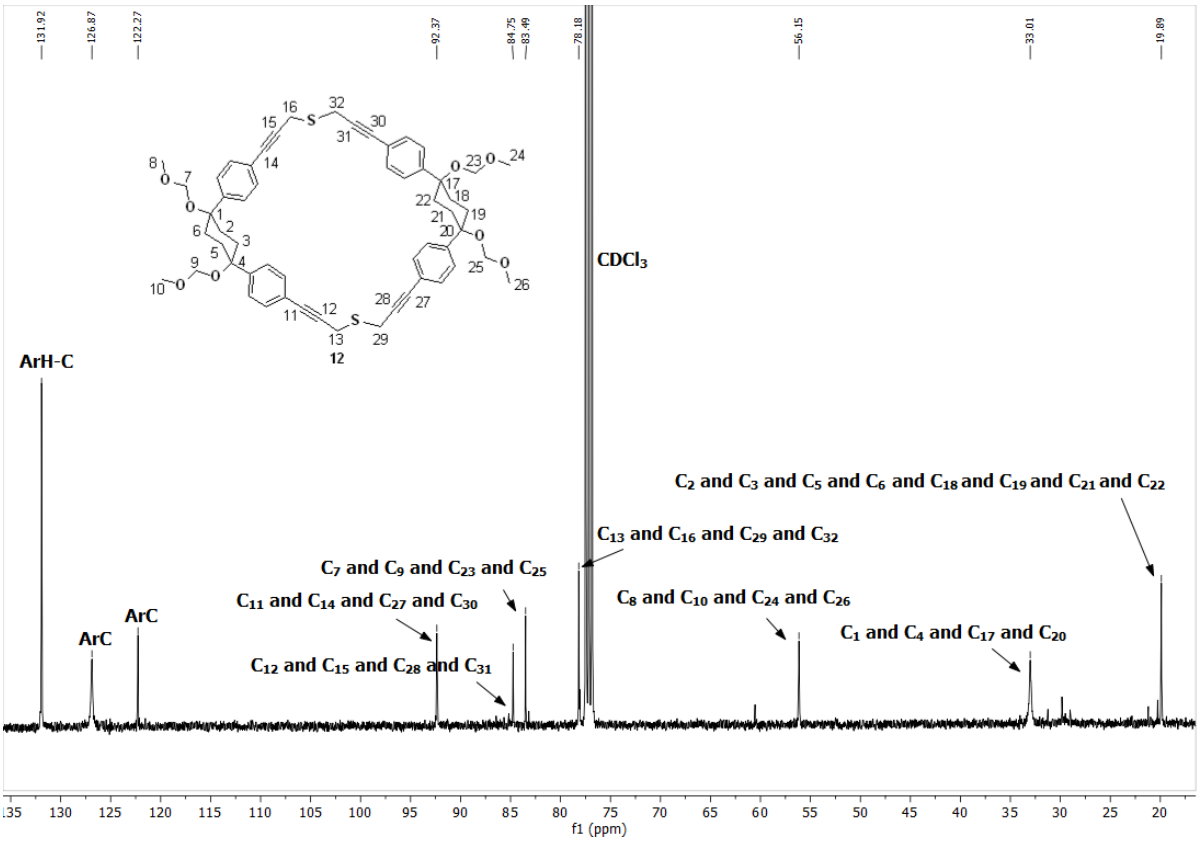

CPP NMR Spectrum 11 ^{13}C NMR spectrum of the sulfur-containing mom-protected macrocycle 12.

CHAPTER 11
REFERENCES

1 A. Fife, P. J. Beasley and D. L. Fertig, *Adv. Neuroimmunol.*, 1996, **6**, 179–190.

2 A. Urruticoechea, R. Alemany, J. Balart, A. Villanueva, F. Viñals and G. Capellá, *Curr. Pharm. Des.*, 2010, **16**, 3–10.

3 J. Ferlay, I. Soerjomataram, R. Dikshit, S. Eser, C. Mathers, M. Rebelo, D. M. Parkin, D. Forman and F. Bray, *Int. J. Cancer*, 2015, **136**, E359–E386.

4 J. Ferlay, H.-R. Shin, F. Bray, D. Forman, C. Mathers and D. M. Parkin, *Int. J. Cancer*, 2010, **127**, 2893–2917.

5 A. Jemal, F. Bray, M. M. Center, J. Ferlay, E. Ward and D. Forman, *CA. Cancer J. Clin.*, 2011, **61**, 69–90.

6 A. Jemal, F. Bray, D. Forman, M. O'Brien, J. Ferlay, M. Center and D. M. Parkin, *Cancer*, 2012, **118**, 4372–4384.

7 F. Bray, A. Jemal, N. Grey, J. Ferlay and D. Forman, *Lancet Oncol.*, 2012, **13**, 790–801.

8 A. Pearce, L. Sharp, P. Hanly, A. Barchuk, F. Bray, M. de Camargo Cancela, P. Gupta, F. Meheus, Y.-L. Qiao, F. Sitas, S.-M. Wang and I. Soerjomataram, *Cancer Epidemiol.*, 2018, **53**, 27–34.

9 D. O. Ochwang'i, C. N. Kimwele, J. A. Oduma, P. K. Gathumbi, J. M. Mbaria and S. G. Kiama, *J. Ethnopharmacol.*, 2014, **151**, 1040–1055.

10 B. Alberts, A. D. Johnson, J. Lewis, D. Morgan, M. Raff, K. Roberts and P. Walter, in *Molecular Biology of the Cell*, Garland Science, New York, 6th edn., 2015, pp. 1091–1144.

11 R. Todd and D. T. Wong, *Anticancer Res.*, 1999, **19**, 4729–4746.

12 O. Prakash, A. Kumar, P. Kumar and Ajeet, *Am. J. Pharmacol. Sci.*, 2013, **1**, 104–115.

13 S. I. Hajdu, *Cancer*, 2011, **117**, 1097–1102.

14 M. M. Olszewski, *Univ. Toronto Med. J.*, 2010, **87**, 181–186.

15 S. I. Hajdu, *Cancer*, 2011, **117**, 2811–2820.

16 S. I. Hajdu, *Cancer*, 2012, **118**, 1155–1168.

17 Y. Hu and L. Fu, *Am. J. Cancer Res.*, 2012, **2**, 340–356.

18 J. Walter, H. Miller and C. K. Bomford, in *A Short Textbook of Radiotherapy*, Churchill Livingstone, New York, 4th edn., 1979, pp. 271–284.

19 V. T. DeVita and S. A. Rosenberg, *N. Engl. J. Med.*, 2012, **366**, 2207–2214.

20 S. I. Hajdu, M. Vadmal and P. Tang, *Cancer*, 2012, **118**, 4914–4928.

21 S. I. Hajdu and M. Vadmal, *Cancer*, 2013, **119**, 4058–4082.

22 H. Schweitzer, *Science,* 1910, **32**, 809–823.

23 H. H. Dale, *Science,* 1924, **60**, 185–191.

24 V. T. Devita and E. Chu, *Cancer Res.*, 2008, **68**, 8643–8653.

25 S. I. Hajdu and F. Darvishian, *Cancer*, 2013, **119**, 1450–1466.

26 M. Fridlender, Y. Kapulnik and H. Koltai, *Front. Plant Sci.*, 2015, **6**, 1–9.

27 S. M. K. Rates, *Toxicon*, 2001, **39**, 603–613.

28 H. Yuan, Q. Ma, L. Ye and G. Piao, *Molecules*, 2016, **21**, 1–18.

29 A. A. Salim, Y.-W. Chin and A. D. Kinghorn, in *Bioactive Molecules and Medicinal Plants*, eds. K. G. Ramawat and J. M. Merillon, Springer, Heilderberg, 2008, pp. 1–24.

30 M. J. Balunas and A. D. Kinghorn, *Life Sci.*, 2005, **78**, 431–441.

31 B. K. Mishra, R. Mishra, S. N. Jena and S. Shukla, *J. Genet.*, 2016, **95**, 705–717.

32 P. López, D. P. K. H. Pereboom-de Fauw, P. P. J. Mulder, M. Spanjer, J. de Stoppelaar, H. G. J. Mol and M. de Nijs, *Food Chem.*, 2018, **242**, 443–450.

33 R. G. Mehta and J. M. Pezzuto, *Curr. Oncol. Rep.*, 2002, **4**, 478–486.

34 M. Greenwell and P. K. S. M. Rahman, *Int. J. Pharm. Sci. Res.*, 2015, **6**, 4103–4112.

35 G. D. Bagchi, D. C. Jain and S. Kumar, *Phytochemistry*, 1997, **44**, 1131–1133.

36 M. Heinrich and H. L. Teoh, *J. Ethnopharmacol.*, 2004, **92**, 147–162.

37 A. J. Manson, H. Hanagasi, K. Turner, P. N. Patsalos, P. Carey, N. Ratnaraj and A. J. Lees, *Brain*, 2001, **124**, 331–340.

38 A. Alvarado-Gonzalez and I. Arce, *J. Clin. Med. Res.*, 2015, **7**, 831–839.

39 A. M. Das, *Appl. Clin. Genet.*, 2017, **10**, 43–48.

40 G. M. Cragg and D. J. Newman, *J. Ethnopharmacol.*, 2005, **100**, 72–79.

41 A. M. Shaikh, B. Shrivastava, K. G. Apte and S. D. Navale, *J. Pharmacogn. Phytochem.*, 2016, **5**, 291–295.

42 M. C. Wani, H. L. Taylor, M. E. Wall, P. Coggon and A. T. McPhail, *J. Am. Chem. Soc.*, 1971, **93**, 2325–2327.

43 A. M. Barbuti and Z.-S. Chen, *Cancers,* 2015, **7**, 2360–2371.

44 K. Priyadarshini and A. U. Keerthi, *Med. Chem.*, 2012, **2**, 139–141.

45 W. T. Stearn and R. E. Schultes, in *The Botany and Chemistry of Cannabis: Proceedings of a Conference organized by The Institute for the Study of Drug Dependance at The Ciba Foundation 9-10 April 1969*, eds. C. R. B. Joyce and S. H. Curry, J. & A. Churchill, London, 1970, pp. 8–12.

46 A. Hazekamp, J. T. Fischedick, M. L. Díez, A. Lubbe and R. L. Ruhaak, in *Comprehensive Natural Products II: Chemistry and Biology*, eds. L. Mander and H.-W. Liu, Elsevier Ltd, Kidlington, 2010, pp. 1033–1084.

47 J. M. McPartland and G. W. Guy, *Bot. Rev.*, 2017, **83**, 327–381.

48 M. A. ElSohly and D. Slade, *Life Sci.*, 2005, **78**, 539–548.

49 R. C. Lynch, D. Vergara, S. Tittes, K. White, C. J. Schwartz, M. J. Gibbs, T. C. Ruthenburg, K. deCesare, D. P. Land and N. C. Kane, *CRC. Crit. Rev. Plant Sci.*, 2016, **35**, 349–363.

50 E. Small, *Bot. Rev.*, 2015, **81**, 189–294.

51 R. C. Clarke and M. D. Merlin, *Bot. Rev.*, 2015, **81**, 295–305.

52 E. B. Russo, *Chem. Biodivers.*, 2007, **4**, 1614–1648.

53 F. H. Liu, H.-R. Hu, G.-H. Du, G. Deng and Y. Yang, *Indian J. Tradit. Knowl.*, 2017, **16**, 235–242.

54 E. J. Brand and Z. Zhao, *Front. Pharmacol.*, 2017, **8**, 1–11.

55 P. Robson, *Br. J. Psychiatry*, 2001, **178**, 107–115.

56 L. M. Borgelt, K. L. Franson, A. M. Nussbaum and G. S. Wang, *Pharmacotherapy*, 2013, **33**, 195–209.

57 A. Mack and J. Joy, in *Marijuana As Medicine?: The Science Beyond the Controversy*, National Academies Press, Washington, 2001, pp. 13–37.

58 J. J. Ransom, 'Anslingerian' Politics: The History of Anti-Marijuana Sentiment in Federal law and How Harry Anslinger's Anti-Marijuana Politics Continue to Prevent the FDA and other Medical Experts from Studying Marijuana's Medical Utility (1991 Third Year Paper), http://nrs.harvard.edu/urn-3:HUL.InstRepos:8965561, (accessed 11 February 2019).

59 A. C. Howlett, *Prostaglandins Other Lipid Mediat.*, 2002, **68**–**69**, 619–631.

60 C. Perkel, *S. Afr. Psychiatry Rev.*, 2005, **8**, 25–30.

61 K. Peltzer and S. Ramlagan, *S. Afr. J. Psychiatry*, 2007, **13**, 126–131.

62 S. Khan, *S. Afr. J. Criminol.*, 2015, **3**, 167–179.

63 D. J. Stein, *S. Afr. Med. J.*, 2016, **106**, 569–570.

64 South African Medical Research Council, Cannabinoids for medicinal use policy brief, http://www.mrc.ac.za/policy-briefs/cannabinoids-medical-use, (accessed 11 February 2019).

65 A. du Plessis, I. Visser and A. Smit, Cannabis Position Paper 2013 by the South African National Cannabis Working Group, https://www.daggacouple.co.za/wp-content/uploads/2013/11/SANCWG-Cannabis-Position-Paper-of-2013.pdf, (accessed 11 February 2019).

66 C. M. Andre, J.-F. Hausman and G. Guerriero, *Front. Plant Sci.*, 2016, **7**, 1–17.

67 L. Combie and W. M. L. Crombie, *Phytochemistry*, 1975, **14**, 409–412.

68 C. Almaguer, C. Schönberger, M. Gastl, E. K. Arendt and T. Becker, *J. Inst. Brew.*, 2014, **120**, 289–314.

69 F. Pollastro, L. De Petrocellis, A. Schiano-Moriello, G. Chianese, H. Heyman, G. Appendino and O. Taglialatela-Scafati, *Fitoterapia*, 2017, **123**, 13–17.

70 L. O. Hanuš, S. M. Meyer, E. Muñoz, O. Taglialatela-Scafati and G. Appendino, *Nat. Prod. Rep.*, 2016, **33**, 1357–1392.

71 M. I. Khan, A. A. Sobocinska, A. M. Czarnecka, M. Król, B. Botta and C. Szczylik, *Curr. Pharm. Des.*, 2016, **22**, 1756–1766.

72 H.-C. Lu and K. MacKie, *Biol. Psychiatry*, 2016, **79**, 516–525.

73 W. A. Devane, F. A. Dysarz, M. R. Johnson, L. S. Melvin and A. C. Howlett, *Mol. Pharmacol.*, 1988, **34**, 605–613.

74 S. Munro, K. L. Thomas and M. Abu-Shaar, *Nature*, 1993, **365**, 61–65.

75 L. Console-Bram, J. Marcu and M. E. Abood, *Prog. Neuropsychopharmacol. Biol. Psychiatry*, 2012, **38**, 4–15.

76 L. A. Matsuda, S. J. Lolait, M. J. Brownstein, A. C. Young and T. I. Bonner, *Nature*, 1990, **346**, 561–564.

77 W. A. Devane, L. Hanuš, A. Breuer, R. G. Pertwee, L. A. Stevenson, G. Griffin, D. Gibson, A. Mandelbaum, A. Etinger and R. Mechoulam, *Science,* 1992, **258**, 1946–1949.

78 T. Sugiura, S. Kondo, A. Sukagawa, S. Nakane, A. Shinoda, K. Itoh, A. Yamashita and K. Waku, *Biochem. Biophys. Res. Commun.*, 1995, **215**, 89–97.

79 F. A. Javid, R. M. Phillips, S. Afshinjavid, R. Verde and A. Ligresti, *Eur. J. Pharmacol.*, 2016, **775**, 1–14.

80 F. A. Iannotti, V. Di Marzo and S. Petrosino, *Prog. Lipid Res.*, 2016, **62**, 107–128.

81 A. C. Porter and C. C. Felder, *Pharmacol. Ther.*, 2001, **90**, 45–60.

82 A. E. Munson, L. S. Harris, M. A. Friedman, W. L. Dewey and R. A. Carchman, *J. Natl. Cancer Inst.*, 1975, **55**, 597–602.

83 R. Ramer, A. Rohde, J. Merkord, H. Rohde and B. Hinz, *Pharm Res.*, 2010, **27**, 2162–2174.

84 Y. Gaoni and R. Mechoulam, *J. Am. Chem. Soc.*, 1964, **86**, 1646–1647.

85 R. Mechoulam, P. Braun and Y. Gaoni, *J. Am. Chem. Soc.*, 1967, **89**, 4552–4554.

86 R. Adams, D. C. Pease and J. H. Clark, *J. Am. Chem. Soc.*, 1940, **62**, 2194–2196.

87 R. Mechoulam and Y. Shvo, *Tetrahedron*, 1963, **19**, 2073–2078.

88 S. Burstein, *Bioorg. Med. Chem.*, 2015, **23**, 1377–1385.

89 P. H. Reggio, R. D. Bramblett, H. Yuknavich, H. H. Seltzman, D. N. Fleming, S. R. Fernando, L. A. Stevenson and R. G. Pertwee, *Life Sci.*, 1995, **56**, 2025–2032.

90 P. Massi, A. Vaccani, S. Ceruti, A. Colombo, M. P. Abbracchio and D. Parolaro, *J. Pharmacol. Exp. Ther.*, 2004, **308**, 838–845.

91 A. Ligresti, A. S. Moriello, K. Starowicz, I. Matias, S. Pisanti, L. De Petrocellis, C. Laezza, G. Portella, M. Bifulco and V. Di Marzo, *J. Pharmacol. Exp. Ther.*, 2006, **318**, 1375–1387.

92 D. J. Hermanson and L. J. Marnett, *Cancer Metastasis Rev.*, 2011, **30**, 599–612.

93 M. B. Morelli, M. Offidani, F. Alesiani, G. Discepoli, S. Liberati, A. Olivieri, M. Santoni, G. Santoni, P. Leoni and M. Nabissi, *Int. J. Cancer*, 2014, **134**, 2534–2546.

94 L. De Petrocellis, A. Ligresti, A. S. Moriello, M. Allarà, T. Bisogno, S. Petrosino, C. G. Stott and V. Di Marzo, *Br. J. Pharmacol.*, 2011, **163**, 1479–1494.

95 P. Massi, M. Solinas, V. Cinquina and D. Parolaro, *Br. J. Clin. Pharmacol.*, 2012, **75**, 303–312.

96 H. C. Kolb, M. G. Finn and K. B. Sharpless, *Angew. Chem. Int. Ed.*, 2001, **40**, 2004–2021.

97 W. D. Sharpless, P. Wu, T. V. Hansen and J. G. Lindberg, *J. Chem. Educ.*, 2005, **82**, 1833–1836.

98 A. Michael, *J. Prakt. Chem.*, 1893, **48**, 94–95.

99 M. M. Heravi, M. Tamimi, H. Yahyavi and T. Hosseinnejad, *Curr. Org. Chem.*, 2016, **20**, 1591–1647.

100 V. V. Rostovtsev, L. G. Green, V. V. Fokin and K. B. Sharpless, *Angew. Chem. Int. Ed.*, 2002,

41, 2596–2599.

101 C. W. Tornøe, C. Christensen and M. Meldal, *J. Org. Chem.*, 2002, **67**, 3057–3064.

102 S. Bernard, D. Defoy, Y. L. Dory and K. Klarskov, *Bioorg. Med. Chem. Lett.*, 2009, **19**, 6127–6130.

103 J. S. Yadav, B. V. S. Reddy, G. M. Reddy and D. N. Chary, *Tetrahedron Lett.*, 2007, **48**, 8773–8776.

104 W. S. Brotherton, H. A. Michaels, J. T. Simmons, R. J. Clark, N. S. Dalal and L. Zhu, *Org. Lett.*, 2009, **11**, 4954–4957.

105 K. R. Reddy, K. Rajgopal and M. L. Kantam, *Synlett*, 2006, 957–959.

106 F. Himo, T. Lovell, R. Hilgraf, V. V. Rostovtsev, L. Noodleman, K. B. Sharpless and V. V. Fokin, *J. Am. Chem. Soc.*, 2005, **127**, 210–216.

107 B. T. Worrell, J. A. Malik and V. V. Fokin, *Science,* 2013, **340**, 457–460.

108 A. Krasiński, V. V. Fokin and K. B. Sharpless, *Org. Lett.*, 2004, **6**, 1237–1240.

109 L. Zhang, X. Chen, P. Xue, H. H. Y. Sun, I. D. Williams, K. B. Sharpless, V. V. Fokin and G. Jia, *J. Am. Chem. Soc.*, 2005, **127**, 15998–15999.

110 B. C. Boren, S. Narayan, L. K. Rasmussen, L. Zhang, H. Zhao, Z. Lin, G. Jia and V. V. Fokin, *J. Am. Chem. Soc.*, 2008, **130**, 8923–8930.

111 M. M. Majireck and S. M. Weinreb, *J. Org. Chem.*, 2006, **71**, 8680–8683.

112 M. Lamberti, G. C. Fortman, A. Poater, J. Broggi, A. M. Z. Slawin, L. Cavallo and S. P. Nolan, *Organometallics*, 2012, **31**, 756–767.

113 L. Liang and D. Astruc, *Coord. Chem. Rev.*, 2011, **255**, 2933–2945.

114 A. E. Speers and B. F. Cravatt, *Chem. Biol.*, 2004, **11**, 535–546.

115 A. J. Link and D. A. Tirrell, *J. Am. Chem. Soc.*, 2003, **125**, 11164–11165.

116 C. D. Hein, X.-M. Liu and D. Wang, *Pharm. Res.*, 2008, **25**, 2216–2230.

117 N. Ma, Y. Wang, B.-X. Zhao, W.-C. Ye and S. Jiang, *Drug Des. Devel. Ther.*, 2015, **9**, 1585–1599.

118 G. Appendino, S. Bacchiega, A. Minassi, M. G. Cascio, L. De Petrocellis and V. Di Marzo, *Angew. Chem. Int. Ed.*, 2007, **46**, 9312–9315.

119 D.-R. Hou, S. Alam, T.-C. Kuan, M. Ramanathan, T.-P. Lin and M.-S. Hung, *Bioorg. Med. Chem. Lett.*, 2009, **19**, 1022–1025.

120 H. Shu, S. Izenwasser, D. Wade, E. D. Stevens and M. L. Trudell, *Bioorg. Med. Chem. Lett.*, 2009, **19**, 891–893.

121 P. W. Szafranski, K. Dyduch, T. Kosciolek, T. P. Wrobel, M. Gomez-Canas, M. Gomez-Ruiz, J. Fernandez-Ruiz and J. Mlynarski, *Lett. Drug Des. Discov.*, 2013, **10**, 169–172.

122 T. Hua, K. Vemuri, M. Pu, L. Qu, G. W. Han, Y. Wu, S. Zhao, W. Shui, S. Li, A. Korde, R. B. Laprairie, E. L. Stahl, J.-H. Ho, N. Zvonok, H. Zhou, I. Kufareva, B. Wu, Q. Zhao, M. A. Hanson, L. M. Bohn, A. Makriyannis, R. C. Stevens and Z.-J. Liu, *Cell*, 2016, **167**, 750–762.

123 X. Li, T. Hua, K. Vemuri, J.-H. Ho, Y. Wu, L. Wu, P. Popov, O. Benchama, N. Zvonok, K. Locke, L. Qu, G. W. Han, M. R. Iyer, R. Cinar, N. J. Coffey, J. Wang, M. Wu, V. Katritch, S. Zhao, G. Kunos, L. M. Bohn, A. Makriyannis, R. C. Stevens and Z.-J. Liu, *Cell*, 2019, **176**, 459–467.

124 M. Meldal and C. W. Tomøe, *Chem. Rev.*, 2008, **108**, 2952–3015.

125 L. B. Krasnova and A. K. Yudin, *Can. J. Chem.*, 2005, **83**, 1025–1032.

126 M. Namutebi, E. M. McGarrigle and V. K. Aggarwal, *Phosphorus, Sulfur Silicon Relat. Elem.*, 2010, **185**, 1250–1272.

127 J. Christoffers, Y. Schukze and J. Pickardt, *Tetrahedron*, 2001, **57**, 1765–1769.

128 M. P. Leal, M. Assali, I. Fernández and N. Khiar, *Chem. Eur. J.*, 2011, **17**, 1828–1836.

129 J. Bonnamour, J. Legros, B. Crousse and D. Bonnet-Delpon, *Tetrahedron Lett.*, 2007, **48**, 8360–8362.

130 J. R. Johansson, T. Beke-Somfai, A. S. Stålsmeden and N. Kann, *Chem. Rev.*, 2016, **116**, 14726–14768.

131 M.-J. Wu, C.-L. Lee, Y.-C. Wu and C.-P. Chen, *Eur. J. Org. Chem.*, 2008, 854–861.

132 L. Lis, E. S. Koltun, H. Liu and S. R. Kass, *J. Am. Chem. Soc.*, 2002, **124**, 1276–1287.

133 L. Crombie and A. D. Heavers, *J. Chem. Soc. Perkin Trans. 1*, 1992, **1**, 1929–1937.

134 S. Bähn, S. Imm, L. Neubert, M. Zhang, H. Neumann and M. Beller, *Chem. Eur. J.*, 2011, **17**, 4705–4708.

135 S. M. A. Rahman, H. Ohno, N. Maezaki, C. Iwata and T. Tanaka, *Org. Lett.*, 2000, **2**, 2893–2895.

136 J.-P. Anselme, *J. Chem. Educ.*, 1997, **74**, 69–72.

137 K. H. Huang, J. Mangette, T. Barta, P. Hughes, E. Hall, Steven and J. Veal, Benzene, Pyridine, and Pyridazine Derivatives (Patent No. WO 2008/024978 A2, pg 114-115),

https://patentscope.wipo.int/search/docs2/pct/WO2008024978/pdf/g3Q031hi3KRlcl8hgunT-P270MBNvspd2PVU8O7KlXTzask7k2vxuGfG1kBNiuVOVGtH5JOe7cIh2VApgw1VLkzes9MGqPSrtddUD9EAh4I0sAD0WeyCKE6uYPs6w6i-?docId=id000000006118880&psAuth=QjiM06Wt8uYeQTf7axas9K8H9WWNBYaLL, (accessed 10 February 2019).

138 E. Weitz and A. Scheffer, *Eur. J. Inorg. Chem.*, 1921, **54**, 2327–2344.

139 C. A. Bunton and G. J. Minkoff, *J. Chem. Soc.*, 1949, 665–670.

140 O. Lifchits, M. Mahlau, C. M. Reisinger, A. Lee, C. Farès, I. Polyak, G. Gopakumar, W. Thiel and B. List, *J. Am. Chem. Soc.*, 2013, **135**, 6677–6693.

141 S. L. Zhang and Z. Q. Deng, *Org. Biomol. Chem.*, 2016, **14**, 7282–7294.

142 M. Miyashita, T. Suzuki and A. Yoshikoshi, *Tetrahedron Lett.*, 1987, **28**, 4293–4296.

143 D. Liotta, W. Markiewicz and H. Santiesteban, *Tetrahedron Lett.*, 1977, **50**, 4365–4368.

144 D. Liotta, U. Sunay, H. Santiesteban and W. Markiewicz, *J. Org. Chem.*, 1981, **46**, 2605–2610.

145 K. B. Sharpless and R. C. Michaelson, *J. Am. Chem. Soc.*, 1973, **95**, 6137–6139.

146 S. K. Karmee, R. Van Oosten and U. Hanefeld, *Tetrahedron: Asymmetry*, 2011, **22**, 1736–1739.

147 S. Abele, R. Inauen, J.-A. Funel and T. Weller, *Org. Process Res. Dev.*, 2011, **16**, 129–140.

148 L.-W. Xu, C.-G. Xia, J.-W. Li and S.-L. Zhou, *Synlett*, 2003, 2246–2248.

149 P. Lakshmipathi and A. V. Rama Rao, *Tetrahedron Lett.*, 1997, **38**, 2551–2552.

150 L.-W. Xu, L. Li, C.-G. Xia, S.-L. Zhou and J.-W. Li, *Tetrahedron Lett.*, 2004, **45**, 1219–1221.

151 L. Castrica, F. Fringuelli, L. Gregoli, F. Pizzo and L. Vaccaro, *J. Org. Chem.*, 2006, **71**, 9536–9539.

152 D. J. Guerin, T. E. Horstmann and S. J. Miller, *Org. Lett.*, 1999, **1**, 1107–1109.

153 J. Andraos, E. Ballerini and L. Vaccaro, *Green Chem.*, 2015, **17**, 913–925.

154 J. B. Stothers and P. C. Lauterbur, *Can. J. Chem.*, 1964, **42**, 1563–1576.

155 O. L. Chapman, U.-P. E. Tsou and J. W. Johnson, *J. Am. Chem. Soc.*, 1987, **109**, 553–559.

156 A. Mohan, V. Ramkumar and S. Sankararaman, *J. Organomet. Chem.*, 2015, **799**–**800**, 115–121.

157 R. Appel, *Angew. Chem. Int. Ed.*, 1975, **14**, 801–811.

158 J. D. Slagle, T. T.-S. Huang and B. Franzus, *J. Org. Chem.*, 1981, **46**, 3526–3530.

159 H. Erfle and R. Pepperkok, *Methods Enzymol.*, 2005, **404**, 1–8.

160 G. Dongmei, S. Dengjun, Z. Liangming and Z. Weiwei, *Afr. Health Sci.*, 2015, **15**, 594–597.

161 S.-H. Lee, J. Yoon, S.-H. Chung and Y.-S. Lee, *Tetrahedron*, 2001, **57**, 2139–2145.

162 P. W. Groundwater, M. Nyerges, I. Fejes, D. E. Hibbs, D. Bendell, R. J. Anderson, A. McKillop, T. Sharif and W. Zhanga, *Arkivoc*, 2012, **5**, 684–697.

163 A. Kozioł, A. Stryjewska, T. Librowski, K. Salat, M. Gawel, A. Moniczewski and S. Lochynski, *Mini-Rev. Med. Chem.*, 2014, **14**, 1156–1168.

164 E. Marsault and M. L. Peterson, *J. Med. Chem.*, 2011, **54**, 1961–2004.

165 A. Grossmann, S. Bartlett, M. Janecek, J. T. Hodgkinson and D. R. Spring, *Angew. Chem. Int. Ed.*, 2014, **53**, 13093–13097.

166 M. S. Seyfried, J. Alzeer and N. W. Luedtke, *Eur. J. Org. Chem.*, 2016, 367–372.

167 V. Montes-García, J. Pérez-Juste, I. Pastoriza-Santos and L. M. Liz-Marzán, *Chem. Eur. J.*, 2014, **20**, 10874–10883.

168 S. Iijima, *Nature*, 1991, **354**, 56–58.

169 H. Omachi, S. Matsuura, Y. Segawa and K. Itami, *Angew. Chem. Int. Ed.*, 2010, **49**, 10202–10205.

170 Y. Segawa, A. Yagi, K. Matsui and K. Itami, *Angew. Chem. Int. Ed.*, 2016, **55**, 5136–5158.

171 H. Takaba, H. Omachi, Y. Yamamoto, J. Bouffard and K. Itami, *Angew. Chem. Int. Ed.*, 2009, **48**, 6112–6116.

172 R. Jasti, J. Bhattacharjee, J. B. Neaton and C. R. Bertozzi, *J. Am. Chem. Soc.*, 2008, **130**, 17646–17647.

173 Y. Segawa, S. Miyamoto, H. Omachi, S. Matsuura, P. Šenel, T. Sasamori, N. Tokitoh and K. Itami, *Angew. Chem. Int. Ed.*, 2011, **50**, 3244–3248.

174 A.-F. Tran-Van and H. A. Wegner, *Beilstein J. Nanotechnol.*, 2014, **5**, 1320–1333.

175 A.-F. Tran-Van, E. Huxol, J. M. Basler, M. Neuburger, J.-J. Adjizian, C. P. Ewels and H. A. Wegner, *Org. Lett.*, 2014, **16**, 1594–1597.

176 A.-F. S. Tran-Van, Reactivity of Strained Systems in Alkyne Cycloaddition Reactions-Synthesis of Substituted Cycloparaphenylenes, https://edoc.unibas.ch/39117/1/PhD Thesis AF Stoessel Tran-Van.pdf, (accessed 5 March 2019).

177 A. Dell'Isola, M. M. W. McLachlan, B. W. Neuman, H. M. N. Al-Mullah, A. W. D. Binks, W.

Elvidge, K. Shankland and A. J. A. Cobb, *Chem. Eur. J.*, 2014, **20**, 11685–11689.

178 R. Chinchilla and C. Nájera, *Chem. Rev.*, 2007, **107**, 874–922.

179 T. Mitra, J. Das, M. Maji, R. Das, U. K. Das, P. K. Chattaraj and A. Basak, *RSC Adv.*, 2013, **3**, 19844–19848.

180 C.-C. Han and R. Balakumar, *Tetrahedron Lett.*, 2006, **47**, 8255–8258.

181 X. Cao, Y. Yang and X. Wang, *J. Chem. Soc., Perkin Trans. 1*, 2002, 2485–2489.

182 S. Schenk, J. Weston and E. Anders, *J. Am. Chem. Soc.*, 2005, **127**, 12566–12576.

183 Y. Miyauchi, K. Johmoto, N. Yasuda, H. Uekusa, S. Fujii, M. Kiguchi, H. Ito, K. Itami and K. Tanaka, *Chem. Eur. J.*, 2015, **21**, 18900–18904.

184 M. Amatore, D. Leboeuf, M. Malacria, V. Gandon and C. Aubert, *J. Am. Chem. Soc.*, 2013, **135**, 4576–4579.